# Oceanologia

**Official Journal of the Polish Academy of Sciences: Institute of Oceanology and Committee on Maritime Research**



**This journal is supported by the Ministry of Science and Higher Education, Warsaw, Poland**

**Indexed in:** ISI Journal Master List, Science Citation Index Expanded, Scopus, Current Contents, Zoological Record, Thomson Scientific SSCI, Aquatic Sciences and Fisheries Abstracts, DOAJ

**IMPACT FACTOR ANNOUNCED FOR 2016 IN THE 'JOURNAL CITATION REPORTS' IS 1.500; 5-year IF is 1.341**

**Publisher**
Elsevier Sp. z o.o.
22, Jana Pawła II Avenue
00-133 Warsaw, Poland

**Associate Publisher**
Justyna Kasprzycka
j.kasprzycka@elsevier.com
+31 20 485 3846

**ISSN 0078-3234**

Oceanologia (2017) 59, 1—17

Available online at www.sciencedirect.com

ScienceDirect

journal homepage: www.journals.elsevier.com/oceanologia/

ORIGINAL RESEARCH ARTICLE

# Tracking trends in eutrophication based on pigments in recent coastal sediments

**Małgorzata Szymczak-Żyła [a], Magdalena Krajewska [a], Aleksandra Winogradow [a], Agata Zaborska [a], Gijs D. Breedveld [b], Grażyna Kowalewska [a,*]**

[a] *Institute of Oceanology, Polish Academy of Sciences, Sopot, Poland*
[b] *Norwegian Geotechnical Institute, Oslo, Norway*

Received 15 June 2016; accepted 22 August 2016
Available online 29 September 2016

**KEYWORDS**
Eutrophication;
Pigments;
Markers;
Sediments;
Baltic Sea;
Norwegian fjords

**Summary** Eutrophication in two different coastal areas — the Gulf of Gdańsk (southern Baltic) and the Oslofjord/Drammensfjord (Norway) — both subject to human pressure and with restricted water exchange with adjacent seas, was investigated and compared. Sediment cores (up to 20 cm long) were collected at 12 stations using a core sampler, 6 in each of the two areas, and divided into sub-samples. The physicochemical parameters characterizing the adjacent water column and near-bottom water, i.e. salinity, oxygen concentration and temperature, were measured during sample collection. Chlorophylls-a, -b and -c, their derivatives and selected carotenoids were determined for all the samples, as were additional parameters characterizing the sediments, i.e. $C_{org}$, $N_{tot}$, $\delta^{13}C$ and $\delta^{15}N$, grain size. $^{210}Pb$ activity was also determined and on that basis sediment mixing and accumulation rates were estimated. The distribution of pigments in sediments was related to environmental conditions, the sampling site location and sediment characteristics. The results are in agreement with other observations that eutrophication in the Gulf of Gdańsk has increased, especially since the 1970s, whereas in the Oslofjord it decreased during the same period. The pigments are better preserved in inner Oslofjord sediments than in those from the Gulf of Gdańsk. The results demonstrate that the sum of chloropigments-a in

* Corresponding author at: Institute of Oceanology, Polish Academy of Sciences, ul. Powstańców Warszawy 55, 81-712 Sopot, Poland. Tel.: +48 587311615.
*E-mail addresses:* szymczak@iopan.gda.pl (M. Szymczak-Żyła), mlawrec@iopan.gda.pl (M. Krajewska), olcia@iopan.gda.pl (A. Winogradow), agata@iopan.gda.pl (A. Zaborska), Gijs.Breedveld@ngi.no (G.D. Breedveld), Kowalewska@iopan.gda.pl (G. Kowalewska).
Peer review under the responsibility of Institute of Oceanology of the Polish Academy of Sciences.

Production and hosting by Elsevier

http://dx.doi.org/10.1016/j.oceano.2016.08.003

sediments calculated per dry weight of sediments is a valuable measure of eutrophication, providing that the monitoring site is selected properly, i.e. sediments are hypoxic/anoxic and non-mixed. Besides, the results confirm previous observations that the percentages of particular chlorophyll-a derivatives in the sum of chloropigments-a are universal markers of environmental conditions in a basin. The ratios of chloropigments-b and chlorophylls-c to the sum of chloropigments-a (ΣChlns-b/ΣChlns-a; Chls-c/ΣChlns-a) may by applied as complementary markers of freshwater and marine organic matter input, respectively.


## 1. Introduction

Eutrophication is one of the most important problems affecting many coastal areas worldwide (e.g. Bianchi et al., 2010; Chen et al., 2001; Fleming-Lehtinen et al., 2015; HELCOM, 2007; Li et al., 2013; Orive et al., 2002). It occurs in aquatic basins of high primary production caused by elevated nutrient concentrations (Edlund et al., 2009; Harmon et al., 2014). The intensive blooms of algae and cyanobacteria (including toxin-producing phytoplankton species), followed by high rates of sedimentation and accumulation, in conjunction with restricted water exchange result in eutrophication, which is manifested by hypoxia/anoxia in the sediments and near-bottom water (Conley et al., 2011; HYPOX, 2016). Oxygen depletion inhibits the growth of benthic organisms — this is reflected in the formation of laminar sediments (Reuss et al., 2005; Zhao et al., 2012). Like darkness and low temperatures, anoxia prevents the remineralization of organic matter in sediments (Hedges and Keil, 1995).

Despite the large body of knowledge relating to eutrophication and its imprint on bottom sediments, it is still not easy to evaluate it quantitatively, analyze its trends in a basin and compare it in different locations. Numerous proxies have been applied to this phenomenon, including organic compounds — principally pigments. These are chlorophyll-a, carotenoids and their derivatives. Chlorophyll-a in water is well known as a marker of primary production and has been used for this purpose in oceanography for over 50 years (e.g. Bianchi and Canuel, 2011; Jeffrey and Mantoura, 1997); the same applies to its derivatives (Bianchi et al., 1997, 2002a,b; Carpenter et al., 1988). However, chlorophyll-a concentrations in water change frequently in time and space, whereas chloropigments-a (chlorophyll-a and its derivatives) in sediments have been shown to be good indicators of the average primary production in a basin (Bianchi et al., 2002a,b; Harris et al., 1996; Stephens et al., 1997; Szymczak-Żyła et al., 2011). Particular sedimentary chlorophyll-a derivatives may be taken as markers of syn- and post-depositional environmental conditions (Szymczak-Żyła et al., 2011). Not only chloropigments but also carotenoids are monitored in sediments as chemotaxonomic and biomass markers; indeed, β-carotene is considered an even better proxy for total algal biomass than chlorophyll-a (Dixit et al., 2000; Leavitt, 1993; Schüller et al., 2013). Numerous papers have focused on chloropigments and carotenoids in recent and old sediments, mainly in lakes (e.g. Hodgson et al., 2004; Leavitt et al., 1997; McGowan et al., 2012; Moorhouse et al., 2014; Pienitz et al., 1992). Pigments have also been tracked in shelf areas (Chen et al., 2001; Li et al., 2012, 2013; Louda et al., 2000; Shankle et al., 2002; Sampere et al., 2008), in large river estuaries in America (Canuel et al., 2009; Chen et al., 2005; Edlund et al., 2009; Wysocki et al., 2006) and Asia (Li et al., 2011; Zhao et al., 2012), in New Zealand fjords (Schüller and Savage, 2011) and off the coast of Antarctica (Sañé et al., 2013). In contrast, not many papers have been written on pigments in European coastal zone sediments (Bianchi et al., 1996; Bourgeois et al., 2011; Reuss et al., 2005; Tselepides et al., 2000) and even fewer on Baltic sediments (Bianchi et al., 2002a,b; Kowalewska, 1997; Kowalewska et al., 2004; Reuss et al., 2005; Savage et al., 2010; Szymczak-Żyła and Kowalewska, 2007), despite the fact that eutrophication and hypoxia were identified as problems in this sea already many years ago (Conley et al., 2009; HELCOM, 2007).

Pigment concentrations in sediments depend on different factors, associated with (1) primary production and sedimentation, (2) pigment stability and (3) post-depositional conditions in sediments. Pigment degrade already in the water column and after deposition in the sediments as a result of senescence, oxidation, herbivore grazing or bacterial degradation (e.g. Bianchi et al., 1988; Louda et al., 1998, 2002; Spooner et al., 1994a,b; Szymczak-Żyła et al., 2006; Welschmeyer and Lorenzen, 1985). The influence of particular factors on pigment content may be different at different sites, so it is not an easy task to compare the extent of eutrophication in different areas based on pigment proxies in sediments, or to make judgements about eutrophication trends (Leavitt, 1993; Reuss et al., 2005).

The aim of this work was to compare eutrophication in different water basins, exemplified by the Gulf of Gdańsk (southern Baltic) and the Oslofjord/Drammensfjord (Norway), and its trends in each one. These two water bodies differ in salinity, geomorphology and the extent of water mixing, but both experience limited exchange of water with the adjacent sea and both are subject to human pressure. The aim was realized by analysing the pigment content in recent sediments in relation to environmental conditions in the near-bottom water as well as sediment characteristics, including accumulation rate, sediment mixing, grain size distribution, carbon and nitrogen content, i.e. parameters and factors associated with eutrophication.

## 2. Material and methods

### 2.1. Study areas

#### 2.1.1. Gulf of Gdańsk

The Gulf of Gdańsk (Fig. 1, area 4940 km$^2$) is part of the southern Baltic Sea (Majewski, 1990). The adjacent

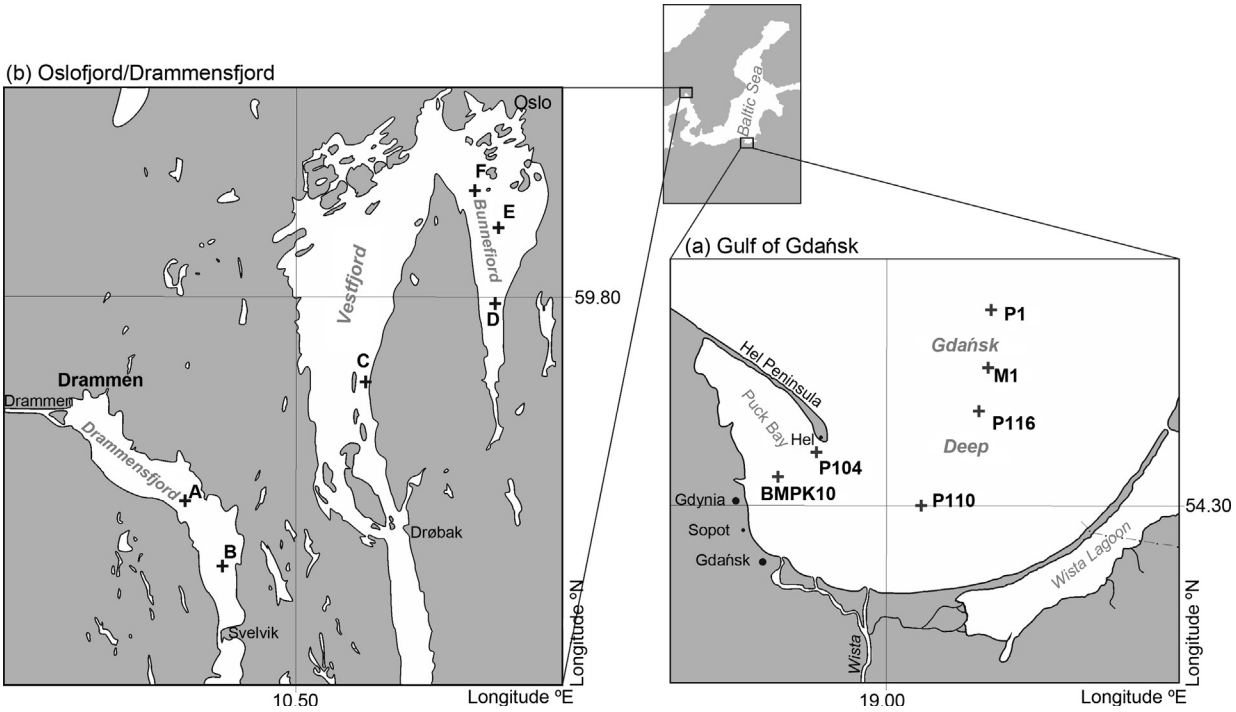


**Figure 1** Location of the sampling sites: (a) Gulf of Gdańsk and (b) Oslofjord/Drammensfjord.

Gdańsk-Sopot-Gdynia conurbation (>1.2 million inhabitants) has a considerable anthropogenic influence on the Gulf. In addition, the Gulf of Gdańsk annually receives some 39 $km^3$ (average flow rate ~1240 $m^3 s^{-1}$) of freshwater from the River Wisła (Vistula) (Pastuszak and Witek, 2012), which corresponds to ~13% of the total volume of Gulf of Gdańsk waters. The catchment area of the River Wisła covers about 54% of the area of Poland (~170 000 $km^2$) and is inhabited by almost 60% of the country's population (~27% of the Baltic catchment area's population), and the river itself accumulates pollutants from industrial, municipal and agricultural effluents; nutrients are especially important. The nutrients and organic matter entering the Gulf with Wisła waters causes high primary production, which, together with the limited water exchange in the Gulf of Gdańsk, results in eutrophication (IMGW, 2013; Witek et al., 1999).

The depth of the Gulf of Gdańsk (average — 59 m; maximum — 118 m) increases seawards from the shallow coastal zone. The salinity of the Gulf's surface waters varies from ~4.5 near the Wisła mouth to ~8 in the northern, deep part of the basin. In its deeper regions (the Gdańsk Deep), vertical stratification of the water occurs, resulting in a halocline at a depth of 60—80 m that separates the more saline deep water (~12.5) from the less saline water at the surface. As vertical water exchange is limited, the bottom water in the deepest areas is hypoxic/anoxic (Conley et al., 2009; IMGW, 2013). The oxygen conditions improve during intermittent inflow events of cold and well-oxygenated seawater from the North Sea through the Danish Straits. Such strong inflows into the Baltic take place once every few years, usually during late autumn or winter (HELCOM, 2013; Mälkki and Perttilä, 2012; Mohrholz et al., 2015). The hydrological conditions and bottom topography strongly differentiate this shallow basin as far as sediment characteristics are concerned. Thus, the sediments in the Gulf vary from coarse sands near the coast to silty clay in the Gdańsk Deep. This and the lack of tides make the Gulf an exceptional natural model basin for studying eutrophication in a marine environment strongly impacted by freshwater input (IMGW, 2013).

### 2.1.2. Oslofjord/Drammensfjord

The Oslofjord (southern Norway) is an approximately 100 km long northward extension of the Skagerrak (Fig. 1). It is divided into an inner and outer fjord by a narrow sound with a sill at 19.5 m water depth (Drøbak Sound). The inner Oslofjord consists of two main basins: the Vestfjord and the Bunnefjord, both with a maximum water depth of about 160 m, separated by a sill at about 50 m water depth. Both fjord basins contain a number of smaller, semi-enclosed basins. The bottom topography of the Oslofjord restricts deeper-water exchange and renewal in the inner fjord. The water masses are stratified with brackish surface water and marine bottom water. Deep water renewals take place in winter with strong northerly winds (Hess et al., 2014). The inner microtidal area, which borders the most densely populated and industrialized area in Norway, has received large amounts of waste waters and nutrients, particularly during the last century. As a consequence of that and the limited water-exchange between the different basins, oxygen-depleted bottom water conditions have developed in several basins (Dale et al., 1999). The nutrient load to the inner Oslofjord reached a maximum around 1970; since then it has decreased considerably, and the oxygen conditions are slowly improving in most basins (Hess et al., 2014).

The outer Oslofjord is connected to the Drammensfjord, which has a length of 20 km and a width of 1.6—3.0 km. It is separated from the Greater Oslofjord by a sill at Svelvik, which was dredged from 6 to 8 m depth around 1900, and to

10 m in 1951 (Smittenberg et al., 2005). Since the 1800s, the redoxcline in Drammensfjord has moved to shallower water depths following the increased influx of organic material from the pulp and paper industry, and from an increasing population and more intensive agriculture in the drainage area (Alve, 1991). Oxygen depletion was first detected in 1899, and the presence of $H_2S$ in June 1933 (Öztürk, 1995; Smittenberg et al., 2005). An incursion of oceanic waters currently occurs once every 3–5 years, mainly between November and May, displacing some of the anoxic bottom waters upwards (Alve, 1995a; Richards, 1965). The shallowest position of the redoxcline occurred in the late 1970s to early 1980s, when it lay at 30–35 m water depth (Magnusson and Næs, 1986). In 1988, following the closing down of industry and the implementation of governmental regulations, it was recorded at about 35 m water depth in the north and about 60 m in the south with anoxic sediments in the deeper parts and oxic sediments in the shallower parts (Alve, 1995b). Recent studies conducted by local authorities (Monitoring of Drammensfjord 2008–2011, NGI, 2010) show that the deep-water dissolved oxygen levels increased from anoxic to a period of oxic conditions following the 2004/2005-dredging of the sill to 12 m depth. The mixing of freshwater from the River Drammen (drainage area ~17 000 $km^2$, average flow rate ~300 $m^3 s^{-1}$), which enters the fjord at its head, gives rise to a brackish surface water layer (salinity 1–10, depending on the season) that is separated from saline bottom water (30.5) below 40 m depth. River regulation has smoothed the annual freshwater supply to the fjord over the last 60 years, reducing the effect of spring flooding and increasing the winter supply. This has shifted the minimum freshwater supply from winter to late summer, thus increasing the residence time of the surface water during summer (Smittenberg et al., 2005).

## 2.2. Sample collection

Sediments were collected at six stations in the Gulf of Gdańsk and six stations in the Oslofjord/Drammensfjord (Fig. 1; Table 1). The stations in the Gulf of Gdańsk were selected so as to cover a wide range of environmental conditions in the study area, i.e. different water depth, salinity, oxygen concentration, sediment type and distance from the coastline. The four stations selected – P110, P116, M1 and P1 – were positioned along the way of Wisła water inflow in the Gulf as far as the Gdańsk Deep. The other two stations were located in Puck Bay, the shallow, western part of the Gulf (Table 1): station BMPK10 in the middle of the Bay and P104 close to the town of Hel, a recreational and sports centre, near intensively used shipping lanes and strong water currents around the tip of the Hel Peninsula.

The stations in the Oslofjord/Drammensfjord were also selected such as to obtain many different locations concerning distance from the open sea, salinity, oxygen concentration and human pressure (Fig. 1; Table 1). Two stations were located in Drammensfjord: A in the middle of the fjord and B

**Table 1** Characteristics of the sampling stations.

| Station | Coordinates | Water depth [m] | Parameters of near-bottom water | | | Sediment accumulation rate [cm $y^{-1}$] | Sediment mixing depth [cm] |
|---|---|---|---|---|---|---|---|
| | | | Salinity | Temp. [°C] | Oxygen [mg $L^{-1}$] | | |
| ***Gulf of Gdańsk*** | | | | | | | |
| P1 | 54°50.042′N 19°19.683′E | 112 | 12.0 | 6.3 | 3.4 | 0.16 ± 0.01 | 0 |
| M1 | 54°44.912′N 19°17.662′E | 95 | 11.7 | 6.4 | 3.9 | 0.16 ± 0.01 | 0 |
| P116 | 54°39.091′N 19°17.575′E | 92 | 10.8 | 6.4 | 0.5 | 0.14 ± 0.01 | 0 |
| P110 | 54°29.986′N 19°06.902′E | 72 | 8.6 | 5.0 | 5.4 | 0.17 ± 0.02 | 3 |
| BMPK10 | 54°33.545′N 18°40.950′E | 31 | 7.5 | 4.9 | 11.1 | No accumulation or max 0.07 ± 0.01 | 12 |
| P104 | 54°34.944′N 18°47.370′E | 55 | 7.6 | 4.5 | 12.1 | No accumulation | 12 |
| ***Oslofjord/Drammensfjord*** | | | | | | | |
| A | 59°41.276′N 10°22.745′E | 113 | 31.2 | 8.0 | 0.3 | 0.11 ± 0.01 | 0 |
| B | 59°38.862′N 10°24.804′E | 122 | 31.0 | 8.2 | 0.5 | 0.27 ± 0.02 | 0 |
| C | 59°45.066′N 10°34.429′E | 154–158 | 32.3 | 8.3 | 9.2 | 0.20 ± 0.02 | 4 |
| D | 59°47.386′N 10°43.154′E | 152 | 32.6 | 9.2 | 1.7 | 0.10 ± 0.03 | 5 |
| E | 59°50.643′N 10°43.557′E | 77 | 33.2 | 8.5 | 0.2 | 0.18 ± 0.01 | 0 |
| F | 59°51.470′N 10°41.710′E | 78 | 33.6 | 8.3 | 1.7 | 0.05 ± 0.01 | 3 |

nearer Svelvik. The other four stations were located in the inner Oslofjord: station C in the deepest, southernmost part of the Vestfjord, and stations D, E and F in the Bunnefjord. Station D was in the deepest and southern-most part of the Bunnefjord, station E in its shallower part, and station F was closest to the port of Oslo.

The sediments were collected during two cruises of r/v 'Oceania': in April 2014 (in the Gulf of Gdańsk) and in June 2014 (in the Norwegian fjords). Sediment samples were taken with a Niemistö core sampler in the Gulf of Gdańsk and with a GEMAX twin-core sampler in the Norwegian fjords; in both cases the core diameter $\Phi$ = 10 cm. Eight cores were collected at each station. All the cores were photographed immediately after collection (Appendix 1). After collection the following layers were taken from each sediment core: 0–1, 1–5, 5–10, 10–15 and 15–20 cm; sub-samples from all the cores collected at the same station were pooled. The additional core for $^{210}$Pb analysis was divided into thinner, 1 cm thick layers from 0 to 10 cm and 2 cm thick layers from 10 to 30 cm sediment depth. All the sub-samples were frozen on board immediately after collection.

## 2.3. Physicochemical seawater parameters

The salinity, temperature and oxygen concentration were measured with a SBE19 probe (vertical profiles in the water column) and with a ProfiLine Multi 197i WTW meter (near-bottom water).

## 2.4. Analyses

### 2.4.1. Pigment analysis

The concentrations of pigments were determined in all samples with HPLC using a procedure described in detail elsewhere (Kowalewska et al., 1996; Szymczak-Żyła et al., 2008).

*2.4.1.1. Pigment extraction from sediments.* A frozen sediment sample (3–5 g) was placed in a glass centrifuge tube and left to thaw. After centrifugation (10 min, 2500 rpm) water was removed and the sample flushed with acetone, stirred, sonicated (2–3 min), centrifuged again, and the extract decanted. The extraction was repeated until the supernatant was colourless (max. 3 times). The acetone extracts were transferred to a separate funnel in which liquid–liquid extraction was performed in the acetone extract:benzene:water system. The benzene layer was then transferred to a glass vial and evaporated to dryness in a stream of argon and stored frozen (−20°C) until HPLC analysis. The extracted sediment was dried at 60°C and weighed. The pigment content was calculated per dry sediment weight.

*2.4.1.2. HPLC pigment analysis.* The sediment extract prepared as above was dissolved in acetone and injected into the HPLC set (Knauer, Germany) with two detectors: diode array (DAD 2800 Knauer) and fluorescence detector (RF-20Axs, Shimadzu, Japan), autosampler (Knauer Optimas, Germany), then into a Lichrospher 100RP-18 endcapped column (250 mm × 4 mm, 5 μm; Merck, Germany) through a guard column (Lichrospher 100RP-18 endcapped, 4 mm × 4 mm; Merck, Germany).

The following pigments were determined: chloropigments-a (chlorophyll-a and its derivatives: pheophorbides-a, pyropheophorbides-a, chlorophyll-a-allomers, chlorophyll-a-epimer, pheophytin-a, pheophytin-a-epimer, pyropheophytin-a and sum of steryl chlorin esters); chloropigments-b (chlorophyll-b and pheophytin-b); sum of chlorophylls-c; carotenoids (fucoxanthin, alloxanthin, diatoxanthin, lutein, zeaxanthin, cantaxanthin, echinenone and β-carotene).

Separations of chloropigments-a and -b were carried out using an HPLC/DAD set, in the A (acetone):B (80:20, acetone: water, v/v) gradient system at a flow rate of 1.0 mL min$^{-1}$. The mobile phase and gradient system was a modified version of that used by Szymczak-Żyła et al. (2008). Absorption spectra were measured over the 360–750 nm range. Pigment concentrations were determined according to the procedure described by Szymczak-Żyła et al. (2008).

Chlorophylls-c were analyzed using an HPLC/FL set, in the A (acetone):B (80:20, acetone:water, v/v) gradient system at a flow rate of 0.5 mL min$^{-1}$. The excitation and emission wavelengths were 440 and 630 nm, respectively. Quantitative data of chlorophylls-c content were obtained according to the procedure described by Kowalewska et al. (1996).

Carotenoid separations were carried out using an HPLC/DAD set, in the A (85:15, methanol:0.5 M ammonium acetate, aq. v/v):B (90:10, acetonitrile:water, v/v): C (ethyl acetate) gradient system at a flow rate of 1.0 mL min$^{-1}$. The mobile phase and gradient system was a modified version of that used by Chen et al. (2001). Carotenoid concentrations in the samples were calculated in the same way as those for chloropigments-a and b (Szymczak-Żyła et al., 2008).

Pigments were identified on the basis of retention time and absorbance spectra compared with pigment standards (DHI, Denmark).

### 2.4.2. Additional analyses

*2.4.2.1. $^{210}$Pb analysis – sediment accumulation rate.* The $^{210}$Pb dating method (Goldberg, 1963) was used to determine the sediment accumulation rate. Sediment samples for $^{210}$Pb dating were freeze-dried and ground in the laboratory. Sediment moisture and porosity were calculated. The $^{210}$Pb activity concentration was measured indirectly by the alpha spectrometry counting of its daughter nuclide $^{210}$Po (Zaborska et al., 2007). In brief, sediment samples were spiked with $^{209}$Po (chemical yield tracer) and digested. Polonium isotopes were spontaneously deposited onto silver discs. These were analyzed for $^{210}$Po and $^{209}$Po activity concentration in a multi-channel analyser (Canberra) equipped with Si/Li detectors. The samples were counted for 1 day. The activity concentration of $^{210}$Po in a sample was determined on the basis of chemical recovery by comparing the measured and spiked activity concentration of $^{209}$Po. Blanks and standards were measured to verify the efficiency of the separation procedure and detection. Standard reference materials (IAEA-326) were used to verify the measurements. One blank sample (without the sediment) was measured with every 7 sediment samples. The environmental background was negligible. The linear accumulation rate (LAR, cm y$^{-1}$) was calculated assuming an exponential decrease in $^{210}$Pb$_{ex}$ with sediment depth (Zaborska et al., 2007).

*2.4.2.2. Grain size analysis.* The fine fractions from sampling stations BMPK10 and P104 and the sediment samples from the other stations were analyzed by laser diffraction using a Fritsch Laser Particle Sizer Analysette-22 (Kramarska

et al., 1996) and recorded at a resolution of 1 ϕ. Sodium pyrophosphate was used to prevent aggregates forming during measurement. Because the sediment samples from the Oslofjord contained carbonates, they were pre-treated with 10% HCl. All sediment samples were treated with 30% $H_2O_2$ before analysis in order to remove organic matter. Sediments from stations BMPK10 and P104 were first passed wet (Myślińska, 1992) through a sieve of mesh diameter of 0.063 mm.

*2.4.2.3. Carbon and nitrogen analyses.* Organic carbon ($C_{org}$), total nitrogen ($N_{tot}$), stable carbon ($\delta^{13}C$) and nitrogen ($\delta^{15}N$) isotope analyses were done in a Flash EA 1112 Series Elemental Analyzer combined with an IRMS Delta V Advantage Isotopic Ratio Mass Spectrometer (Thermo Electron Corp., Germany). Dry, homogeneous samples of the sediments were weighed (2–4 mg for the Baltic Sea sediment samples, 20–25 mg for the Oslofjord/Drammensfjord sediment samples) into silver vials and acidified with 2 M HCl (Chang et al., 1991; Hedges and Stern, 1984). The $C_{org}$ and $N_{tot}$ concentrations are stated as percentages of the bulk of the dry sample after removal of carbonates. Quality control of the organic carbon measurements was carried out with standards (Thermo Electron Corp.). The accuracy and precision (average recovery 99.1 ± 2.0%) of the methodology were satisfactory. Isotopic ratios $\delta^{13}C$ and $\delta^{15}N$ were calculated using laboratory working pure reference gases $CO_2$ and $N_2$ calibrated against IAEA standards: CO-8 and USGS40 for $\delta^{13}C$ and N-1 and USGS40 for $\delta^{15}N$. The $\delta^{13}C$ results are given in the conventional delta notation, i.e. versus PDB for $\delta^{13}C$ and versus air for $\delta^{15}N$.

## 2.5. Statistical analysis

The results were statistically processed using STATISTICA 12.5 software (StatSoft, Poland): correlation analysis, cluster analysis and principal component analysis (PCA) were used. Non-parametric methods (e.g. R-Spearman correlation analysis) were applied to cases where the basic conditions necessary for using parametric methods were not fulfilled (tested with the Shapiro–Wilk and Brown-Forsyth tests). Correlation analysis was used to evaluate the relationships between the pigment contents, pigment ratios in the sediment and the environmental parameters. A correlation of $p < 0.05$ was regarded as significant. Cluster analysis (Ward's method, Euclidean distance) was used to produce a classification of the sampling stations taking into account sediment characteristics (pigment content, grain size, organic carbon and nitrogen content) and near-bottom water parameters. Relationships between the content of pigments, ratio of particular pigments in the sediment samples and other measured parameters were also checked using PCA.

# 3. Results

## 3.1. Pigment distribution

The highest pigment concentrations were found in sediments collected from the Gdańsk Deep, where the concentration of e.g. ΣChlns-a in the surface (0–1 cm) layer of sediments ranged from ~350 nmol $g^{-1}$ d.w. (dry weight of sediment) at station P110 to ~800 nmol $g^{-1}$ d.w. at station P1 (Fig. 2). Relative to the Gdańsk Deep area, the sediments from Puck Bay (stations BMPK10, P104) contained much lower amounts of pigments (e.g. ΣChlns-a in 0–1 cm layer ~80 nmol $g^{-1}$ d.w.). From the Oslofjord/Drammensfjord, only the sediments from the Bunnefjord were rich in pigments, where the concentration of ΣChlns-a in the surface (0–1 cm) layer of sediments ranged from ~130 nmol $g^{-1}$ d.w. at station F to ~320 nmol $g^{-1}$ d.w. at station E (Fig. 2). A considerably lower pigment content was determined in Drammensfjord (~35 nmol $g^{-1}$ d.w. at station A and ~60 nmol $g^{-1}$ d.w. at station B) and in Vestfjord (station C ~35 nmol $g^{-1}$ d.w.).

The concentration ranges of parent chloropigments and carotenoids in the surface (0–1 cm) sediment layer were as follows: 4–227 nmol $g^{-1}$ d.w. (chl-a), 0.2–15 nmol $g^{-1}$ d.w. (chl-b), 0.2–8.5 nmol $g^{-1}$ d.w. (chls-c), 3.5–387 nmol $g^{-1}$ d.w. (fuco), 0.5–45 nmol $g^{-1}$ d.w. (diato), 1–82 nmol $g^{-1}$ d.w. (lut) and 0–256 nmol $g^{-1}$ d.w. (β-car) (Table 2). The profiles of all pigment concentrations resembled that of the sum of chloropigments-a.

Pigment concentrations were distinctly higher in the surface (0–1 cm) layer than in the deeper sediment layers of the Gulf of Gdańsk (Fig. 2). This was not observed in the samples from the Oslofjord/Drammensfjords, where the surface layer pigment concentrations are comparable to or even lower than in the deeper layers.

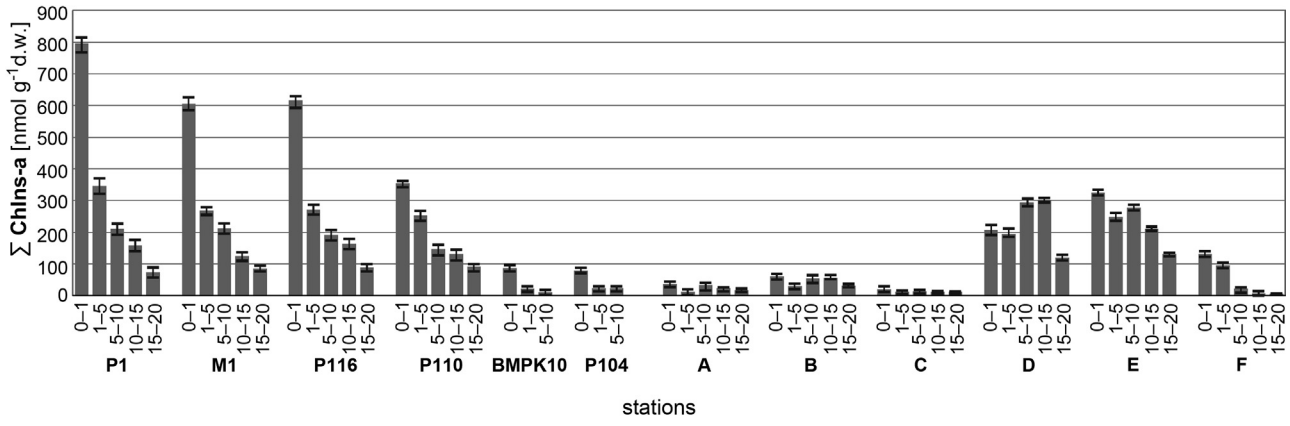


**Figure 2** Average contents [nmol $g^{-1}$ d.w.] of the sum of chloropigments-a (ΣChlns-a); $n = 2$.

**Table 2** Average contents of selected pigments [nmol $g^{-1}$ d.w.] in the surface (0–1 cm) sediment layer; $n = 2$.

| Station | Chl-*a* | Chl-*b* | Chls-*c* | Fuco | Diato | Lut | β-car |
|---|---|---|---|---|---|---|---|
| ***Gulf of Gdańsk*** | | | | | | | |
| P1 | 227.4 | 14.8 | 8.5 | 386.6 | 45.0 | 81.7 | 255.8 |
| M1 | 164.3 | 12.3 | 5.7 | 204.1 | 36.2 | 76.2 | 207.9 |
| P116 | 194.3 | 13.1 | 6.7 | 268.3 | 34.9 | 67.3 | 184.7 |
| P110 | 176.9 | 7.4 | 6.5 | 144.4 | 12.8 | 29.1 | 67.6 |
| BMPK10 | 35.3 | 1.4 | 1.8 | 27.6 | 1.4 | 4.3 | 14.3 |
| P104 | 32.9 | 1.4 | 1.8 | 41.1 | 4.4 | 3.4 | 13.1 |
| ***Oslofjord/Drammensfjord*** | | | | | | | |
| A | 9.3 | 1.1 | 0.2 | 3.5 | 0.5 | 4.6 | 8.0 |
| B | 22.3 | 1.6 | 0.5 | 12.6 | 3.5 | 10.0 | 19.5 |
| C | 4.3 | 0.2 | 0.3 | 8.9 | 0.9 | 1.3 | 0.0 |
| D | 83.9 | 5.1 | 3.1 | 79.3 | 23.0 | 24.5 | 89.0 |
| E | 79.4 | 5.3 | 5.1 | 90.8 | 34.3 | 27.2 | 119.6 |
| F | 32.5 | 1.5 | 2.3 | 23.5 | 18.3 | 21.3 | 104.1 |

## 3.2. Physicochemical parameters of seawater

All the stations in the Oslofjord/Drammensfjord were characterized by a much higher salinity both in the water column and in the near-bottom water, and the halocline was at a shallower depth, than in the Gulf of Gdańsk (Table 1, Appendix 2). The temperature of the near-bottom water was higher and more evenly distributed in the Norwegian fjords than in the Gulf of Gdańsk. In the Gulf of Gdańsk higher temperatures were recorded at the stations in the Gdańsk Deep than at the shallower stations, in Puck Bay. There was anoxia in the near-bottom water at one station (P116, oxygen concentration – 0.5 mg $L^{-1}$) in the Gdańsk Deep, while three other stations in the Gdańsk Deep (P1, M1 and P110) had low oxygen concentration (3.5–5.4 mg $L^{-1}$). Only two shallow-water stations (BMPK10 and P104) had a high oxygen concentration. All but one of the stations in the Norwegian fjords exhibited anoxia/hypoxia. The exception was station C (Vestfjord) with the higher oxygen concentration (9.2 mg $L^{-1}$) (Table 1).

## 3.3. Sediment characteristics

### 3.3.1. $^{210}$Pb – sediment accumulation rates

$^{210}Pb_{tot}$ in the surface (0–1 cm) layer varied significantly depending on sampling region – from ~82 to ~650 Bq $kg^{-1}$ in the Gulf of Gdańsk and from ~120 to ~280 Bq $kg^{-1}$ in the Oslofjord (Appendix 3). The $^{210}Pb_{tot}$ values for the Gulf of Gdańsk cores concur with those recently reported by several authors (Suplińska and Pietrzak-Flis, 2008; Zaborska et al., 2014; Zalewska et al., 2015). The $^{210}Pb_{tot}$ results for Norwegian fjord sediments are also comparable to those obtained by other authors (Dolven and Alve, 2010; Smittenberg et al., 2005; Zegers et al., 2003).

Most of the $^{210}Pb_{tot}$ activity concentration profiles showed an exponential decrease along the core, although sediment mixing and/or extremely low net sedimentation was apparent at some stations. The $^{210}Pb_{tot}$ profiles of Norwegian fjord sediments (C, D, F) indicated disturbances in the surface sediments (3–5 cm) caused by human or animal activity and/or by currents (Table 1; Appendix 3). Similar $^{210}Pb_{tot}$ profiles were reported by Dolven and Alve (2010) and Smittenberg et al. (2005) for the Oslofjord sediments. According to those authors these sediments exhibited numerous disturbances as well as mixing in both the upper and lower parts of the cores. In the fjords (this work) there was no mixing at three stations: A, B and E. In the Gdańsk Deep no sediment mixing was found to have occurred at three stations (P1, M1, P116), while there was slight (3 cm) mixing at station P110 and intensive mixing at the shallow-water stations BMPK10 and P104 down to 12 cm depth (Table 1).

The stations in the Gdańsk Deep were characterized by intermediate linear accumulation rates (LARs) ranging from 0.14 cm $y^{-1}$ (station P116) to 0.17 cm $y^{-1}$ (station P110) (Table 1). The LAR was not calculated for station P104 in Puck Bay, since the $^{210}Pb_{tot}$ activity concentration profile did not decrease with depth there. At station BMPK10, the $^{210}Pb_{tot}$ profile showed very little decrease with depth, and it was difficult to calculate the LAR (no accumulation at all or no more than 0.07 cm $y^{-1}$). The last two stations were located in relatively shallow areas (30–50 m), where the coarser sediment fraction prevailed as a result of local currents transferring fine particulate matter to deeper areas. LARs ranging from 0.05 cm $y^{-1}$ (station F) to 0.18 cm $y^{-1}$ (station E) were measured for eastern Oslofjord (Bunnefjord) sediments. Station C in the western Oslofjord (Vestfjord) displayed the second highest LAR of 0.20 cm $y^{-1}$. In the Drammensfjord, the LARs were 0.11 cm $y^{-1}$ (station A) and 0.27 cm $y^{-1}$ (station B) (Table 1).

The LARs obtained in this study for the Gdańsk Deep stations (0.14–0.17 cm $y^{-1}$) agree with the values reported for this region (0.1–0.24 cm $y^{-1}$, Pempkowiak, 1991; Suplińska and Pietrzak-Flis, 2008; Zaborska et al., 2014; Zalewska et al., 2015). Few data on sediment accumulation rates in the Oslofjord have been reported. Pau and Hammer (2013) estimated accumulation rates in the northern part of the Vestfjord. They report LARs from 0.04 to 0.18 cm $y^{-1}$, depending on the bottom depth (with higher rates in deeper areas). Their results generally agree well with the LARs obtained in this work (from 0.5 to 0.20 cm $y^{-1}$). Dolven and Alve (2010) and Dolven et al. (2013) studied both parts of the Oslofjord. They found very large and variable accumulation rates of 0.1–0.3 cm $y^{-1}$ in the northern Bunnefjord and even larger rates of *ca* 0.4 cm $y^{-1}$ in its southern part. Extremely large LARs of 1.3–2.5 cm $y^{-1}$ and very high fluxes of $^{210}$Pb have been reported for the southern Vestfjord (Dolven and Alve, 2010). In the Drammensfjord, sediment accumulation rates from 0.15 to 0.25 cm $y^{-1}$ were measured by Smittenberg et al. (2005) and Huguet et al. (2007), which is in agreement with the results of this work.

### 3.3.2. Grain size

The grain size fractions are presented as the sum of sand (>0.063 mm), silt (from 0.063 to 0.004 mm) and clay (<0.004 mm). The sediments richest in sand were at stations P104 and BMPK10 (Table 3; Appendix 4). The silt fractions were the largest at the stations in the Gdańsk Deep and the eastern Oslofjord (Bunnefjord). The content of the smallest grain size (<0.004 mm) fraction was the highest in the Drammensfjord and the Vestfjord (station C).

### 3.3.3. Carbon and nitrogen

Organic carbon concentrations in sediments of the Gdańsk Deep were by far the highest of all the samples studied

(5–8%) (Table 3; Appendix 4). The lowest concentrations were in Puck Bay (BMPK10, P104) (1–3.4%). The organic carbon content in the samples from the Norwegian fjords were in between those values: the highest content was for stations in the Bunnefjord – from 1.5 to 4.5% at D and E, and 7% in the 1–5 cm layer of sediments at F. The values were lower in the Drammensfjord (1.4–2.5%). The $\delta^{13}C$ values measured for sediment cores ranged from −26.9‰ to −20.5‰. The distinctly higher values were measured for four (C, D, E, F) sediment cores collected from the Oslofjords (from −22.3‰ to −20.5‰). The $\delta^{15}N$ values measured for the Baltic Sea sediments ranged from ~2‰ to 3.7‰, while for the Norwegian fjord sediments from ~1.6‰ to 3.5‰ (Appendix 4).

## 4. Discussion

### 4.1. Environmental conditions and the pigment record in sediments

Chloropigments-a content in recent sediments is a good, well-documented indicator of productivity in both lacustrine and marine sediments (e.g. Kowalewska et al., 2004; Leavitt and Hodgson, 2001; Louda et al., 2000; Szymczak-Żyła and Kowalewska, 2007; Villanueva and Hastings, 2000). The method based on determining chloropigments-a in sediments (calculated per dry weight of sediment, not normalized to organic carbon) yields the average eutrophication picture for an area. The pigment contents in the sediments discussed in this paper (Fig. 2, Table 2) are in accordance with previous studies of the Gulf of Gdańsk. Szymczak-Żyła et al. (2011) reported that the average sum of chloropigments-a (ΣChlns-a) in the Gdańsk Deep sediments was ~400 nmol $g^{-1}$ d.w. (in 0–1 cm). In that work the highest value (~900 nmol $g^{-1}$ d.w.) was recorded in May 2003. This was a consequence of the intense algal bloom (Chl-a ~20 mg $m^{-3}$) that had taken place in April 2003 (IMGW, 2009). The high value of pigments determined in the surface (0–1 cm) sediment layer (ΣChlns-a ~800 nmol $g^{-1}$ d.w.) of the Gdańsk Deep in April 2014 (this paper) indicates that productivity in this area is still high. The concentration of pigments in sediments depends not only on primary production but also other factors influencing sedimentation, hydrological and depositional conditions. Taking into account the concentration of pigments (ΣChlns-a) in the surface (0–1 cm) sediment layer and sediment characteristics, including organic carbon and total nitrogen content, grain size distribution and near-bottom water parameters (salinity, temperature and oxygen concentration), hierarchical cluster analysis (dendrogram of the sampling stations – Fig. 3a) showed that sediments in the Gdańsk Deep (stations P1 and P110, M1 and P116) differ from those at the other Gulf of Gdańsk stations, i.e. those in Puck Bay (BMPK10, P104). Furthermore, the Gulf of Gdańsk stations differ significantly from those in the Oslofjord/Drammensfjord area (Fig. 3a). Principal Component Analysis (PCA) was applied to check these results and to find the most significant factor affecting the pigment concentration in the sediments of the study areas (Fig. 3b and c). The PCA data matrix model explains over 90% of the total variations with the first two principal components. The considerably lower pigment content in the Puck Bay sediments corresponds with the good oxic conditions in the near-bottom water and the high content of sand fraction (Fig. 3b and c), which is due to the strong water currents in this area. A high positive and significant correlation of ΣChlns-a with the percentage of organic carbon ($r = 0.92$, $p < 0.05$) and the percentage of the fine sediment fraction <0.063 mm ($r = 0.88$, $p < 0.05$) was obtained for all the samples from the Gulf of Gdańsk. Shankle et al. (2002) has observed that sediment grain size is an important factor affecting pigment content in sediments. The pigment-rich Gdańsk Deep sediments contain large quantities of organic carbon, total nitrogen and silt fraction (Fig. 3b and c). Anoxia in the near-bottom water and sediments prevents the decomposition of organic matter and preserves pigments in the Gdańsk Deep sediments. The pigment concentration correlates negatively with the oxygen content in the near-bottom water ($r = -0.9$, $p < 0.05$), which

**Table 3** Sediment characteristics: grain size, organic carbon ($C_{org}$), total nitrogen ($N_{tot}$), stable carbon ($\delta^{13}C$) and nitrogen ($\delta^{15}N$) content in the surface (0–1 cm) sediment layer.

| Station | Grain size [%] | | | $C_{org}$ [%] | $N_{tot}$ [%] | $\delta^{13}C$ [‰] | $\delta^{15}N$ [‰] |
|---|---|---|---|---|---|---|---|
| | Sand >0.063 mm | Silt 0.063–0.004 mm | Clay <0.004 mm | | | | |
| ***Gulf of Gdańsk*** | | | | | | | |
| P1 | 0.8 | 75.8 | 23.4 | 8.13 | 1.14 | −25.3 | 3.72 |
| M1 | 0 | 73.5 | 26.5 | 6.90 | 0.94 | −25.4 | 2.51 |
| P116 | 0 | 73.2 | 26.8 | 7.22 | 1.02 | −25.2 | 2.21 |
| P110 | 1.4 | 76.5 | 22.1 | 6.65 | 0.98 | −25.2 | 2.52 |
| BMPK10 | 53.9 | 35.4 | 10.7 | 3.36 | 0.37 | −25.2 | 2.46 |
| P104 | 64.1 | 28.7 | 7.2 | 1.62 | 0.22 | −25.2 | 3.52 |
| ***Oslofjord/Drammensfjord*** | | | | | | | |
| A | 0 | 51.9 | 48.1 | 2.03 | 0.15 | −25.9 | 2.75 |
| B | 0 | 54.8 | 45.2 | 1.60 | 0.15 | −25.2 | 1.23 |
| C | 0 | 54.1 | 45.9 | 2.97 | 0.23 | −21.7 | 1.02 |
| D | 0 | 67.5 | 32.5 | 2.58 | 0.33 | −22.0 | 2.29 |
| E | 0 | 63.8 | 36.2 | 1.58 | 0.19 | −22.0 | 2.99 |
| F | 0 | 63.9 | 36.1 | 3.74 | 0.33 | −21.5 | 2.32 |

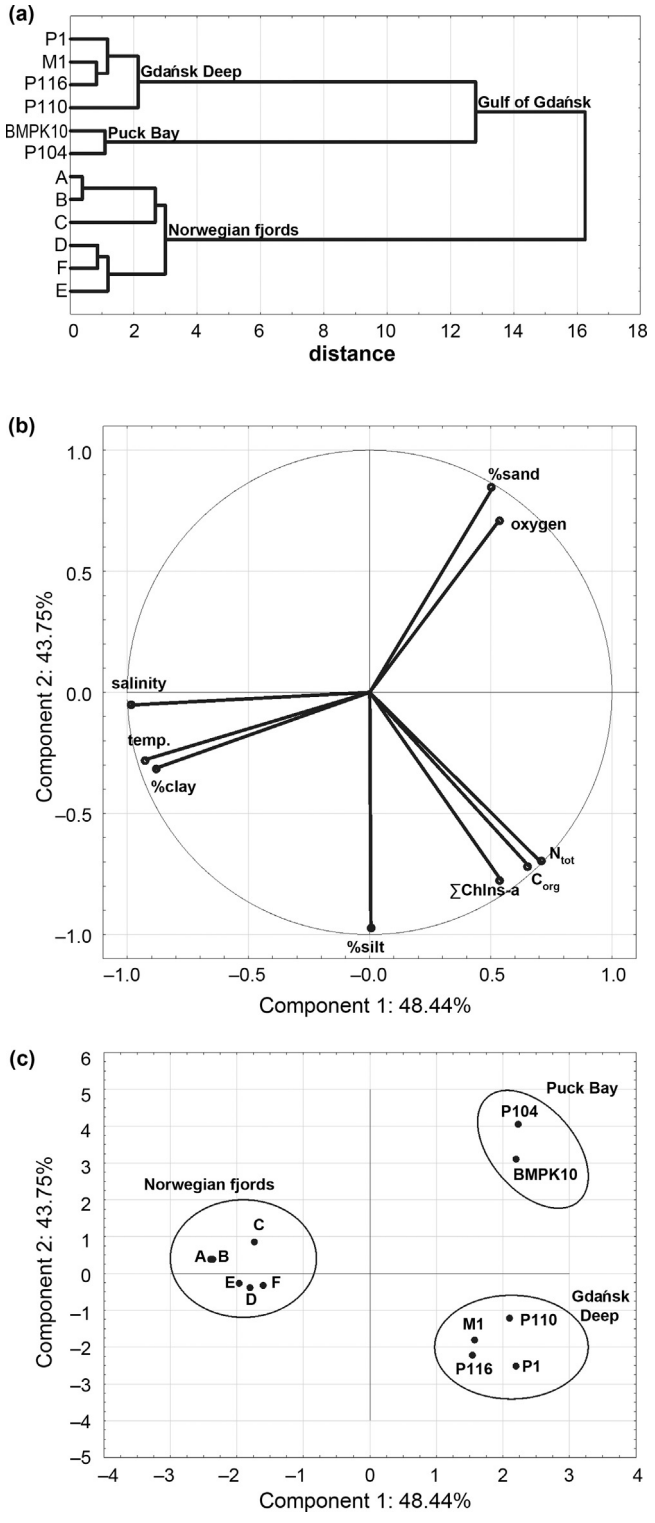


**Figure 3** Results of the statistical analysis: (a) hierarchical dendrogram of sampling stations (cluster analysis — Ward's method, Euclidean distance) based on characteristics of the surface (0—1 cm) sediment layer: chloropigments-a content (∑Chlns-a), organic carbon ($C_{org}$) and total nitrogen ($N_{tot}$) content, grain size (%sand, %silt, %clay) and near-bottom water parameters (salinity, temperature and oxygen concentration); (b) scatter plot of principal component loading by individual variables; (c) scatter plot of principal component object scores by sampling sites.

is in agreement with the observations of other authors that oxygen is one of the most significant factors affecting the pigment concentration in sediments (Bianchi et al., 2000; Reuss et al., 2005; Villanueva and Hastings, 2000). Gulf of Gdańsk sediments differ significantly from the Oslofjord/Drammensfjord sediments (Fig. 3a and c), which have a higher clay fraction content and higher near-bottom water salinity and temperature. The near-bottom waters of most of the Norwegian fjord areas studied here, except Vestfjord, were anoxic/hypoxic (Table 1). In the Oslofjord/Drammensfjord areas studied, only the sediments of the Bunnefjord were rich in pigments, while in the Drammensfjord, despite the anoxic/hypoxic conditions, there were far fewer pigments in the sediments (Fig. 2, Table 2). This is indicative of this area's low productivity, or that a large proportion of pigments is degraded to colourless products in the water column. All this demonstrates that chloropigments-a in surface sediments are a reflection of the eutrophication of the basin.

Pigment concentrations are distinctly higher in the surface (0—1 cm) layer, which might have been formed in the past 5—7 years, than in deeper sediment layers of the Gulf of Gdańsk (Fig. 2). This tallies with our previous observations (Szymczak-Żyła and Kowalewska, 2007) and those of other authors (Stephens et al., 1997; Villanueva and Hastings, 2000) that the pigment content decreases the fastest in the surface sediment layer. In the deeper layers pigment transformation proceeds much more slowly, especially in anoxic basins. However, this was not observed in the samples from the Oslofjord/Drammensfjord, where pigment concentrations in the surface layer are comparable to or even lower than in the deeper layers (Fig. 2). This suggests decreasing primary production and that conditions in the Norwegian fjords are more propitious to pigment preservation in sediments. The topography of the fjords being what it is (see Section 2.1.2), the pigments remain undecomposed for many years. In the Gulf of Gdańsk vertical mixing and bottom-water exchange is limited but not within the same range as in the fjords.

Sediments differed not only in the content of pigments but also in the percentage of particular chlorophyll-a derivatives in their sum. Our previous observations from Gulf of Gdańsk studies showed that the percentage of particular sedimentary chlorophyll-a derivatives may be taken to be markers of syn- and post-depositional environmental conditions (Szymczak-Żyła et al., 2011). Chlorophyll-a allomers are characteristic of sediments originating from an oxygenated coastal zone. Chlorophyll-a and pheophorbides-a indicate the presence of comparatively fresh material (Louda et al., 1998, 2002). Pyropheophorbides-a are mainly a marker for grazing by zooplankton and/or zoobenthos (Bianchi et al., 1998, 2002a, b; Head and Harris, 1996; Szymczak-Żyła et al., 2006). Finally, pyropheophytin-a and the steryl derivatives occur mainly in anoxic sediments (Chen et al., 2001; Louda et al., 2000; Shankle et al., 2002; Szymczak-Żyła et al., 2011; Villanueva and Hastings, 2000). Based on these observations, we named indicators of processes ('grazing') and environmental conditions ('oxic' and 'anoxic') (Fig. 4a—c). There was a high (almost 20%) percentage of 'grazing' chlorophyll-a derivatives (pyropheophorbides-a) in the Puck Bay sediments (stations BMPK10 and P104), which corresponds with the sediment mixing results. The $^{210}Pb_{tot}$ profile in the sediments indicated intensive mixing at the shallow-water Puck Bay stations down to 12 cm depth (Table 1). The pigment results

presented in this paper suggest that the sediments there were probably disturbed by animal activity. In the Norwegian fjords the sediments at stations C, D, F were also mixed. The high percentage of 'grazing' derivatives at stations C and F suggests that benthic activity is responsible for sediment mixing in these areas. Indeed, a large biomass of benthic animals (Polychaetes) was observed already during sampling at station F (Appendix 1). However, at station A, where the sediments were not mixed, the high percentage of 'grazing' derivatives suggests intense zooplankton activity in the water column. Two stations with mixed sediments (P110 and D) did not have a high proportion of 'grazing' indicators. This can be explained by mixing by abiotic factors (e.g. currents) at these sampling sites.

The maximum percentage of chlorophyll-*a*-allomers, which form under oxic conditions, ('oxic' indicator) was in the sediments from the Puck Bay stations and in Vestfjord (station C), while derivatives characteristic of anoxic conditions (pyropheophytin-a and the steryl chlorin esters – 'anoxic' indicator) were found in sediments from the Gdańsk Deep and the remaining Norwegian fjord stations (A, B, D, E, F) (Fig. 4b and c). This is indicative of oxic/anoxic conditions in the near-bottom water (Table 1).

## 4.2. Freshwater and seawater influences

Eutrophication occurs in coastal areas impacted by inorganic nutrient loads, by nutrients bound to organic matter and restricted water exchange. The traditional proxies used for determining organic matter sources are the carbon-to-nitrogen ratio (C $N^{-1}$) and the stable isotopes of these two elements ($\delta^{13}C$, $\delta^{15}N$) (Fontugne and Jouanneau, 1987; Maksymowska et al., 2000; Szczepańska et al., 2012), but the ranges characteristic of different organic matter sources are broad and frequently overlap (Cravotta, 1997; Schulz and Zabel, 2006). The use of these three proxies for sediments often yields different information, so that determining the origin of organic matter is difficult. The use of $\delta^{15}N$ as an indicator for sediments is particularly ambiguous, because nitrogen is fractionated in the trophic network rather than during photosynthesis. The typical nitrogen isotopic composition ($\delta^{15}N$) of marine phytoplankton in temperate seas varies from 3.0‰ to 12.0‰. Freshwater phytoplankton isotopic signatures mentioned in the literature have $\delta^{15}N$ around 5‰ (Schulz and Zabel, 2006).

The C $N^{-1}$ results for five (P1, M1, P116, P110, P104) of the six sediment cores from the Gulf of Gdańsk (range from ~8 to ~10) indicate a mixed marine and terrigenous origin of the sedimentary organic matter (Szczepańska et al., 2012). The exception is station BMPK10, for which the measured values are higher (from 10.5 to 13.4), indicating a more terrigenous origin. The $\delta^{13}C$ values (from −25.7‰ to −25‰) indicate that the organic matter in all the cores consists of a mixture of terrestrial and marine matter. This is in agreement with the conclusion drawn from the C $N^{-1}$ ratio and data published earlier for this area (Szczepańska et al., 2012; Voss et al., 2000). The $\delta^{15}N$ values measured for the Baltic Sea sediments ranged from ~2‰ to 3.7‰. The stable nitrogen signature recorded in this study is similar to that of Voss et al. (2000), who noted that this signature is indicative of marine phytoplankton. This observation thus contradicts the C $N^{-1}$ ratio and $\delta^{13}C$ results.

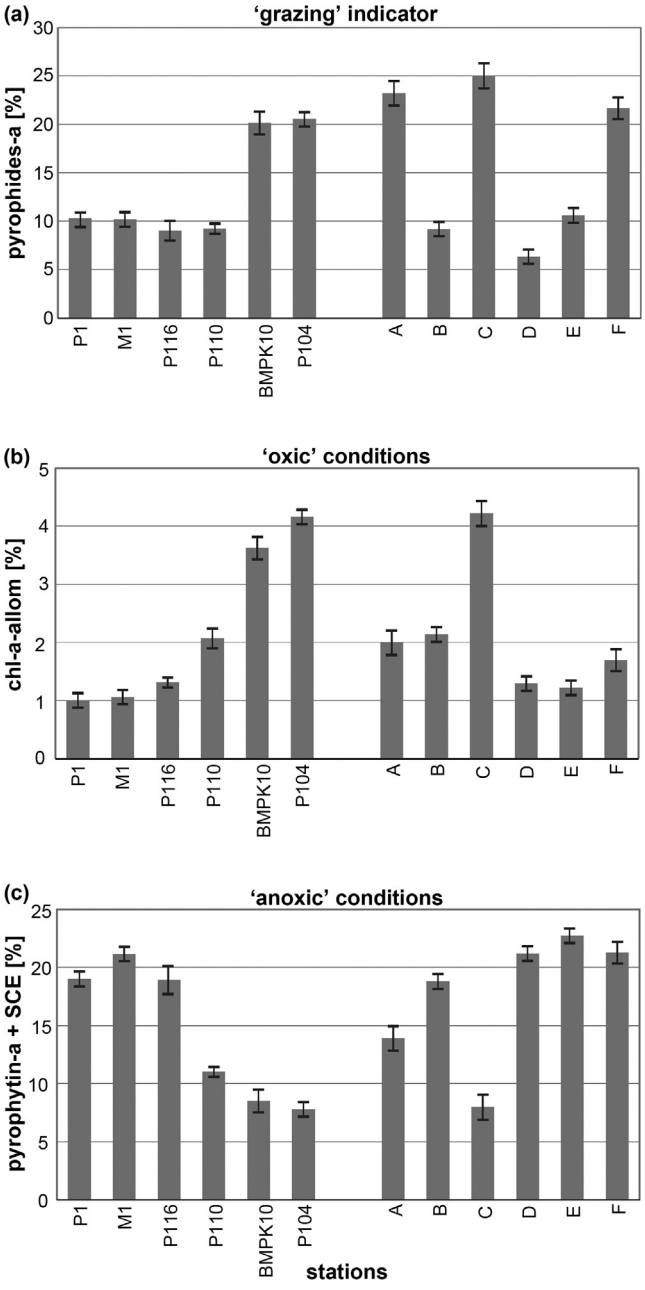


**Figure 4** Average percentage of particular chlorophyll-*a* derivatives in the sum of chloropigments-a: (a) pyropheophorbides-a ('grazing' indicator); (b) chlorophyll-*a*-allomers ('oxic' indicator); (c) sum of pyropheophytin-a and steryl chlorin esters ('anoxic' indicator); $n = 2$.

The C $N^{-1}$ ratios encountered in the cores from the Norwegian fjords ranged from ~9 to ~19. These values were close to those obtained by other authors for the same area (Smittenberg et al., 2005). The highest values were measured for the sediment core collected from station A and are indicative of the terrigenous provenance of the organic matter. The C $N^{-1}$ ratio for the sediment cores from stations B and C ranges from 12.6 to 14.8, indicating that the organic matter is a mixture of terrestrial and marine material. The lowest ratios (from 9 to 12) were for sediments at stations D and E and was closer to the values for freshly deposited marine phytoplankton (Kenney et al., 2010). The $\delta^{13}C$ values measured for

sediment cores collected from the Oslofjord (Stations C, D, E, F) (from −22.3‰ to −20.5‰; Appendix 4) point to the marine provenance of the organic matter. The values for the sediment cores from Drammensfjord (A and B) are lower, from −26.9‰ to −25.0‰, which indicates that the organic matter in those sediments is a mixture of terrestrial and marine materials. The results for sediment cores A and B are similar to the results obtained by other authors (Huguet et al., 2007; Smittenberg et al., 2005), but differ from the conclusion for station A based on the C $N^{-1}$ ratio. The $\delta^{15}N$ values measured for the Norwegian fjord sediments ranged from 1.6‰ to 3.5‰ (Appendix 4), indicating that the organic matter there originated from phytoplankton or terrestrial organisms (Schulz and Zabel, 2006). All the cores display a great variation of $\delta^{15}N$ with depth, demonstrating the varying origin and fate of organic matter, especially in the Norwegian fjord. Generally, in our work $\delta^{15}N$ values are smaller in the fjord sediments, especially in the Drammensfjord, than in the Gulf of Gdańsk sediments; this can be explained by the different main sources of organic matter for these two water areas, maybe because of the higher input of sewage (Cravotta, 1997) or undecomposed macrophyta (Bucholc et al., 2014; Kenney et al., 2010) which characterize the higher $\delta^{15}N$, in the Gulf of Gdańsk.

Having the above in mind, the chlorophyll-b and chlorophylls-c to sum of chloropigments-a ratios (Chl-b/ΣChlns-a; Chls-c/ΣChlns-a) were validated as markers of riverine and marine provenance of organic matter, respectively. These ratios depend on the initial concentrations of the parent (Chl-b and Chls-c) pigments in the matter undergoing sedimentation and their stability. Even though chlorophyll-*b* and -*c* are less stable than chlorophyll-*a* (Leavitt and Hodgson, 2001), these markers can enrich our knowledge about the origin of organic matter. Previous studies of southern Baltic Sea sediments have shown that the ratios of chlorophylls-c and -b to chlorophyll-a depends on the proportions of diatoms and green algae in the total Baltic phytoplankton. Chlorophyll-c/chlorophyll-a ratios were higher in samples from marine areas (Kowalewska et al., 1996). The authors suggested that the above ratios in the sediment can be used as an indicator for fresh and marine organic matter in the adjacent waters.

The results of this work indicate that the Chl-b/ΣChlns-a ratio was higher in the Gdańsk Deep (stations P1–P116) and Drammensfjord (stations A and B) than in the other sediments studied (Fig. 5a). Both areas are strongly influenced by riverine water. The Gdańsk Deep is a sink for organic matter carried by the River Wisła into the Gulf of Gdańsk (Jankowski

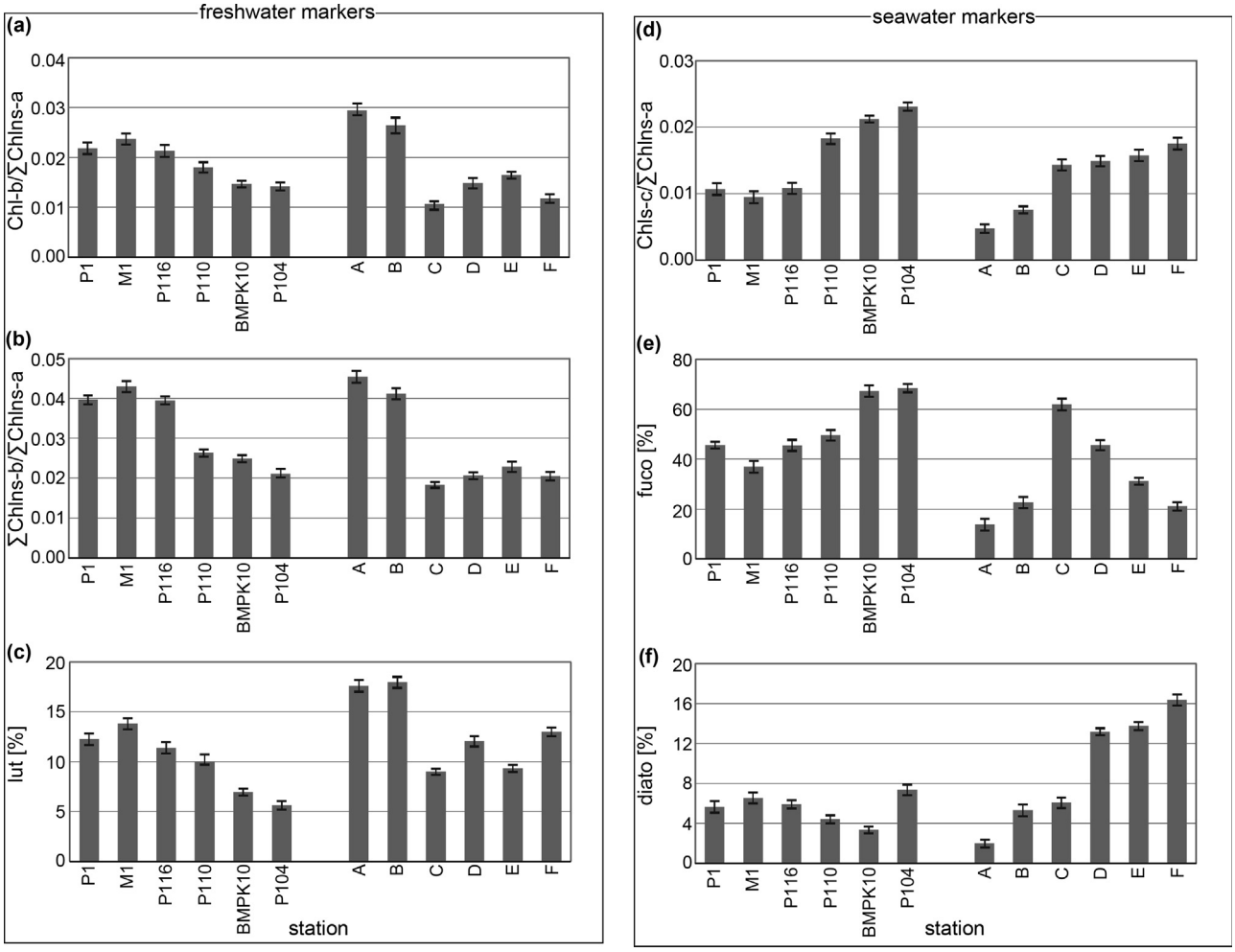


**Figure 5** Pigment ratios: (a) chlorophyll-b to chloropigments-a ratio (Chl-b/ΣChlns-a); (b) sum of chloropigments-b to chloropigments-a ratio (ΣChlns-b/ΣChlns-a); (c) percentage of lutein in the sum of carotenoids (%lut); (d) chlorophylls-c to chloropigments-a ratio (Chls-c/ΣChlns-a); (e) percentage of fucoxanthin in the sum of carotenoids (%fuco); (f) percentage of diatoxanthin in the sum of carotenoids (%diato).

and Staśkiewicz, 1994), while Drammensfjord accumulates in sediments freshwater organic matter from the River Drammen (Fig. 1). The highest chl-b/ΣChlns-a ratio was recorded in sediments at station A (Drammensfjord), located close to the mouth of the river, where blooms of green algae *Botryococcus brauni* (Kützing) were observed (Smittenberg et al., 2005). The high correlation between the percentage of lutein in the sum of carotenoids (%lut) and chl-b/ΣChlns-a ($r = 0.7$ and 0.87, $p < 0.05$) for the Gulf of Gdańsk and the Norwegian fjords, respectively, showed that even though lutein is more stable than chlorophyll-b and is recognized as a marker of green algae (Leavitt and Hodgson, 2001), the Chl-b/ΣChlns-a ratio is also a good marker of green algal biomass, which is more abundant in freshwater environments than that of diatoms and dinoflagellates (Bellinger and Sigee, 2010). In sediment samples with a large proportion of chlorophyll-b derivatives, such as the Gulf of Gdańsk (Fig. 5b and c), the higher correlation between %lut and the ΣChlns-b/ΣChlns-a (the sum of chlorophyll-b and its derivatives to the sum of chloropigments-a) ratio ($r = 0.98$, $p < 0.05$) suggests that it is an even better marker than chl-b/ΣChlns-a.

The highest Chls-c/ΣChlns-a ratio was recorded at stations BMPK10 and P104 in the Gulf of Gdańsk and in the Oslofjord samples (stations C–F) (Fig. 5d). There is a high correlation between Chls-c/ΣChlns-a and the percentage of fucoxanthin (the pigment occurring mainly in diatoms (Jeffrey and Vesk, 1997)) in the sum of carotenoids (%fuco) for the Gulf of Gdańsk sediments ($r = 0.92$, $p < 0.05$) and a high correlation with the percentage of diatoxanthin (%diato) for the Oslofjord ($r = 0.87$, $p < 0.05$) (Fig. 5e and f). This suggests that the diatoms are the main source of chlorophylls-*c* in the Gulf of Gdańsk sediments, while in the Oslofjord, besides diatoms, also other marine species containing diatoxanthin such as dinoflagellates. The exception there was station C (Vestfjord) with the high percentage of fucoxanthin (~60%, Fig. 5e). Both phytoplankton groups (diatoms and dinoflagellates) contain not only chlorophyll-a but also chlorophylls-c (Jeffrey and Vesk, 1997). These groups of phytoplankton, though present in both sea- and freshwater, occur in the greatest proportions in waters of seas and oceans, especially in the temperate zones (Sverdrup and Armbrust, 2008). The Chls-c/ΣChlns-a ratio in sediments, proposed in this paper, could be a marker of seawater influences.

Principal Component Analysis (PCA) was applied to validate these results. The proxies for the 0–1 cm sediment layer, both that proposed in this work (ΣChlns-b/ΣChlns-a; Chls-c/ΣChlns-a) and the traditional one (C $N^{-1}$; $\delta^{13}C$; $\delta^{15}N$, as additional variables), were considered (Fig. 6a and b). The PCA data matrix model explains over 90% of the total variations with the first two principal components. The first principal component explains ~66% of the variations and is strongly correlated with four of the variables. It increases with increasing of ΣChlns-b/ΣChlns-a ratio and the percentage of lutein in the sum of carotenoids, and with decreasing of Chls-c/ΣChlns-a ratio and the percentage of fucoxanthin. The second principal component (~27% of the total variance) increases with increasing of percentage of diatoxanthin in the sum of carotenoids. The greatest input to organic matter in the sediments at the stations in Drammensfjord (stations A, B) is from freshwater organisms, containing chlorophyll-*b* (green algae and higher plants). The greatest input to organic matter in the sediments at the Oslofjord stations is from

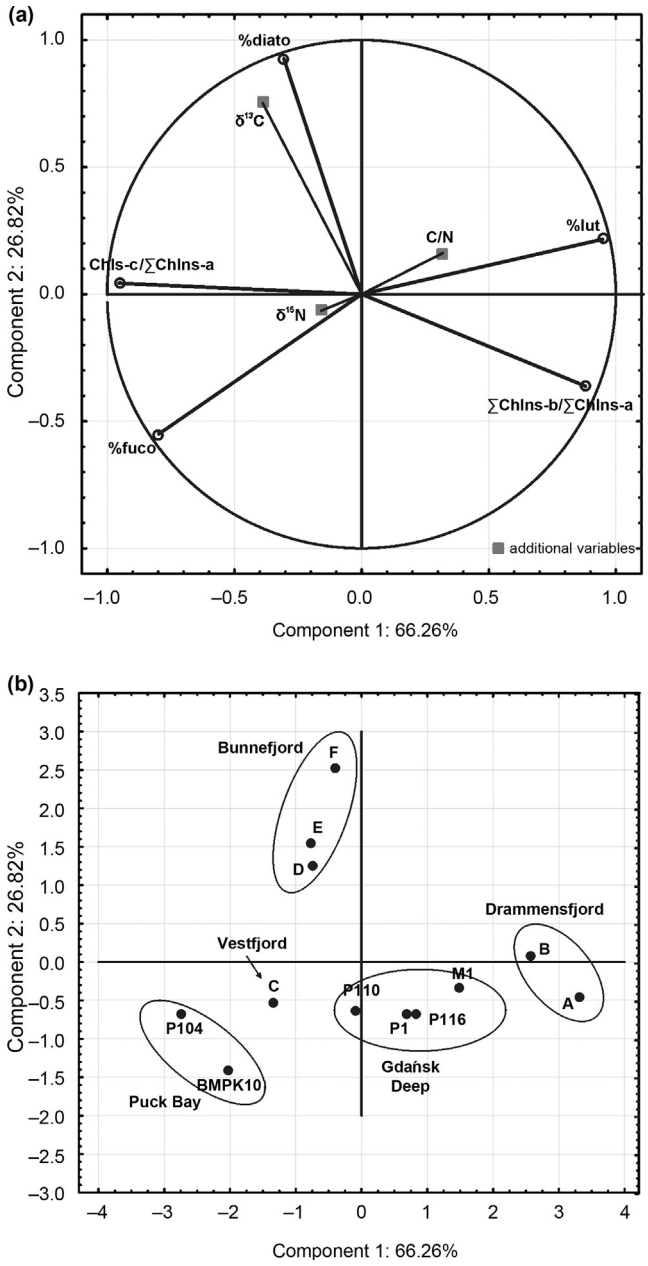


**Figure 6** Results of the statistical analysis: scatter plot of (a) principal component loading by individual variables; (b) principal component object scores by sampling sites based on proposed indicators of the source of organic matter (ΣChlns-b/ΣChlns-a; Chls-c/ΣChlns-a), percentages of particular carotenoids in the sum of carotenoids (%fuco, %lut, %diato) and traditional proxies as additional variables (C $N^{-1}$; $\delta^{13}C$; $\delta^{15}N$) for the 0–1 cm sediment layer.

marine organisms containing chlorophylls-c, such as diatoms and dinoflagellates (Fig. 6a and b). The $\delta^{13}C$ values measured for sediment cores collected from the Oslofjord are in agreement with these pigment markers. The results of this work have confirmed the previous observations for the Gulf of Gdańsk (Kowalewska et al., 1996). Chls-c/ΣChlns-a may thus be a simple marker of seawater organic matter input and ΣChlns-b/ΣChlns-a a marker of freshwater organic matter

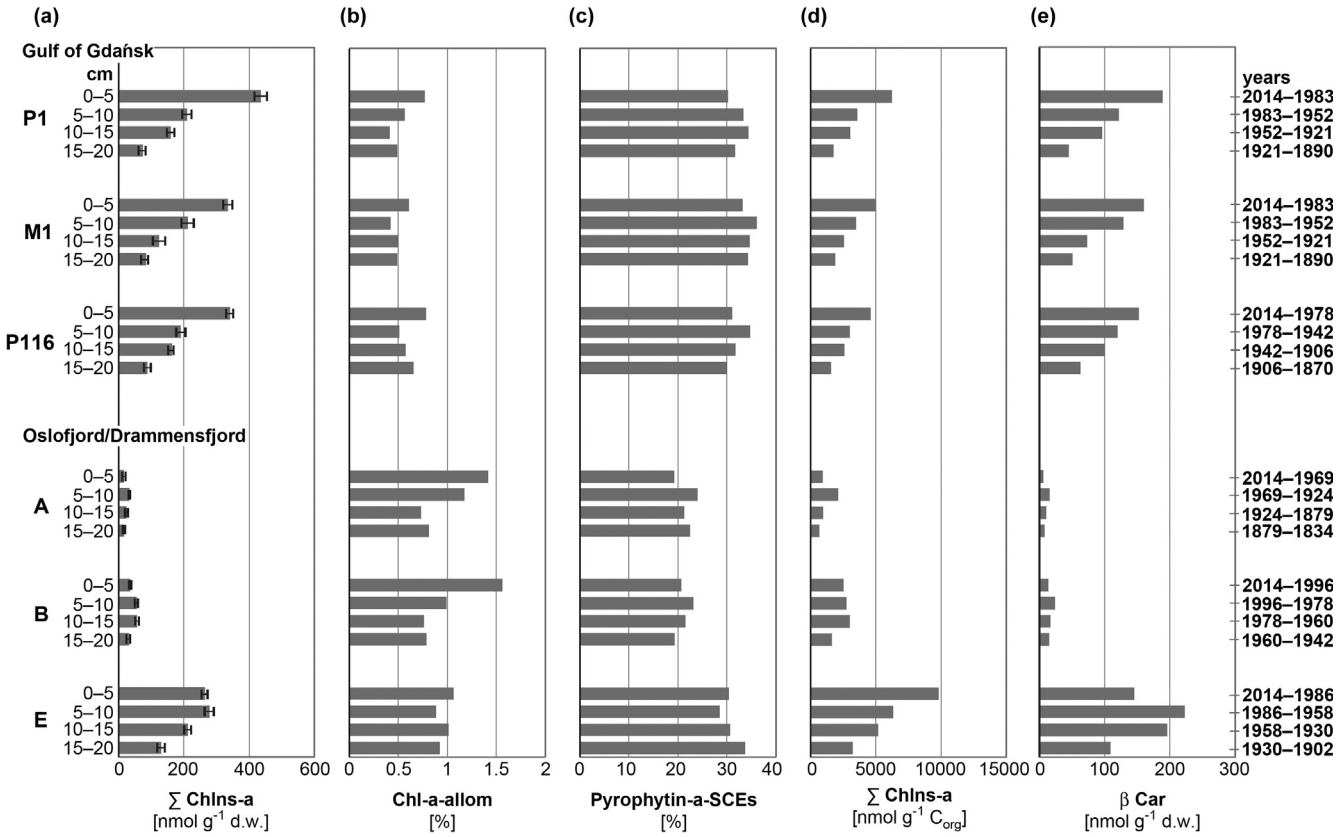


**Figure 7** Pigment content profiles for selected non-mixed sediments: (a) ΣChlns-a [nmol $g^{-1}$ d.w.]; (b) the percentage of chlorophyll-a-allomers in the sum of chloropigments-a ('oxic' indicator); (c) percentage of the sum of pyropheophytin-a and steryl chlorin esters in the sum of chloropigments-a ('anoxic' indicator); (d) ΣChlns-a [nmol $g^{-1}$ $C_{org}$]; (e) β-carotene [nmol $g^{-1}$ d.w.].

input, complementing the traditional proxies, which are often ambiguous and contradictory, especially $\delta^{15}N$ (Kenney et al., 2010; Schulz and Zabel, 2006; Torres et al., 2012).

### 4.3. Eutrophication trends

Six stations were selected for tracking eutrophication trends in the two basins. These were stations with unmixed sediments according to the $^{210}Pb$ analysis (Table 1): three in the Gdańsk Deep (P1, M1, P116), two in the Drammensfjord (A and B) and one in the Oslofjord (E). Looking at the sum of chloropigments-a profiles for these stations (Fig. 7a), one can see that there is a temporal increase in the chloropigments-a content in the sediments at all the Gdańsk Deep stations; this is particularly obvious in the surface sediments, which were formed in the last 30—40 years. The pigment contents were averaged for 0—5 cm basing on weighted mean for 0—1 cm and 1—5 cm layers. This is in agreement with other observations that eutrophication of the southern Baltic increased in the 1970s (Fleming-Lehtinen et al., 2015). In the Oslofjord/Drammensfjord maximum of chloropigments-a content corresponds to deeper layers (A, 5—10 cm; B, 10—15 cm; E, 5—10 cm), formed when the nutrient load was at its highest in the 1970s (Hess et al., 2014). This indicates a decrease in eutrophication in the past 30—40 years. Moreover, one can see that allo-chlorophyll-*a* derivatives forming in oxic conditions (Fig. 7b) take minimum values in the sediments accumulated during the 1970s, and in general are lower in the Gulf of Gdańsk than in the Oslofjord/Drammensfjord. The derivatives preserved in old sediments — 'anoxic' indicators (pyropheophytin-a and steryl chlorins) — have opposite profiles to allo-chlorophylls and in general are more abundant in sediments of the Gulf of Gdańsk than in the Oslofjord/Drammensfjord, although the chloropigments-a at station E are the richest in these compounds (Fig. 7c), indicating a high level of anoxia. The sum of chloropigments-a normalized to the organic carbon content (Fig. 7d) demonstrates similar trends to those of chloropigments-a calculated to dried weight of sediments, with the exception of station E, where there is an increase in the surface 0—5 cm layer in comparison with the next 5—10 cm. This difference is obvious, as normalization of the chloropigments-a content mirrors a stage in the decomposition of pigments, not their content in the sediments. The β-carotene profiles are similar to those for chloropigments-a (Fig. 7e), which indicates that chloropigments-a, despite being less stable than β-carotene (Leavitt and Hodgson, 2001), are good markers for tracking eutrophication trends.

## 5. Conclusions

Comparison of pigments in the sediments in the two basins shows that eutrophication in the Gulf of Gdańsk has increased over the last 30—40 years but has decreased in the Oslofjord/Drammensfjord during the same period. The results presented in this paper prove that the sum of chloropigments-a in

sediments, calculated per dry weight of sediment, is a valuable measure of eutrophication in an area. The advantage of chloropigments-a over the other proxies (e.g. β-carotene) is that the percentage of particular chlorophyll-a derivatives (pyropheophorbides-a, chlorophyll-a-allomers, pyropheophytin-a and steryl chlorin esters) in the sum of chloropigments-a provide information on syn- and post-depositional environmental conditions. They are universal markers of grazing, oxic and anoxic conditions in a basin. The sum of chloropigments-b to chloropigments-a ratio (ΣChlns-b/ΣChlns-a) is a marker of freshwater organic matter input and the chlorophylls-c to chloropigments-a ratio (Chls-c/ΣChlns-a) is a marker of seawater organic matter input. When applying these markers for tracking eutrophication trends it is very important to select a suitable monitoring site, i.e. where the sediments are unmixed (laminated) and hypoxic/anoxic.

## Acknowledgements

This work was carried out within the framework of the Polish-Norwegian Research Programme operated by the National Centre for Research and Development under the Norwegian Financial Mechanism 2009—2014, grant no. 196128. M. Krajewska received funds from the Leading National Research Centre (KNOW) for the Centre for Polar Studies for the period 2014—2018. We extend our gratitude to Dr Anna Filipkowska, Dr Ludwik Lubecki, Dr Ilona Złoch and Dr Andrzej Kadłubicki of the Institute of Oceanology, PAN, Sopot, Poland, Dr Tomasz M. Ciesielski from NTNU, Trondheim, Norway and Dr Amy M.P. Oen of NGI, Oslo, Norway for their help in organizing the cruise in the Oslofjord/Drammensfjord and for their assistance with the sample collection. We also thank the crew of the 'Oceania' for their help and the very pleasant working atmosphere during the two cruises to the Gulf of Gdańsk and the Norwegian fjords. We thank Urszula Pączek, MSc, of the National Geological Institute, Marine Branch (PIG-PIB) in Gdańsk, for the grain size analysis.

## Appendix A. Supplementary data

Supplementary data associated with this article can be found, in the online version, at doi:10.1016/j.oceano.2016.08.003.

## References

Alve, E., 1991. Foraminifera, climatic change and pollution: a study of Late Holocene sediments in Drammensfjord, SE Norway. Holocene 1 (3), 243—261, http://dx.doi.org/10.1177/095968369100100306.

Alve, E., 1995a. Benthic foraminiferal responses to estuarine pollution: a review. J. Foramin. Res. 25 (3), 190—203.

Alve, E., 1995b. Benthic foraminiferal distribution and recolonization of formerly anoxic environments in Drammensfjord, southern Norway. Mar. Micropal. 25 (2—3), 169—186, http://dx.doi.org/10.1016/0377-8398(95)00007-N.

Bellinger, E.G., Sigee, D.C., 2010. Freshwater Algae. Identification and Use as Bioindicators. Wiley-Blackwell, Hoboken, 271 pp.

Bianchi, T.S., Baeur, J.E., Druffel, E.R.M., Lambert, C.D., 1998. Pyropheophorbide-*a* as a tracer of suspended particulate organic-matter from the NE Pacific continental margin. Deep-Sea Res. Pt. II 45 (4—5), 715—731, http://dx.doi.org/10.1016/S0967-0645(97)00099-4.

Bianchi, T.S., Canuel, E.A., 2011. Chemical Biomarkers in Aquatic Ecosystem. Princeton Univ. Press, 396 pp.

Bianchi, T.S., Dawson, R., Sawangwong, P., 1988. The effects of macrobenthic deposit-feeding on the degradation of chloropigments in sandy sediments. J. Exp. Mar. Biol. Ecol. 122 (3), 243—255, http://dx.doi.org/10.1016/0022-0981(88)90126-8.

Bianchi, T.S., Demetropoulos, A., Hadjichristophorou, M., Argyrou, M., Baskaran, M., Lambert, C., 1996. Plant pigments as biomarkers of organic matter sources in sediments and coastal waters of Cyprus (eastern Mediterranean). Estuar. Coast. Shelf Sci. 42 (1), 103—115, http://dx.doi.org/10.1006/ecss.1996.0008.

Bianchi, T.S., DiMarco, S.F., Cowan, J.H., Hetland, R.D., Chapman, P., Day, J.W., Allison, M.A., 2010. The science of hypoxia in the Northern Gulf of Mexico: a review. Sci. Total Environ. 408 (7), 1471—1484, http://dx.doi.org/10.1016/j.scitotenv.2009.11.047.

Bianchi, T.S., Engelhaupt, E., McKee, B.A., Miles, S., Elmgren, R., Hajdu, S., Savage, C., Baskaran, M., 2002a. Do sediments from coastal sites accurately reflect time trends in water column phytoplankton? A test from Himmerfjärden Bay (Baltic Sea proper). Limnol. Oceanogr. 47 (5), 1537—1544.

Bianchi, T.S., Johansson, B., Elmgren, R., 2000. Breakdown of phytoplankton pigments in Baltic sediments: effects of anoxia and loss of deposit-feeding macrofauna. J. Exp. Mar. Biol. Ecol. 251 (2), 161—183, http://dx.doi.org/10.1016/S0022-0981(00)00212-4.

Bianchi, T.S., Rolff, C., Lambert, C.D., 1997. Sources and composition of particulate organic carbon in the Baltic Sea: the use of plant pigments and lignin-phenols as biomarkers. Mar. Ecol. Prog. Ser. 156, 25—31.

Bianchi, T.S., Rolff, C., Widbom, B., Elmgren, R., 2002b. Phytoplankton pigments in Baltic Sea seston and sediments: seasonal variability, fluxes, and transformations. Estuar. Coast. Shelf Sci. 55 (3), 369—383, http://dx.doi.org/10.1006/ecss.2001.0911.

Bourgeois, S., Pruski, A.M., Sun, M.-Y., Buscail, R., Lantoine, F., Kerhervé, P., Vétion, G., Rivière, B., Charles, F., 2011. Distribution and lability of land-derived organic matter in the surface sediments of the Rhône prodelta and the adjacent shelf (Mediterranean Sea, France): a multi proxy study. Biogeosciences 8 (11), 3107—3125, http://dx.doi.org/10.5194/bg-8-3107-2011.

Bucholc, K., Szymczak-Żyła, M., Lubecki, L., Zamojska, A., Hapter, P., Tjernström, E., Kowalewska, G., 2014. Nutrient content in macrophyta collected from southern Baltic Sea beaches in relation to eutrophication and biogas production. Sci. Total Environ. 473—474, 298—307, http://dx.doi.org/10.1016/j.scitotenv.2013.12.044.

Canuel, E.A., Lerberg, E.J., Dickhut, R.M., Kuehl, S.A., Bianchi, T.S., Wakeham, S.G., 2009. Changes in sediment and organic carbon accumulation in a highly-disturbed ecosystem: The Sacramento-San Joaquin River Delta (California, USA). Mar. Pollut. Bull. 59 (4—7), 154—163, http://dx.doi.org/10.1016/j.marpolbul.2009.03.025.

Carpenter, S.R., Leavitt, P.R., Elser, J.J., Elser, M.M., 1988. Chlorophyll budgets: response to food web manipulation. Biogeochemistry 6 (2), 79—90.

Chang, F.Y., Kao, S.J., Liu, K.K., 1991. Analysis of organic and carbonate carbon in sediments. Acta Oceanogr. Taiwan 27, 140—150.

Chen, N., Bianchi, T.S., McKee, B.A., 2005. Early diagenesis of chloropigment biomarkers in the lower Mississippi River and Louisiana shelf: implications for carbon cycling in a river-dominated margin. Mar. Chem. 93 (2—4), 159—177, http://dx.doi.org/10.1016/j.marchem.2004.08.005.

Chen, N., Bianchi, T.S., McKee, B.A., Bland, J.M., 2001. Historical trends of hypoxia on the Louisiana shelf: application of pigments as biomarkers. Org. Geochem. 32, 543—561.

Conley, D.J., Björck, S., Bonsdorff, E., Carstensen, J., Destouni, G., Gustafsson, B.G., Hietanen, S., Kortekaas, M., Kuosa, H., Meier, H.E.M., Müller-Karulis, B., Nordberg, K., Norkko, A., Nürnberg, G., Pitkänen, H., Rabalais, N.N., Rosenberg, R., Savchuk, O.P., Slomp, C.P., Voss, M., Wulff, F., Zillén, L., 2009. Hypoxia-related

processes in the Baltic Sea. Crit. Rev. 43 (10), 3412—3420, http://dx.doi.org/10.1021/es802762a.

Conley, D.J., Carstensen, J., Aigars, J., Axe, P., Bonsdorff, P., Eremina, T., Haahti, B.-M., Humborg, C., Jonsson, P., Kotta, J., Lännegren, C., Larsson, U., Maximov, A., Rodriguez Medina, M., Lysiak-Pastuszak, E., Remeikaitė-Nikienė, N., Walve, J., Wilhelms, S., Zillén, L., 2011. Hypoxia is increasing in the coastal zone of the Baltic Sea. Environ. Sci. Technol. 45 (16), 6777—6783, http://dx.doi.org/10.1021/es201212r.

Cravotta III, C.A., 1997. Use of stable isotopes of carbon, nitrogen, and sulfur to identify sources of nitrogen in surface waters in the Lower Susquehanna River Basin, Pennsylvania. US Geological Survey Water Supply Paper 2497. 1—68.

Dale, B., Thorsen, T.A., Fjelisa, A., 1999. Dinoflagellate cysts as indicators of cultural eutrophication in the Oslofjord, Norway. Estuar. Coast. Shelf Sci. 48 (3), 371—382, http://dx.doi.org/10.1006/ecss.1999.0427.

Dixit, A.S., Hall, R.I., Leavitt, P.R., Quinlan, R., Smol, J.P., 2000. Effects of sequential depositional basins on lake response to urban and agricultural pollution: a palaeoecological analysis of the Qu'Appelle Valley, Saskatchewan, Canada. Freshwater Biol. 43 (3), 319—337, http://dx.doi.org/10.1046/j.1365-2427.2000.00516.x.

Dolven, J.K., Alve, E., 2010. Naturtilstanden i indre Oslofjord. Rapport No. 106. Inst. Geofag, UiO, 86 pp.

Dolven, J.K., Alve, E., Rygg, B., Magnusson, J., 2013. Defining past ecological status and in situ reference conditions using benthic foraminifera: a case study from the Oslofjord, Norway. Ecol. Indic. 29, 219—233, http://dx.doi.org/10.1016/j.ecolind.2012.12.031.

Edlund, M.B., Engstrom, D.R., Triplett, L.D., Lafrancois, B.M., Leavitt, P.R., 2009. Twentieth century eutrophication of the St. Croix River (Minnesota—Wisconsin, USA) reconstructed from the sediments of its natural impoundment. J. Paleolimnol. 41 (4), 641—657, http://dx.doi.org/10.1007/s10933-008-9296-1.

Fleming-Lehtinen, V., Andersen, J.H., Carstensen, J., Łysiak-Pastuszak, E., Murray, C., Pyhälä, M., Laamanen, M., 2015. Recent developments in assessment methodology reveal that the Baltic Sea eutrophication problem is expanding. Ecol. Indic. 48, 380—388, http://dx.doi.org/10.1016/j.ecolind.2014.08.022.

Fontugne, M.R., Jouanneau, J.M., 1987. Modulation of the particulate organic carbon flux to the ocean by a macrotidal estuary — evidence from measurements of carbon isotopes in organic matter from the Gironde system. Estuar. Coast. Shelf Sci. 24 (3), 13—47, http://dx.doi.org/10.1016/0272-7714(87)90057-6.

Goldberg, E.D., 1963. Geochronology with lead-210. In: Radioactive Dating. IAEA, Vienna, 121—131.

Harmon, T.S., Smoak, J.M., Waters, M.N., Sanders, C.J., 2014. Hydrologic fragmentation-induced eutrophication in Dove Sound, Upper Florida Keys, USA. Environ. Earth Sci. 71 (10), 4387—4395, http://dx.doi.org/10.1007/s12665-013-2832-y.

Harris, P.G., Zhao, M., Rosell-Melé, A., Tiedemann, R., Sarnthein, M., Maxwell, J.R., 1996. Chlorin accumulation rate as a proxy for quaternary marine primary productivity. Nature 383 (6595), 63—65, http://dx.doi.org/10.1038/383063a0.

Head, E.J.H., Harris, L.R., 1996. Chlorophyll destruction by *Calanus* spp. grazing on phytoplankton: kinetics, effects of ingestion rate and feeding history, and a mechanistic interpretation. Mar. Ecol. Prog. Ser. 135 (1—3), 223—235.

Hedges, J.I., Keil, R.G., 1995. Sedimentary organic matter preservation: an assessment and speculative synthesis. Mar. Chem. 49 (2—3), 81—115, http://dx.doi.org/10.1016/0304-4203(95)00008-F.

Hedges, J.I., Stern, J.H., 1984. Carbon and nitrogen determinations of carbonate containing solids. Limnol. Oceanogr. 29 (3), 657—663.

HELCOM, 2007. Activities 2006. Overview. In: Baltic Sea Environment Proceedings No. 112.

HELCOM, 2013. Climate change in the Baltic Sea Area HELCOM thematic assessment in 2013. In: Baltic Sea Environment Proceedings No. 137.

Hess, S., Alve, E., Reuss, N.S., 2014. Benthic foraminiferal recovery in the Oslofjord (Norway): responses to capping and re-oxygenation. Estuar. Coast. Shelf Sci. 147, 87—102, http://dx.doi.org/10.1016/j.ecss.2014.05.012.

Hodgson, D.A., Vyverman, W., Verleyen, E., Sabbe, K., Leavitt, P.R., Taton, A., Squier, A.H., Keely, B.J., 2004. Environmental factors influencing the pigment composition of in situ benthic microbial communities in east Antarctic lakes. Aquat. Microb. Ecol. 37 (3), 247—263.

Huguet, C., Smittenberg, R.H., Boer, W., Sinninghe Danste, J.S., Schouetn, S., 2007. Twentieth century proxy records of temperature and soil organic matter input in the Drammensfjord, southern Norway. Org. Geochem. 38 (11), 1838—1849, http://dx.doi.org/10.1016/j.orggeochem.2007.06.015.

HYPOX Report Summary, 2016. Final Report Summary — HYPOX (In situ monitoring of oxygen depletion in hypoxic ecosystem of coastal and open seas, and land-locked water bodies). Proj. Ref. 226213, EU 2016, FP7-ENVIRONMENT, http://cordis.europa.eu/result/rcn/159559_en.html.

IMGW — Instytut Meteorologii i Gospodarki Wodnej, Jakusik, E., Krzymiński, W., Łysiak-Pastuszak, E., Zalewska, T., 2013. Bałtyk Południowy w 2012 r. Charakterystyka wybranych elementów środowiska. IMGW, PIB, Warszawa.

IMGW — Instytut Meteorologii i Gospodarki Wodnej, Miętus, M., Łysiak-Pastuszak, E., Zalewska, T., Krzymiński, W., 2009. Bałtyk Południowy w 2003 r. Charakterystyka wybranych elementów środowiska. IMGW, Gdynia, Warszawa.

Jankowski, A., Staśkiewicz, A., 1994. Prądy. In: Majewski, A., Lauer, Z. (Eds.), Atlas Morza Bałtyckiego. IMGW, Warszawa, 85—92.

Jeffrey, S.W., Mantoura, R.F.C., 1997. Development of pigment methods for oceanography: SCOR-supported Working Groups and objectives. In: Jeffrey, S.W., Mantoura, R.F.C., Wright, S.W. (Eds.), Phytoplankton Pigments in Oceanography. SCOR-UNESCO Publ., Paris, 19—36.

Jeffrey, S.W., Vesk, M., 1997. Introduction to marine phytoplankton and their pigment signatures. In: Jeffrey, S.W., Mantoura, R.F.C., Wright, S.W. (Eds.), Phytoplankton Pigments in Oceanography. SCOR-UNESCO Publishing, 37—84.

Kenney, W.F., Brenner, M., Curtis, J.H., Schelske, C.L., 2010. Identifying sources of organic matter in sediments of shallow lakes using multiple geochemical variables. J. Paleolimnol. 44 (4), 1039—1052, http://dx.doi.org/10.1007/s10933-010-9472-y.

Kowalewska, G., 1997. Chlorophyll *a* and its derivatives in recent sediments of the southern Baltic Sea collected in the years 1992—1996. Oceanologia 39 (4), 413—432.

Kowalewska, G., Wawrzyniak-Wydrowska, B., Szymczak-Żyła, M., 2004. Chlorophyll a and its derivatives in sediments of the Odra estuary as a measure of its eutrophication. Mar. Pollut. Bull. 49 (3), 148—153, http://dx.doi.org/10.1016/j.marpolbul.2004.02.003.

Kowalewska, G., Witkowski, A., Toma, B., 1996. Chlorophylls *c* in bottom sediments as markers of diatom biomass in the southern Baltic Sea. Oceanologia 38 (2), 227—249.

Kramarska, R., Smagała, S., Uścinowicz, S., 1996. Analiza porównawcza wyników badań uziarnienia osadów przy zastosowaniu laserowego miernika, Analysette 22. Archiwum OGM PIG-PIB, Gdańsk.

Leavitt, P.R., 1993. A review of factors that regulate carotenoid and chlorophyll deposition and fossil pigment abundance. J. Paleolimnol. 9 (2), 109—127, http://dx.doi.org/10.1007/BF00677513.

Leavitt, P.R., Hodgson, D.A., 2001. Sedimentary pigments. In: Smol, J.P., Birks, H.J., Last, W.M. (Eds.), Tracking Environmental Change Using Lake Sediments. Kluwer Acad. Publ., Dordrecht, 295—325.

Leavitt, P.R., Vinebrooke, R.D., Donald, D.B., Smol, J.P., Schindler, D.W., 1997. Past ultraviolet radiation environments in lakes derived from fossil pigments. Nature 388 (6641), 457—459, http://dx.doi.org/10.1038/41296.

Li, X., Bianchi, T.S., Allison, M.A., Chapman, P., Mitra, S., Zhang, Z., Yang, G., Yu, Z., 2012. Composition, abundance and age of total organic carbon in surface sediments from the inner shelf of the East China Sea. Mar. Chem. 145—147, 37—52, http://dx.doi.org/10.1016/j.marchem.2012.10.001.

Li, X., Bianchi, T.S., Allison, M.A., Chapman, P., Yang, G., 2013. Historical reconstruction of organic carbon decay and preservation in sediments on the East China Sea shelf. J. Geophys. Res. Biogeosci. 118 (3), 1079—1093, http://dx.doi.org/10.1002/jgrg.20079.

Li, X., Bianchi, T.S., Yang, Z., Osterman, L.E., Allison, M.A., DiMarco, S.F., Yang, G., 2011. Historical trends of hypoxia in Changjiang River estuary: applications of chemical biomarkers and microfossils. J. Marine Syst. 86 (3—4), 57—68, http://dx.doi.org/10.1016/j.jmarsys.2011.02.003.

Louda, J.W., Li, J., Liu, L., Winfree, M.N., Baker, E.W., 1998. Chlorophyll-a degradation during cellular senescence and death. Org. Geochem. 29 (5—7), 1233—1251, http://dx.doi.org/10.1016/S0146-6380(98)00186-7.

Louda, J.W., Liu, L., Baker, E.W., 2002. Senescence- and death-related alternation of chlorophylls and carotenoids in marine phytoplankton. Org. Geochem. 33 (12), 1635—1653, http://dx.doi.org/10.1016/S0146-6380(02)00106-7.

Louda, J.W., Loitz, J.W., Rudnick, D.T., Baker, E.W., 2000. Early diagenetic alteration of chlorophyll-a and bacteriochlorophyll-a in a contemporaneous marl ecosystem; Florida Bay. Org. Geochem. 31, 1561—1580.

Magnusson, J., Næs, K., 1986. Basisundersøkelser I Drammensfjorden 1982-84. Delrapport 6. Hydrografi, vannkvalitet og vannutskiftninge. NIVA, overvåkningsrapporrt 243/86, 77 pp.

Majewski, A., 1990. Morfometria i hydrografia zlewiska. In: Majewski, A. (Ed.), Zatoka Gdańska. IMGW, Wyd. Geolog, Warszawa, 10—19.

Maksymowska, D., Richard, P., Piekarek-Jankowska, H., Riera, P., 2000. Chemical and isotopic composition of the organic matter sources in the Gulf of Gdansk (Southern Baltic Sea). Estuar. Coast. Shelf Sci. 51 (5), 585—598, http://dx.doi.org/10.1006/ecss.2000.0701.

Mälkki, P., Perttilä, M., 2012. Baltic Sea water exchange and oxygen balance. In: Haapala, I. (Ed.), From the Earth's Core to Outer Space (Lecture Notes in Earth System Sciences). Springer-Verlag, Berlin, 151—161.

McGowan, S., Barker, P., Haworth, E.Y., Leavitt, P.R., Maberly, S.C., Pates, J., 2012. Humans and climate as drivers of algal community change in Windermere since 1850. Freshwater Biol. 57 (2), 260—277, http://dx.doi.org/10.1111/j.1365-2427.2011.02689.x.

Mohrholz, V., Naumann, M., Nausch, G., Krüger, S., Gräwe, U., 2015. Fresh oxygen for the Baltic Sea — an exceptional saline inflow after a decade of stagnation. J. Marine Syst. 148, 152—166, http://dx.doi.org/10.1016/j.jmarsys.2015.03.005.

Moorhouse, H.L., McGowan, S., Jones, M.D., Barker, P., Leavitt, P.R., Brayshaw, S.A., Haworth, E.Y., 2014. Contrasting effects of nutrients and climate on algal communities in two lakes in the Windermere catchment since the late 19th century. Freshwater Biol. 59 (12), 2605—2620, http://dx.doi.org/10.1111/fwb.12457.

Myślińska, E., 1992. Laboratoryjne badania gruntów. PWN, Warszawa, 52—74.

NGI, 2010. Miljøovervåkning av indre Drammensfjord. Årsrapport 2009. NGI-Rapp. 20081432-00-68-R. Datert 15. mars 2010.

Orive, E., Elliot, M., de Jonge, V.N., 2002. Nutrients and eutrophication in estuaries and coastal waters. In: Proceedings of the 31st Symposium of the ECSA. 3—7 July 2000, Bilbao, Spain. Kluwer Acad. Publ., Dordrecht, 526 pp.

Öztürk, M., 1995. Trends of trace metals (Mn, Fe, Co, Ni, Cu, Zn, Cd, and Pb) distributions at the oxic-anoxic interface and in the sulfidic water of the Drammensfjord. Mar. Chem. 48 (3—4), 329—342, http://dx.doi.org/10.1016/0304-4203(95)92785-Q.

Pastuszak, M., Witek, Z., 2012. Discharges of water and nutrients by the Vistula and Oder rivers draining Polish territory. In: Pastuszak, M., Igras, J. (Eds.), Temporal and Spatial Differences in Emission of Nitrogen and Phosphorus from Polish Territory to the Baltic Sea. National Mar. Fisher. Res. Inst./Fertilizer Research Institute (INSOL), Gdynia/Puławy, 311—353.

Pau, M., Hammer, O., 2013. Sediment mapping and long-term monitoring of currents and sediment fluxes in pockmarks in the Oslofjord, Norway. Mar. Geol. 346, 262—273, http://dx.doi.org/10.1016/j.margeo.2013.09.012.

Pempkowiak, J., 1991. Enrichment factors of heavy metals in the Southern Baltic surface sediments dated with $^{210}$Pb and $^{137}$Cs. Environ. Int. 17 (5), 421—428, http://dx.doi.org/10.1016/0160-4120(91)90275-U.

Pienitz, R., Walker, I.R., Zeeb, B.A., Smol, J.P., Leavitt, P.R., 1992. Biomonitoring past salinity changes in an athalassic subarctic lake. Int. J. Salt Lake Res. 1 (2), 91—123, http://dx.doi.org/10.1007/BF02904364.

Reuss, N., Conley, D.J., Bianchi, T.S., 2005. Preservation conditions and the use of sediment pigments as a tool for recent ecological reconstruction in four Northern European estuaries. Mar. Chem. 95 (3—4), 283—302, http://dx.doi.org/10.1016/j.marchem.2004.10.002.

Richards, F.A., 1965. Anoxic basins and fjords. In: Riley, J.P., Skirrow, G. (Eds.), Chemical Oceanography, vol. 1.. Acad. Press, London, pp. 611—643.

Sampere, T.P., Bianchi, T.S., Wakeham, S.G., Allison, M.A., 2008. Sources of organic matter in surface sediments of the Louisiana Continental margin: effects of major depositional/transport pathways and Hurricane Ivan. Cont. Shelf Res. 28 (17), 2472—2487, http://dx.doi.org/10.1016/j.csr.2008.06.009.

Sañé, E., Isla, E., Grémare, A., Escoubeyrou, K., 2013. Utility of amino acids as biomarkers in polar marine sediments: a study on the continental shelf of Larsen region, Eastern Antarctic Peninsula. Polar Biol. 36 (11), 1671—1680, http://dx.doi.org/10.1007/s00300-013-1386-5.

Savage, C., Leavitt, P.R., Elmgrenb, R., 2010. Effects of land use, urbanization, and climate variability on coastal eutrophication in the Baltic Sea. Limnol. Oceanogr. 55 (3), 1033—1046, http://dx.doi.org/10.4319/lo.2010.55.3.1033.

Schüller, S.E., Allison, M.A., Bianchi, T.S., Tian, F., Savage, C., 2013. Historical variability in past phytoplankton abundance and composition in Doubtful Sound, New Zealand. Cont. Shelf Res. 69, 110—122, http://dx.doi.org/10.1016/j.csr.2013.09.021.

Schüller, S.E., Savage, C., 2011. Spatial distribution of diatom and pigment sedimentary records in surface sediments in Doubtful Sound, Fiordland, New Zealand. New Zeal. J. Mar. Fresh. 45 (4), 591—608, http://dx.doi.org/10.1080/00288330.2011.561865.

Schulz, H.D., Zabel, M., 2006. Marine Geochemistry. Springer-Verlag, Berlin, Heidelberg, 574 pp.

Shankle, A.M., Goericke, R., Franks, P.J.S., Levin, L.A., 2002. Chlorin distribution and degradation in sediments within and below the Arabian Sea oxygen minimum zone. Deep-Sea Res. Pt. I 49 (6), 953—969, http://dx.doi.org/10.1016/S0967-0637(01)00077-2.

Smittenberg, R.H., Baas, M., Green, M.J., Hopmans, E.C., Schouten, S., Sinninghe Danste, J.S., 2005. Pre- and post-industrial environmental changes as revealed by the biogeochemical sedimentary record of Drammensfjord, Norway. Mar. Geol. 214 (1—3), 177—200, http://dx.doi.org/10.1016/j.margeo.2004.10.029.

Spooner, N., Harvey, H.R., Pearce, G.E.S., Eckardt, C.B., Maxwell, J. R., 1994a. Biological defunctionalisation of chlorophyll in the aquatic environment II: action of endogenous algal enzymes and aerobic bacteria. Org. Geochem. 22 (3—5), 773—780, http://dx.doi.org/10.1016/0146-6380(94)90138-4.

Spooner, N., Keely, B.J., Maxwell, J.R., 1994b. Biologically mediated defunctionalization of chlorophyll in the aquatic environment I: senescence/decay of the diatom *Phaeodactylum tricornutum*. Org. Geochem. 21 (5), 509—516, http://dx.doi.org/10.1016/0146-6380(94)90101-5.

Stephens, M.P., Kadko, D.C., Smith, C.R., Latasa, M., 1997. Chlorophyll-a and pheopigments as tracers of labile organic carbon at the central equatorial Pacific seafloor. Geochim. Cosmochim. Acta 61 (21), 4605—4619.

Suplińska, M.M., Pietrzak-Flis, Z., 2008. Sedimentation rates and dating of bottom sediments in the Southern Baltic Sea region. Nukleonika 53 (2), 105—111.

Sverdrup, K.A., Armbrust, E.V., 2008. An Introduction to the World's Oceans, 9th edn. McGraw-Hill, Columbus, United States, 521 pp.

Szczepańska, A., Zaborska, A., Maciejewska, A., Kuliński, K., Pempkowiak, J., 2012. Distribution and origin of organic matter in the Baltic Sea sediments dated with $^{210}$Pb and $^{137}$Cs. Geochronometria 39 (1), 1—9, http://dx.doi.org/10.2478/s13386-011-0058-x.

Szymczak-Żyła, M., Kowalewska, G., 2007. Chloropigments *a* in the Gulf of Gdańsk (Baltic Sea) as markers of the state of this environment. Mar. Pollut. Bull. 55 (10—12), 512—528, http://dx.doi.org/10.1016/j.marpolbul.2007.09.013.

Szymczak-Żyła, M., Kowalewska, G., Louda, J.W., 2011. Chlorophyll-a and derivatives in recent sediments as indicators of productivity and depositional conditions. Mar. Chem. 125 (1—4), 39—48, http://dx.doi.org/10.1016/j.marchem.2011.02.002.

Szymczak-Żyła, M., Louda, J.W., Kowalewska, G., 2008. Comparison of extraction and HPLC methods for marine sedimentary chloropigment determinations. J. Liq. Chromatogr. Relat. Technol. 31 (8), 1162—1180, http://dx.doi.org/10.1080/10826070802000699.

Szymczak-Żyła, M., Wawrzyniak-Wydrowska, B., Kowalewska, G., 2006. Products of chlorophyll *a* transformation by selected benthic organisms in the Odra Estuary (Southern Baltic Sea). Hydrobiologia 554 (1), 155—164, http://dx.doi.org/10.1007/s10750-005-1016-5.

Torres, I.C., Inglett, P.W., Brenner, M., Kenney, W.F., Ramesh Reddy, K., 2012. Stable isotope ($\delta^{13}$C and $\delta^{15}$N) values of sediment organic matter in subtropical lakes of different trophic status. J. Paleolimnol. 47 (4), 693—706, http://dx.doi.org/10.1007/s10933-012-9593-6.

Tselepides, A., Polychronaki, T., Marrale, D., Akoumianaki, I., Dell'Anno, A., Pusceddu, A., Danovaro, R., 2000. Organic matter composition of the continental shelf and bathyal sediments of the Cretan Sea (NE Mediterranean). Prog. Oceanogr. 46 (2—4), 311—344, http://dx.doi.org/10.1016/S0079-6611(00)00024-0.

Villanueva, J., Hastings, D.W., 2000. A century-scale record of the preservation of chlorophyll and its transformation products in anoxic sediments. Geochim. Cosmochim. Acta 64 (13), 2281—2294, http://dx.doi.org/10.1016/S0016-7037(99)00428-7.

Voss, M., Larsen, B., Leivuori, M., Vallius, H., 2000. Stable isotope signals of eutrophication in Baltic Sea sediments. J. Marine Syst. 25 (3—4), 287—298, http://dx.doi.org/10.1016/S0924-7963(00)00022-1.

Welschmeyer, N.A., Lorenzen, C.J., 1985. Chlorophyll budgets: zooplankton grazing and phytoplankton growth in temperate fjord and Central Pacific Gyres. Limnol. Oceanogr. 30 (1), 1—21.

Witek, Z., Ochocki, S., Nakonieczny, J., Podgórska, B., Drags, A., 1999. Primary production and decomposition of organic matter in the epipelagic zone of the Gulf of Gdańsk, an estuary of the Vistula. ICES J. Mar. Sci. 56 (Suppl. A), 3—14.

Wysocki, L.A., Bianchi, T.S., Powell, R.T., Reuss, N., 2006. Spatial variability in the coupling of organic carbon, nutrients, and phytoplankton pigments in surface waters and sediments of the Mississippi River plume. Estuar. Coast. Shelf Sci. 69 (1—2), 47—63, http://dx.doi.org/10.1016/j.ecss.2006.03.022.

Zaborska, A., Carroll, J., Papucci, C., Pempkowiak, J., 2007. Intercomparison of alpha and gamma spectrometry techniques used in $^{210}$Pb geochronology. J. Environ. Radioactiv. 93 (1), 38—50, http://dx.doi.org/10.1016/j.jenvrad.2006.11.007.

Zaborska, A., Winogadow, A., Pempkowiak, J., 2014. Caesium-137 distribution, inventories and accumulation history in the Baltic Sea sediments. J. Environ. Radioactiv. 127, 11—25, http://dx.doi.org/10.1016/j.jenvrad.2013.09.003.

Zalewska, T., Woroń, J., Danowska, B., Suplińska, M., 2015. Temporal changes in Hg, Pb, Cd, and Zn environmental concentrations in the southern Baltic Sea sediments dated with $^{210}$Pb method. Oceanologia 57 (1), 32—43, http://dx.doi.org/10.1016/j.oceano.2014.06.003.

Zegers, B.N., Lewis, W.A., Booij, K., Smittenberg, R.H., Boer, W., de Boer, J., Boon, J.P., 2003. Levels of polybrominated diphenyl ether flame retardants in sediment cores from Western Europe. Environ. Sci. Technol. 37 (17), 3803—3807, http://dx.doi.org/10.1021/es034226o.

Zhao, J., Bianchi, T.S., Li, X., Allison, M.A., Yao, P., Yu, Z., 2012. Historical eutrophication in the Changjiang and Mississippi delta-front estuaries: stable sedimentary chloropigments as biomarkers. Cont. Shelf Res. 47, 133—144, http://dx.doi.org/10.1016/j.csr.2012.07.005.

Oceanologia (2017) 59, 18—27

Available online at www.sciencedirect.com

ScienceDirect

journal homepage: www.journals.elsevier.com/oceanologia/

ORIGINAL RESEARCH ARTICLE

# Application of Dean's curve to investigation of a long-term evolution of the southern Baltic multi-bar shore profile

**Grzegorz R. Cerkowniak** *, **Rafał Ostrowski, Zbigniew Pruszak**

*Institute of Hydro-Engineering, Polish Academy of Sciences (IBW PAN), Gdańsk, Poland*

Received 29 February 2016; accepted 10 June 2016
Available online 24 June 2016

**KEYWORDS**
Cross-shore profile;
Bars;
Shoreline position;
Dean's curve;
Nearshore sediment resources

**Summary** The paper presents the results of studies on the long-term evolution of the multi-bar cross-shore profiles. The analysis is focused on time-dependent variability of shoreline position, a modified parameter *A* of the conventional Dean's equation and a parameter *F* describing the amount of nearshore sediment resources in the multi-bar cross-shore profile. The study also deals with interrelationships between these quantities. The analysis is carried out using field data collected at Lubiatowo, Poland, on the dissipative shore, representative for the south Baltic. The considered coastal segment is found to be stable in the long-term scale. The results of analysis show that the parameter *A* can either increase or decrease together with the shoreline advance. It is concluded that the shoreline position change is a parameter unsatisfactorily representative for behaviour of the seashore. The use of the Dean's approximation for estimation of the sediment resources *F* on the multi-bar seashore profiles is found reasonable to eliminate the effects of peculiarities of such shores.


* Corresponding author at: Institute of Hydro-Engineering of the Polish Academy of Sciences (IBW PAN), Kościerska 7, 80-328 Gdańsk, Poland. Tel.: +48 58 522 2933; fax: +48 58 552 4211.
*E-mail address:* g.cerkowniak@ibwpan.gda.pl (G.R. Cerkowniak).
Peer review under the responsibility of Institute of Oceanology of the Polish Academy of Sciences.

ELSEVIER | Production and hosting by Elsevier

## 1. Introduction

A typical sandy multi-bar coastal zone constitutes a complex morphological system described by a characteristic cross-shore profile with large bed forms (bars) and a shoreline, as well as a beach and dunes. While behaviour of the shoreline and beach forms is the key indicator of coastal dynamics in the longshore direction, the spatial-temporal evolution of the subaqueous cross-shore profile is driven mostly by processes

http://dx.doi.org/10.1016/j.oceano.2016.06.001

occurring in the direction perpendicular to the shoreline. Variety and intensity of coastal morphological changes depend on impact of waves and currents. This impact has a random character and is variable in time and space. Recently, the severity of extreme marine hydrological and hydrodynamic events is said to increase due to climate change (see e.g. Shaltout et al., 2015; Tsoukala et al., 2016). The morphological changes are observed across the entire coastal zones built of sandy sediments, even at the depths of 15—17 m (see e.g. Uścinowicz et al., 2014). On the other hand, in some cases, extensive technical interventions in the shallow water coastal regions have minor influence on nearshore morphodynamics (see e.g. Kubowicz-Grajewska, 2015).

Loss of wave energy due to breaking in the surf zone is strictly related to the presence of underwater bars. A well-developed bar system causes multiple wave breaking and as a result smaller part of deep-water wave energy reaches the shoreline vicinity and the beach than in a case of shore profile without bars (see e.g. Komar, 1998; Pruszak et al., 2008). The cross-shore profile shape can be therefore assumed as a key factor ruling the wave breaking and energy dissipation process. The layout and number of seabed forms (bars) on the cross-shore profile is an indicator of the wave breaking pattern. The number of bars is frequently said to depend on seabed inclination and sediment grain sizes, as well as on the offshore wave climate (see Dolan, 1983; Katoh and Yanagishima, 1993; Moore et al., 2003; Pruszak et al., 1999).

The precise quantitative assessment of evolution of a coast is very difficult, particularly in a case of the multi-bar sandy sea shore. Many coastal parameters are subject to changes which can be of various quality. For instance, retreat of the dune toe can be accompanied by the shoreline advance but in some circumstances both the shoreline and dune toe can move either landwards or seawards. Erosion observed simultaneously at the dune, emerged part of the beach and the shoreline can be compensated by accumulation of huge amounts of sand in the nearshore region, e.g. by volumetric expansion of the bar system. The situation becomes even more complicated if the coastal morphodynamics is considered in multi-scale time domains. Thus, there has been a need to elaborate a reliable method of accurate estimation of coastal evolution trends. Such a method, proposed herein, seems to yield reasonable results independently of peculiarities of an analysed seashore segment.

Analysis of selected parameters of the multi-bar shore profile is a fundamental aim of the present study. The study concentrates on interrelationship between the parameter $A$ of the modified Dean's curve approximating each cross-shore profile, shoreline position with respect to the long-term mean and the parameter $F$ describing the amount of sediment resources in the nearshore part of the coastal zone. In the present analysis, the temporal scale of decades has been considered (period from 1987 to 2008) and the coastal zone with 2—5 bars. The parameter $F$, expressing nearshore sand resources and resistance of seashore to erosion, has been defined in accordance with the Dutch approach, adapted by Cieślak (2001).

## 2. Study site and field data

The analysis was carried out by use of data collected on the typical south Baltic shore, namely at the Coastal Research Station (CRS) in Lubiatowo. The station was established in 1968 and has been operated by the Institute of Hydro-Engineering of the Polish Academy of Sciences (IBW PAN). Since 1970s, numerous field surveys have been carried out at CRS Lubiatowo during which a lot of data have been collected. Some of these data have been used in studies published in scientific papers. The present article contains the Lubiatowo data unused till now, as well as the data already utilised but within a new interpretation.

The mean nearshore slope is $\beta = 0.015$ (0.04 at maximum very close to the shoreline) and the seabed is built of fine quartz sand having the median grain diameter equal to $d_{50} = 0.22$ mm. The Baltic can be assumed as the non-tidal or micro-tidal sea and water motion is therefore generated only by wind-driven waves and currents. The underwater bar system consists of 3—5 bars. The first stable bar occurs about 100—120 m from the shoreline, the second one ca. 250 m, the third one 400—450 m while the fourth one often overlaps with the fifth one constituting a large form 650—750 m from the shoreline. Aside from these stable bars, there is also an ephemeral bar in the form of a flat shoal located near the shoreline. The view of the considered coastal segment, its location in the south Baltic Sea and the layout of exemplary analysed cross-shore profiles are shown in Fig. 1.

The presence and layout of bars, together with instantaneous wave conditions, imply numbers and locations of wave breakings. In mild and moderate wave conditions, waves break over the first bar and sometimes also in the region of the second bar, that means 100—250 m from the shoreline. During storms, waves are subject to multiple breaking and constitute a few breaker lines over the bars located farther seawards. If the waves are very small, they reach the nearshore zone unaffected by the seabed and break in close shoreline vicinity. A typical storm of average intensity generates waves having a significant height of $H_s = 2.5$ m at water depth of $h \approx 15$ m. The maximum significant wave height can reach $H_s$ equal to 3.5—4.5 m. In such conditions, wave period is equal to 5—8 s (while it does not exceed ca. 4.5 s in mild conditions). Due to wave transformation and breaking on the cross-shore profile, a part of wave energy $E$ dissipates which qualitatively depends on the incipient (deep-water) wave height. For instance, as calculated by Pruszak et al. (2008), the deep-water waves higher than 1.5 m loose at least 60% of their energy in the nearshore zone of CRS Lubiatowo site (which implies that not more than 40% of wave energy reaches the shoreline vicinity).

Within the present study, cross-shore transects stretching several hundred metres seawards (most often about 900—1000 m) and shoreline positions along 2.6 km coastal segment have been analysed. The bathymetric profiles spaced by 100 m from each other have been measured since 1987 while the shoreline position data have been collected since 1983. The analysis has been focused on three selected profiles, numbered 6, 11 and 21 (see Fig. 1). The variability of cross-shore transect no. 21 in the period from 1987 to 2008 is shown in Fig. 2a while the shoreline evolution in the same time is presented in Fig. 2b. Locations of the selected profiles 6, 11 and 21 are also shown in Fig. 2a.

It can be seen in Fig. 2a that the changes in bottom ordinates attain 4 m while Fig. 2b implies that the scope of variability of shoreline position at some locations is almost 100 m.

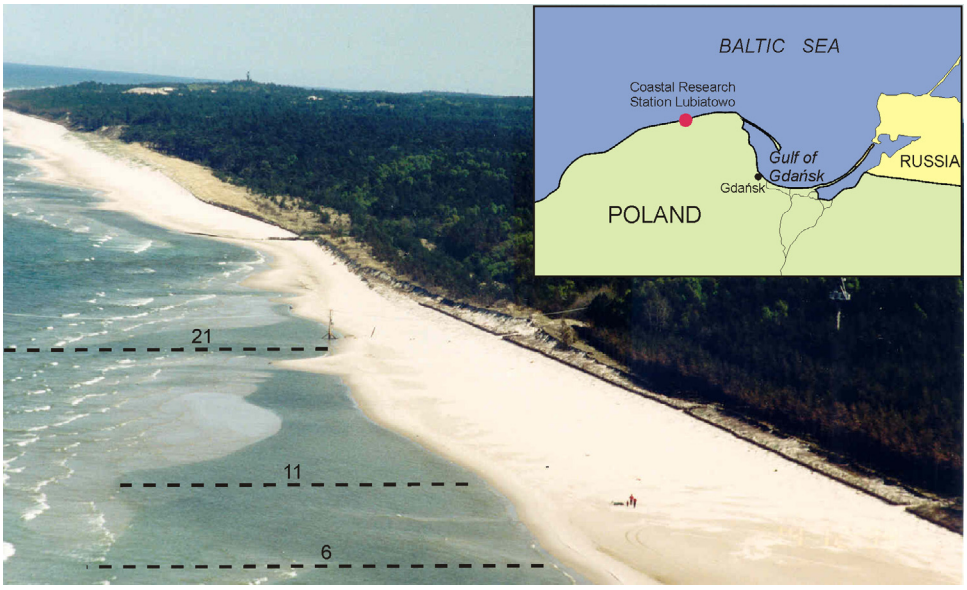


**Figure 1** Location of the study site, its view and layout of exemplary cross-shore profiles.

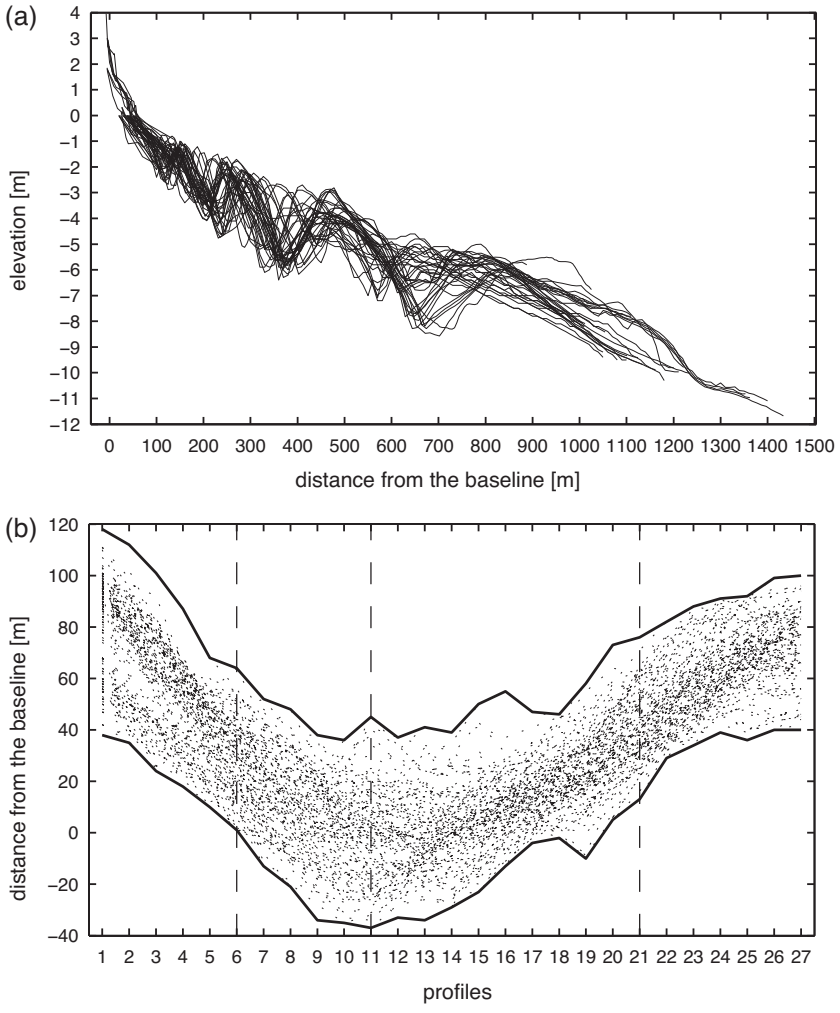


**Figure 2** Long-term variability of the cross-shore profile (a) and shoreline position (b) at CRS Lubiatowo in the period from 1987 to 2008.

## 3. Analysis

### 3.1. Approximated equilibrium seabed profile

The measured cross-shore profile can be approximated by the classical curve proposed by Dean (1976, 1985):

$$y' = A \cdot x'^{2/3}, \tag{1}$$

in which $x'$ and $y'$ are the cross-shore distance and the water depth in the coordinate system shown in Fig. 3. The parameter $A$ is a so-called "profile scale parameter" with dimensions of length to the 1/3 power. Basing on the linear wave theory, Dean (1977, 2002) has shown that Eq. (1) is consistent with uniform wave energy dissipation per unit volume within the surf zone and the shape described by Eq. (1) defines the "equilibrium beach profile".

In this system, however, the approximating function is vertical at the shoreline which is unreal. To get rid of this inconvenience, Pruszak et al. (1997) modified Dean's approximation by application of displacement of the shoreline point to location where the line of the nearshore mean seabed inclination ($\tan\alpha$) is tangent to Dean's curve, as shown in Fig. 3. The modified Dean's function reads as follows:

$$y = A \cdot (x + x_o)^{2/3} - A \cdot x_o^{2/3} = A \cdot \left\{ \left[ x + \frac{8}{27} \left( \frac{A}{\tan\alpha} \right)^3 \right]^{2/3} - \left( \frac{2A}{3\tan\alpha} \right)^2 \right\}. \tag{2}$$

The measured cross-shore transects have been approximated by Eq. (2) using the least-square method. This ensured determination of Dean's parameter $A$ for each measurement of the analysed shore profiles. The time-dependent values of the parameter $A$ for profiles 6, 11 and 21 are shown in Fig. 4.

It can be seen in Fig. 4 that the parameter $A$ value oscillates in the range from 0.075 to 0.107. Further, no distinct periodicity is visible. There is a decreasing trend for all three analysed profiles which can suggest that the nearshore zone has become shallower during the considered period.

The parameter $A$ quantitatively represents the shore stability. Small values of $A$ are typical for accumulative shores while high $A$ values indicate steep shores, vulnerable to wave impact and erosion. Coastal erosion is basically identified as the shoreline retreat which most often corresponds to retreat of the entire cross-shore profile. In some cases, however, regression of the shoreline is compensated by accumulation of sediment in the nearshore zone, e.g. in the form of underwater bars. Evolution of the shoreline $\delta$ at the considered cross-shore transects with respect to the time-averaged shoreline position is drawn in Fig. 5, in which the positive and negative values stand for the shoreline advance and retreat, respectively.

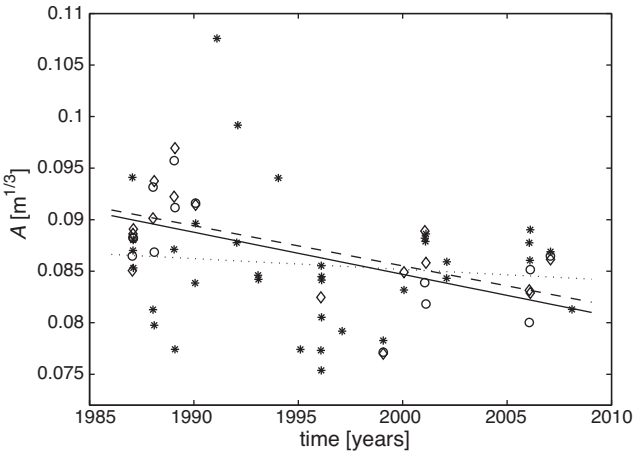


**Figure 4** Variability of parameter $A$ in time with trend lines for profiles 6 (circle, solid line), 11 (diamond, dashed line) and 21 (asterisk, dotted line).

The linear trends presented in Fig. 5 indicate the long-term shore accretion at profiles 6 and 21. The scatter around the approximating line is distinctly less for the profile no. 6 than for the profile no. 21 which implies that the profile no. 21 is more dynamic than the profile no. 6. It can be seen in Fig. 5 that the profile no. 11 has also been very dynamic. In this case, however, the approximating line reveals a significant trend of the shoreline retreat.

More detailed insight into shore profile change is obtained by analysis of the parameter $A$ as a function of shoreline position $\delta$. The results of such calculations are shown in Fig. 6.

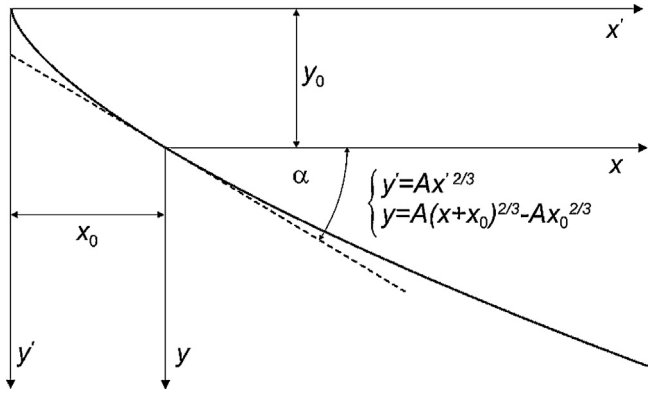


**Figure 3** Modified Dean's curve.

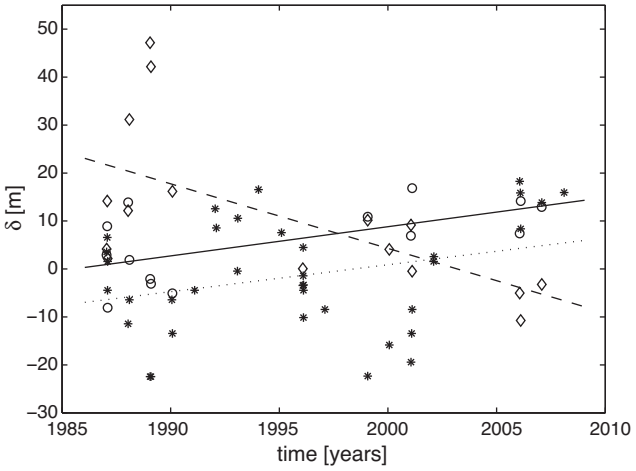


**Figure 5** Shoreline evolution $\delta(t)$ with trend lines at profiles 6 (circle, solid line), 11 (diamond, dashed line) and 21 (asterisk, dotted line).

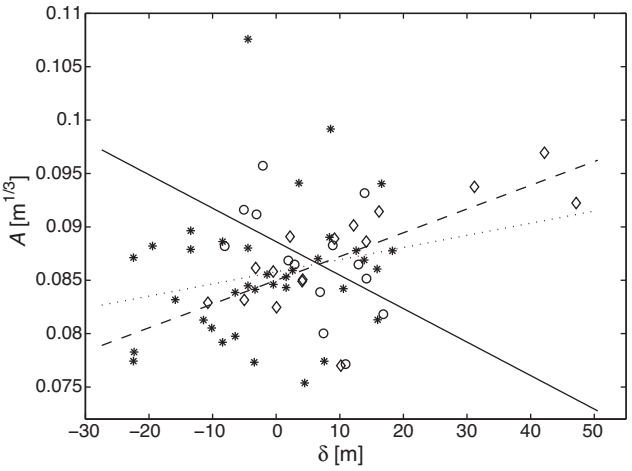


**Figure 6** Parameter $A$ as a function of shoreline position $\delta$ with trend line for profiles 6 (circle, solid line), 11 (diamond, dashed line) and 21 (asterisk, dotted line).

The results of analysis plotted in Fig. 6 show the increasing parameter $A$ together with the shoreline advance at profiles 11 (small deviations from the approximation) and 21 (very large scatter from the approximating line). Simultaneous increase of $A$ and $\delta$ denotes steepening of the cross-shore profile together with the seaward shoreline displacement. As regards the profile no. 21, the most considerable scatter is visible. For the profile no. 6, the increase of $A$ is accompanied by decrease of $\delta$. This denotes a case in which the shoreline advance occurs on the cross-shore profile becoming shallower (accumulation of sediment on the entire profile). In general, it can be concluded from Fig. 6 that the considered sea shore can behave variously and the shoreline position $\delta$ is a parameter the evolution of which does not reflect behaviour of the entire cross-shore shape.

It should be pointed out that similar values of the parameter $A$ of Dean's function (Eq. (1)) and the modified Dean's function (Eq. (2)) can be obtained for various shapes of the multi-bar cross-shore transects. This is illustrated in Fig. 7 where the exemplary approximations of the profile no. 11 by use of the modified Dean's curve (Eq. (2)) for 1989, 2001 and 2007 are shown. The caption of Fig. 7 indicates that the parameter $A$ is almost the same for 2001 and 2007 (with relatively exact approximations in both cases) while the cross-shore reliefs differ considerably. For 1989 (with a satisfactorily good approximation), the parameter $A$ is only slightly bigger than for 2001 and 2007 while the cross-shore shape for this year is totally different than observed in 2001 and 2007.

As depicted in Fig. 7, the actual cross-shore transects were subject to conversion from the 5-bar profile in 1989 to 2-bar profiles in 2001 and 2007. As mentioned before, the approximation goodness is better for the profile displaying smaller number of bars. In particular, it can be seen in Fig. 7 that the offshore part of the profile (350 m from the shoreline and farther) is perfectly well approximated by the modified Dean's function. It could have been expected as the approach of Dean was originally proposed for sea shores having no bars or small numbers (no more than 1–2) of bars.

## 3.2. Nearshore sediment resources

In view of the previous considerations, evolution of shoreline position does not reflect actual erosion or accretion of the sea shore. For a sandy coast, the amount of non-cohesive sediments constituting the nearshore seabed indicates the shore character, namely whether it is erosive or accumulative. According to Cieślak (2001), on the south Baltic coast, including the Polish seashore, the above feature is represented by sediments deposited in the zone between the dune foot (landward edge of the emerged part of the beach, located about 2.0 m above the mean sea level) and the depth of 6–7 m. This part of the cross-shore transect, namely beyond the ordinates +2 m and −6 m (or −7 m) ought to be taken into account while determining the sediment resources in the sandy coastal zone, see Fig. 8.

The nearshore sediment resources volume per one metre along the shoreline [$m^3\ m^{-1}$], i.e. the area of the cross-shore profile denoted as $F$ in Fig. 8, depends on the boundary ordinate $y_2$ which delineates the seaward limit of analysis ($x_2$). This boundary can be assumed identical to the classical coastal engineering parameter: the depth of closure, at which the nearbed lithodynamic processes become distinctly less intensive than in the nearshore zone. In the present study, the value $y_2 = -6$ m has been assumed.

The time series of the actual variable $F$ and of the variable $F$ determined from the Dean's approximation are shown in Fig. 9a and b, respectively.

Fig. 9a and b reveal increasing linear trends for almost all profiles, both with respect to the variable $F$ determined for the actual cross-shore transects and for $F$ determined using the Dean's-approximated profiles, which implies that the sediment resources at the analysed coastal segment have grown in the long run (since 1987). The amount of nearshore sediments represented by $F$ mostly lies in the range of 1600–2000 $m^3\ m^{-1}$ and 1750–2100 $m^3\ m^{-1}$ for the actual and Dean's-approximated profiles, respectively. In view of the study published by Dubrawski and Zawadzka (2006), in which the quantity $F$ determined in the same way for the erosive shore segments in Kołobrzeg (west part of the Polish coast) has been reported to be equal to 1000–1200 $m^3\ m^{-1}$ only, the considered seashore at CRS Lubiatowo can be assumed as stable or even accumulative. This finding can be supported by analysis of Hel Peninsula (ca. 40–70 km eastwards of CRS Lubiatowo) seashore stability carried out by Ostrowski and Skaja (2011). Analysed in that study, the root part of Hel Peninsula is subject to regular intensive artificial beach nourishment which is necessary to provide accumulative features of this shore segment (wide beach and high ordinate of the dune toe). The respective values of $F$ calculated analogously (with $y_1 = +2$ m and $y_2 = -6$ m) for the root part of Hel Peninsula in 2003–2008 range from 1200 $m^3\ m^{-1}$ to 2000 $m^3\ m^{-1}$. The above considerations suggest that the parameter $F$ is an indicator of the coastal resistance (or vulnerability) to erosion. For individual south Baltic shore segments this value is different. Since this criterion is site-specific, depending on local conditions (e.g. wave climate and grain size), it ought to be determined for each considered site separately.

By intuition, variability of the parameter $F$ ought to be distinctly correlated with the shoreline position changes which means e.g. that the bigger shoreline advance is

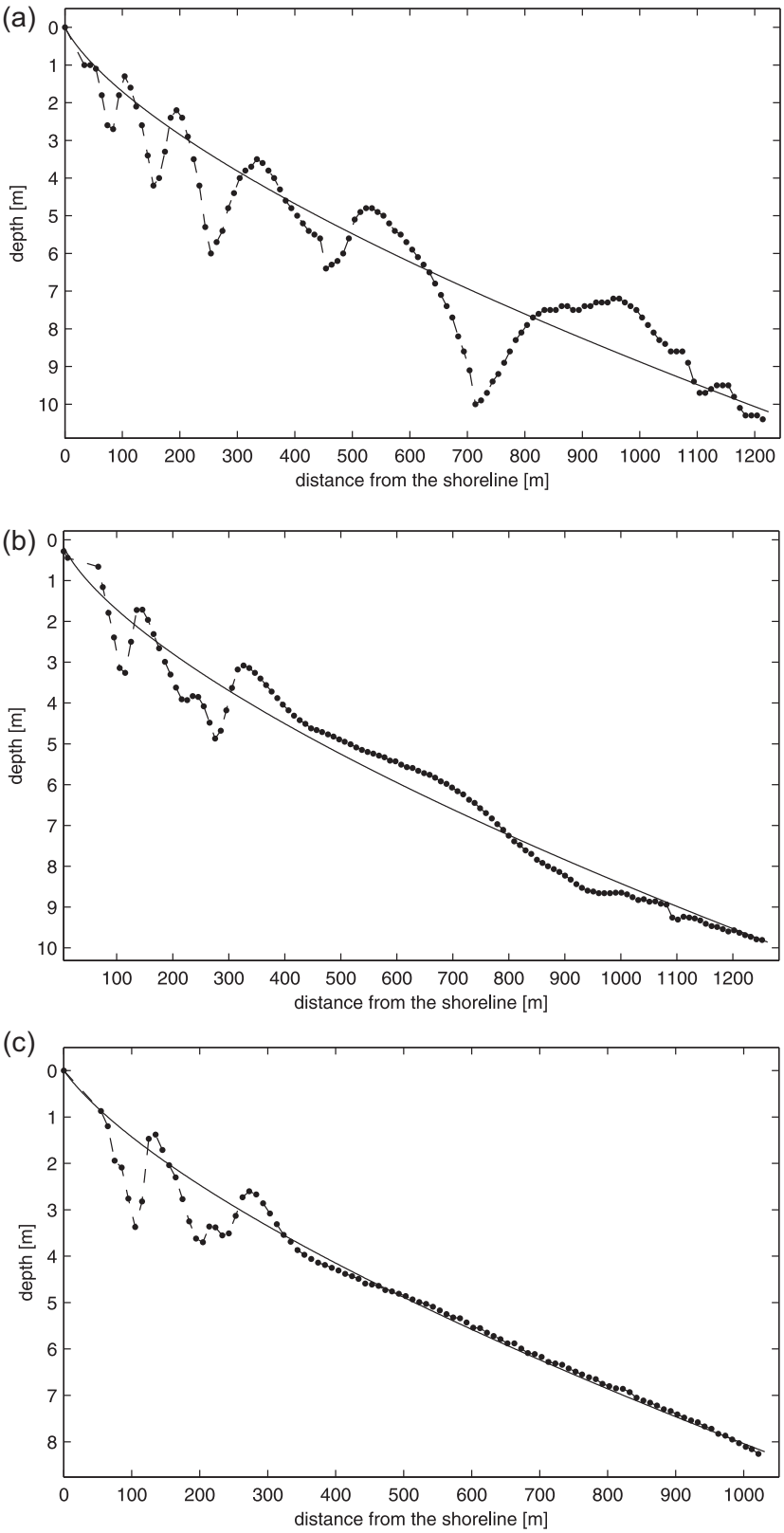


**Figure 7** Results of approximation of profile no. 11 by modified Dean's function: for 1989 with $A = 0.0922$ and $R^2 = 0.847$ (a), for 2001 with $A = 0.0858$ and $R^2 = 0.963$ (b) and for 2007 with $A = 0.0861$ and $R^2 = 0.957$ (c).

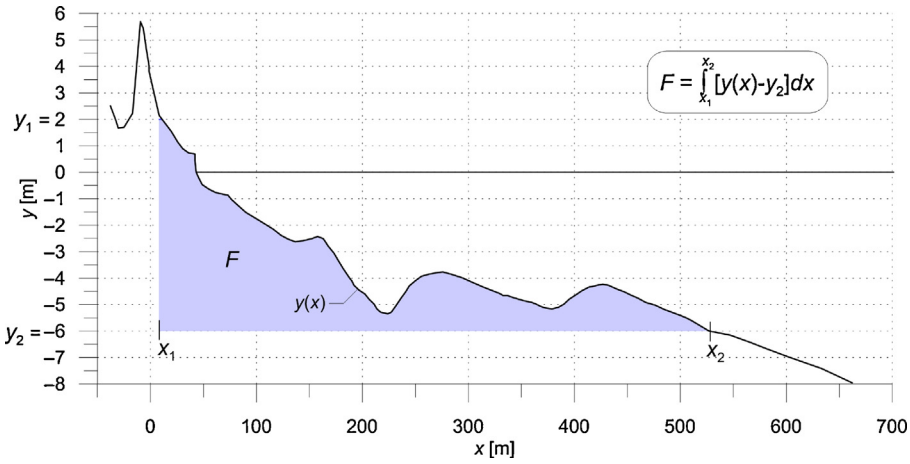


**Figure 8** Definition of nearshore sediment resources *F*, after Cieślak (2001).

observed the higher value of *F* is obtained from the calculations. This is not entirely confirmed by results of analysis shown in Fig. 10a and b for the actual and Dean's-approximated shore profiles.

The trend lines plotted in Fig. 10a and b clearly show that in some cases the shoreline evolution can take place independently of the nearshore seabed profile change. This is particularly visible for the profile no. 11 where the shoreline advance $\delta$ is not related with the increase of the sediment resources *F* in the nearshore zone. For the profile no. 21 the considerable seaward movement of shoreline position is accompanied by merely a slight growth of sediment resources while for the profile no. 6 the beach accretion at the shoreline corresponds to distinct sediment accumulation in the

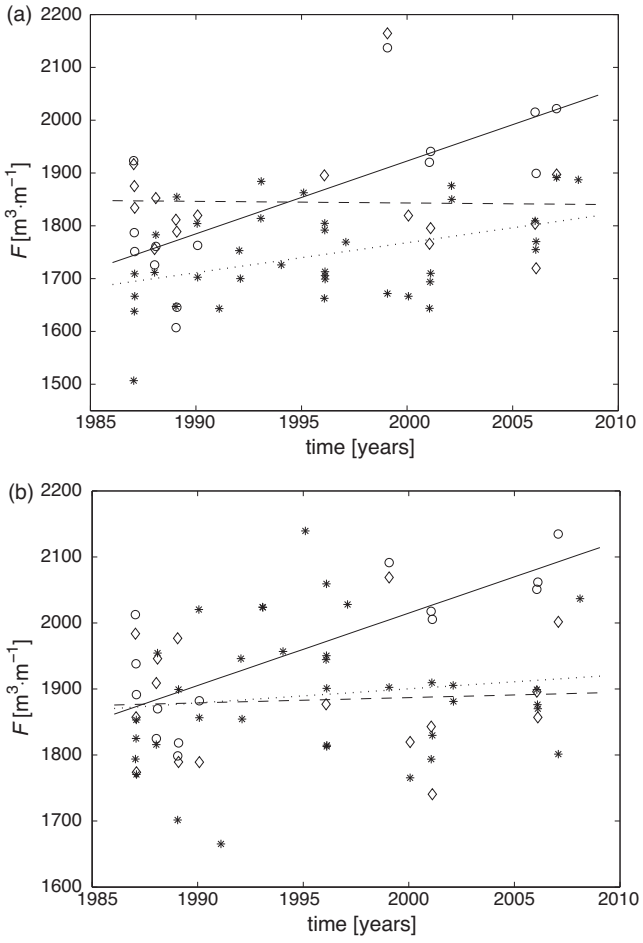


**Figure 9** Variability of sediment resources *F* (a) and sediment resources *F* calculated for Dean's curve (b) in time with trend lines for profiles 6 (circle, solid line), 11 (diamond, dashed line) and 21 (asterisk, dotted line).

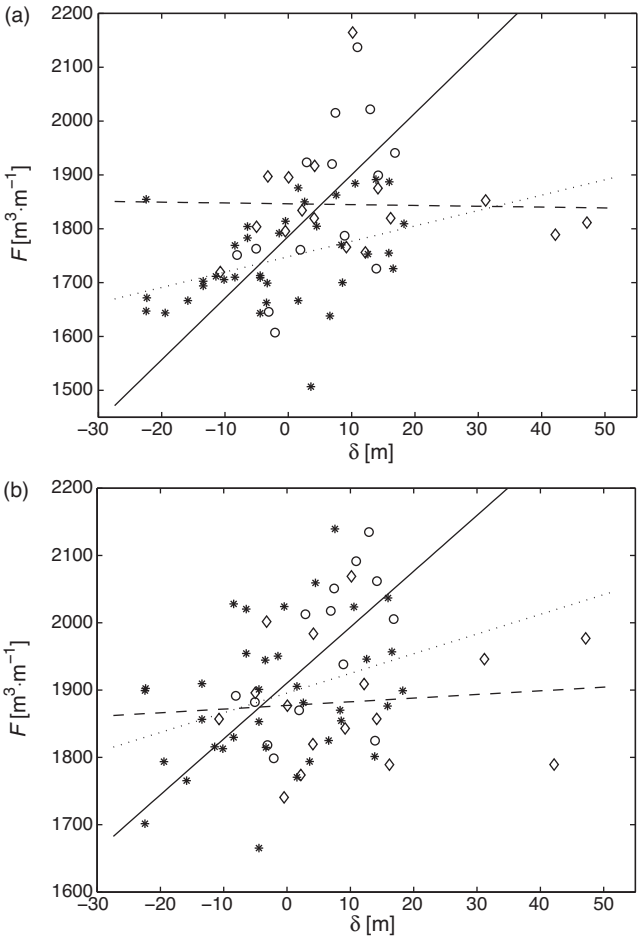


**Figure 10** Sediment resources $F$ (a) and sediment resources $F$ calculated for Dean's curve (b) as a function of shoreline position $\delta$ with trend lines for profiles 6 (circle, solid line), 11 (diamond, dashed line) and 21 (asterisk, dotted line).

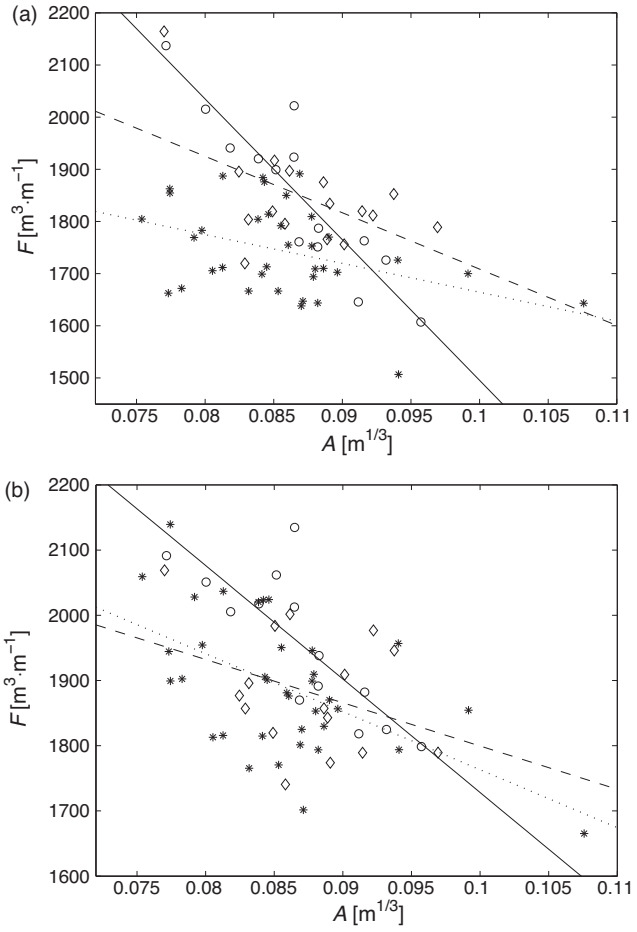


**Figure 11** Sediment resources $F$ (a) and sediment resources $F$ calculated for Dean's curve (b) as a function of parameter $A$ with trend line for profiles 6 (circle, solid line), 11 (diamond, dashed line) and 21 (asterisk, dotted line).

entire nearshore zone ($F$ significantly proportional to $\delta$). Such various dependencies of $F$ on $\delta$ result from the fact that the shoreline position is sensitive to any (even very weak) hydrodynamic conditions while the sea bottom at bigger depths (5–7 m) is subject to changes during more severe conditions. Secondly, in some circumstances the emerged part of the shore profile can quickly evolve due to aeolian processes and influence the parameter $F$ while the shoreline position and the nearshore seabed can remain unchanged at the same time.

In contrast to the ambiguity of the relationship between the nearshore sediment resources $F$ and the shoreline position $\delta$, a more clear mutual association between the parameter $F$ and Dean's coefficient $A$ can be expected. Typically, volumetric increase of the nearshore sand resources is accompanied by flattening of the non-bar profile which results in decrease of the parameter $A$ in Dean's curve. For the multi-bar shore, the bars may be located closer or further to each other, can be more or less steep, higher or lower. These features can distinctly imply the value of $F$, even if the coefficient $A$ remains similar. Yielded by the present analysis, the parameter $A$ decreases with growing $F$ for all cases presented in Fig. 11a and b. It is worthwhile noting, however, that the inclinations of the approximating lines differ significantly from each other, particularly in Fig. 11a (the actual value of $F$ versus the parameter $A$). This results from the bottom relief of the analysed coastal segment at which, as mentioned before, the multi-bar characteristics can yield the same or similar values of $A$ for variety of cross-shore profile shapes. It should be noted again that the wind-induced evolution of the emerged beach influences the parameter $F$ while it has no meaning to the parameter $A$.

For the multi-bar shore, identification of $x_2$ (see Fig. 8) in the calculation of $F$ can be problematic since the depth $y_2$ (−6 m) may occur at a few locations (Fig. 7a). Secondly, bars are very dynamic forms and can migrate, evolve, disappear, appear, bifurcate and join with each other, even in short time scales. For instance, the outer bar can in fact contribute to sediment resource defined by the approach of Cieślak (2001), although being formally not taken into account due to the depths exceeding $y_2$. A question arises whether the commonly used approximation of the real cross-shore profile by the Dean's curve is reliable enough to calculate the sediment resources $F$ on the basis of such approximation. The positive answer to this question would eliminate doubts which can appear when the quantity $F$ does not comprise huge amounts

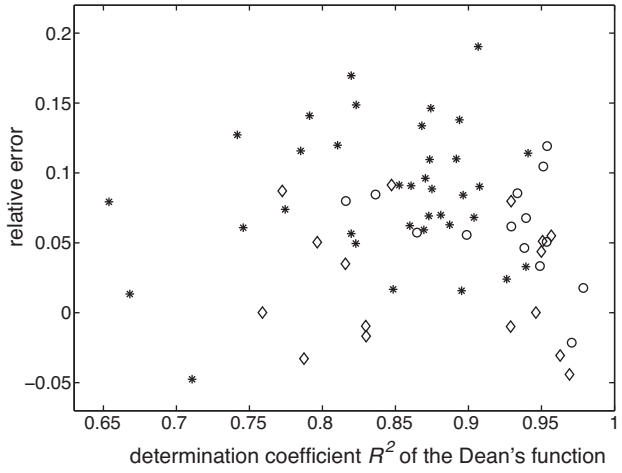


**Figure 12** Relative error between sediment resources $F$ calculated for the real profile and approximated by the Dean's curve as a function of determination coefficient $R^2$ of the Dean's approximation for profiles 6 (circle), 11 (diamond) and 21 (asterisk).

of sand accumulated in the outer bar, as illustrated in Fig. 7a and Fig. 8. In such a case, the sediment resources are underestimated. One can also imagine the contrary situation, when the sea bed inclination becomes significantly steeper just beyond the outer boundary of the calculation domain (corresponding to the ordinate $y_2 = -6$ m). In the latter case, the nearshore sediment resources can be underestimated. Calculation of the parameter $F$ for the Dean's approximation of the entire cross-shore transect seems to be a reasonable solution which can dispel the above uncertainty.

The answer to the respective query is provided by the results of computations presented in Fig. 12 which shows the relative error in determination of $F$ for the real and Dean's-approximated nearshore sea bottom shape.

It can be seen in Fig. 12 that the accuracy in calculation of the quantity $F$ for the Dean's-approximated seabed profile with respect to the actual $F$ value is quite good, having the relative error (vertical axis) not exceeding 0.2. This takes place independently of goodness of the Dean's approximation, expressed by the determination coefficient $R^2$ (horizontal axis). This finding constitutes a good basis to use of the Dean's approximation for estimation of the sediment resources on the multi-bar seashore profiles in order to eliminate the effects of peculiarities of such shores.

## 4. Conclusions

The analysis of variability of the parameter $A$ characterising the Dean's curve show that this parameter can behave independently of the shoreline migration. In contrast to the classical knowledge on no-bar or single-bar seashore, according to which coastal erosion is inevitably represented either by increase of the parameter $A$ (deepening of the nearshore profile) or by maintenance of the same value of $A$ (retreat of the entire profile), the multi-bar shore erosion can be accompanied by decrease of $A$ (shoreline retreat with simultaneous accumulation of sediment within the bar system). The parameter $A$ has thus been found not to be a fully representative indicator of the multi-bar cross-shore profile evolution.

It has also been definitely confirmed that the changes of shoreline position (especially in the short-term time scales) are not always correlated with changes of the coastal sediments amount. Hence, features of the entire nearshore sea bottom relief ought to be considered in analysis of coastal morphodynamics. For the multi-bar dissipative sandy coast, typical in the south Baltic, the seashore zone stretching from the dune toe (ordinates of about +2 m) to the depth of ca. −6 m has been found representative for estimation of the sediment resources $F$. In order to get rid of the effects of peculiarities of the multi-bar cross-shore profiles and related possible underestimations or overestimations, the parameter $F$ is proposed to be calculated for the seabed shape approximated by the Dean's curve. It has been proved that such approach eliminates the bias caused by the profile peculiarities and, at the same time, does not produce significant inaccuracies in comparison to analysis of actual cross-shore transects. The proposed method can be applied in a variety of time scales: from short-term coastal changes (hours and days) to long-term evolution (decades).

Finally, the nearshore sediment resources $F$ can be treated as an indicator of the shore stability. For individual south Baltic shore segments this value is different. Since this criterion is site-specific, depending on local conditions (e.g. wave climate and grain size), it ought to be determined for each considered site separately.

## Acknowledgement

The study was sponsored by the Ministry of Science and Higher Education, Poland, under the IBW PAN statutory programme No. 2 which is hereby gratefully acknowledged.

## References

Cieślak, A., 2001. Outline of the seashore protection strategy. Inż. Mor. Geotech. 22 (2), 65–73, (in Polish).

Dean, R.G., 1976. Beach erosion: causes, processes, and remedial measures. Crit. Rev. Environ. Contr. 6 (3), 259–296.

Dean, R.G., 1977. Equilibrium Beach Profiles: US Atlantic and Gulf Coasts. Ocean Eng. Tech. Rep. No. 12. Dep. Civil Eng., College Mar. Stud., Univ. Delaware, Newark, 45 pp.

Dean, R.G., 1985. Physical modeling of littoral processes. In: Dalrymple, R.A. (Ed.), Physical Modelling in Coastal Engineering. A. A. Balkema, Rotterdam, Boston, 119–139.

Dean, R.G., 2002. Beach Nourishment. Theory and Practice, Advanced Series on Ocean Engineering, vol. 18. World Sci. Publ. Co. Pte. Ltd., 399 pp.

Dolan, T.J., 1983. Wave mechanisms for the formation of multiple longshore bars with emphasis on the Chesapeake Bay. (MCE thesis). Univ. Delaware, Newark, 208 pp.

Dubrawski, R., Zawadzka, E., 2006. Future of the Polish Sea Shores. Wyd. IM, Gdańsk, 302 pp., (in Polish).

Katoh, K., Yanagishima, S., 1993. Beach erosion in a storm due to infragravity waves. Rep. Port Harbour Res. Inst., Nagase, Yokosuka 31 (5), 73–102.

Komar, P.D., 1998. Beach Processes and Sedimentation, 2nd ed. Prentice Hall, Upper Saddle River, NJ, 544 pp.

Kubowicz-Grajewska, A., 2015. Morpholithodynamical changes of the beach and the nearshore zone under the impact of submerged breakwaters – a case study (Orłowo Cliff, the Southern Baltic). Oceanologia 57 (2), 144–158, http://dx.doi.org/10.1016/j.oceano.2015.01.002.

Moore, L.J., Sullivan, C., Aubrey, D.G., 2003. Interannual evolution of multiple longshore sand bars in a mesotidal environment, Truro, Massachusetts, USA. Mar. Geol. 196 (3—4), 127—143, http://dx.doi.org/10.1016/S0025-3227(03)00028-8.

Ostrowski, R., Skaja, M., 2011. Dependence of Hel Peninsula seashore stability on artificial nourishment. Inż. Mor. Geotech. 32 (6), 495—502, (in Polish).

Pruszak, Z., Różyński, G., Szmytkiewicz, M., Skaja, M., 1999. Quasi-seasonal morphological shore evolution response to variable wave climate. In: Kraus, N.C., McDougal, W.G. (Eds.), Proc. 4th International Symposium on Coastal Engineering and Science of Coastal Sediment Processes, vol. 2. ASCE, Reston, 1081—1093.

Pruszak, Z., Różyński, G., Zeidler, R.B., 1997. Statistical properties of multiple bars. Coast. Eng. 31 (4), 263—280, http://dx.doi.org/10.1016/S0378-3839(97)00010-0.

Pruszak, Z., Szmytkiewicz, P., Ostrowski, R., Skaja, M., Szmytkiewicz, M., 2008. Shallow-water wave energy dissipation in a multi-bar coastal zone. Oceanologia 50 (1), 43—58.

Shaltout, M., Tonbol, K., Omstedt, A., 2015. Sea-level change and projected future flooding along the Egyptian Mediterranean coast. Oceanologia 57 (4), 293—307, http://dx.doi.org/10.1016/j.oceano.2015.06.004.

Tsoukala, V.K., Chondros, M., Kapelonis, Z.G., Martzikos, N., Lykou, A., Belibassakis, K., Makropoulos, C., 2016. An integrated wave modelling framework for extreme and rare events for climate change in coastal areas — the case of Rethymno, Crete. Oceanologia 58 (2), 71—89, http://dx.doi.org/10.1016/j.oceano.2016.01.002.

Uścinowicz, S.1., Jegliński, W., Miotk-Szpiganowicz, G., Nowak, J., Pączek, U., Przezdziecki, P., Szefler, K., Poręba, G., 2014. Impact of sand extraction from the bottom of the southern Baltic Sea on the relief and sediments of the seabed. Oceanologia 56 (4), 857—880, http://dx.doi.org/10.5697/oc.56-4.857.

Oceanologia (2017) 59, 28—36

Available online at www.sciencedirect.com

ScienceDirect

journal homepage: www.journals.elsevier.com/oceanologia/

ORIGINAL RESEARCH ARTICLE

# The impact of tides and waves on near-surface suspended sediment concentrations in the English Channel

**Nicolas Guillou** [a,*], **Aurélie Rivier** [a,b], **Georges Chapalain** [a], **Francis Gohin** [b]

[a] *Laboratoire de Génie Côtier et Environnement (LGCE), Cerema/DTecEMF/DS, Plouzané, France*
[b] *ODE-DYNECO-PELAGOS, Ifremer, Centre de Bretagne, Technople Brest-Iroise, Plouzané, France*

Received 5 April 2016; accepted 23 June 2016
Available online 9 July 2016

**KEYWORDS**
Sediment transport;
Numerical modeling;
Satellite;
ROMS;
MERIS;
MODIS

**Summary** Numerous ecological problems of continental shelf ecosystems require a refined knowledge of the evolution of suspended sediment concentrations (SSC). The present investigation focuses on the spatial and temporal variabilities of near-surface SSC in coastal waters of the English Channel (western Europe) by exploiting numerical predictions from the Regional Ocean Modeling System ROMS. Extending previous investigations of ROMS performances in the Channel, this analysis refines, with increased spatial and temporal resolutions, the characterization of near-surface SSC patterns revealing areas where concentrations are highly correlated with evolutions of tides and waves. Significant tidal modulations of near-surface concentrations are thus found in the eastern English Channel and the French Dover Strait while a pronounced influence of waves is exhibited in the Channel Islands Gulf. Coastal waters present furthermore strong SSC temporal variations, particularly noticeable during storm events of autumn and winter, with maximum near-surface concentrations exceeding 40 mg $l^{-1}$ and increase by a factor from 10 to 18 in comparison with time-averaged concentrations. This temporal variability strongly depends on the granulometric distribution of suspended sediments characterized by local bimodal contributions of silts and sands off coastal irregularities of the Isle of Wight, the Cotentin Peninsula and the southern Dover Strait.


* Corresponding author. Tel.: +33 2 98 05 67 39; fax: +33 2 98 05 67 21.
*E-mail address:* nicolas.guillou@cerema.fr (N. Guillou).
Peer review under the responsibility of Institute of Oceanology of the Polish Academy of Sciences.

ELSEVIER | Production and hosting by Elsevier

http://dx.doi.org/10.1016/j.oceano.2016.06.002

## 1. Introduction

An accurate knowledge of suspended sediment concentrations (SSC) is required for numerous ecological issues of continental shelf ecosystems. SSC influence thus water clarity, limiting the amount of light available to phytoplankton for photosynthesis and the biological primary production (Hoppe, 1984). Suspended particulates may also absorb and transport polluting substances such as heavy metals or radioactive materials with harmful consequences in terms of water quality (Haarich et al., 1993). A refined estimation of suspended sediment transport rates constitutes finally a prerequisite of coastal engineering applications dealing with maintenance dredging projects of estuaries or harbors.

Recognized as an important coastal ecosystem of northwestern European shelf seas, the English Channel (Fig. 1) has been the subject of numerous studies dedicated to suspended sediment transport. Initially based on in situ observations along transects in the Wight-Cotentin area and the Dover Strait (Dupont et al., 1993; Eisma and Kalf, 1979; Van Alphen, 1990; Velegrakis et al., 1997), first investigations exhibited a spatial "zonation" between (1) high turbid coastal waters with mean near-surface SSC of 10–35 mg $l^{-1}$ and (2) central waters with low concentrations of 2–3 mg $l^{-1}$. Numerical modeling tools were then implemented to extend these local analyses focusing on effects of major hydrodynamic forcings of tides and waves (Gerritsen et al., 2000; Grochowski et al., 1993; Guillou and Chapalain, 2011; Guillou et al., 2009; Velegrakis et al., 1999). Three-dimensional (3D) predictions exhibited, in particular, remote advective and diffusive transport of silts ($d < 30$ μm) during spring tide with noticeable effects on grain-size variability of suspended sediments. Impacts of waves were furthermore quantified with SSC increase by a factor between 10 and 20 in exposed coastal areas during storm events.

Nevertheless, whereas these simulations provided interesting insights about temporal and spatial SSC variabilities in the English Channel complemented further local evaluations (Rahbani, 2015), numerical studies remained primary restricted to the vicinity of measurement sites. Broad-scale assessments of near-surface SSC have however been conducted relying on satellite monitoring of ocean color (Fettweis et al., 2007, 2012; Gohin et al., 2005; Gohin, 2011). Despite the reduced number of high-quality images fully covering the whole area over long time periods and the low accuracy of satellite observations (Wozniak, 2014), the refined analysis of remote-sensing images exhibited close correlations between observed SSC and hydrodynamic forcings of tides and waves (Rivier et al., 2012). Satellite-retrieved observations have thus been considered in numerous assessments of numerical simulations investigating regional variabilities of near-surface SSC at increased spatial and temporal resolutions in the English Channel (Guillou et al., 2015; Menesguen and Gohin, 2006; Souza et al., 2007; Sykes and Barcelia, 2012). Nevertheless, the attention was primary dedicated to approach of major SSC patterns and improvements of numerical predictions neglecting accurate evaluations about the roles of tides and waves on SSC variabilities.

The present study investigates the spatial and temporal variabilities of near-surface SSC under combined influences of tides and waves relying on numerical simulations established by Guillou et al. (2015) in the English Channel (Section 2). Predictions are first exploited to assess the global effects at the scale of the Channel identifying areas where concentrations are highly correlated with the evolutions of tides and waves (Section 3.1). Further investigation is then conducted about the temporal variabilities of nearshore SSC patterns quantifying effects of waves on near-surface concentrations in shallow waters (Section 3.2). The influence of

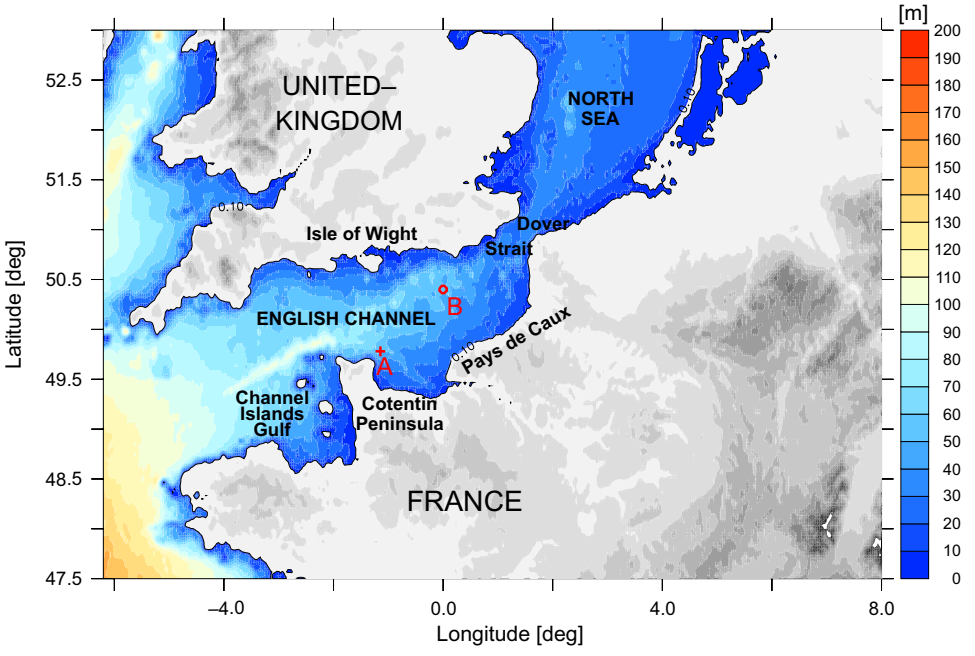


**Figure 1** Bathymetry of the English Channel with locations of points A and B.

the granulometric distribution of suspended sediments is finally analyzed with a particular focus off coastal irregularities characterized by a local heterogeneity of grain sizes of suspended particles (Section 3.3).

## 2. Numerical modeling

Numerical modeling is based on the 3D multicomponent sediment transport model ROMS (Regional Ocean Modeling System) (Haidvogel et al., 2000; Warner et al., 2008) assessed against satellite-retrieved observations from raw remote-sensing images for the year 2008 (Guillou et al., 2015). Major characteristics of numerical model and performances evaluation are briefly described hereafter. Further details are available in Guillou et al. (2015).

The modeling system, implemented with a horizontal resolution of 3 km, takes into account the spatial distribution of seabed sediments by applying the interpolation method proposed by Leprêtre et al. (2006) to a series of available bottom sediment samples in the English Channel. Tidal free-surface elevations at open boundaries derive from harmonic components of TPOEX/Poseidon 6 database (Egbert and Erofeeva, 2002) while wind speeds above free surface are provided by meteorological ALADIN (Bénard, 2004; Météo-France). Waves effects are included following the parameterization adopted by Soulsby et al. (1993) on interactions between wave and current bottom boundary layers, with wave input parameters taken from the IOWAGA (Integrated Ocean WAves for Geophysical and other Applications) database (Ifremer, Ardhuin et al., 2011). Sediment transport is finally computed for the four finest grain size classes of silts ($d_1$ = 25 μm), very fine sands ($d_2$ = 75 μm), fine sands ($d_3$ = 150 μm) and medium sands ($d_4$ = 350 μm). SSC inputs of fine suspended particles ($d_1$ = 25 μm) are considered at open boundaries according to the statistical model developed by Rivier et al. (2012). ROMS is finally run during two years, 2007 and 2008, considering the first year as an initialization period.

Predictions are assessed against local and synoptic observations of near-surface SSC derived from raw MODIS/AQUA (MODerate resolution Imaging Spectroradiometer, NASA) and MERIS (MEdium Resolution Imaging Spectrometer, ESA) satellite images (Gohin, 2011). Whereas points predictions show a general tendency to underestimate highest observed concentrations in winter following results from Sykes and Barcelia (2012), the local evaluation confirms model's capability to approach observed spring-neap tidal modulations of near-surface concentrations (Fig. 2). Synoptic evaluations exhibit furthermore model's performances in approaching the large-scale variability of near-surface SSC characterized by (1) strong horizontal gradients in nearshore regions and (2) a prominent turbid area around the Isle of Wight (Fig. 3). These predictions approach also secondary features identified in the vicinity of protruding headlands and isles along the English and French coastlines.

## 3. Results and discussion

### 3.1. Global effects of tides and waves

ROMS' implementation by Guillou et al. (2015) in the English Channel primary focused on improvements of predictions neglecting further investigations about the effects of tides and waves on near-surface SSC variability. Numerical results are exploited here to assess spatial and temporal variabilities of near-surface concentrations in relation to major hydrodynamic forcings of tides and waves. Fig. 4 shows the maximum predicted near-surface SSC during the year 2008 and its relative increase with respect to yearly-averaged concentrations. Temporal variations of surface concentrations are particularly pronounced in the most turbid areas of the English Channel. Whereas offshore waters show weak SSC variations in relation to reduced concentrations and near-bed resuspensions, coastal waters exhibit significant evolutions at a distance up to 10 km from French and English coastlines. This spatial "zonation" between high turbid coastal waters and low turbid central waters confirms previous investigations conducted by Fettweis et al. (2012) or Lafite et al. (2000) in the English Channel.

These variations of near-surface coastal SSC appear primary associated with waves effects on seabed sediments. As exhibited by Grochowski and Collins (1994), sand-sized particles may be disturbed by wave activity during more than 20 % of a year over most of nearshore waters of the English

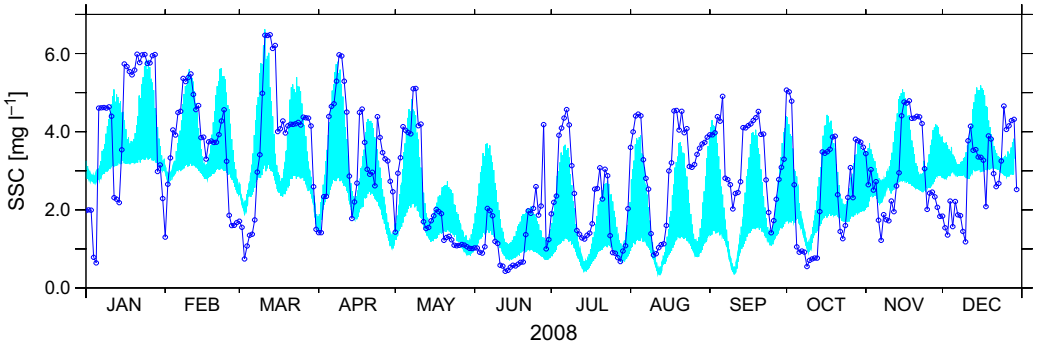


**Figure 2** Time series of suspended sediment concentrations (SSC) (light blue) observed and (dark blue) predicted off the Cotentin Peninsula (point A). (For interpretation of the references to color in this figure legend, the reader is referred to the web version of this article.)
Adapted from Guillou et al. (2015).

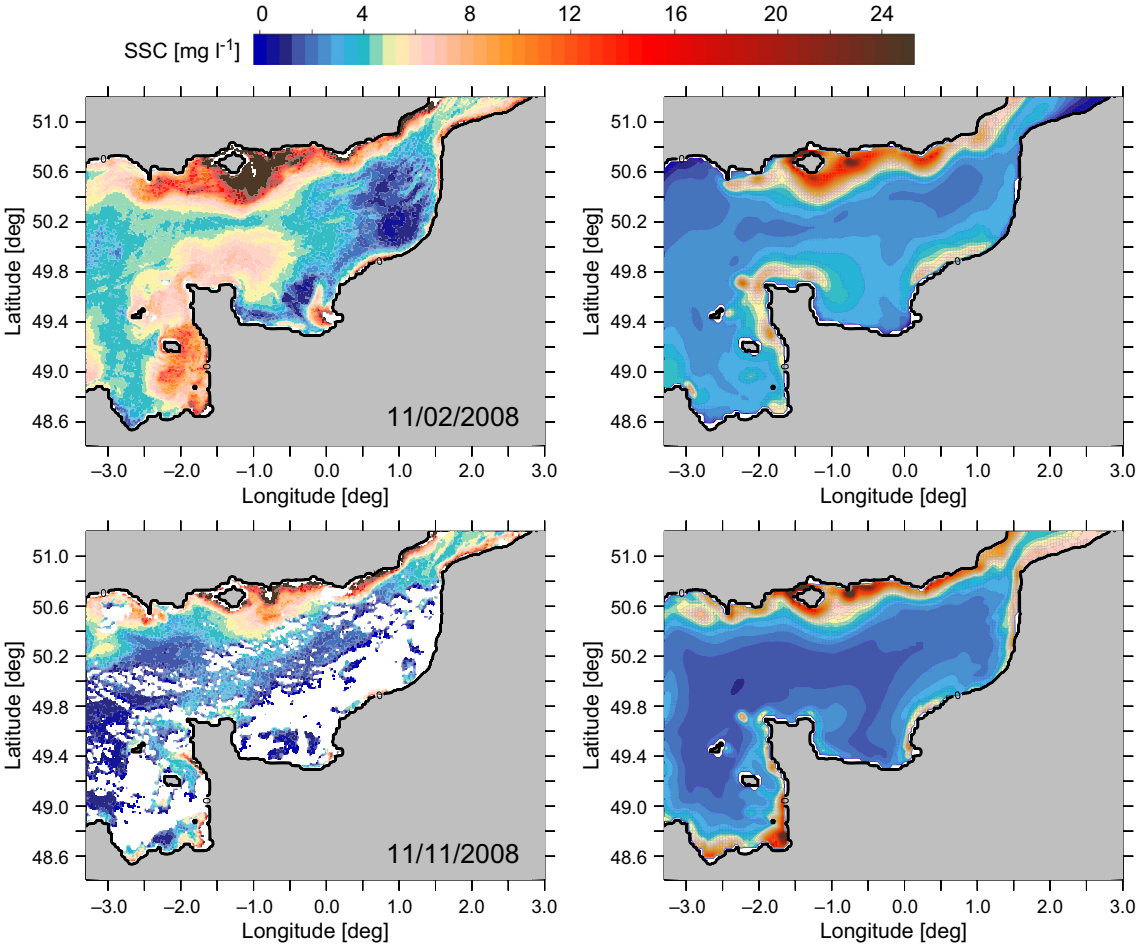


**Figure 3** Near-surface suspended sediment concentrations (SSC) observed (right) and computed (left) for stormy for stormy wave conditions and spring (11 February 2008) and mean (11 November 2008) tides.
Adapted from Guillou et al. (2015).

Channel. This period corresponds globally to storm waves conditions of autumn and winter. In the present investigation, the associated near-surface concentrations present thus strong temporal variations with mean values over 8 mg $l^{-1}$ against less than 4 mg $l^{-1}$ in summer and spring (Fig. 5). Maximum near-surface SSC are furthermore reaching values over 40 mg $l^{-1}$ with increase by a factor from 10 to 18 in comparison with time-averaged concentrations (Fig. 4b). Whereas seldom in situ SSC measurements are available in the English Channel to confirm these values, comparable increase have been reported from field studies near the Isle of Wight by Velegrakis et al. (1997). These predictions are also consistent with broader observations conducted in the southern North Sea off Maplin Sand (UK) by Owen and Thorn (1978). Predicted increase factors fall finally in the range of numerical values obtained by Gerritsen et al. (2000) in the eastern English Channel.

Influences of tides and waves on near-surface SSC are finally investigated displaying Pearson's correlation coefficients between (1) predicted concentrations and (2) integrated parameters characterizing the local evolution of hydrodynamic forcings. These site-specific explanatory parameters are (1) the tidal free-surface elevation and (2) the significant wave height at point B in the eastern English Channel (Fig. 1). Point B corresponds to the offshore lightship 62305 of the UK Meteorological Office. Resulting spatial distributions of correlation coefficients (Fig. 6) refine the cartography previously established by Rivier et al. (2012) on the basis of remote-sensing images over the period 2003–2009. Indeed, applying statistical treatments on satellite images, an initial cartography was obtained identifying, at a coarse spatial resolution of 36 km, areas of the English Channel where near-surface SSC are highly correlated with spring-neap tidal variations. Strong tidal modulations of near-surface concentrations were exhibited in the eastern English Channel with null to low influence in the western Channel in relation to dominant waves conditions. Whereas the present investigation is restricted to the year 2008, the resulting spatial distributions of correlation coefficients (Fig. 6) confirm the large-scale influence of tides on near-surface SSC modulations. Spring-neap tidal correlations appear however moderated in the Channel Islands Gulf where waves are predominantly influencing the evolution of near-surface SSC. The refined spatial resolution obtained by the exploitation of numerical predictions reveals finally a strong influence of tidal cycles along the French southern Dover Strait corroborating previous estimations performed by Guillou et al. (2009) and Guillou and Chapalain (2011) in these areas.

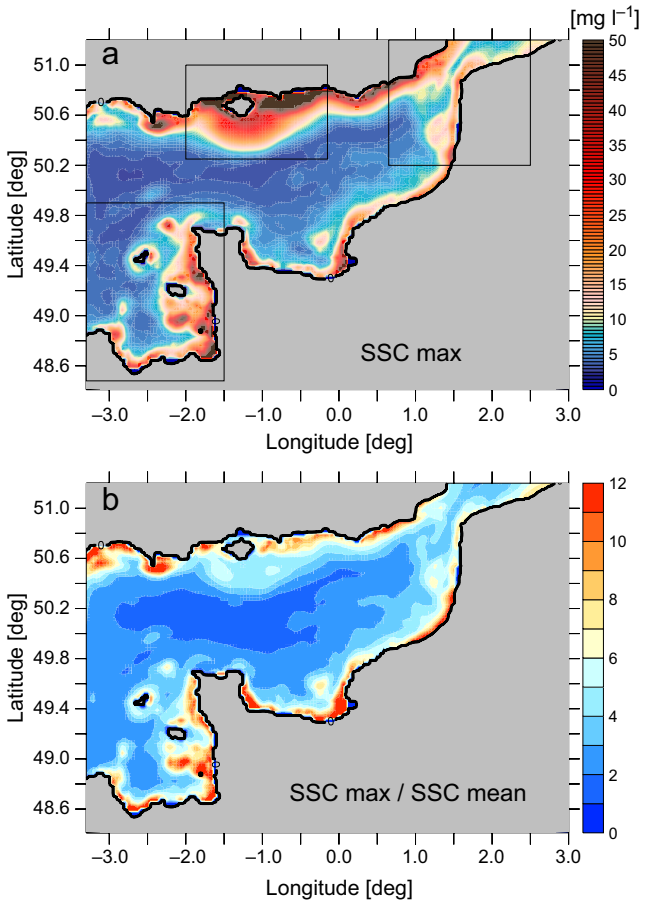


**Figure 4** (a) Maximum predicted near-surface suspended sediment concentrations (SSC) in 2008 with the areas of interest delineated in black rectangles. (b) Relative increase of predicted near-surface suspended sediment concentrations with respect to averaged concentrations for the year 2008.

### 3.2. Variability of nearshore near-surface SSC patterns

Further investigation is conducted focusing on the temporal variability of (1) nearshore concentrations patterns separating French and English coastal waters and (2) areas with the highest contributions around the Isle of Wight, in the Channel Island Gulf and in the Dover Strait (Fig. 4a). Mean near-surface SSC of French and English waters show nearly similar temporal evolutions in spring and summer whereas more significant differences are exhibited in winter (Fig. 7a). In January, maximum concentrations are thus reaching peak values over 16 mg $l^{-1}$ in English coastal waters while maximum concentrations remain below 10 mg $l^{-1}$ in French waters. These differences are mainly associated with the contribution of the area of high concentrations identified around the Isle of Wight (Fig. 7b). The evolution of near-surface SSC of English coastal waters is directly correlated with the temporal variability of concentrations around the Isle of Wight. As identified in Fig. 6, this latter region experiences significant influences of tide and wave forcings corroborating previous investigations performed by Velegrakis et al. (1997, 1999). Tidal currents influence thus advection of finest suspended particles along the west-eastern direction modulating the longshore extension of the turbid area around the Isle of Wight at semi-diurnal frequencies. This evolution is modulated by waves which impact the northern offshore extension of this area with noticeable effects during storm events when near-surface concentrations are reaching values of 20 mg $l^{-1}$ at a distance of 20 km from the Isle of Wight (Figs. 3 and 4).

In addition to this prominent area, two major nearshore resuspensions regions are identified in (1) the Channel Islands Gulf and (2) the Dover Strait (Fig. 4a). Confirming previous investigations performed in Section 3.1 (Fig. 6), averaged concentrations in these areas are strongly influenced by tides with spring-neap modulations of predicted SSC (Fig. 7b). Waves are however found to impact the variability of concentrations in coastal waters with noticeable effects between the months of October and February. This influence is exhibited in the central part of the Dover Strait where waves modify very clearly the "zonation" between central and coastal waters. Confirming previous estimates performed by Eisma and Kalf (1979), Lafite et al. (2000), Mc Cave (1973) and Van Alphen (1990), three main areas of resuspensions are thus revealed: (1) the English coastline with weakest coastal SSC, (2) the transitional zone of gravel and pebbles deposits where no resuspension occurs and (3) the French coastal zone showing the highest concentrations.

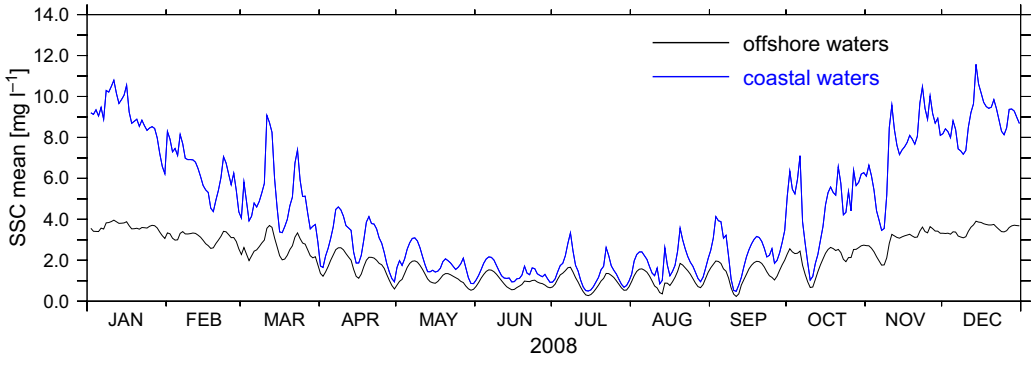


**Figure 5** Time series of predicted averaged near-surface suspended sediment concentrations (SSC) in coastal and offshore waters of computational domain.

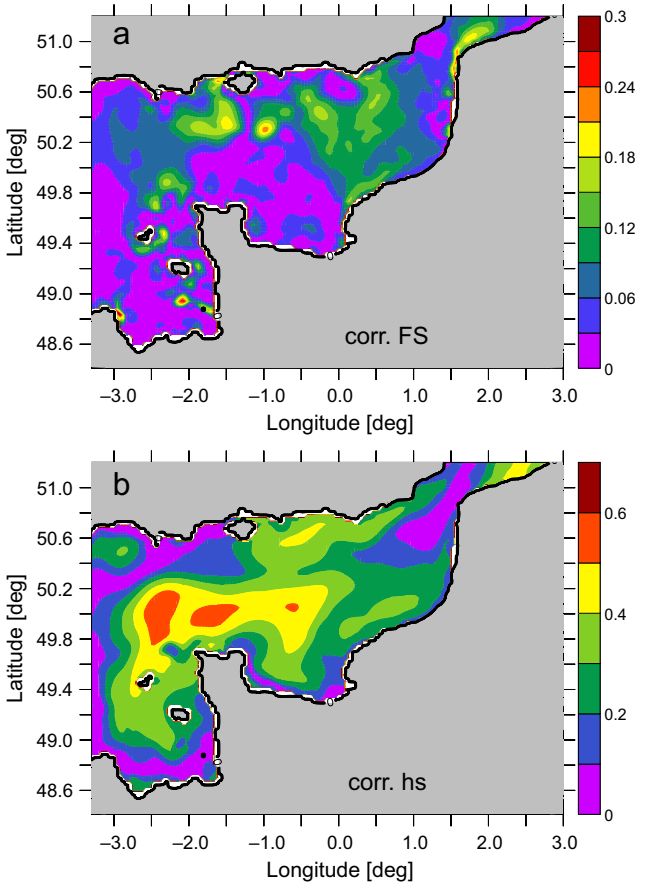


**Figure 6** Correlation coefficients between predicted near-surface suspended sediment concentrations (SSC) and (a) predicted tidal free-surface elevation and (b) observed significant wave height at point B in 2008.

### 3.3. Influence of the granulometric distribution of suspended sediments

As exhibited by Sykes and Barcelia (2012), the granulometric distribution of near-surface suspended sediments influences the temporal variability of the total SSC. Strong temporal variabilities may thus appear as a result of a bi-modal distribution of silts and sands. Indeed, sands contribution to mean concentrations is generally characterized by quarter-diurnal variations in relation to local resuspensions whereas silts evolution may be semi-diurnal as a consequence of remote advection (Jago et al., 1993; Van der Molen et al., 2009). In the English Channel, these processes have been identified on the basis of a comparison between numerical predictions and in situ measurements by (1) Guillou et al. (2009) and Guillou and Chapalain (2011) in the southern Dover Strait and (2) Velegrakis et al. (1997) in the south-eastern edge of the Isle of Wight. These effects are particularly noticeable in nearshore waters in relation to increased influences of waves on the sea floor (Grochowski and Collins, 1994). In the present investigation, bi-modal distributions are thus exhibited off coastal irregularities of the Channel Islands Gulf, the Isle of Wight, the Cotentin Peninsula and the southern Dover Strait (Fig. 8). These nearshore grain-size variabilities contrast with the nearly uniform grain-size distribution of offshore near-surface SSC characterized by an average silt contribution over 90%.

This local heterogeneity of suspended concentrations has to be considered when processing satellite reflectance data. In this study, the backscattering coefficient by unit mass has been considered constant for a given area neglecting inherent optical properties of suspended particles in relation to size and composition (Gohin, 2011; Rivier et al., 2012). This assumption may thus result in differences in the estimation of near-surface SSC from remote-sensing data particularly noticeable in the highly localized energetic regions of the

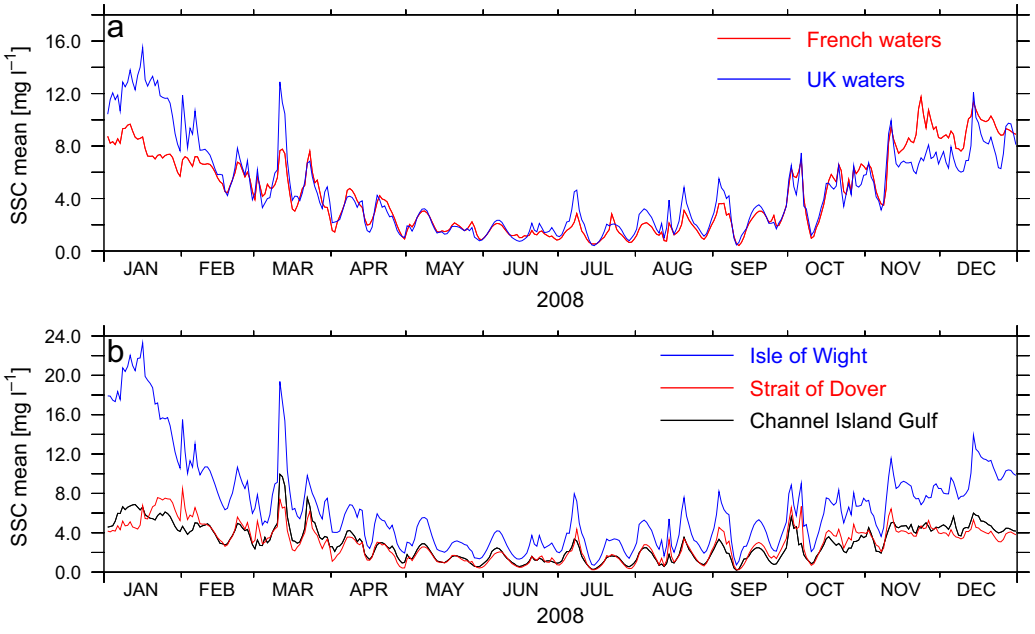


**Figure 7** Time series of predicted averaged near-surface suspended sediment concentrations (SSC) over different areas of computational domain.

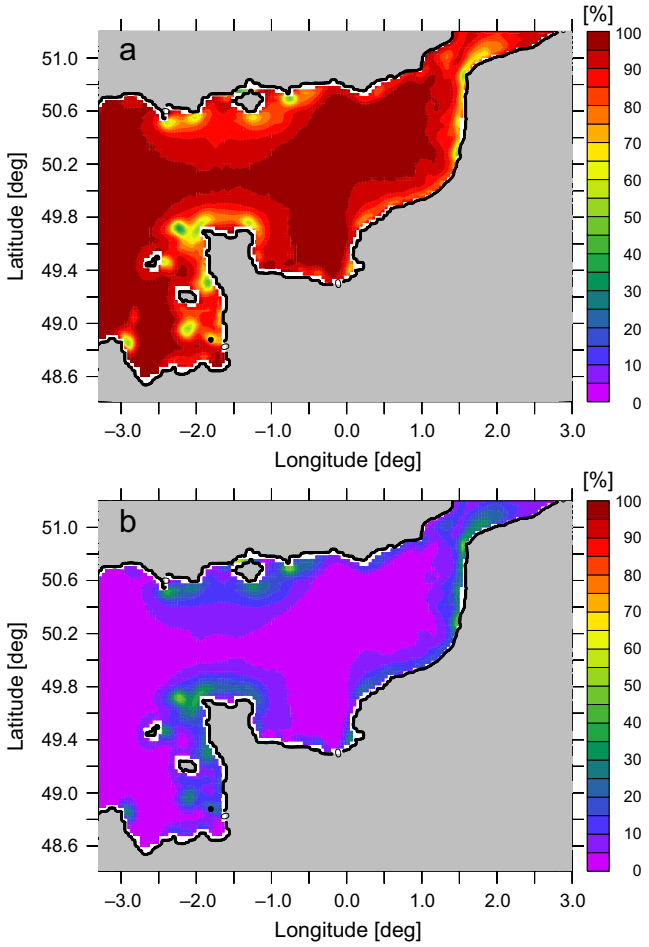


**Figure 8** Percentages of (a) silts and (b) sands in the mean predicted near-surface suspended sediment concentrations (SSC) in 2008.

English Channel (Bowers and Binding, 2006; Bowers and Braithwaite, 2012; Lubac and Loisel, 2007). Integrating the grain-size variability of near-surface concentrations may improve estimations derived from remote-sensing data in the nearshore areas.

## 4. Conclusions

Numerical predictions from the Regional Ocean Modeling System ROMS assessed against satellite-retrieved images have been exploited to investigate the spatial and temporal variabilities of near-surface SSC in coastal waters of the English Channel. The main outcomes of the present study are the following:

1. Predictions exhibit significant temporal variations of near-surface concentrations in coastal waters with increase from 10 to 18 in comparison with time-averaged values. Considering the refined spatial resolution of the computational mesh, two cartographies are produced exhibiting correlations of near-surface SSC with tidal free-surface elevation and significant wave height. Waves influence is exhibited in the Channel Islands Gulf while strong tidal correlations are revealed in the southern Dover Strait.
2. The granulometric distribution of near-surface suspended sediments has been identified exhibiting local bi-modal distributions of silts and sands with a strong influence on SSC variabilities. Whereas near-surface SSC appears predominantly composed of silts, sands may contribute locally to suspended concentrations in the most energetic areas of the English Channel. This may furthermore result in local grain-size heterogeneity of suspended sediments with possible biases in the estimation of associated concentrations from remote-sensing images.

The present study provides interesting insights about the spatial and temporal variabilities of near-surface SSC in the English Channel complemented previous studies based on remote-sensing data. This research will naturally benefit from extended comparisons of numerical predictions with in situ observations based on acoustic and/or optical devices in conjunction with direct sampling of surface water for evaluation of measurements accuracy. Taking into account errors usually associated with remote-sensing images during rougher sea states, these in situ measurements will confirm model's performances in the most turbid areas during storm events. This objective will be achieved with longer simulations covering major measurements campaigns in the English Channel. This long-term evaluation of near-surface SSC will also assess the variability of suspended sediment transport in relation to the inter-annual variability of wave climate in the English Channel. The present modeling focuses furthermore on disturbances induced by tides and waves on near-surface SSC neglecting a refined evaluation of predicted concentrations distributions in the entire water column, exhibiting, in particular, near-bed concentrations. Further investigations are thus required about effects of tides and waves on near-bed sediments. Whereas further studies can be conducted about the role of wind on near-surface concentrations, another prospective of this research will also consist in incorporating fluxes of fresh waters and sediments through river boundaries. These developments will finally aim at improved estimations of sediment fluxes through the English Channel.

## Acknowledgements

The authors are particularly grateful to MyOcean project (European Commission, http://www.myocean.eu) and the Space Agencies for providing access to ocean color data from MODIS (NASA) and MERIS (ESA). Wave data were supplied by the IOWAGA project (http://wwz.ifremer.fr/iowaga/Products). Wind fields data of the meteorological model ALADIN were provided by Météo-France. Simulations were performed on computer facilities CAPARMOR ("Calcul PARallèle Mutualisé pour l'Océanographie et la Recherche"). The present paper is a contribution to the research programs HERMES and FLUSED of the Cerema (DTEMF/DS/LGCE, Laboratory of Coastal Engineering and Environment) (http://memphys-lgce.fr.ht).

## References


Ardhuin, F., Hanafin, J., Quilfen, Y., Chapron, B., Queffeulou, P., Obrebski, M., 2011. Calibration of the IOWAGA global wave hindcast (1991–2011) using ECMWF and CFSR winds. In: 12th Int. Workshop on Wave Hindcasting and Forecasting, Kohala Coast, Hawaii.

Bénard, P., 2004. ALADIN-NH/AROME dynamical core; status and possible extension to IFS. In: Proc. ECMWF Seminar on Recent Developments in Numerical Methods for Atmosphere and Ocean Modelling, Reading, UK, 27–40.

Bowers, D.G., Binding, C.E., 2006. The optical properties of mineral suspended particles: a review and synthesis. Estuar. Coast. Shelf Sci. 67 (1–2), 219–230, http://dx.doi.org/10.1016/j.ecss.2005.11.010.

Bowers, D.G., Braithwaite, K.M., 2012. Evidence that satellite sense the cross-sectional area of suspended particles in shelf seas and estuaries better than their mass. Geo-Mar. Lett. 32 (2), 165–171, http://dx.doi.org/10.1007/s00367-011-0259-6.

Dupont, J.P., Collins, M.B., Lafite, R., Nash, L., Huault, M.F., Shimwell, S.J., Chaddock, S., Brunet, C., Wartel, M., Lamboy, M., 1993. Annual variations in suspended particulate matter within the Dover Strait. Oceanol. Acta 16 (5–6), 507–516.

Egbert, G., Erofeeva, S., 2002. Efficient inverse modeling of barotropic ocean tides. J. Atmos. Ocean. Technol. 19 (2), 183–204, http://dx.doi.org/10.1175/1520-0426(2002)019%3C0183:EIMOBO%3E2.0.CO;2.

Eisma, D., Kalf, J., 1979. Distribution and particle size of suspended matter in the Southern North Sea. Neth. J. Sea Res. 13 (2), 298–324, http://dx.doi.org/10.1016/0077-7579(79)90008-5.

Fettweis, M., Monbaliu, J., Baeye, M., Nechad, B., Van den Eynde, D., 2012. Weather and climate induced variability of surface suspended particulate matter concentration in the North Sea and the English Channel. Methods Oceanogr. 3–4, 25–39, http://dx.doi.org/10.1016/j.mio.2012.11.001.

Fettweis, M., Nechad, B., Van den Eynde, D., 2007. An estimate of the suspended particulate matter (SPM) transport in the southern North Sea using Sea WiFS images, in situ measurements and numerical model results. Cont. Shelf Res. 27 (10–11), 1568–1583, http://dx.doi.org/10.1016/j.csr.2007.01.017.

Gerritsen, H., Vos, R., der Kaaij, T.V., Lane, A., Boon, J., 2000. Suspended sediment modelling in a shelf sea (North Sea). Coast. Eng. 41 (1–3), 317–352, http://dx.doi.org/10.1016/S0378-3839(00)00042-9.

Gohin, F., 2011. Annual cycles of chlorophyll-*a*, non-algal suspended particulate matter and turbidity observed from space and in-situ in coastal waters. Ocean Sci. 7 (5), 705–732, http://dx.doi.org/10.5194/os-7-705-2011.

Gohin, F., Loyer, S., Lunven, M., Labry, C., Froidefond, J.M., Delmas, D., Huret, M., Herbland, A., 2005. Satellite-derived parameters for biological modelling in coastal waters: illustration over the eastern continental shelf of the Bay of Biscay. Remote Sens. Environ. 95 (1), 29–46, http://dx.doi.org/10.1016/j.rse.2004.11.007.

Grochowski, N.T.L., Collins, M.B., 1994. Wave activity on the sea-bed of the English Channel. J. Mar. Biol. Assoc. U. K. 74 (3), 739–742, http://dx.doi.org/10.1017/S0025315400047792.

Grochowski, N.T.L., Collins, M.B., Boxall, S.R., Salomon, J.C., 1993. Sediment transport predictions for the English Channel, using numerical models. J. Geol. Soc. (London, U.K.) 150 (3), 683–695, http://dx.doi.org/10.1144/gsjgs.150.4.0683.

Guillou, N., Chapalain, G., 2011. Modelling impact of northerly wind generated waves on sediments resuspensions in the Dover Strait and adjacent waters. Cont. Shelf Res. 31 (18), 1894–1903, http://dx.doi.org/10.1016/j.csr.2011.08.011.

Guillou, N., Chapalain, G., Thais, L., 2009. Three-dimensional modeling of tide-induced suspended transport of seabed multi-component sediments in the eastern English Channel. J. Geophys. Res. 114, C07025, http://dx.doi.org/10.1029/2008JC004791.

Guillou, N., Rivier, A., Gohin, F., Chapalain, G., 2015. Modeling near-surface suspended sediment concentration in the English Channel. J. Mar. Sci. Eng. 3 (2), 193–215, http://dx.doi.org/10.3390/jmse3020193.

Haarich, M., Kienz, W., Krause, M., Schmidt, G.P.Z.D., 1993. Heavy metal distribution in different compartments of the northern North Sea and adjacent areas. Ocean Dyn. 45 (5), 313–336, http://dx.doi.org/10.1007/BF02225884.

Haidvogel, D.B., Arango, H.G., Hedstrom, K., Beckman, A., Malanotte-Rizzoli, P., Shchepetkin, A.F., 2000. Model evaluation experiments in the North Atlantic Basin: simulations in nonlinear terrain-following coordinates. Dyn. Atmos. Oceans 32 (3–4), 239–281, http://dx.doi.org/10.1016/S0377-0265(00)00049-X.

Hoppe, H.G., 1984. Attachment of bacteria: advantage or disadvantage for survival in the aquatic environment. In: Marshall, K.C. (Ed.), Microbial Adhesion and Aggregation, Life Sci. Res. Rep. ñ131. Springer-Verlag, New York, 283–303, http://dx.doi.org/10.1007/978-3-642-70137-5_19.

Jago, C.F., Bale, A.J., Green, M.O., Howarth, M.J., Jones, S.E., McCave, I.N., Millward, G.E., Morris, A.W., Rowden, A.A., Williams, J.J., Hydes, D., Turner, A., Huntley, D., Van Leussen, W., 1993. Resuspension processes and Seston dynamics, southern North Sea. Philos. Trans. R. Soc. Lond. A 343 (1669), 475–491, http://dx.doi.org/10.1098/rsta.1993.0060.

Lafite, R., Shimwell, S., Grochowski, N., Dupont, J.P., Nash, L., Salomon, J.C., Cabioch, L., Collins, M., Gao, S., 2000. Suspended particulate matter fluxes through the Straits of Dover, English Channel: observations and modelling. Oceanol. Acta 23 (6), 687–699, http://dx.doi.org/10.1016/S0399-1784(00)00144-4.

Leprêtre, A., Chapalain, G., Carpentier, P., 2006. A spatial interpolation method of granulometric properties of superficial sediments. Bull. Soc. Geol. Fr. 177 (2), 89–95, http://dx.doi.org/10.2113/gssgfbull.177.2.89.

Lubac, B., Loisel, H., 2007. Variability and classification of remote sensing reflectance spectra in the eastern English Channel and southern North Sea. Remote Sens. Environ. 110 (1), 45–58, http://dx.doi.org/10.1016/j.rse.2007.02.012.

Mc Cave, I.N., 1973. Mud in the North Sea science. In: Goldberg, E.D. (Ed.), North Sea Science. M.I.T. Press, 75–100.

Menesguen, A., Gohin, F., 2006. Observation and modelling of natural retention structures in the English Channel. J. Mar. Syst. 63 (3–4), 244–256, http://dx.doi.org/10.1016/j.jmarsys.2006.05.004.

Owen, M., Thorn, M., 1978. Effect of waves on sand transport by currents. In: Proc. 16th Conf. Coastal Eng. Hamburg, 1675–1687, doi:10.9753/icce.v16.%25p.

Rahbani, M., 2015. A comparison between the suspended sediment concentrations derived from DELFT3D model and collected using transmissometer – a case study in tidally dominated area of Dithmarschen Bight. Oceanologia 57 (1), 44–49, http://dx.doi.org/10.1016/j.oceano.2014.06.002.

Rivier, A., Gohin, F., Bryère, P., Petus, C., Guillou, N., Chapalain, G., 2012. Observed vs. predicted variability in non-algal suspended particulate matter concentration in the English Channel in relation to tides and waves. Geo-Mar. Lett. 32 (2), 139–151, http://dx.doi.org/10.1007/s00367-011-0271-x.

Soulsby, R.L., Hamm, L., Klopman, G., Myrhaug, D., Simons, R.R., Thomas, G.P., 1993. Wave–current interaction within and outside the bottom boundary layer. Coast. Eng. 21 (1–3), 41–69, http://dx.doi.org/10.1016/0378-3839(93)90045-A.

Souza, A.J., Holt, J.T., Proctor, R., 2007. Modelling SPM on the NW European shelf seas. In: Balson, P, Collins, M. (Eds.), Coastal and Shelf Sediment Transport. Geol. Soc., London, 147–158, http://dx.doi.org/10.1144/GSL.SP.2007.274.01.14.

Sykes, P.A., Barcelia, R.M., 2012. Assessment and development of a sediment model within an operational system. J. Geophys. Res. 117, C04036, http://dx.doi.org/10.1029/2011jc007420.

Van Alphen, J., 1990. A mud balance for Belgian-Dutch coastal waters between 1969 and 1986. Neth. J. Sea Res. 25 (1—2), 19—30, http://dx.doi.org/10.1016/0077-7579(90)90005-2.

Van der Molen, J., Bolding, K., Greenwoord, N., Mills, D.K., 2009. A 1-D vertical multiple grain size model of suspended particulate matter in combined currents and waves in shelf seas. J. Geophys. Res. 114, F01030, http://dx.doi.org/10.1029/2008jf001150.

Velegrakis, A.F., Gao, S., Lafite, R., Dupont, J.P., Huault, M.F., Nash, L.A., Collins, M.B., 1997. Resuspension and advection processes affecting suspended particulate matter concentrations in the central English Channel. J. Sea Res. 38 (1—2), 17—34, http://dx.doi.org/10.1016/S1385-1101(97)00041-5.

Velegrakis, A.F., Michel, D., Collins, M.B., Lafite, R., Oikonomou, E. K., Dupont, J.P., Huault, M.F., Lecouturier, M., Salomon, J.C., Bishop, C., 1999. Sources, sinks and resuspension of suspended particulate matter in the eastern English Channel. Cont. Shelf Res. 19 (15—16), 1933—1957, http://dx.doi.org/10.1016/S0278-4343(99)00047-3.

Warner, J.C., Sherwood, C.R., Signell, R.P., Harris, C.K., Arango, H. G., 2008. Development of a three-dimensional, regional, coupled wave, current, and sediment-transport model. Comput. Geosci. 34 (10), 1284—1306, http://dx.doi.org/10.1016/j.cageo.2008.02.012.

Wozniak, S.B., 2014. Simple statistical formulas for estimating biogeochemical properties of suspended particulate matter in the southern Baltic Sea potentially useful for optical remote sensing applications. Oceanologia 56 (1), 7—39, http://dx.doi.org/10.5697/oc.56-1.007.

Oceanologia (2017) 59, 37—48

Available online at www.sciencedirect.com

ScienceDirect

journal homepage: www.journals.elsevier.com/oceanologia/

ORIGINAL RESEARCH ARTICLE

# Characteristics and inter-annual changes in temperature, salinity and density distribution in the Gulf of Riga

**Maris Skudra** [a,b,*], **Urmas Lips** [a]

[a] *Marine Systems Institute, Tallinn University of Technology, Tallinn, Estonia*
[b] *Latvian Institute of Aquatic Ecology, Riga, Latvia*

Received 12 January 2016; accepted 4 July 2016
Available online 16 July 2016

**KEYWORDS**
Gulf of Riga;
Temperature;
Salinity;
Vertical stratification;
Internal Rossby radius

**Summary** Available CTD profiles from the Gulf of Riga (May—August, 1993—2012) were analyzed to study inter-annual and long-term changes in temperature, salinity and density in relation to river runoff and atmospheric forcing (e.g. Baltic Sea Index). To describe temporal changes in vertical stratification, the upper mixed layer (UML) and deep layer (DL) parameters were estimated. On average the UML depth increases from 8.7 m in May to 9.0, 11.5 and 13.7 m in June, July and August, respectively, and the UML temperature increases from 8.0°C to 12.5, 18.7 and 18.6°C (May, June, July and August) while the UML salinity increases from 4.90 g kg$^{-1}$ to 5.14, 5.28 and 5.38 g kg$^{-1}$, respectively. High correlation ($r$ = −0.82) was found between the inter-annual changes in river runoff (spring) and mean salinity in the UML in August as well as between DL mean salinity ($r$ = 0.88) and density ($r$ = 0.84) in the Irbe Strait and DL mean salinity and density in the Gulf of Riga. Inter-annual changes in the UML depth as well as in DL salinity and density had a significant correlation with the changes in Baltic Sea Index. The strongest stratification (August) can be observed in the years with the highest UML temperature and the highest river run-off in spring. We suggest that the predicted increase in water temperature and changes in river run-off due to the climate change would result in faster development of the seasonal thermocline in spring and stronger vertical stratification in summer.


* Corresponding author at: Marine Systems Institute, Tallinn University of Technology, Akadeemia Rd. 15A, 12618 Tallinn, Estonia. Tel.: +371 28740641; fax: +372 620 4301.
*E-mail address:* maris.skudra@msi.ttu.ee (M. Skudra).
Peer review under the responsibility of Institute of Oceanology of the Polish Academy of Sciences.

Production and hosting by Elsevier

http://dx.doi.org/10.1016/j.oceano.2016.07.001

## 1. Introduction

The Gulf of Riga (GoR) is a relatively closed basin in the eastern part of the Baltic Sea with surface area of 17,913 $km^2$ and volume 405 $km^3$ (Leppäranta and Myrberg, 2009). It has two openings – the Irbe Strait (sill depth of 25 m and cross-section of 0.4 $km^2$) in the western part and the Suur Strait (sill depth of 5 m and cross-section of 0.04 $km^2$) in the northern part of the gulf with 70–80% (Petrov, 1979) of the water exchange occurring through the Irbe Strait. The mean depth of the GoR is 26 m which is about two times less than in the Baltic Sea. The deepest regions of the gulf are situated to the east and southeast from Ruhnu Island where depth reaches about 56 m, although, the deepest spot in the whole GoR is Mersraga Trough (width about 50 m and length 4.5 km) with the depth of 66 m (Stiebrins and Väling, 1996) situated approximately 13 km to the north from the village of Mersrags.

The catchment area of the GoR consists of 134,000 $km^2$ with five major rivers discharging into the GoR – Daugava, Lielupe, Gauja, Pärnu and Salaca. First three are located in the southern part of the gulf where approximately 86% of all river run-off occurs (Berzinsh, 1995) and latter two in the eastern part. Annual mean run-off to the gulf in 1950–2012 has been stated as 1013.5 $m^3 s^{-1}$ (Kronsell and Andersson, 2014) or approximately 32 $km^3$ which is about 7.9% of the volume of the gulf. It has been showed that river run-off together with the limited water exchange are the main reasons for the observed horizontal salinity difference in the surface layer – salinity decreases from the Irbe Strait to the southern part of the gulf (see e.g. Berzinsh, 1980, 1995; Stipa et al., 1999). The strongest difference can be observed in April and May when the influence of the river discharge is at its maximum and salinity decreases from about 6.0 PSU (Practical Salinity Scale) in the Irbe Strait to 2.0 PSU and less close to the mouths of Daugava and Lielupe. Slight surface salinity difference (about 1.0–1.5 PSU) can be observed also across the gulf from west to east during April (Stipa et al., 1999).

Water temperature in the GoR has a seasonal pattern – during November–February cooling of the whole water column occurs, March–April marks the start of the water column warming from surface layers which intensifies and reaches maximum during May–August and is again followed by a steady cooling during September–October. Data analysis during 1963–1990 revealed that mean temperature for the whole water column in winter, spring, summer and autumn was 0.0, 2.8, 12.0 and 9.0°C, respectively (Berzinsh, 1995). It was reported (Raudsepp, 2001) that seasonal changes in thermal stratification are consistent with the annual cycle of air-sea heat exchange. Due to these seasonal characteristics the whole water column in the GoR is thermally well mixed during December–March, whereas, seasonal thermocline starts to develop in April and the strongest stratification can be observed in August. More detailed analysis on stratification in the GoR is described in the research by Stipa et al. (1999).

According to the previous studies (Berzinsh, 1980, 1995) there have been two periods with opposite tendencies regarding salinity – from beginning of 1960s till 1977 average salinity increased (average rate of 0.035 PSU per year), whereas, from 1977 till early 1990s salinity decreased (0.041 PSU per year) which was mainly related to the dynamics of long-term river run-off. Similar decline of salinity was also observed within different layers (expressed as mean values at 0, 10, 20, 30, 40 and 50 m) of the GoR (Raudsepp, 2001). Remote sensing data for 1990–2008 has showed a strong increase of the sea surface temperature (SST) in the GoR – about 0.8–1.0°C per decade with similar or slightly higher values only in the Gulf of Finland and Bothnian Bay (BACC, 2015). Long-term changes in both, temperature and salinity, not only influence the physical characteristics of the GoR but they can have an impact to the whole ecosystem of the gulf. For example, Jurgensone et al. (2011) reported that the temperature increase would affect the phytoplankton community in the GoR suggesting a shift from dinoflagellates to chlorophytes in summer. Kotta et al. (2009) stated that the reduction in salinity had negative consequences for most of the benthic invertebrate species referring to their salinity tolerance. In general, the dynamics of zooplankton, zoobenthos and fish in the GoR primarily relies on climatic conditions.

The main goal of the present study was to describe the vertical characteristics of temperature, salinity and density fields and their inter-annual variability in the GoR based on the CTD data collected during 1993–2012 (May–August) as well as possible connection of revealed changes with different forcing factors. Previous studies have mainly focused on short-term analysis of temperature and salinity data (Kõuts and Håkansson, 1995; Stipa et al., 1999) and/or covered only the time period until 1995 (Raudsepp, 2001). In addition, present research aimed to estimate the baroclinic Rossby radius on the basis of the existing CTD profiles with a similar approach as used by Alenius et al. (2003) for the Gulf of Finland. Based on the results of this analysis and taking into account the latest climate change predictions we also suggest what could happen in the future.

## 2. Material and methods

Present paper analyzed the CTD data collected in 1993–2012 during various monitoring programmes and research projects conducted by Latvian Institute of Aquatic Ecology, Marine Systems Institute at Tallinn University of Technology and Institute of Food Safety, Animal Health and Environment (Latvia) and their predecessors. Vertical profiles of different parameters were acquired with following CTD profilers – AROP 500, SBE 19plus SeaCAT, SBE 19 SeaCAT, Neil Brown Mark III and Idronaut OS320plus.

In total 3558 CTD casts were processed and 863 CTD casts were used in the present study from the period of May–August, 1993–2012 with Gulf of Riga borders set along 58°N latitude and 22.6°E longitude (Fig. 1). CTD profiles were processed and analyzed with vertical resolution of 0.5 m (constant for all profiles) and only stations with depth over 20 m were used. Availability of CTD profiles differed widely between the years and months (Table 1).

Upper mixed layer (UML) depth was estimated using smoothed (2.5 m moving average) vertical profiles of density and the UML depth was defined at each vertical profile as the shallowest depth where the density difference between consecutive data points was equal or exceeded 0.05 kg $m^{-3}$. The latter value was derived empirically as a value which best reflects the start of pycnocline and, thus,

**Table 1** The available CTD casts by year and month.

| Year | May | June | July | August | Total |
|---|---|---|---|---|---|
| 1993 | 15 | — | — | 11 | 26 |
| 1994 | 6 | 5 | 10 | 12 | 33 |
| 1995 | 19 | 17 | 15 | 15 | 66 |
| 1996 | 15 | — | — | 3 | 18 |
| 1997 | — | 3 | — | — | 3 |
| 1998 | 4 | 3 | — | 12 | 19 |
| 1999 | 2 | — | 9 | — | 11 |
| 2000 | — | — | — | 18 | 18 |
| 2001 | 29 | — | 8 | 20 | 57 |
| 2002 | 31 | 7 | 17 | 19 | 74 |
| 2003 | 31 | 9 | 10 | 30 | 80 |
| 2004 | 23 | 5 | 3 | 13 | 44 |
| 2005 | 11 | 9 | — | 12 | 32 |
| 2006 | 14 | — | 10 | 18 | 42 |
| 2007 | 29 | — | 17 | 23 | 69 |
| 2008 | 31 | 4 | 6 | 9 | 50 |
| 2009 | 28 | — | 3 | 24 | 55 |
| 2010 | 40 | — | 6 | 31 | 77 |
| 2011 | 20 | — | 6 | 15 | 41 |
| 2012 | 7 | 10 | 5 | 26 | 48 |
| Total | 355 | 72 | 125 | 311 | 863 |

the depth of UML. Smoothed vertical profiles of density were used to avoid possible fluctuations which might mislead the correct distinction of the UML by exceeding the selected density difference (0.05 kg $m^{-3}$) between consecutive data points. Deep layer (DL) was defined as a layer with depth >35 m and all estimated parameter characteristics of DL were obtained only from profiles deeper than 35 m. The salinity in the present study was expressed as absolute salinity [g $kg^{-1}$] and derived from CTD measured salinity values (on Practical Salinity Scale) using freely available software "Ocean Data View" (Schlitzer, 2010) and following TEOS-10 (Thermodynamic Equation Of Seawater — 2010) guidelines and Feistel et al. (2010).

River run-off data were calculated from monthly mean flow rates [$m^3$ $s^{-1}$] of four biggest rivers in Latvia discharging into the Gulf of Riga — Daugava, Gauja, Lielupe and Salaca (data provided by Latvian Environment, Geology and Meteorology Centre). The mouths of Daugava, Gauja and Lielupe are located in southern part, whereas, the mouth of Salaca in eastern part of the Gulf of Riga.

Available wind data were acquired from Sõrve (1995—2012), Ruhnu (2003—2012), Kihnu (1993—2011) and Pärnu (1993—2012) meteorological stations provided by Estonian Environment Agency. To characterize the atmospheric forcing conditions over the Gulf of Riga we analyzed the monthly-averaged Baltic Sea Index (BSI), which is the difference of normalized sea level pressures between Szczecin in Poland and Oslo in Norway (Lehmann et al., 2002; values provided by Andreas Lehmann).

Mean values of studied CTD parameters in May—August were estimated at the beginning as a simple arithmetic means of every month in each year. These values were further used to obtain the monthly mean values for the whole research period of 1993—2012 from which finally one mean value was derived for each parameter. For more detailed CTD parameter analyses we used only data from May and August and only those monthly mean values where available amount of CTD casts was equal or exceeded 5 casts in a month.

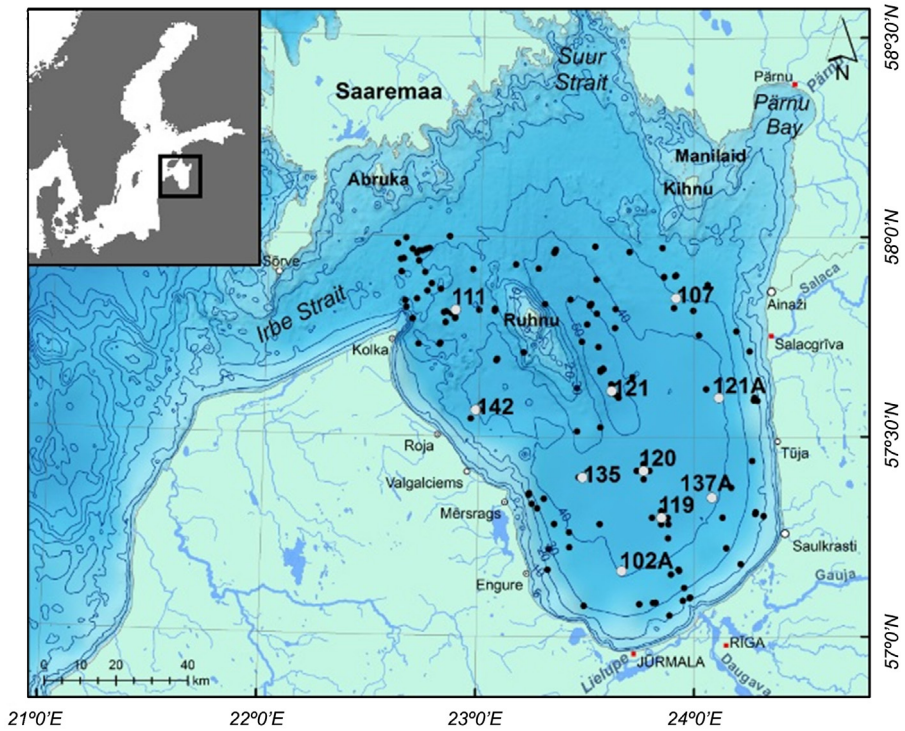


**Figure 1** Bathymetric map of the Gulf of Riga with CTD cast locations indicated with black dots (all stations) and white dots (10 main stations with station labels).

Rossby radius was calculated numerically solving eigenvalue problem using Runge—Kutta scheme combined with trial-and-error approach. See Chelton et al. (1998) for more detailed information about definition and calculation of Rossby radius.

In order to analyze the dynamics of various parameters in different parts of the GoR ten "main" stations (102A, 135, 142, 111, 119, 120, 121, 137A, 121A, 107) were chosen determined by the data availability from these stations (Fig. 1).

## 3. Results

### 3.1. Upper mixed layer

From analyzed 863 CTD casts we were able to define UML in 533 of them. Regarding monthly distribution of defined UML, from 356 CTD casts in May we defined UML in 133 (37%) of them and from 75 (June), 125 (July) and 311 (August) casts we defined UML in 35 (48%), 98 (78%) and 267 (85%) of them, respectively.

The mean UML depth derived from all available CTD casts in the Gulf of Riga in the period of 1993—2012 (May—August) was 10.7 m. The shallowest mean UML depth in the research period was found in May (8.7 m), it was deeper in June (9.0 m) and July (11.5 m) but the deepest UML was detected in August (13.7 m) (Fig. 2).

The UML mean salinity and temperature in the whole period were 5.17 g kg$^{-1}$ and 14.5°C, whereas density (expressed as sigma-t which is seawater density, where density value of 1000 kg m$^{-3}$ has been subtracted) — 2.95 kg m$^{-3}$. Salinity and temperature increased from 4.90 g kg$^{-1}$ and 8.0°C in May to 5.14 g kg$^{-1}$ and 12.5°C in June, to 5.28 g kg$^{-1}$ and 18.7°C in July and 5.38 g kg$^{-1}$ and 18.6°C in August, respectively. Mean UML density in May, June, July and August was 3.59, 3.32, 2.39 and 2.48 kg m$^{-3}$, respectively (Fig. 2).

#### 3.1.1. August

Greater amount of CTD casts in August allowed us to make more detailed inter-annual and long-term analysis of UML characteristics and suggest probable factors which may have impact on different UML parameters. The mean vertical structure of salinity in the GoR during 1993—2012 showed that salinity was about 5.3 g kg$^{-1}$ at the surface and around 6.0 g kg$^{-1}$ in the bottom layer, whereas, the mean vertical structure of temperature showed typical two-layer formation with thermocline situated approximately at 10—30 m depth (Fig. 3).

During the period of 1993—2012, the UML mean depth varied between different parts (10 main stations) of the GoR. Results showed that the UML mean depth was shallower in the western (W) part of the gulf ranging between 12.3 and 13.3 m (stations 111, 142, 135 and 102A), whereas, in the eastern (E) part the UML mean depth was deeper ranging between 14.6 and 15.4 m (stations 107, 121A and 137A). When looking at the section from the W to the E part of the GoR (stations 142-121-121A), an increase of the UML mean depth (start of the thermocline) can be observed (12.3, 14.2 and 14.6 m, respectively), thus, suggesting occurrence of differences between the two coastal areas in the gulf. The UML mean salinity also varied spatially during the research period. Results from 10 main stations revealed that on average the UML mean salinity was higher in the E part of the GoR (5.53, 5.42 and 5.37 g kg$^{-1}$ at stations 107, 121A and 137A, respectively) and slightly lower values were observed in the W part of the gulf (5.36, 5.31, 5.31 and 5.29 g kg$^{-1}$ at stations 111, 142, 135 and 102A, respectively). As expected, the UML mean salinity decreased towards the southern (S) part of the GoR where influence of river run-off is more pronounced than in the northern (N) part of the gulf.

The inter-annual variations of UML mean depth, temperature, salinity and density in August were noticeable but no clear tendency or trend could be detected in the period 1993—2012 (Fig. 4). Results from years 1993, 1994 and 2008 should be regarded with caution regarding the mean conditions in the gulf because of spatial distribution of stations in these years — in 1993 and 1994 the data only from the N and northwestern (NW) part and in 2008 only from the S part of the Gulf of Riga were available. This circumstance might explain rather big peaks in 1993 (UML mean depth) and 1994 (UML mean depth, temperature, density). Apart from that, the UML mean depth varied mainly between 10 and 20 m in the whole study period. Regarding the mean salinity, temperature and density, years 2003, 2006 and 2010 stand out from the whole period of inter-annual variability. Two salinity peaks were observed in 2003 (5.58 g kg$^{-1}$)

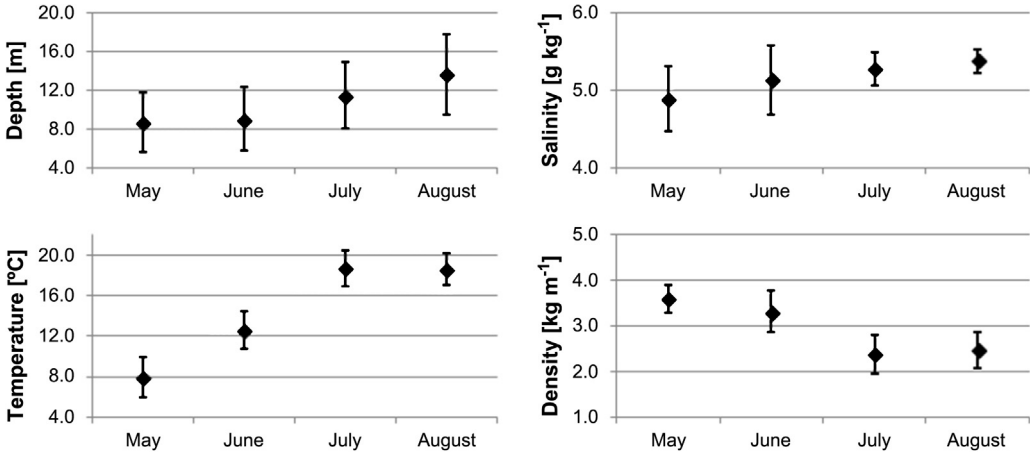


**Figure 2** Mean characteristics of upper mixed layer between 1993 and 2012 (May—August) with standard deviations.

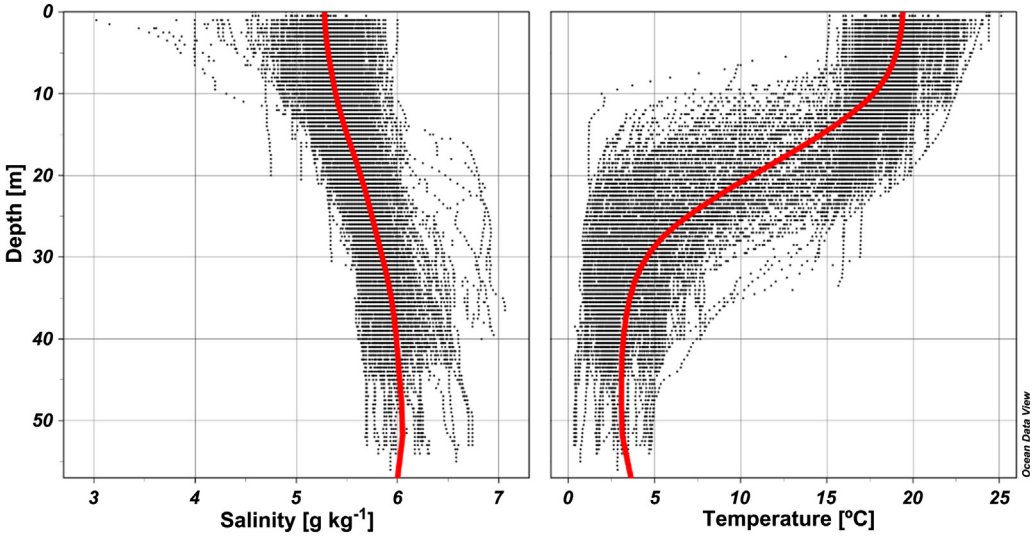


**Figure 3** Scatter plot of vertical profiles of salinity and temperature in August, 1993—2012. The red line represents the mean vertical profile for the whole period. (For interpretation of the references to colour in this figure legend, the reader is referred to the web version of this article.)

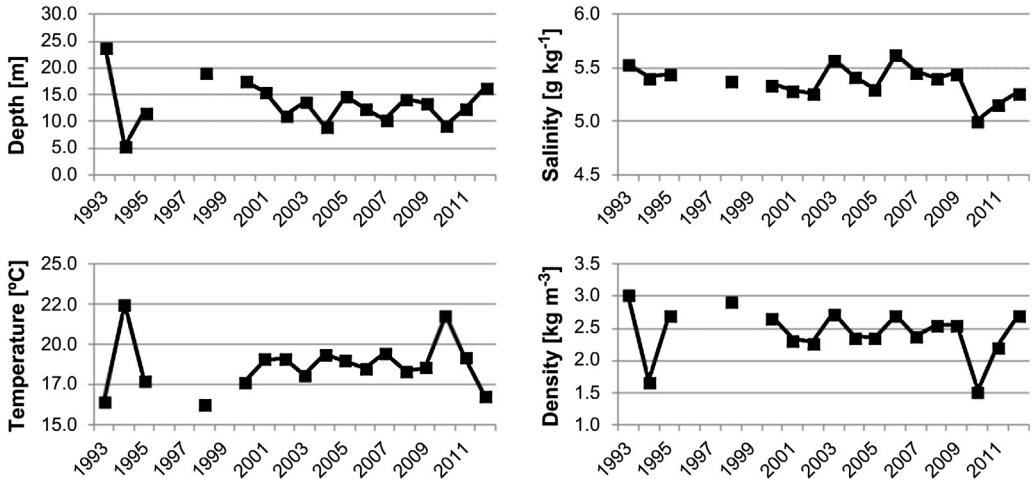


**Figure 4** Inter-annual variability of mean characteristics of upper mixed layer in August, 1993—2012.

and 2006 (5.63 g kg$^{-1}$), respectively. However, year 2010 stood out as a year with the lowest salinity (5.01 g kg$^{-1}$) and density (1.53 kg m$^{-3}$) as well as with the second largest UML mean temperature (21.8°C) in the whole period. In addition, correlation was found between the UML mean temperature and UML mean depth ($r = -0.84$, $n = 17$, $p < 0.05$). Correlation remained significant ($r$ values ranging from $-0.58$ to $-0.8$, $p < 0.05$) throughout the GoR when looking at specific parts (ten main stations).

A rather high correlation ($r = -0.66$, $n = 17$, $p < 0.05$) during 1993—2012 was found between the UML mean salinity (August) and mean river run-off in spring (March—May). Correlation increased even more ($r = -0.82$, $n = 14$, $p < 0.05$) when years 1993, 1994 and 2008 were taken out of calculations due to the insufficient data in regard of their spatial distribution. The above mentioned correlation remained high almost throughout the whole GoR when looking at specific parts/stations (Table 2) — the highest correlation was found in the S and southwestern (SW) part of the GoR at stations 119 ($r = -0.85$, $n = 13$, $p < 0.05$), 102A ($r = -0.80$, $n = 15$, $p < 0.05$) and 135 ($r = -0.81$, $n = 13$, $p < 0.05$), respectively. The lowest correlation was found in the E part of GoR at the stations 137A ($r = -0.66$, $n = 15$, $p < 0.05$), 121A ($r = -0.63$, $n = 14$, $p < 0.05$) and 107 ($r = -0.49$, $n = 14$, $p > 0.05$), respectively, with correlation decreasing further away from the S part of the GoR. A remarkably high correlation was still observed at the stations 121 ($r = -0.77$, $n = 17$, $p < 0.05$), 142 ($r = -0.77$, $n = 14$, $p < 0.05$) and 111 ($r = -0.76$, $n = 18$, $p < 0.05$), respectively, despite being relatively far away from the freshwater sources mostly located in the S part of the GoR.

The estimated UML parameters in August were correlated with the Baltic Sea Index and significant correlation was found between inter-annual changes of the UML mean depth and BSI in 1993—2012. The best correlation ($r = 0.71$, $n = 14$, $p < 0.05$) was found using mean BSI values from the period of June—August and excluding years 1993, 1994 and 2008 from the calculations as it was done before. Correlation was somewhat scattered when looking at specific parts/stations of the GoR (Table 2) — the highest correlation was found along

**Table 2** Correlation between the upper mixed layer characteristics and various forcing factors in the Gulf of Riga during 1993–2012. Bold numbers indicate significant correlation ($p < 0.05$), $n$ shows the number of years used in the analysis and "All stations" row shows the correlation between the average upper mixed layer characteristics over all stations and forcing factors.

| Station | $n$ | UML salinity (August) and river runoff (March–May) | UML depth (August) and Baltic Sea Index (June–August) | UML depth (August) and wind speed (August) |
|---|---|---|---|---|
| 111 | 18 | **−0.76** | **0.71** | **0.64** |
| 142 | 14 | **−0.77** | 0.43 | 0.51 |
| 135 | 13 | **−0.81** | **0.88** | 0.37 |
| 102A | 15 | **−0.80** | **0.74** | 0.51 |
| 119 | 13 | **−0.85** | **0.56** | 0.34 |
| 120 | 13 | **−0.71** | 0.18 | 0.13 |
| 121 | 17 | **−0.77** | 0.41 | 0.37 |
| 137A | 15 | **−0.66** | 0.40 | 0.41 |
| 121A | 14 | **−0.63** | **0.66** | **0.56** |
| 107 | 14 | **−0.49** | **0.55** | 0.01 |
| All stations | 14 | **−0.63** | **0.71** | **0.59** |

SW and W part of the GoR at stations 102A ($r = 0.74$, $n = 15$, $p < 0.05$), 135 ($r = 0.88$, $n = 13$, $p < 0.05$) and 111 ($r = 0.71$, $n = 18$, $p < 0.05$), respectively. Lower correlation was obtained at stations 107 ($r = 0.55$, $n = 14$, $p < 0.05$) and 121A ($r = 0.66$, $n = 14$, $p < 0.05$) in the E part of the GoR and at station 119 ($r = 0.56$, $n = 13$, $p < 0.05$) in the S part of the gulf but no significant correlation was found in the remaining stations — 137A, 120, 121 and 142. In addition, a probable link between the UML mean depth and wind speed (measured at the Sõrve meteorological station) was searched from the same period. Significant correlation was found ($r = 0.59$, $n = 14$, $p < 0.05$) between the UML mean depth in August and average wind speed (August). However, if we look at the specific parts/stations of the GoR then significant correlation was obtained only at two stations — 111 ($r = 0.64$, $n = 16$, $p < 0.05$) in the NW part and 121A ($r = 0.56$, $n = 14$, $p < 0.05$) in the E part of the GoR (Table 2).

## 3.2. Deep layer

Altogether, 558 CTD casts during the period of May–August, 1993–2012 with depth >35 m were available for deep layer analysis. The mean salinity, temperature and density derived for the whole period was 5.99 g kg$^{-1}$, 2.2°C and 4.68 kg m$^{-3}$, respectively.

Monthly mean salinity and density for the whole period showed negligible variations in the DL during May–August when the mean salinity and density fluctuated only by 0.06 g kg$^{-1}$ and 0.04 kg m$^{-3}$ between the months. Monthly mean DL temperature increased steadily from 1.4°C (May) to 1.9°C (June), 2.5°C (July) and 3.0°C (August), respectively (Fig. 5).

Greater amount of CTD casts in May and August allowed us to make more detailed inter-annual and long-term analysis about DL characteristics. Similarly to UML dynamics, inter-annual variations of mean temperature, salinity and density were evident but no clear tendency or trend could be detected in May or August during the period of 1993–2012 (Fig. 6). Results from years 1993 (stations only in NW part) in May and 1993, 1994 and 2008 in August should be regarded with caution regarding the mean conditions in the gulf because of spatial distribution of stations in these years (see Section 3.1.1). This might explain rather big salinity peak in 1994 (August). Apart from 1994, the peaks of DL mean salinity in August, 2006 and 2010 coincided well with similar peaks in May (seen also in density), whereas, the salinity peak

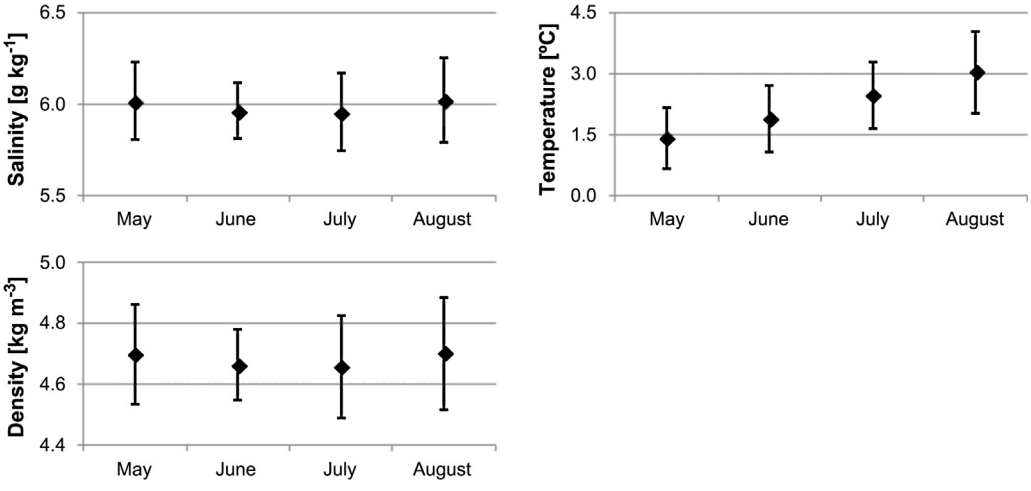


**Figure 5** Mean characteristics of deep layer between 1993 and 2012 (May–August) with standard deviations.

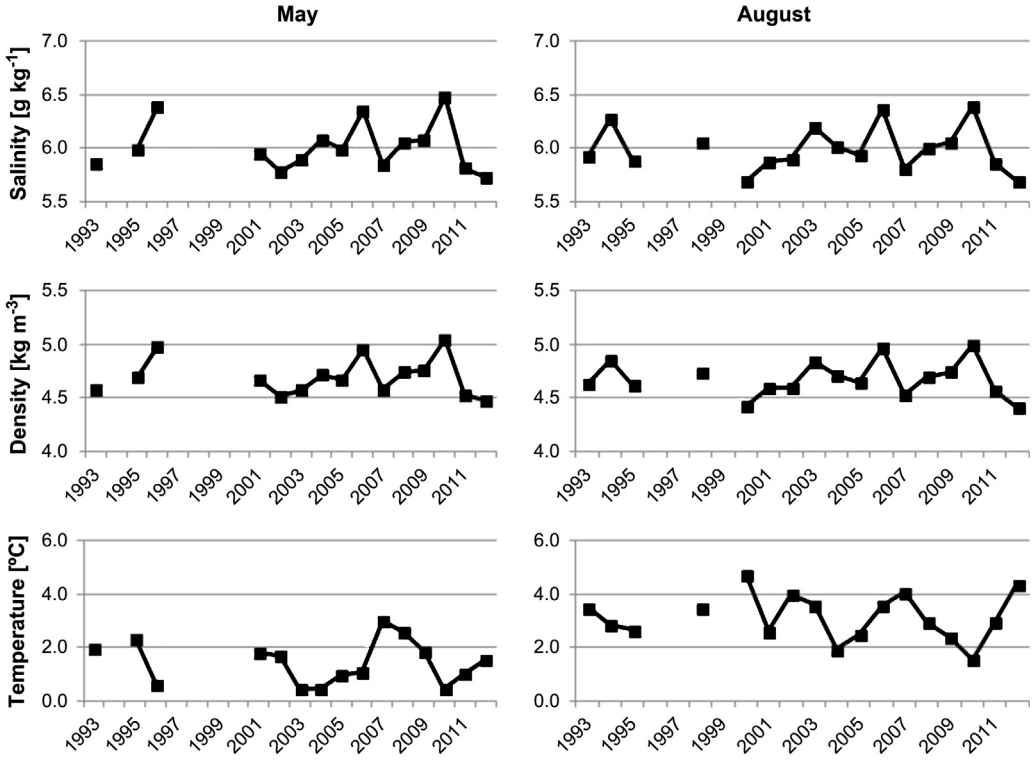


**Figure 6** Inter-annual variability of mean characteristics of deep layer in May (left column) and August (right column), 1993—2012.

in 2003 was more pronounced in August (6.20 g $kg^{-1}$) than in May (5.89 g $kg^{-1}$) suggesting of more saline water inflow sometime between May and August. In May 1996 the second largest (6.40 g $kg^{-1}$) mean salinity was observed from the whole study period, whereas, in August only data from one station (121) was available with mean salinity of 6.46 g $kg^{-1}$.

As majority of water exchange between the GoR and Baltic Sea takes place through the Irbe Strait a possible connection was expected between DL characteristics in the Irbe Strait and DL in the GoR. High correlation ($r = 0.88$, $n = 12$, $p < 0.05$) during 1993—2012 was found in August between DL mean salinity in the Irbe Strait and DL mean salinity in the GoR. Similar correlation ($r = 0.84$, $n = 12$, $p < 0.05$) was observed regarding the DL mean density in both locations. Correlation between the previously mentioned DL mean salinity in the Irbe Strait and GoR was slightly different when looking at specific parts/stations of the GoR — the highest correlation was observed at the stations near the Irbe Strait and along the W coast of the gulf (stations 111, 142 and 135 with $r = 0.94$, 0.95 and 0.93, respectively, $p < 0.05$). Towards the S and southeastern (SE) part of the GoR correlation steadily decreased ($r = 0.83$, 0.76 and 0.71 at stations 102A, 119 and 137A, respectively, $p < 0.05$) whereas correlation was even lower in the central and E part of the gulf (stations 120, 121 and 121A with $r = 0.68$, 0.49 and 0.59, respectively, correlation not being significant at latter 2 stations). Analyzing all the data from May, the previously described connection between the DL mean parameters in the Irbe Strait and GoR was not significant regarding salinity and density. Nevertheless, when looking at specific stations significant correlation was still observed regarding salinity at 2 stations closest to the Irbe strait (111 and 142 with $r = 0.70$ and 0.67, respectively, $n = 10$, $p < 0.05$). Regarding density, the correlation was significant ($r = 0.72$, $n = 10$, $p < 0.05$) only at station 111.

The DL characteristic parameters in May and August were also correlated with the Baltic Sea Index. As expected, neither in May nor in August significant correlation was detected between BSI and any parameter characterizing DL when analyzing mean values from the whole GoR. Nevertheless, at some occasions in May the correlation was evident when using BSI averaged over May and March—May. In both cases significant negative correlation was found in S part of the gulf (station 119) between BSI (May and March—May) and salinity ($r = -0.55$ and $-0.61$, respectively) as well as density ($r = -0.58$ and $-0.65$, respectively, $n = 16$, $p < 0.05$). Similar negative correlation was observed at station 137A between averaged BSI (March—May) and salinity as well as density ($r = -0.57$ and $-0.59$, respectively). This negative correlation tendency between BSI and salinity and density was evident in other stations as well, although, it was not significant ($p > 0.05$).

### 3.3. Vertical stratification in August

Inter-annual and long-term variability of different parameters in May and August was analyzed in previous sections. To study the vertical stratification and its variability we used the month of August which had the best data coverage during the whole study period (Fig. 7). The average salinity, density (sigma-t) and temperature difference between the UML and DL during 1993—2012 was 0.62 g $kg^{-1}$, 2.22 kg $m^{-3}$ and 15.5°C, respectively. Year 2010 remarkably stood out as a year where difference between the UML and DL characteristics was the greatest — difference in salinity, density and

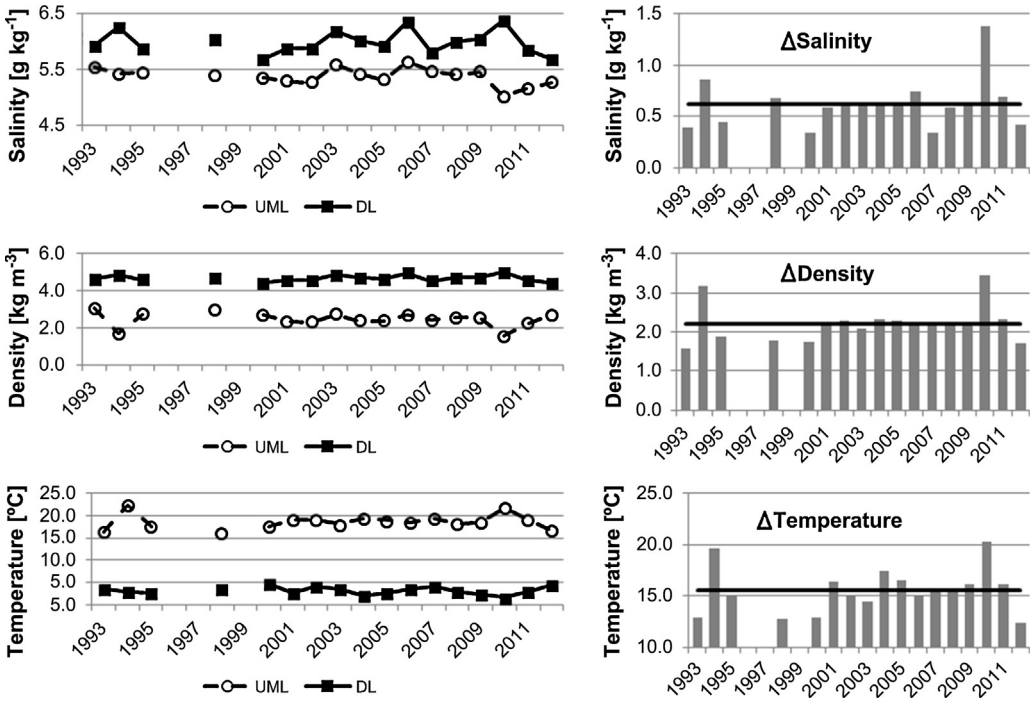


**Figure 7** Mean salinity, density (sigma-t) and temperature in the upper mixed layer and deep layer in August 1993–2012 (left column) and their differences between the two layers (right column). Differences are given as deep layer minus upper mixed layer for salinity and density, and opposite for temperature; solid line represents the mean difference during 1993–2012.

temperature was 1.38 g kg$^{-1}$, 3.46 kg m$^{-3}$ and 20.2°C, respectively. Salinity in the UML was the lowest (5.01 g kg$^{-1}$), whereas, in DL the highest (6.39 g kg$^{-1}$) from the whole period. Similar situation was observed regarding density – UML was characterized with the lowest (1.53 kg m$^{-3}$) and DL with the highest density (4.99 kg m$^{-3}$) in the whole period. The lowest DL mean temperature (1.6°C) was also observed in 2010 but the highest UML mean temperature (22.5°C) was observed in 1994 with the UML mean temperature in 2010 slightly lower at 21.8°C. In 1994 there was also observed rather high difference in mean salinity and density between UML and DL but this result should be treated with caution as in 1994 the data was available only from the N and NW part of the GoR.

Baltic Sea Index and river run-off was used to see whether any correlation could be found between the inter-annual changes of vertical stratification (expressed as salinity difference ($\Delta S$) and density difference ($\Delta D$) between the DL and UML and temperature difference ($\Delta T$) between the UML and DL) and forcing factors. Results showed that there was no significant correlation between BSI mean values (values from August, June–August and July–August were tested) and any mentioned parameters ($\Delta S$, $\Delta D$ and $\Delta T$). On contrary, significant positive correlation was found between the river run-off in spring and corresponding $\Delta S$, $\Delta D$ and $\Delta T$with coefficient $r = 0.52$, 0.62 and 0.65, respectively ($n = 17$, $p < 0.05$).

## 3.4. Rossby radius

To estimate the characteristic values of Rossby radius in the GoR and, thus, corresponding scales of mesoscale features (eddies etc.) and to see whether there are some trends evident, we calculated Rossby radius in May and August using all available CTD profiles from ten main stations during 1993–2012.

The overall mean Rossby radius in May was roughly 2 times less than in August – 1.6 and 3.2 km, respectively. Inter-annual variability of mean Rossby radius was characteristic for both months but no conclusive trend could be observed in neither of them (Fig. 8). Although in August, in the beginning of 1990s the two lowest values of Rossby radius were observed (1993 and 1996), data only from 3 out of 10 stations were available and, thus, these results should be treated with caution. Similar situation was in August 1994 and in May 1993, 1994, 1998 and 1999. Nevertheless, August 2001, 2005 and 2010 stood out as years with the highest Rossby radius with values exceeding 3.5 km, whereas, in May, on the contrary, the lowest Rossby values in 2003 (0.9 km) and 2007 (1.2 km) were more distinguishable from the whole period.

During 1993–2012 the mean Rossby radius in May varied from 0.9–1.9 km, whereas, in August from 2.2–3.9 km. Although the mean Rossby radius is definitely higher in August than in May also some similarities and differences can be detected when looking at the spatial distribution of mean

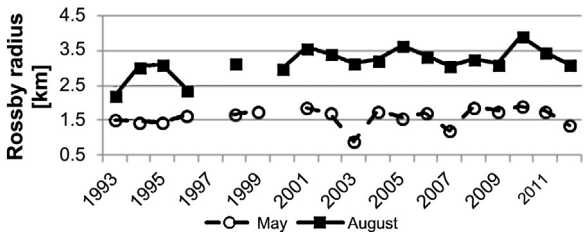


**Figure 8** Mean Rossby radius in May and August during 1993–2012.

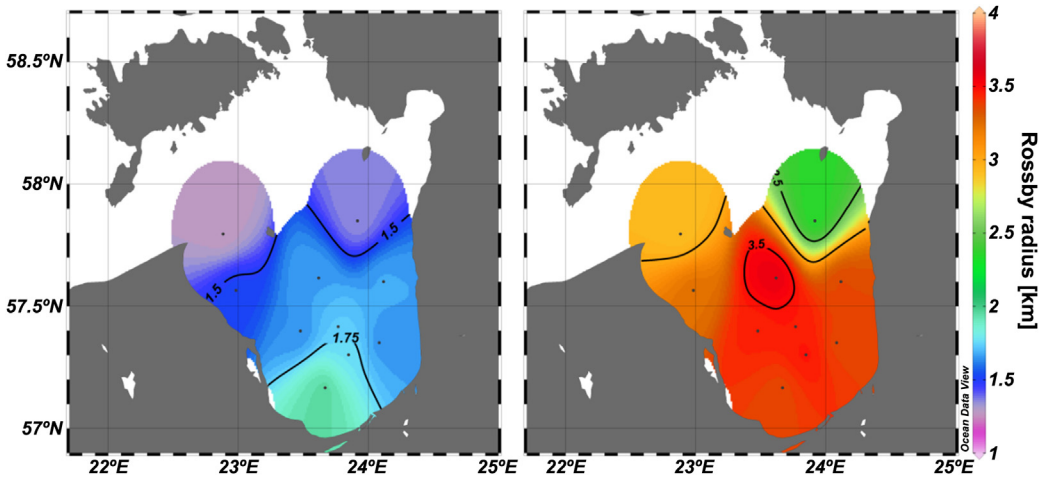


**Figure 9** Mean Rossby radius in May (left) and August (right) at 10 main stations in the Gulf of Riga during 1993–2012.

Rossby radius in both months (Fig. 9). The lowest mean Rossby radius values can be observed at stations 111, 142 and 107 in both months – 1.3, 1.5 and 1.3 in May and 2.9, 3.2 and 2.3 km in August, respectively. In May the highest mean Rossby radius values can be seen in the S part of the GoR at stations 102A and 119 (2.0 and 1.8 km, respectively), whereas, in August the maximum value was found in the central part of the gulf at station 121 (3.6 km). In August the mean Rossby radius in the E part (3.4 km at stations 121A and 137A) and SW part (3.4 km at station 102A) was also somewhat lower (0.1 km on average) than at other stations situated more in the central (120 and 119) part of the GoR.

## 4. Discussion

Estimation of UML depth from CTD profiles, to our knowledge, has not been done before in the GoR with similar approach as in the present study. Although Stipa et al. (1999) and Tamminen and Seppälä (1999) concluded before that mixed layer depth increases from spring to late summer, both studies relied on the data from 4 surveys during 1993–1995 and referred to the data from one section when talking about mixed layer depth. Consequently, we needed to compare our findings with some other regions than GoR. Resembling research in the Gulf of Finland (GoF) by Liblik and Lips (2011) using CTD profiles and analyzing the vertical structure of the water column showed that the UML mean depth in the GoF (12.8 m) during 1987–2008 (June–August) is about 1.4 m deeper than in our findings about the GoR (using also June–August). The UML mean salinity in the GoR during 1993–2012 (May–August) was practically identical to those findings in the GoF (although they used Practical Salinity Scale as opposed to Absolute Salinity in our case), whereas, the UML mean temperature in June, July and August was about 0.7–1.8°C higher in the GoR, probably, due to the fact that the GoR is a shallower water basin accumulating and releasing the heat more rapidly. If the UML characteristics are quite similar in both water basins mentioned before, then substantial differences can be seen in the DL characteristics, mainly, due to the fact that both water basins are hydrographically diverse – GoR is a rather shallow, semi-enclosed sub-basin of the Baltic Sea as opposed to the GoF which is much more deeper and has an open access to the Baltic Sea. Thus, the DL mean salinity is about 2.5 g $kg^{-1}$ higher in the GoF than in the GoR and mean temperature is lowest in the cold intermediate layer (as opposed to the DL) which, on the other hand, is not typical in the GoR where the lowest temperatures occur in the DL itself.

Analyzing the temperature and salinity values in the GoR at standard depths from 1973–1995 Raudsepp (2001) concluded that the mean salinity difference between surface and bottom is about 1 PSU which is substantially higher than what we obtained (0.62 g $kg^{-1}$) analyzing the month of August when the strongest stratification is expected. Comparing both studies we suggest that this difference between the surface and bottom layers is basically due to the increased bottom layer salinity during 1973 to 1995. In our study we had almost identical mean salinity (6.0 g $kg^{-1}$) in the DL (average from 35 m till bottom of the profile) from May to August in 1993–2012, whereas, in the results reported by Raudsepp (2001) at approximately 35 m depth salinity was around 6.1 PSU and increased more in the DL (about 6.5 PSU at the bottom). In addition, Raudsepp (2001) used Practical Salinity Scale for salinity, so each salinity value in his work is even higher if compared to Absolute Salinity, which is used in the present study. On the other hand, Stipa et al. (1999) reported of the density difference between the surface and deep waters in the middle of the summer being 1.5–2 kg $m^{-3}$ using years 1993–1995 in their study. This is somewhat similar, although, a bit lower than we found out (2.2 kg $m^{-3}$) in our research during 1993–2012 (August).

Obtained mean Rossby radius values in May during 1993–2012 (0.9–1.9 km) were on average 2–2.5 times smaller than in the study where Rossby radius values from the model results were presented (Lips et al., 2016b). Such a discrepancy is caused by the different approaches used to calculate the Rossby radius. It has been showed before that in the whole Baltic Sea (Fennel et al., 1991) as well as in specific parts as the Gulf of Finland (Alenius et al., 2003) the Rossby radius has seasonal characteristics with minimum values during the autumn and winter and maximum values occurring in the summer mainly due to the strong stratification. Our results from the August correspond to these maximum Rossby radius values quite well exceeding the values in May almost two times. The stratification is strongest during the August in the GoR and the highest UML mean depth in August served as

a good indicator for this in our research. In May, on the other hand, the GoR is partially stratified with mainly shallow UML but in approximately 2/3 of the CTD casts we were not able to detect distinctly developed UML in May. Strength of the stratification in the GoR is the main reason for Rossby radius differences in May and August. In August the Rossby radius was larger in the deeper parts (smaller in shallower parts) of the GoR which is in accordance to what has been found in the GoF (Alenius et al., 2003) and worldwide (Chelton et al., 1998). Nevertheless, in May the largest Rossby radius was observed in the S part of the gulf rather than in the central, deeper part. We suggest that this could be related to maximum river run-off occurring in spring and strongly influencing the surface layers starting from the S part of the gulf, thus, promoting stratification as well.

Seasonal changes in the UML mean depth in the GoR (May–August) showed similar characteristics as reported by Tamminen and Seppälä (1999) on the basis of data from 1993–1995 in the GoR and by Liblik and Lips (2011) using long-term data in the GoF, with depth increasing with each consecutive month. Estimated UML mean depth in the GoR in summer was shallower and mean temperature was warmer than that of the GoF, mainly because GoR is a shallower water basin than the GoF. The UML mean temperature also increased during May–August following the air temperature raise and, in general, this temperature dynamics corresponds well with previous studies (e.g. Berzinsh, 1995; Raudsepp, 2001) about seasonal variations of temperature in the GoR. Finally, the UML mean salinity during May–August increased steadily as well in the GoR and this dynamics is in accordance with previously mentioned study by Raudsepp (2001) where it was described that lower surface salinity in May is due to the maximum river run-off in the spring. A bit older studies by Berzinsh (1980, 1987) covering the periods 1963–1976 and 1971–1982, respectively, showed that mean salinity in June can be as low as in May and that the surface layer (0–10 m) mean salinity continued to slightly decrease also after May in June and the following increase started again from July. In these last two studies one can observe that the mean surface salinity is about 1.0 g $kg^{-1}$ higher than we found in our results during 1993–2012. Seasonal changes in the DL characteristics are minor mainly due to the fact that there is no direct influence from the atmosphere.

Inter-annual variability dominated in our results during 1993–2012 and they did not reveal any unequivocal trends or tendencies in the UML or DL characteristics as opposed to previous studies where it was reported, for example, that salinity increased during 1960–1977 (e.g. Berzinsh, 1980, 1995) and decreased from the end of 1970s till the start of 1990s (Berzinsh, 1995; Raudsepp, 2001). Based on the data from 1976–2008 at four monitoring stations (standard depths) in the central and S part of the GoR, Jurgensone et al. (2011) reported about general increase of water temperature in the summer (June–September). Based on the satellite data during 1990–2004, Siegel et al. (2006) showed a positive trend in the yearly mean SST of the Baltic Sea with summer and autumn dominating this trend and positive summer trend being highest in the northern Baltic Sea. Similar analysis of remote sensing data from 1990–2008 (BACC, 2015) showed an increase of SST specifically in the GoR by about 1.0°C per decade. However, our results based on the CTD data in August did not show similar pattern with unequivocal temperature increase in the GoR during 1993–2012, although, apart from 1994, in general the UML mean temperature has increased from 1993–2010. Jurgensone et al. (2011) also noticed a salinity decrease before 1993 and a slight increase afterwards, whereas, there was no apparent trend in the stratification strength expressed as density difference between the surface (0–10 m) and subsurface layer. The latter corresponds well to our findings about the stratification strength (expressed as difference between the UML and DL) in August, whereas, we did not find any pronounced increase (or decrease) in the mean salinity in August during 1993–2012. Nevertheless, our results from August show that the mean salinity in last 3 years of the research period has been fairly lower compared with the values from the beginning of the 1990s.

Spatial distribution of the UML mean salinity from ten main stations in August showed higher salinity in the E coast than the W coast. In addition, the UML mean depth in August showed shallower UML depth in the W coast than in the central and E part of the gulf (UML mean depth in E part only slightly exceeded that in the central part). Therefore, it allows us to suggest that in the summer there is evident thermocline slope and corresponding sea level slope (opposite to the thermocline slope) between the two coasts and it is steeper in the W part of the GoR. Prevailing winds from WSW during the research period also indicate higher sea level in the E coast of the GoR. Thus, due to the average sea level gradient the general northward flow is dominating in the western part of the open gulf. This type of water flow is in accordance with the recent model results (Lips et al., 2016a) where it was reported that anticyclonic circulation exists in the GoR during summer forming a water tongue with lower salinity in the W part of the GoR.

High correlation found between the UML mean salinity (August) and the river run-off in spring during 1993–2012 confirmed the results of previous studies in the GoR (e.g. Berzinsh, 1995; Raudsepp, 2001) where it was shown that river run-off is the main factor for the salinity variations. A bit unexpected was the fact that high connection between these two factors was found not only in the S part of the gulf (majority of the freshwater discharges in this part) but, basically, throughout the gulf (10 main stations) and, especially, in the stations near the Irbe Strait. However, the mentioned model study by Lips et al. (2016a) also showed that during summer the anticyclonic (clockwise) circulation pattern dominates in the GoR, thus, transporting fresher surface waters from the south to north along the W coast of the gulf. Taking into account that our results showed also weaker correlation between the UML mean salinity and river run-off in spring on the E coast of the gulf, we feel that this general anticyclonic circulation (in the summer during stratified conditions) fits well with our findings and helps to explain them.

During the research period BSI (June–August) was found to be related ($r = 0.71$) to the UML mean depth (August) in the GoR. A positive BSI corresponds to an anomalous sea level pressure difference between Szczecin in Poland and Oslo in Norway (north-south distance of approximately 600 km) which means that the westerlies are prevailing over the Baltic Sea. If the BSI increases the winds from west are dominating and becoming stronger and, in general, stronger influence from the atmosphere should initiate more mixing in

the UML and, thus, make it deeper. Obtained significant correlation between the average wind speed (August) and UML mean depth ($r = 0.59$) also adds up to this relation. Nevertheless, the results from 10 main stations showed that not always this correlation between the BSI and UML mean depth (as well as wind speed and UML mean depth) is significant and that it varies in different parts of the gulf which might be due to, for example, upwelling and downwelling events (e.g. Lehmann and Myrberg, 2008; Lehmann et al., 2012; Lips et al., 2009) or other factors which might have local influence on the water masses (mesoscale structures like eddies, filaments etc.). We suggest that, although atmospheric forcing undoubtedly plays an important role affecting the UML depth, it is only a part of explanation and more detailed research should be carried out in this direction to come up with more justified conclusions which are based on the data with better spatial and temporal resolution as we had.

At some occasions in May a connection (negative correlation) was found between the BSI (March–May) and DL mean salinity and density. We suggest that this is caused by the stronger winds and corresponding more intense vertical mixing. Although this negative correlation was not significant in all parts of the GoR (the overall correlation and correlation at some main stations was just over the chosen significance level of $p < 0.05$), it still was evident as a common tendency in all main stations. Taking into account that in May, on average, the GoR is not characterized by fully developed and permanent stratification, this might as well serve as a factor favouring water column mixing and transferring the impact of the atmosphere to the deep layers.

Inter-annual variations of the DL mean salinity in the GoR (August) are related to the DL mean salinity in the Irbe Strait (August). Best correlation was found in the W part of the gulf close to the Irbe Strait with correlation steadily decreasing towards the S part of the GoR, thus, suggesting that the inflow through the Irbe Strait continues anticlockwise along the W coast and penetrating deeper in the GoR. This corresponds well to what was previously reported regarding saline water inflow through Irbe Strait and further movement of the saline deep waters into the GoR (e.g. Berzinsh, 1995; Lilover et al., 1998).

For numerical modelling purposes in order to resolve mesoscale processes it is important to estimate the Rossby radius in the GoR. Our estimates of the Rossby radius in May and August showed that numerical models with horizontal grid spacing 1 km or less should be applied. Nevertheless, our temporal and spatial resolution of the CTD data did not allow us to determine Rossby radius in winter when the Rossby radius values are usually the lowest. Alenius et al. (2003) showed that the Rossby radius summer values are approximately 1.75 times the winter values in the centre of the Gulf of Finland. However, they also emphasized that the analysis is somewhat biased due to temporal distribution of the observations. Taking into account that the GoR is a shallower water basin than GoF and the water column is usually thoroughly mixed from the end of autumn till early spring, we speculate that Rossby radius in winter and early spring should be even lower than 1 km.

As previously discussed river run-off plays a major role affecting the salinity dynamics in the whole GoR. In addition to that, we also found a significant connection (positive correlation) between the mean river run-off in spring and stratification in August (expressed as difference between the temperature, salinity and density in the UML and DL) during 1993–2012. As river run-off increases it increases not only the salinity difference between the UML and DL but strengthens temperature and density difference as well. It means that river run-off in the GoR serves as instantaneous source of changes but it can also have further impact on the whole water column after some time. Maximum stratification found in 2010 serves as a good example for previously mentioned connection – in 2010 the second largest (after 1994) river run-off in spring was observed from the whole research period with following maximum strength of stratification observed later in August. Similar pattern can be observed in 1994 which was characterized by the largest river run-off in spring from the whole period. Although salinity difference between the UML and DL is considerably lower than in 2010 we suggest that this is due to the rather poor spatial distribution of the data (data available only from the N part of the gulf which is not affected by river run-off at the same level as the S part) and, judging by differences in temperature and density, the stratification in 1994 was at least as strong as in 2010.

Latest projections of the future climate change (BACC, 2015) continue to predict a significant water temperature increase in the Baltic Sea region similarly as it was stated before (BACC, 2008). Current study and results obtained using the CTD profiles from 20 years allows us to foresee the possible situation and changes in the GoR. We suggest that if the water temperature will continue to increase then the warming would generate a stronger stratification conditions in the GoR in summer. Furthermore, stronger stratification is likely to favour the oxygen depletion in the deeper parts of the gulf and following hypoxic or, at some cases, even anoxic conditions. Thus, the previously detected parts with low oxygen concentration or no oxygen at all (Hansson et al., 2009) in the GoR could expand in wider areas. Due to the projected strong decrease in sea-ice extent (BACC, 2015) the spring bloom could start earlier with possible shifts in dominating species characteristics as it was already suggested by Jurgensone et al. (2011). Moreover, with projected increase in the river run-off in winter (BACC, 2015), the nutrient amounts will also increase suggesting longer spring blooms with higher biomass.

Since 1977 there is an evident salinity decrease in the Baltic Proper and the GoR. Although it is not so pronounced since the beginning of the 1990s, most of the studies about future scenarios (see BACC, 2015) predict further salinity decrease. If so, then increase of freshwater species in the coastal areas is likely to occur.

While precipitation and evapotranspiration were projected to increase in the GoR region, the mean annual river run-off was projected to decrease. However, strong seasonal changes with shift of the maximum river run-off from spring to winter were also projected. We suggest that, due to the above mentioned factors, the salinity minimum usually observed (in the surface layers) starting from the spring in the S part of the gulf will also shift in accordance to changes in the river run-off seasonal dynamics. Earlier maximum river run-off together with water temperature increase could benefit for the faster development of permanent stratification in the GoR. Strong stratification could be observed already in May or even earlier as opposed to only partially

stratified conditions (May) shown in the present study. Due to the stronger and earlier stratification in spring which hinders the vertical mixing, riverine water discharging mainly into the S part of the gulf could be transported for longer distances away from the coast. Such freshwater dynamics would have an impact on surrounding water masses by, for example, bringing more nutrient-rich water in the surface layers and increasing total suspended matter content in the areas where it was previously not observed or the effect was minor.

In conclusion, we showed that relatively large inter-annual variations dominated in the temporal variability of different UML and DL parameters and no clear long-term trend could be detected in the GoR during 1993—2012. The UML mean depth was found to be related to the Baltic Sea Index. River run-off proved to be a major driving force for the salinity dynamics and a substantial contributor to enhancing the strength of the stratification in summer. The analysis of inter-annual variations in density difference between the UML and DL revealed that the strongest stratification was observed in the years with the highest UML mean temperature and highest river run-off during spring. We suggest that the predicted water temperature increase and seasonal changes in river run-off will result in a stronger stratification in the GoR.

## Acknowledgements

This work was supported by institutional research funding IUT19-6 of the Estonian Ministry of Education and Research, the DoRa programme activity 4 “Doctoral studies of talented international students in Estonian universities”. We thank our colleagues who have participated in the analyzed CTD data collection during 1993—2012. We are grateful to Viesturs Berzinsh and Andreas Lehmann who provided CTD data and BSI values, respectively.

## References

Alenius, P., Nekrasov, A., Myrberg, K., 2003. Variability of the baroclinic Rossby radius in the Gulf of Finland. Cont. Shelf Res. 23 (6), 563—573.

BACC, 2008. Assessment of Climate Change for the Baltic Sea Basin. Springer Verlag, Berlin, 35—221.

BACC, 2015. Second Assessment of Climate Change for the Baltic Sea Basin. SpringerOpen, Geesthacht, 69—263.

Berzinsh, V., 1980. Interannual and seasonal changes of water salinity in the Gulf of Riga. Rybokhozyaistvennye issledovaniya (Balt-NIIRKH), vol. 15, Avots, Riga, 3—12, (in Russian).

Berzinsh, V., 1987. Hydrological dividing of the open part of the Gulf of Riga. In: Andrusaitis, G.P., Laganovska, R.Y., Apine, S.O. (Eds.), Hydrochemical and Hydrobiological Characteristics and Dividing of the Coastal Part of the Baltic Sea, Gulf of Riga and Gulf of Finland, Zinatne, Riga, 7—20, (in Russian).

Berzinsh, V., 1995. Hydrology. In: Ojaveer, O. (Ed.), Ecosystem of the Gulf of Riga Between 1920 and 1990. Estonian Acad. Publ., Tallinn, 7—32.

Chelton, D.B., DeSzoeke, R.A., Schlax, M.G., Naggar, K.E., Siwertz, N., 1998. Geographical variability of the first baroclinic Rossby radius of deformation. J. Phys. Oceanogr. 28 (3), 433—460.

Feistel, R., Weinreben, S., Wolf, H., Seitz, S., Spitzer, P., Adel, B., Nausch, G., Schneider, B., Wright, D.G., 2010. Density and absolute salinity of the Baltic Sea 2006—2009. Ocean Sci. 6 (1), 3—24.

Fennel, W., Seifert, T., Kayser, B., 1991. Rossby radii and phase speeds in the Baltic Sea. Cont. Shelf Res. 11 (1), 23—36.

Hansson, M., Axe, P., Andersson, L., 2009. Extent of anoxia and hypoxia in the Baltic Sea, 1960—2009. SMHI Report Mo 2009-214, http://www.smhi.se/polopoly_fs/1.10354!Oxygen_timeseries_1960_2009.pdf.

Jurgensone, I., Carstensen, J., Ikauniece, A., Kalveka, B., 2011. Long-term changes and controlling factors of phytoplankton community in the Gulf of Riga (Baltic Sea). Estuaries Coasts 34 (6), 1205—1219.

Kotta, J., Kotta, I., Simm, M., Põllupüü, M., 2009. Separate and interactive effects of eutrophication and climate variables on the ecosystem elements of the Gulf of Riga. Estuar. Coast. Shelf Sci. 84 (4), 509—518.

Kõuts, T., Håkansson, B. (Eds.), 1995. Observations of Water Exchange, Currents, Sea Levels and Nutrients in the Gulf of Riga. SMHI RO Series No. 23, Norrköping. 141 pp.

Kronsell, J., Andersson, P., 2014. Total and regional runoff to the Baltic Sea. HELCOM Baltic Sea Environment Fact Sheets, http://www.helcom.fi/baltic-sea-trends/environment-fact-sheets/ (accessed: 11 November 2015).

Lehmann, A., Krauss, W., Hinrichsen, H.-H., 2002. Effects of remote and local atmospheric forcing on circulation and upwelling in the Baltic Sea. Tellus A 54 (3), 299—316.

Lehmann, A., Myrberg, K., 2008. Upwelling in the Baltic Sea — a review. J. Marine Syst. 74 (Suppl.), S3—S12.

Lehmann, A., Myrberg, K., Höflich, K., 2012. A statistical approach to coastal upwelling in the Baltic Sea based on the analyses of satellite data for 1990—2009. Oceanologia 54 (3), 369—393, http://dx.doi.org/10.5697/oc.54-3.369.

Leppäranta, M., Myrberg, K., 2009. Physical Oceanography of the Baltic Sea. Praxis Publ. Ltd., Chichester, 46 pp.

Liblik, T., Lips, U., 2011. Characteristics and variability of the vertical thermohaline structure in the Gulf of Finland in summer. Boreal Environ. Res. 16 (Suppl. A), 73—83.

Lilover, M.J., Lips, U., Laanearu, J., Liljebladh, B., 1998. Flow regime in the Irbe strait. Aquat. Sci. 60 (3), 253—265.

Lips, I., Lips, U., Liblik, T., 2009. Consequences of coastal upwelling events on physical and chemical patterns in the central Gulf of Finland (Baltic Sea). Cont. Shelf Res. 29 (15), 1836—1847.

Lips, U., Zhurbas, V., Skudra, M., Väli, G., 2016a. A numerical study of circulation in the Gulf of Riga, Baltic Sea. Part I: Whole-basin gyres and mean currents. Cont. Shelf Res. 112, 1—13.

Lips, U., Zhurbas, V., Skudra, M., Väli, G., 2016b. A numerical study of circulation in the Gulf of Riga, Baltic Sea. Part II: Mesoscale features and freshwater transport pathways. Cont. Shelf Res. 115 (1), 44—52.

Petrov, V.S., 1979. Water balance and water exchange between the Gulf of Riga and the Baltic Proper. In: Sbornik rabot rizhskoj gidrometeorologicheskoj observatorii, 18, Riga. 20—40, (in Russian).

Raudsepp, U., 2001. Interannual and seasonal temperature and salinity variations in the Gulf of Riga and corresponding saline water inflow from the Baltic Proper. Hydrol. Res. 32 (2), 135—160.

Schlitzer, R., 2010. Ocean Data View, http://odv.awi.de.

Siegel, H., Gerth, M., Tschersich, G., 2006. Sea surface temperature development of the Baltic Sea in the period 1990—2004. Oceanologia 48 (S), 119—131.

Stiebrins, O., Väling, P., 1996. Bottom Sediments of the Gulf of Riga. Geological Survey of Latvia, Riga, 4 pp.

Stipa, T., Tamminen, T., Seppälä, J., 1999. On the creation and maintenance of stratification in the Gulf of Riga. J. Marine Syst. 23 (1—3), 27—49.

Tamminen, T., Seppälä, J., 1999. Nutrient pools, transformations, ratios, and limitation in the Gulf of Riga, the Baltic Sea, during four successional stages. J. Marine Syst. 23 (1—3), 83—106.

Oceanologia (2017) 59, 49—56

Available online at www.sciencedirect.com

ScienceDirect

journal homepage: www.journals.elsevier.com/oceanologia/

ORIGINAL RESEARCH ARTICLE

# Effect of physicochemical parameters on zooplankton in the brackish, coastal Vistula Lagoon

**Ewa Paturej, Agnieszka Gutkowska, Jacek Koszałka *, Magdalena Bowszys**

*Department of Tourism, Recreation and Ecology, University of Warmia and Mazury, Olsztyn, Poland*

Received 11 August 2015; accepted 8 August 2016
Available online 21 August 2016

**KEYWORDS**
Physicochemical properties;
Zooplankton;
Brackish waters;
Coastal lagoon

**Summary** This paper analyzes whether physicochemical properties significantly influence the occurrence of zooplankton in a brackish reservoir. The studies were carried out on the Vistula Lagoon in August and September from 2006 to 2009 at 32 research sites. The environmental conditions in the Vistula Lagoon varied widely. At the time of the investigation, 17 species of rotifers, six species of Cladocera, and ten species of Copepoda were noted, and the total density of plankton fauna ranged from 145 to 765 ind. $dm^{-3}$. Statistical analysis demonstrated a significant correlation between the occurrence of some zooplankton species and certain environmental parameters, whereas the sampling sites were grouped according to study years. The zooplankton systems recorded at the research sites in 2006 constitute the most disparate group. Thus, it can be concluded that physicochemical properties might significantly impact both individual species (depending on their environmental demands) and entire zooplankton clusters.


## 1. Introduction

The instability of environmental conditions is a typical feature of brackish waters such as estuaries or lagoons (Cognetti and Maltagliati, 2000). Changes in abiotic factors are reflected in the biochemical activity of both vertebrates and invertebrates. These factors determine the rate of metabolic transformations, the efficacy of immune systems, and reaction patterns of bodies to stressors (Kinne, 1964; Roddie et al., 1984).

Studies to date of the Vistula Lagoon have focused on the physicochemical characters of the water (Nawrocka and Kobos, 2011; Paturej and Kruk, 2011; Witek et al., 2010), the biota composition of the pelagic zone (Dmitrieva and

* Corresponding author at: Department of Tourism, Recreation and Ecology, University of Warmia and Mazury, Oczapowskiego 5, 10-957 Olsztyn, Poland. Tel.: +48 89 524 51 89/523 41 89; fax: +48 89 523 41 16.
*E-mail address:* jacko@uwm.edu.pl (J. Koszałka).
Peer review under the responsibility of Institute of Oceanology of the Polish Academy of Sciences.

ELSEVIER Production and hosting by Elsevier

http://dx.doi.org/10.1016/j.oceano.2016.08.001

Semenova, 2012; Psuty and Wilkońska, 2009), or the bottom area of the lagoon (Rychter et al., 2011; Warzocha et al., 2016).

Zooplankton is one of the most important biotic elements that impact all functional aspects of aqueous ecosystems including food chains and trophic networks, energy flow, and the circulation of matter. They occupy a central position in pelagic zone food webs (Lampert, 1997). The occurrence and distribution of plankton fauna depend on a number of factors such as climate change, habitat physicochemical properties, and biotic factors (Ahmad et al., 2011; Alexander, 2012; Cottenie et al., 2001; Rajagopal et al., 2010; Richardson, 2008). Environmental factors are also important elements; for instance, water temperature impacts the growth and development of organisms and can influence their mortality (Hall and Burns, 2001). Different species show varied tolerances to increases or reductions in temperature ranges, and particularly sensitive individuals are eliminated by them (Andrulewicz et al., 2008; Tunowski, 2009). In addition, salinity has a significant impact on organisms, because it requires them to adjust the saline concentrations in their bodies to the surrounding environment. Changes in salinity are the direct cause of some species disappearing and others occurring (Ojaveer et al., 2010). Environmental factors can also prompt organisms to migrate in order to avoid unfavorable environmental conditions, i.e., excessively high or low salinity. Variations in salinity can also contribute indirectly to food shortages and, consequently, they impact zooplankton abundance (Perumal et al., 2009). Water pH can also have an impact on zooplankton; low pH causes reduced zooplankton abundance, as well as decreased biodiversity and the loss of some species (Dehui, 1995; Ivanova and Kazantseva, 2006; Yamada and Ikeda, 1999), whereas alkaline conditions that accompany high primary production favors the growth and abundance of zooplankton (Bednarz et al., 2002; Mustapha, 2009). The availability of light determines the distribution of producers, and this indirectly impacts the diversity and distribution of animals. It also influences the vertical migration of plankton that require a specific intensity of light for many physiological processes. Light also exerts an indirect impact on other physical factors such as temperature and water color (Andrulewicz et al., 2008). Oxygen dissolved in water, which is required for the survival of all aquatic organisms, is another important abiotic factor. Oxygen deficiencies can directly influence organism mortality. In addition, indirect influences are observed through predator–prey interactions since hypoxia influences mobile species to change their horizontal or vertical distribution (Decker et al., 2004). Many authors (Kudari and Kanadami, 2008; Paturej, 2005, 2006; Pinto-Coelho et al., 2005; Wang et al., 2007; Yildiz et al., 2007) claim that the trophic status of a reservoir, i.e., the availability of nutrients, significantly impacts the structure and abundance of zooplankton. When trophic conditions are modest, large, herbivorous forms (Calanoida copepods, large water fleas) dominate, while in fecund waters small detritivore forms and predatory organisms (Cyclopoida copepods, small water fleas, rotifers) occur abundantly (González et al., 2011).

The objective of the study was to determine whether physicochemical properties such as water temperature, salinity, pH, and water transparency, particulate matter, oxygen concentration, nutrient concentrations, and chlorophyll *a* significantly impacted zooplankton occurrence.

## 2. Material and methods

The study was conducted in the Polish part of the brackish Vistula Lagoon located in the southern part of the Baltic Sea. The lagoon is a broad, shallow reservoir with an average depth that does not exceed 2.6 m and a surface area of 328 km$^2$ (Chubarenko and Margoński, 2008). Salinity ranges from 0.5 to 6.0 PSU depending on the intensity of freshwater and brackish water inflows (Kruk et al., 2012). Samples were collected at the end of the summer season in August and September from 2006 to 2009 from 32 sampling sites (Fig. 1).

The zooplankton was collected either with a Ruttner sampler or a 10 dm$^{-3}$ bucket at shallow, coastal sites. The biological material (30 dm$^{-3}$) was concentrated on an Apstein plankton mesh (with a 30 μm net size), fixed with Lugol solution, and preserved in 4% formalin. The zooplankton was examined microscopically and classified into one of three groups of planktonic animals: Rotifera, Cladocera, or Copepoda. The abundance of planktonic fauna was also determined. The zooplankton structure was estimated using the dominance and stability indicators proposed by Kasprzak and Niedbała (1981).

Measurements of physicochemical environmental factors were taken simultaneously with plankton sampling. Water transparency was determined with a Secchi disk and temperature, oxygen concentration, salinity, and pH were measured in situ with a HACH HQd Field Case oxygen probe (RUGGED) and a WTW Multi 350i probe. Particulate matter were determined with the direct weighing method (Hermanowicz et al., 1999). Chemical analyses were performed on unfiltered water samples to determine total phosphorus, orthophosphates, ammonium nitrogen, nitrate nitrogen, total nitrogen, and chlorophyll *a*. Pheophytin was determined in a laboratory as soon as possible after sampling. Ammonium nitrogen was determined spectrophotometrically with the indophenol method according to PN-C-04576-01:1976. Nitrate nitrogen (V) was measured colorimetrically with phenol disulphonic acid according to PN 73/C-04576/08-1973. The concentration of total nitrogen was determined as the sum of nitrate nitrogen and Kjeldahl's nitrogen measured with Kjeldahl's method (Golterman and Clymo, 1969). Total phosphorus and orthophosphates were determined with the

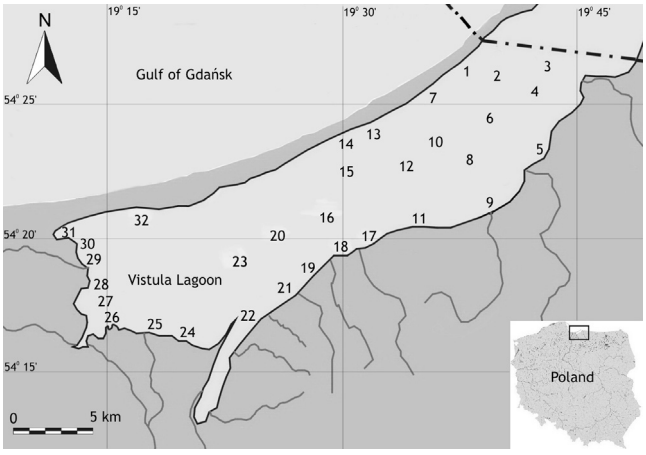


**Figure 1** Location of the research sites on the Vistula Lagoon.

method using ammonium molybdenate based on Standard Methods (1999), whereas sampling and measurements of chlorophyll *a* were carried out according to ISO 10519:1997. Samples for chlorophyll *a* determinations were kept cool and in the dark until they were moved to the laboratory (within 4 h), where the water samples were filtered and immediately elaborated using a mechanical grinder and anhydrous ethanol (99.8%) as the extraction solvent. The chlorophyll *a* concentration was measured using a spectrophotometer (Shimadzu UV 1601) with an adjustment for pheopigments.

The results were processed with statistical methods using CANOCO version 4.52 (Ter Braak and Šmilauer, 2003). Before statistical analyses, zooplankton abundance was log $(x + 1)$ transformed to improve normality (Zar, 2010). All species and forms (*Keratella cochlearis f. tecta*) identified were included in the analyses. Nauplii and copepodites were excluded from the analyses since their identification to the species was impossible.

Environmental variables were analyzed for redundancy using Pearson's correlation. If two variables were highly correlated ($r > 0.6$ or $r < -0.6$), the variable which showed the higher overall mean correlation was excluded from further analyses. Except for pH, $O_2$, chlorophyll *a*, and N-$NH_4$, the environmental variables were log-transformed or log + 1 transformed (TN and N-$NO_3$) to approximate normal distribution.

Detrended Correspondence Analysis (DCA) was used to determine if RDA (Redundancy Analysis) or Canonical Correspondence Analysis (CCA) would be appropriate to evaluate associations between lagoon water physicochemistry and zooplankton abundance. The DCA ordination gradient was in the range of 3–4 standard deviations (3.33 SD), which implied that both linear and unimodal methods were appropriate for the data (Jongman et al., 1995). Thus, CCA was used to describe the relationships among the zooplankton species and the environmental variables selected for further analyses. The analyses were performed with focus scaling on inter-species distances (biplot scaling type). Environmental variables with variance inflation factors (VIF) <20 were selected for the following forward selection to avoid multicollinearity with other variables.

The automatic forward selection procedure (Ter Braak and Šmilauer, 2002) was used to select the contribution of environmental variables in the explanation of the species data set. This procedure computes the significance of a given variable and the stepwise cumulative variance explained with all the selected variables in the model. The statistical significance of eigenvalues and species-environment correlations for the axes generated by the CCA were tested with the Monte Carlo method based on 999 permutations including the unrestricted permutation. *P* values ≤0.05 were considered statistically significant.

## 3. Results

During the period studied, the Vistula Lagoon was characterized by extremely variable environmental conditions (Table 1). The water temperature was typical of the months in which the samples were collected and did not drop below 10°C. Water transparency was low at up to 0.5 m, which is

**Table 1** Average values of the physicochemical parameters of the Vistula Lagoon in 2006–2009 (mean ± std. dev. (range)).

| | 2006 | 2007 | 2008 | 2009 |
|---|---|---|---|---|
| *T* [°C] | 20.5 ± 0.6 (19.7–22.1) | 14.7 ± 2.4 (14.0–18.9) | 18.7 ± 3.8 (10.9–20.7) | 19.8 ± 2.0 (16.0–20.5) |
| SDV [m] | 0.45 ± 0.04 (0.35–0.50) | 0.35 ± 0.08 (0.25–0.45) | 0.35 ± 0.06 (0.25–0.45) | 0.27 ± 0.03 (0.20–0.30) |
| pH [–] | 8.72 ± 0.18 (8.23–8.94) | 8.67 ± 0.35 (8.22–9.25) | 8.64 ± 0.13 (8.4–8.8) | 7.69 ± 0.40 (7.0–8.4) |
| Particulate matter [mg dm$^{-3}$] | 58 ± 12 (49–88) | 56 ± 19 (12–84) | 78.57 ± 22 (57–138) | 95 ± 16 (68–120) |
| Salinity [PSU] | 2.9 ± 0.7 (1.4–3.8) | 3.43 ± 1.90 (1.2–9.3) | 4.1 ± 0.4 (3.1–4.4) | 3.5 ± 0.6 (2.3–4.5) |
| Oxygen [mg dm$^{-3}$] | 7.9 ± 1.2 (6.8–11.4) | 8.3 ± 2.0 (7.6–13.2) | 10.0 ± 1.0 (8.7–12.9) | 9.8 ± 0.6 (8.4–10.6) |
| Chl *a* [μg dm$^{-3}$] | 32.77 ± 24.54 (13.11–101.57) | 32.76 ± 11.71 (26.21–68.80) | 81.91 ± 14.31 (38.23–102.39) | 61.43 ± 25.98 (36.86–141.98) |
| Pheophytin [μg dm$^{-3}$] | 132.4 ± 35.1 (29.29–167.14) | 5.49 ± 6.02 (0.00–20.79) | 8.61 ± 17.52 (0.00–92.82) | 2.5 ± 0.56 (0.00–24.46) |
| TP [μg dm$^{-3}$] | 191 ± 35 (163–261) | 152 ± 39 (91–213) | 210 ± 49 (104–284) | 186.1 ± 36.23 (130–260) |
| SPR [μg dm$^{-3}$] | 24 ± 10 (9–50) | 16 ± 7 (0–65) | 14 ± 10 (1–42) | 14 ± 12 (1–50) |
| TN [mg dm$^{-3}$] | 0.63 ± 0.11 (0.39–0.89) | 1.25 ± 0.25 (0.88–1.74) | 1.71 ± 0.27 (1.18–2.15) | 1.62 ± 0.24 (1.03–2.12) |
| N-$NO_3$ [mg dm$^{-3}$] | 0.01 ± 0.006 (0.01–0.03) | 0.07 ± 0.02 (0.05–0.11) | 0.04 ± 0.016 (0.02–0.08) | 0.03 ± 0.013 (0.01–0.07) |
| N-$NH_4$ [mg dm$^{-3}$] | 0.02 ± 0.01 (0.005–0.045) | 0.02 ± 0.01 (0.012–0.064) | 0.03 ± 0.007 (0.01–0.04) | 0.03 ± 0.014 (0.01–0.07) |

**Table 2** Species composition, dominance and frequency of the zooplankton community in the Vistula Lagoon over the experimental period.

| | | Dominance [%][a] | Frequency [%][b] |
|---|---|---|---|
| *Anureopsis fissa* (Gosse, 1851) | Anu fis | 0.0 | 6.3 |
| *Asplanchna priodonta* Gosse, 1850 | Asp pri | 0.2 | 40.6 |
| *Brachionus angularis* Gosse, 1851 | Bra ang | 2.3 | 53.1 |
| *Brachionus calyciflorus* Pallas, 1766 | Bra cal | 0.9 | 31.3 |
| *Brachionus leydigii* Cohn, 1862 | Bra ley | 0.1 | 3.1 |
| *Colurella colurus* Ehrenberg, 1830 | Col col | 0.0 | 6.3 |
| *Euchlanis dilatata* Ehrenberg, 1832 | Euc dil | 0.0 | 6.3 |
| *Filinia longiseta* Ehrenberg, 1834 | Fil lon | 12.2 | 62.5 |
| *Keratella cochlearis f. tecta* (Gosse, 1886) | Ker cot | 10.8 | 96.9 |
| *Keratella cochlearis cochlearis* (Gosse, 1851) | Ker coc | 54.1 | 93.8 |
| *Keratella quadrata* (Müller, 1786) | Ker qua | 0.2 | 31.3 |
| *Polyarthra dolichoptera* Idelson, 1925 | Pol dol | 0.1 | 12.5 |
| *Polyarthra platyptera* Ehrenberg, 1838 | Pol pla | 1.8 | 18.8 |
| *Polyarthra vulgaris* (Carlin, 1943) | Pol vul | 0.5 | 25.0 |
| *Pompholyx sulcata* Hudson, 1885 | Pom sul | 0.2 | 21.9 |
| *Synchaeta baltica* Ehrenberg, 1834 | Syn bal | 0.1 | 15.6 |
| *Trichocerca pusilla* (Lauterborn, 1898) | Tri pus | 0.5 | 34.4 |
| *Trichocerca similis* (Wierzejski, 1893) | Tri sim | 0.5 | 12.5 |
| *Bosmina longirostris* (Müller, 1785) | Bos lon | 0.0 | 15.6 |
| *Ceriodaphnia quadrangula* (Müller, 1785) | Cer qua | 0.2 | 21.9 |
| *Chydorus sphaericus* (Müller, 1776) | Chy sph | 4.4 | 34.4 |
| *Diaphanosoma brachyurum* (Liévin, 1848) | Dia bra | 3.2 | 81.3 |
| *Leptodora kindtii* (Focke, 1844) | Lep kin | 0.0 | 6.3 |
| *Sida cristalina* (Müller, 1776) | Sid cri | 0.0 | 9.4 |
| *Acartia bifilosa* (Giesbrecht, 1881) | Aca bif | 0.1 | 21.9 |
| *Acartia longiremis* (Dana, 1846) | Aca lon | 1.7 | 81.3 |
| *Acartia tonsa* (Dana, 1846) | Aca ton | 1.1 | 75.0 |
| *Centropages hamatus* (Lilljeborg, 1853) | Cen ham | 0.0 | 3.1 |
| *Cyclops kolensis* Lindberg, 1956 | Cyc kol | 0.2 | 25.0 |
| *Cyclops vicinus* Ulyanin, 1875 | Cyc vic | 0.3 | 21.9 |
| *Eurytemora affinis* (Poppe, 1880) | Eur aff | 2.7 | 71.9 |
| *Eurytemora lacustris* (Poppe, 1887) | Eur lac | 1.1 | 28.1 |
| *Mesocyclops leuckarti* (Claus, 1857) | Mes leu | 0.1 | 6.3 |
| *Thermocyclops oithonoides* (Sars, 1863) | The oit | 0.2 | 25.0 |

[a] Dominance classes according to Kasprzak and Niedbała (1981): >10.0% eudominant species, 5.1–10.0% dominant species, 2.1–5.0% subdominant species, ≤1.0% sub-recedent species.
[b] Frequency criterion according to Tischler (1949) as cited in Trojan (1980): 100–76% (absolutely constant species), 75–51% (constant species), 50–26% (accesoric species), 25–0% (random species).

a characteristic phenomenon in vast, shallow brackish reservoirs that are estuary-like, such as the Vistula Lagoon. Water pH oscillated from neutral to slightly alkaline. The particulate matter concentration in the water did not drop below 50 mg $dm^{-3}$. Salinity, however, oscillated widely depending on the distance from sampling site to the open Baltic. Oxygen conditions were good in the years studied, and high levels of nutrients and chlorophyll *a* were recorded. Pheophytin concentrations, which were lower than chlorophyll *a* concentration except in 2006, indicated that conditions for zooplankton growth were good.

The Vistula Lagoon zooplankton included organisms from three taxonomic groups: Rotifera, Cladocera, and Copepoda. They were predominantly freshwater organisms that are highly tolerant of wide ranges of salinity. In addition, some brackish and marine taxa were observed. In total, 33 species were recorded, most of which belonged to Rotifera (17), followed by six Cladocera and ten copepod species. The species *K. cochlearis* was predominant in the qualitative structure of plankton fauna, while other commonly represented taxa included *Brachionus angularis*, *Filinia longiseta*, *Polyarthra platyptera*, *Chydorus sphaericus*, *Diaphanosoma brachyurum*, *Acartia longiremis* and *Eurytemora affinis* (Table 2).

The quantitative analysis of the samples indicated that the total density of zooplankton in the Vistula Lagoon ranged, on average, from 145 to 765 ind. $dm^{-3}$ (Fig. 2). Among rotifers, the most abundant was *K. cochlearis* with the highest density at the stations sampled of 6059 ind. $dm^{-3}$ and *F. longiseta* at 835 ind. $dm^{-3}$. Among plankton crustaceans, high numbers were recorded for *Ch. sphaericus* (1533 ind. $dm^{-3}$) and *D. brachyurum* (433 ind. $dm^{-3}$), while among copepods *A. longiremis* (162 ind. $dm^{-3}$) and *E. affinis* (208 ind. $dm^{-3}$) were numerous.

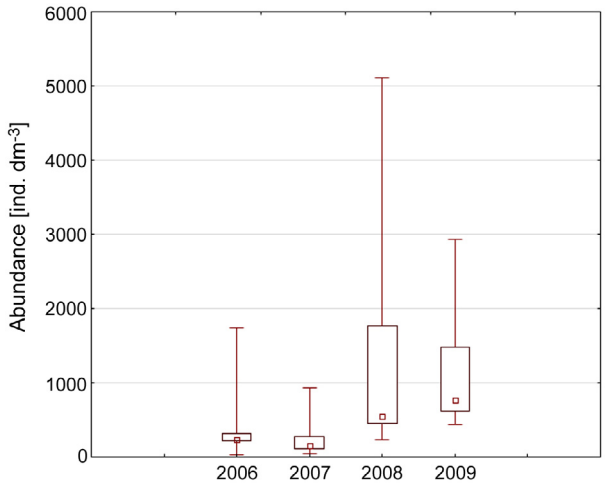


**Figure 2** Average abundance of zooplankton in the Vistula Lagoon.

Canonical Correspondence Analysis was performed for 34 taxa and eleven environmental variables. Among all 13 variables (Table 1), Secchi Disc Visibility (SDV) and pheophytin were not included in the analyzed dataset since they were strongly correlated with the variables selected. The variance inflation factor (VIF) of environmental variables included in the analysis displayed very low values and did not exceed the threshold of >4. All 11 factors were included in the final CCA. Variables used in the ordination explained 35% of the total variability of the zooplankton. The first and second canonical axes explained 10.5% (eigenvalue 0.250) and 9.6% (eigenvalue 0.228), respectively, of the variance in the species data and 30.1% and 27.3%, respectively, of the variance in species-environment relationships (Table 3).

The species–environment correlation of all axes became significant in the Monte Carlo permutation test ($F = 2.988$, $P < 0.01$). The CCAs showed that six of the examined environmental variables related significantly with the zooplankton assemblages (Table 4). The assemblages correlated most strongly with the concentration of total nitrogen (TN), although pH also influenced zooplankton distribution heavily.

Along the gradient of the first axis, the largest correlation between environmental variables and sample location was for $N\text{-}NO_3$ concentration ($r = -0.48$), along the second axis this was negatively correlated with TN concentration ($r = -0.70$) and suspended solids ($r = -0.56$) and was positively correlated with pH ($r = 0.63$). The largest correlation with the third axis was associated with $N\text{-}NH_4$ concentration ($r = 0.57$), while the fourth axis was associated with $O_2$ concentration ($r = 0.42$).

**Table 4** Environmental variables selected by the automatic forward procedure, in order of their inclusion in the model during the 'environmental' partial Canonical Correspondence Analysis of the species assemblages. The additional variance of each variable explains at the time of inclusion (i.e., conditional effect, lambda A) the marginal effect of each variable lambda (1), the statistics of the Monte Carlo significance test for the forward procedure ($F$) and the associated probability ($P$) for each variable.

| Variable | $\lambda_1$ | $\lambda_A$ | $P$ | $F$ |
|---|---|---|---|---|
| TN[a] | 0.20 | 0.20 | 0.002 | 6.42 |
| pH[a] | 0.20 | 0.18 | 0.002 | 6.45 |
| T[a] | 0.12 | 0.06 | 0.010 | 2.32 |
| PM | 0.12 | 0.03 | 0.292 | 1.14 |
| $N\text{-}NO_3$ | 0.11 | 0.04 | 0.092 | 1.54 |
| PSU | 0.11 | 0.04 | 0.064 | 1.68 |
| chl a[a] | 0.09 | 0.05 | 0.026 | 1.99 |
| $N\text{-}NH_4$[a] | 0.09 | 0.10 | 0.002 | 3.49 |
| $O_2$ | 0.09 | 0.05 | 0.072 | 1.66 |
| SPR[a] | 0.07 | 0.06 | 0.006 | 2.30 |
| TP | 0.04 | 0.02 | 0.414 | 1.02 |

[a] Variable significant ($P < 0.05$).

The CCA biplot for species and environmental variables indicated that taxa such as *Ceriodaphnia quadrangula* were positively correlated with nitrates, *Leptodora kindtii* was positively correlated with temperature, and species such as *Synchaeta baltica*, *Anuraeopsis fissa*, and *Brachionus leydigii* were negatively correlated with pH (Fig. 3).

The sampling sites are grouped according to the years in which the experiments were conducted. The plankton clusters recorded at sampling sites in 2006 are the most disparate group (Fig. 4). The community structure of the zooplankton in the Vistula Lagoon in 2006 appears to be strongly affected by temperature, while nitrogen concentration was indicated as a negative influence. The zooplankton diversity in the lagoon in 2009 appeared to be strongly affected by low pH. The zooplankton assemblages observed in 2007 and 2008 were not close to any of the physicochemical arrows, indicating that more than one factor or unmeasured factors were likely to have been important controllers of taxonomic diversity in these years of the study.

**Table 3** Summary of CCA results for the abundance of zooplankton taxa and 11 environmental variables. All axes were significant following Monte-Carlo permutation procedures.

| Axes | 1 | 2 | 3 | 4 | Total inertia |
|---|---|---|---|---|---|
| Eigenvalues | 0.250 | 0.228 | 0.101 | 0.074 | 2.380 |
| Species–environment correlations | 0.824 | 0.865 | 0.716 | 0.697 | |
| Cumulative percentage variance | | | | | |
| of species data | 10.5 | 20.1 | 24.3 | 27.5 | |
| of species–environment relation | 30.1 | 57.4 | 69.5 | 78.4 | |
| Sum of all eigenvalues | | | | | 2.380 |
| Sum of all canonical eigenvalues | | | | | 0.833 |

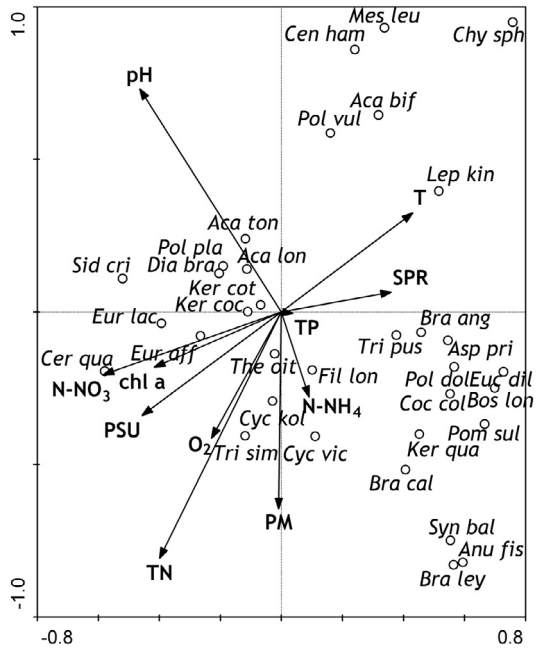


**Figure 3** Canonical Correspondence Analysis (CCA) ordination plot for species composition and environmental variables (T, temperature; PSU, salinity; pH, water reaction; PM, particulate matter; chl a, chlorophyll *a*; $O_2$, dissolved oxygen; N-$NO_3$, nitrate nitrogen; N-$NH_4$, ammonium nitrogen; TN, total nitrogen; TP, total phosphorus; SPR, soluble reactive phosphorus). Code for species in Table 2.

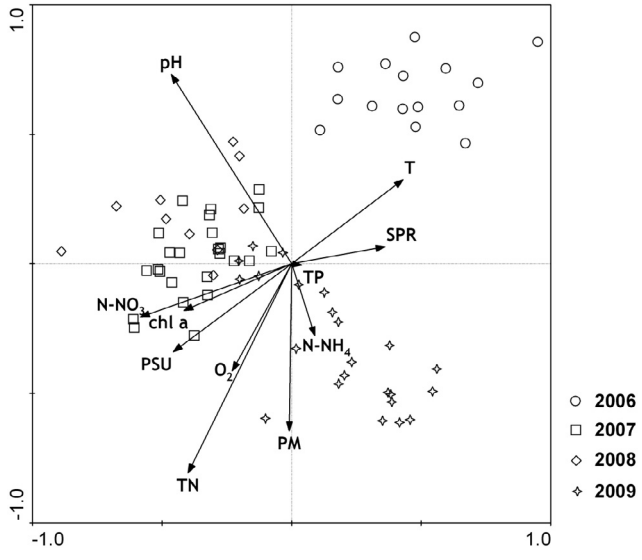


**Figure 4** The CCA ordination diagram of samples and environmental variables (T, temperature; PSU, salinity; pH, water reaction; PM, particulate matter; chl a, chlorophyll *a*; $O_2$, dissolved oxygen; N-$NO_3$, nitrate nitrogen; N-$NH_4$, ammonium nitrogen; TN, total nitrogen; TP, total phosphorus; SPR, soluble reactive phosphorus).

## 4. Discussion

Variations in the physicochemical properties of water bring about changes in the composition and abundance of aquatic organisms. Different environmental factors play important roles in the development and abundance of zooplankton (Suresh et al., 2011). Plankton fauna are found across a wide range of environmental conditions, yet the presence of some species is limited by factors such as dissolved oxygen, pH, temperature, salinity, or other physical and/or chemical properties (Ahmad et al., 2011). In the study presented here, no distinct tendencies of zooplankton grouping depending on a given environmental parameter were observed. Some species showed a clear reaction to a given factor; *L. kindtii*, a water flea, was one of them with abundance increases at higher water temperatures. This regularity was confirmed under laboratory conditions by Vijverberg and Koelewijn (2004). These authors recorded growth rates that were comparable at 15°C, 17.5°C, and 20°C, but at higher temperatures (25°C) growth was distinctly faster. Bowersox et al. (2014) also observed the close relation between the occurrence of *Leptodora* and water temperature. Other species did not show any correlation with this parameter, which is surprising since many authors have proved that the abundance and species diversity of zooplankton depend on temperature (Cognetti and Maltagliati, 2000; Gophen, 2012; Kaya et al., 2010; Marques et al., 2006; Paturej, 2006; Sebastian et al., 2012; Stelzer, 1998). An analogical situation was observed for salinity. There were no significant relations between this parameter and the abundance of zooplankton, which contrasts with data in the literature that emphasize the impact of salinity on plankton fauna (Cognetti and Maltagliati, 2000; Dube et al., 2010; Gao et al., 2008; Laprise and Dodson, 1994; Marques et al., 2006; Paturej, 2005, 2009; Silva et al., 2009; Telesh and Khlebovich, 2010). This could be explained by the specificity of the lagoon studied, which is inhabited mainly by species with a high tolerance to wide salinity ranges. In the present study, these were euryhaline rotifers of freshwater origin such as the genera *Brachionus* and *Trichocerca* and the species of *K. cochlearis*, *F. longiseta*, and *Pompholyx sulcata* (Fontaneto et al., 2006). The copepods were represented by typically freshwater species, i.e., *E. affinis*, and marine species of *Acartia* genus — *A. tonsa* and *A. longiremis*. Water fleas were also found occasionally, because, as typically freshwater organisms, they do not tolerate high salinity (Boix et al., 2007, 2008; Brucet et al., 2009). Interestingly, there was a negative correlation between the abundance of *A. fissa*, *B. leydigii*, and *S. baltica* and water pH. These organisms demonstrate a high degree of tolerance to pH changes (Koste, 1978; Radwan et al., 2004); therefore, this must have resulted from the impact of another factor, for instance, predatory pressure or strong water currents. Rotifers play a very important role in estuarine environments (Holst et al., 1998; Margoński et al., 2006), and, in the present study, three dominant species comprised over 78% of the total numbers of zooplankton. Among them, only *F. longiseta* appears to have been affected mainly by ammonia concentrations, while influence of more than one of the measured environmental variables was noted with regard to the most abundant species of *K. cochlearis* (and its *tecta* form).

While analyzing the influence of physicochemical properties on the sampling sites, it was observed that the samples were grouped by years, which could have stemmed from a diversity of environmental variables that were noted in subsequent years of the study. In 2006, salinity was low and temperatures were high, whereas in 2009 pH was low. The results of CCA showed opposite directions in temperature and salinity gradients, which could suggest higher inflows of colder waters from the Baltic Sea in 2009 than in 2006. This could have had a marked influence on changes in zooplankton community structure between these two years. Different living conditions for plankton organisms form annually, which means that the clusters found in the lagoon do not have a fixed taxonomic "skeleton" and are formed and mixed depending on the abiotic factors in a given year that are, in turn, shaped by the varied impact of factors associated with the proximity of the open sea or freshwater inputs from rivers. Thus, the present study demonstrated that physicochemical properties played a major role in creating zooplankton species structure and could also significantly impact entire zooplankton clusters.

## Acknowledgements

This study was carried out as part of the research projects *Monitoring the Vistula Lagoon water quality on the basis of satellite remote sensing (MONTRANSAT)* co-financed by the European Union from European Regional Development Fund, and *System of environmental and spatial information as the background for sustainable management of the Vistula Lagoon ecosystem (VISLA)* financed by the Polish-Norwegian Research Fund.

## References

Ahmad, U., Parveen, S., Khan, A.A., Kabir, H.A., Mola, H.R.A., Ganai, A.H., 2011. Zooplankton population in relation to physico-chemical factors of a sewage-fed pond of Aligarh (UP), India. BLM 3 (SI2), 336—341.

Alexander, R., (diss.) 2012. Interactions of zooplankton and phytoplankton with cyanobacteria. Univ. Nebraska, 69 pp.

Andrulewicz, E., Szymelfenig, M., Urbański, J., Węsławski, J.M., 2008. The Baltic Sea — What is Worth Knowing. Astra Print Shop, Gdynia, 113 pp., (in Polish).

Bednarz, T., Starzecka, A., Mazurkiewicz-Boroń, G., 2002. Microbiological processes accompanying the blooming of algae and cyanobacteria. Wiad. Botan. 46 (1—2), 45—55, (in Polish).

Boix, D., Gascón, S., Sala, J., Badosa, A., Brucet, S., López-Flores, R., Martinoy, M., Gifre, J., Quintana, X., 2008. Patterns of composition and species richness of crustaceans and aquatic insects along environmental gradients in Mediterranean water bodies. Hydrobiologia 597 (1), 53—69.

Boix, D., Sala, J., Gascón, S., Martinoy, M., Gifre, J., Brucet, S., Badosa, A., López-Flores, R., Quintana, X., 2007. Comparative diversity of crustaceans and aquatic insects from various water body types in coastal Mediterranean wetlands. Hydrobiologia 584 (1), 347—359.

Bowersox, B.J., Scarnecchia, D.L., Miller, S.E., 2014. Distribution, abundance and vertical migrations of *Leptodora kindtii* in a mainstream Missouri River reservoir, Montana, USA. J. Freshwater Ecol. 29 (2), 171—186.

Brucet, S., Boix, D., Gascón, S., Sala, J., Quintana, X.D., Badosa, A., Søndergaard, M., Lauridsen, T.L., Jeppesen, E., 2009. Species richness of crustacean zooplankton and trophic structure of brackish lagoons in contrasting climate zones: north temperate Denmark and Mediterranean Catalonia (Spain). Ecography 32 (4), 692—702.

Chubarenko, B., Margoński, P., 2008. The Vistula Lagoon. In: Schiewer, U. (Ed.), Ecology of Baltic Coastal Waters. Ecol. Stud. Springer-Verlag, Berlin-Heidelberg, 167—195.

Cognetti, G., Maltagliati, F., 2000. Biodiversity and adaptive mechanisms in brackish water fauna. Mar. Pollut. Bull. 40 (1), 7—14.

Cottenie, K., Nuytten, N., Michels, E., De Meester, L., 2001. Zooplankton community structure and environmental conditions in a set of interconnected ponds. Hydrobiologia 442 (1—3), 339—350.

Decker, M.B., Breitburg, D.L., Purcell, J.E., 2004. Effects of low dissolved oxygen on zooplankton predation by the ctenophore *Mnemiopsis leidyi*. Mar. Ecol.-Prog. Ser. 280, 163—172.

Dehui, Z., 1995. Effects of low pH on zooplankton in some suburban waterbodies of Chongqing City. J. Environ. Sci. 7 (1), 31—35.

Dmitrieva, O.A., Semenova, A.S., 2012. Seasonal dynamics and trophic interactions of phytoplankton and zooplankton in the Vistula Lagoon of the Baltic Sea. Oceanology 52 (6), 785—789.

Dube, A., Jayaraman, G., Rani, R., 2010. Modelling the effects of variable salinity on the temporal distribution of plankton in shallow coastal lagoons. J. Hydro-Environ. Res. 4 (3), 199—209.

Fontaneto, D., De Smet, W.H., Ricci, C., 2006. Rotifers in saltwater environments, re-evaluation of an inconspicuous taxon. J. Mar. Biol. Assoc. U.K. 86 (4), 623—656.

Gao, Q., Xu, Z., Zhuang, P., 2008. The relation between distribution of zooplankton and salinity in the Changjiang Estuary. Chin. J. Oceanol. Limnol. 26 (2), 178—185.

Golterman, H.L., Clymo, R.S., 1969. Methods for Chemical Analysis of Fresh Waters. Blackwell Scientific, Oxford, 172 pp.

González, E.J., Matos, M.L., Peñaherrera, C., Merayo, S., 2011. Zooplankton abundance, biomass and trophic state in some Venezuelan Reservoirs. In: Atazadeh, I. (Ed.), Biomass and Remote Sensing of Biomass. InTech, Rijeka, 57—74.

Gophen, M., 2012. The ecology of *Keratella cochlearis* in Lake Kinneret (Israel). Open J. Modern Hydrol. 2 (1), 1—6.

Hall, C.J., Burns, C.W., 2001. Effects of salinity and temperature on survival and reproduction of *Boeckella hamata* (Copepoda: Calanoida) from a periodically brackish lake. J. Plankton Res. 23 (1), 97—103.

Hermanowicz, W., Dojlido, J., Dożańska, W., Koziorowski, B., Zerbe, J., 1999. Physicochemical Analyses of Water and Sewage. Arkady, Warszawa, 556 pp., (in Polish).

Holst, H., Zimmermann, H., Kausch, H., Koste, W., 1998. Temporal and spatial dynamics of planktonic rotifers in the Elbe Estuary during spring. Estuar. Coast. Shelf Sci. 47 (3), 261—273.

ISO 10519:1997 (International Organization for Standardization), 1997. Determination of Chlorophyll Content. International Organization for Standardization, Switzerland, 24 pp.

Ivanova, M.B., Kazantseva, T.I., 2006. Effect of water pH and total dissolved solids on the species diversity of pelagic zooplankton in lakes: a statistical analysis. Russ. J. Ecol. 37 (4), 264—270.

Jongman, R.H.G., Ter Braak, C.J.F., Van Tongeren, O.F.R., 1995. Data Analysis in Community and Landscape Ecology. Cambridge Univ. Press, Cambridge, 324 pp.

Kasprzak, K., Niedbała, W., 1981. Biocenotic indicators in quantitative research. In: Górny, M., Grüm, L. (Eds.), Methods Applied in Soil Zoology, PWN, Warszawa, 397—416, (in Polish).

Kaya, M., Fontaneto, D., Segers, H., Altindağ, A., 2010. Temperature and salinity as interacting drivers of species richness of planktonic rotifers in Turkish continental waters. J. Limnol. 69 (2), 297—304.

Kinne, O., 1964. Physiologische und ökologische Aspekte des Lebens in Ästuarien. Helgoland. Wiss. Meer. 11 (3), 131—156.

Koste, W., 1978. Rotatoria. Die Rädertiere Mitteleuropas. Ein Bestimmungswerk, begründet von Max Voigt. Überordnung Monogononta. Gebrüder Borntraeger, Berlin-Stuttgart, 673 pp.

Kruk, M., Rychter, A., Mróz, M., 2012. The Vistula Lagoon. Environment and its Research in the VISLA Project. Wyd. PWSZ, Elbląg, 178 pp.

Kudari, V.A., Kanadami, R.D., 2008. Impact of changed trophic status on the zooplankton composition in six water bodies of Dharwad district, Karnataka state (South India). Environ. Monit. Assess. 144 (1—3), 301—313.

Lampert, U., 1997. Zooplankton research: the contribution of limnology to general ecological paradigms. Aquat. Ecol. 31 (1), 19—27.

Laprise, R., Dodson, J.J., 1994. Environmental variability as a factor controlling spatial patterns in distribution and species diversity of zooplankton in the St. Lawrence Estuary. Mar. Ecol.-Prog. Ser. 107, 67—81.

Margoński, P., Horbowa, K., Grzyb, A., Krajewska-Sołtys, A., Linkowski, T.B., 2006. Food composition of herring larvae in the Vistula Lagoon (southern Baltic Sea): impact of hydrological factors and changes in zooplankton community structure. ICES CM Documents 2006/F 03, 17 pp., http://www.ices.dk/sites/pub/CM%20Doccuments/2006/F/F0306.pdf.

Marques, S.C., Azeiteiro, U.M., Marques, J.C., Neto, J.M., Pardal, M.A., 2006. Zooplankton and ichthyoplankton communities in a temperate estuary: spatial and temporal patterns. J. Plankton Res. 28 (3), 297—312.

Mustapha, M.K., 2009. Zooplankton assemblage of Oyun Reservoir, Offa, Nigeria. Rev. Biol. Trop. 57 (4), 1027—1047.

Nawrocka, L., Kobos, J., 2011. The trophic state of the Vistula Lagoon: an assessment based on selected biotic and abiotic parameters according to the Water Framework. Oceanologia 53 (3), 881—894, http://dx.doi.org/10.5697/oc.53-3.881.

Ojaveer, H., Jaanus, A., MacKenzie, B., Martin, G., Olenin, S., Radziejewska, T., Telesh, I., Zettler, M.L., Zaiko, A., 2010. Status of biodiversity in the Baltic Sea. PLoS One 5 (9), http://dx.doi.org/10.1371/journal.pone.0012467.

Paturej, E., 2005. Zooplankton of seaside lakes in the coastal region of the Baltic Sea. Wyd. UWM, Olsztyn, 129 pp., (in Polish).

Paturej, E., 2006. Assessment of the trophic state of the coastal Lake Gardno based on community structure and zooplankton-related indices. Electr. J. Polish Agricult. Univ. 9 (2), http://www.ejpau.media.pl/volume9/issue2/art-17.html.

Paturej, E., 2009. A zooplankton-based study of coastal lakes. Baltic Coast. Zone 13 (2), 25—32.

Paturej, E., Kruk, M., 2011. The impact of environmental factors on zooplankton communities in the Vistula Lagoon. Oceanol. Hydrobiol. St. 40 (2), 37—48.

Perumal, V., Rajkumar, M., Perumal, P., Rajasekar, T.K., 2009. Seasonal variations of plankton diversity in the Kaduviyar estuary, Nagapattinam, southeast coast of India. J. Environ. Biol. 30 (6), 1035—1046.

Pinto-Coelho, R., Pinel-Alloul, B., Méthot, G., Havens, K.E., 2005. Crustacean zooplankton in lakes and reservoirs of temperate and tropical regions: variation with trophic status. Can. J. Fish. Aquat. Sci. 62 (2), 348—361.

PN 73/C-04576/08-1973, 1973. Water and sewage. Studies on the content of nitrogen compounds. Measuring nitrate nitrogen. Colorimetric method with phenol-disulphonic acid, 4 pp.

PN-C-04576-01:1976, 1976. Water and sewage. Studies on the content of nitrogen compounds. Measuring ammonium nitrogen with a colorimetric indol-phenolic method, 3 pp.

Psuty, I., Wilkońska, H., 2009. The stability of fish assemblages under unstable conditions: a ten year series from the Polish part of the Vistula Lagoon. Arch. Polish Fish. 17 (2), 65—76.

Radwan, S., Bielańska-Grajner, I., Ejsmont-Karabin, J., 2004. Rotifers (Rotifera). Wyd. Uniw. Łódz., Łódź, 447 pp., (in Polish).

Rajagopal, T., Thangamani, A., Sevarkodiyone, S.P., Sekar, M., Archunan, G., 2010. Zooplankton diversity and physico-chemical conditions in three perennial ponds of Virudhunagar district, Tamilnadu. J. Environ. Biol. 31 (3), 265—272.

Richardson, A.J., 2008. In hot water: zooplankton and climate change. ICES J. Mar. Sci. 65 (3), 279—295.

Roddie, B.D., Leakey, R.J.G., Berry, A.J., 1984. Salinity-temperature tolerance and osmoregulation in *Eurytemora affinis* (Poppe) (Copepoda: Calanoida) in relation to its distribution in the zooplankton of the upper reaches of the Forth estuary. J. Exp. Mar. Biol. Ecol. 79 (2), 191—211.

Rychter, A., Paturej, E., Jabłońska-Barna, I., 2011. Animals of the Vistula Lagoon. In: Kruk, M., Rychter, A., Mróz, M. (Eds.), Vistula Lagoon, 67—90, (in Polish).

Sebastian, P., Stibor, H., Berger, S., Diehl, S., 2012. Effects of water temperature and mixed layer depth on zooplankton body size. Mar. Biol. 159 (11), 2431—2440.

Silva, A.M.A., Barbosa, J.E.L., Medeiros, P.R., Rocha, R.M., Lucena-Filho, M.A., Silva, D.F., 2009. Zooplankton (Cladocera and Rotifera) variations along a horizontal salinity gradient and during two seasons (dry and rainy) in a tropical inverse estuary (Northeast Brazil). Pan-Am. J. Aquat. Sci. 4 (2), 226—238.

APHA, AWWA, WEF, Washington, D.C., 1496 pp.

Stelzer, C.P., 1998. Population growth in planktonic rotifers. Does temperature shift the competitive advantage for different species? Hydrobiologia 387—388, 349—353.

Suresh, S., Thirumala, S., Ravind, H.B., 2011. Zooplankton diversity and its relationship with physicochemical parameters in Kundavada Lake, of Davangere District, Karnataka, India. ProEnvironment 4 (7), 56—59.

Telesh, I.V., Khlebovich, V.V., 2010. Principal processes within the estuarine salinity gradient: a review. Mar. Pollut. Bull. 61 (4—6), 149—155.

Ter Braak, C.J.F., Šmilauer, P., 2002. CANOCO Reference Manual and User's Guide to Canoco for Windows: Software for Canonical Community Ordination (Version 4.5). Microcomputer Power, Ithaca, 500 pp.

Ter Braak, C.J.F., Šmilauer, P., 2003. Program CANOCO, Version 4.52. Biometris — Quantitative Methods in the Life and Earth Sciences. Plant Research International, Wageningen Univ. & Res. Centre, Wageningen.

Tischler, W., 1949. Grundzüge der terrestrischen Tierökologie. F. Vieweg & Sohn, Braunscheig, 220 pp.

Trojan, P., 1980. General Ecology. PWN, Warszawa, 419 pp., (in Polish).

Tunowski, J., 2009. Zooplankton structure in heated lakes with differing thermal regimes and water retention. Arch. Polish Fish. 17 (4), 291—303.

Vijverberg, J., Koelewijn, H.P., 2004. Effect of temperature on development and growth of the raptorial cladoceran *Leptodora kindtii* under laboratory conditions. Freshwater Biol. 49 (11), 1415—1422.

Wang, S., Xie, P., Wu, S., Wu, A., 2007. Crustacea zooplankton distribution patterns and their biomass as related to trophic indicators of 29 shallow subtropical lakes. Limnologica 37 (3), 242—249.

Warzocha, J., Szymanek, L., Witalis, B., Wodzinowski, T., 2016. The first report on the establishment and spread of the alien clam *Rangia cuneata* (Mactridae) in the Polish part of the Vistula Lagoon (southern Baltic). Oceanologia 58 (1), 54—58, http://dx.doi.org/10.1016/j.oceano.2015.10.001.

Witek, Z., Zalewski, M., Wielgat-Rychert, M., 2010. Nutrient stocks and fluxes in the Vistula Lagoon at the end of the twentieth century. Wyd. Nauk. Akad. Pom., Słupsk-Gdynia, 186 pp.

Yamada, Y., Ikeda, T., 1999. Acute toxicity of lowered pH to some oceanic zooplankton. Plankton Biol. Ecol. 46 (1), 62—67.

Yildiz, Ş., Altindağ, A., Ergönül, M.B., 2007. Seasonal fluctuations in the zooplankton composition of a eutrophic lake: Lake Marmara (Manisa, Turkey). Turk. J. Zool. 31 (2), 121—126.

Zar, J.H., 2010. Biostatistical Analysis. Prentice-Hall, New York, 944 pp.

Oceanologia (2017) 59, 57—68

Available online at www.sciencedirect.com

ScienceDirect

journal homepage: www.journals.elsevier.com/oceanologia/

ORIGINAL RESEARCH ARTICLE

# Testing the performance of empirical remote sensing algorithms in the Baltic Sea waters with modelled and *in situ* reflectance data

**Martin Ligi [a,1,*], Tiit Kutser [b,1], Kari Kallio [c], Jenni Attila [c], Sampsa Koponen [c], Birgot Paavel [b], Tuuli Soomets [b], Anu Reinart [a]**

[a] *Tartu Observatory, Nõo Parish, Tartu County, Estonia*
[b] *Estonian Marine Institute, University of Tartu, Tallinn, Estonia*
[c] *Finnish Environment Institute, Helsinki, Finland*

Received 4 April 2016; accepted 8 August 2016
Available online 24 August 2016

**KEYWORDS**
Band-ratio algorithm;
Marine optics;
Baltic Sea

**Summary** Remote sensing studies published up to now show that the performance of empirical (band-ratio type) algorithms in different parts of the Baltic Sea is highly variable. Best performing algorithms are different in the different regions of the Baltic Sea. Moreover, there is indication that the algorithms have to be seasonal as the optical properties of phytoplankton assemblages dominating in spring and summer are different. We modelled 15,600 reflectance spectra using HydroLight radiative transfer model to test 58 previously published empirical algorithms. 7200 of the spectra were modelled using specific inherent optical properties (SIOPs) of the open parts of the Baltic Sea in summer and 8400 with SIOPs of spring season. Concentration range of chlorophyll-*a*, coloured dissolved organic matter (CDOM) and suspended matter used in the model simulations were based on the actually measured values available in literature. For each optically active constituent we added one concentration below actually measured minimum and one concentration above the actually measured maximum value in order to test the performance of the algorithms in wider range. 77 *in situ* reflectance spectra from rocky (Sweden) and sandy

* Corresponding author at: Tartu Observatory, Observatooriumi 1, Tõravere 61602, Nõo Parish, Tartu County, Estonia. Tel.: +372 51 39 778; fax: +372 696 2555.
*E-mail addresses:* ligi@to.ee (M. Ligi), tiit.kutser@sea.ee (T. Kutser), kari.y.kallio@ymparisto.fi (K. Kallio), Anu.Reinart@to.ee (A. Reinart).
[1] These authors contributed equally to this work.
Peer review under the responsibility of Institute of Oceanology of the Polish Academy of Sciences.

Production and hosting by Elsevier

http://dx.doi.org/10.1016/j.oceano.2016.08.002

(Estonia, Latvia) coastal areas were used to evaluate the performance of the algorithms also in coastal waters. Seasonal differences in the algorithm performance were confirmed but we found also algorithms that can be used in both spring and summer conditions. The algorithms that use bands available on OLCI, launched in February 2016, are highlighted as this sensor will be available for Baltic Sea monitoring for coming decades.


## 1. Introduction

Water reflectance data collected with field radiometers has mainly been used for satellite data calibration and validation purposes. However, handheld devices and portable autonomous systems on ferries, jetties, and buoys have become remote sensing tools in their own, as they allow collecting fast and frequent data about the state of waterbodies (Alikas et al., 2015; Groetsch et al., 2014; Simis and Olsson, 2013). Processing the radiometer, as well as satellite data, can be carried out in different ways. A "classical" approach is developing empirical relationships between band-ratios (colour indices), their combinations or more sophisticated parameters and water characteristics, like chlorophyll-*a* concentration. The disadvantages of the empirical methods are that they tend to be local (need tuning for a particular waterbody) or even seasonal (Metsamaa et al., 2006), and need to be developed for each sensor used.

An alternative approach is physics-based analytical methods, where full modelled spectra are used for retrieving chlorophyll-*a*, suspended matter and CDOM (coloured dissolved organic matter) are becoming more and more popular in interpretation of aquatic remote sensing data. Such methods have also been used for more than two decades (Arst and Kutser, 1994; Kutser et al., 2001) and advanced to inversion procedures like Sambuca (Dekker et al., 2011), Bomber (Giardino et al., 2012) retrieving inherent optical water properties (IOPs) and shallow water bottom type simultaneously. There are also neural network type approaches like the method developed for MERIS (Doerffer and Schiller, 2007). The disadvantages of analytical methods, that use water leaving reflectance as the source for water quality parameters calculations, are that they are computationally expensive and require very high-quality input data (*e.g.* perfect atmospheric correction) that is often difficult to achieve. The requirement of high quality input data refers to the spectral library and other model inversion methods. Neural networks can be trained to produce reasonable results even if the reflectance spectra are unrealistic.

It has been shown by many authors (Beltran-Abaunza et al., 2014; Darecki and Stramski, 2004; Kratzer et al., 2008; Reinart and Kutser, 2006) that ocean colour algorithms based on the ratio of blue and green bands (like the OC4v6 developed for retrieving chlorophyll-*a*) provided by different space agencies do not perform well in such optically complex waterbodies like the Baltic Sea. There have been remote sensing activities in different parts of the Baltic Sea and variety of empirical algorithms have been proposed (Attila et al., 2013; Beltran-Abaunza et al., 2014; Darecki et al., 2003, 2005, 2008; Härmä et al., 2001; Koponen et al., 2007; Kowalczuk et al., 2005a, 2010; Kutser, 2004; Kutser et al., 2005a, 2006; Woźniak et al., 2008). However, the algorithms proposed are usually local; applying them in other parts of the sea requires tuning of the algorithms. Moreover, previous studies suggested that there may be need for seasonal water quality algorithms in the Baltic Sea as phytoplankton assemblages in spring and summer are different and their optical properties are very different (Erm et al., 2008; Feistel et al., 2008; Kowalczuk et al., 2005b; Wasmund and Uhlig, 2003). This means that, on the one hand, creating the spectral library necessary for retrieving water properties in the Baltic Sea has to contain reflectance spectra for different seasons. On the other hand, it also suggests that it may be difficult to find band-ratio type algorithms that perform well during the whole year.

As seen in the MERIS ATBD (Doerffer and Schiller, 1997), neural networks have several complicated steps in their calculation. Therefore, the computations may take time, when large satellite images are processed. Empirical algorithms can be used to define initial values for analytical processing to speed up the process by narrowing down the range of variation. For example, the inversion procedures do not have to use the whole spectral library, but only parts of it when approximate concentrations of chlorophyll-*a*, CDOM and suspended matter have been estimated by band-ratio type algorithms. Many satellite instruments are configured to measure water-leaving signal only at a few spectral bands. It means that analytical methods are not always easily usable in interpretation of data from such sensors. Simple band-ratio type remote sensing algorithms are often a good option for retrieving water quality parameters from multispectral data, but these algorithms may also be used in the case of sensors with better spectral resolution as they are computationally fast and easy to use. Therefore, these computationally simple algorithms are also widely used in remote sensing (Ammenberg et al., 2002; Gitelson et al., 2009; Kallio et al., 2001; Koponen et al., 2007).

Our aim was to test whether there are simple empirical algorithms, that use only few spectral channels, which allow estimating chlorophyll-*a*, CDOM and suspended matter concentrations in the Baltic Sea. In an ideal case these algorithms should work all year round, but finding even seasonal algorithms that perform well would be a step forward. The tested algorithms were taken from previously published papers. The reflectance data used in this study was partly simulated with HydroLight radiative model using both summer and spring sets of SIOPs. The concentrations of chlorophyll-*a*, suspended matter and CDOM used in the model simulations covered the whole known range for the Baltic

**Table 1** Concentrations used in the spring simulations.

| Variable | Concentrations | | | | | | | | | | | | | | *N* |
|---|---|---|---|---|---|---|---|---|---|---|---|---|---|---|---|
| Chl [$\mu g\ l^{-1}$] | 0.10 | 1.0 | 2.0 | 4.0 | 6.0 | 8.0 | 10.0 | 14.0 | 20.0 | 26.0 | 32.0 | 42.0 | 84.0 | 250.0 | 14 |
| TSM [$mg\ l^{-1}$] | 0.05 | 0.4 | 0.8 | 1.3 | 1.8 | 2.3 | 4.0 | 5.7 | 7.4 | 8.9 | 18.0 | 50.0 | | | 12 |
| $a_{CDOM}(412)$ [$m^{-1}$] | 0.05 | 0.2 | 0.3 | 0.5 | 0.7 | 0.9 | 1.2 | 1.5 | 3.0 | 20.0 | | | | | 10 |

**Table 2** Concentrations used in the summer simulations.

| Variable | Concentrations | | | | | | | | | | | | *N* |
|---|---|---|---|---|---|---|---|---|---|---|---|---|---|
| Chl [$\mu g\ l^{-1}$] | 0.10 | 0.8 | 1.7 | 2.5 | 3.3 | 4.2 | 6.2 | 8.2 | 10.2 | 12.8 | 26.0 | 120.0 | 12 |
| TSM [$mg\ l^{-1}$] | 0.05 | 0.2 | 0.3 | 0.8 | 1.3 | 1.8 | 3.4 | 5.0 | 6.6 | 8.1 | 16.0 | 50.0 | 12 |
| $a_{CDOM}(412)$ [$m^{-1}$] | 0.05 | 0.2 | 0.3 | 0.5 | 0.7 | 0.9 | 1.2 | 1.5 | 3.0 | 20.0 | | | 10 |

Sea. *In situ* measured data was available for rocky coast of the Baltic Sea (Sweden) and sandy coastal areas (Estonia and Latvia). This datasets allowed evaluating the performance of empirical algorithms for the whole Baltic Sea and two distinctly different seasons. The coastal dataset allowed extending the results to nearshore waters where the concentrations of optically active substances may be beyond those usually observed in the areas reachable by research vessels and were represented by modelled spectra.

## 2. Material and methods

58 different previously published empirical algorithms were tested. Out of the 58, listed in Table 4, 30 were for chlorophyll-*a* (CHL), 20 for the total suspended matter (TSM) and 8 for coloured dissolved organic matter (CDOM). As some publications give the algorithm with the concentration as the output, but others do not, we have only used the general form of the approaches for comparison (*e.g.* band-ratio to concentration) and calculated the slopes and intercepts from our database. Many algorithms were not used in this study, as they were for case 1 waters and for concentrations too low for the Baltic Sea.

Hydrolight radiative transfer software was used to produce a spectral library of Baltic Sea waters. HydroLight is a commercial software product of Sequoia Scientific, Inc. It is a well-known radiative transfer numerical model that computes radiance distributions and derived quantities, such as irradiances and reflectances, for natural water bodies. Using Hydrolight, spectral radiance distribution can be computed as a function of depth, direction, and wavelength within the water. Water-leaving and reflected-sky radiances are computed separately. HydroLight has to be parameterized with SIOPs of the particular water body under investigation and the number of the optically active substances used in the model can be predefined by the user. The illumination conditions (solar zenith angle, cloudiness) and the state of the sea surface (wind) can be defined by the user. The model uses concentrations of optically active substances as input. A detailed description of the HydroLight software can be found in Mobley and Sundman (2013a, 2013b). Mobley (1994) describes the theoretical basis for the solution of radiative transfer modelling equations. A methodology to use the Hydrolight model for creating spectral libraries in automated Matlab software simulations was generated in the framework of the Finnish national project EOMORE and the EU/FP7 project GLaSS (Global Lakes Sentinel Services). It is shortly described in Attila et al. (2015).

The model simulations were carried out with the SIOPs of summer and spring situations. Concentrations of optically active substances (Tables 1 and 2) were also slightly different. The concentrations were defined based on the statistical distribution of the concentrations in the database collected on R/V Aranda over the Baltic Sea. One concentration below the minimum measured value and one concentration above the measured maximum value were added to the concentration ranges in order to expand the modelling range. The concentrations were selected in the range that should be realistic for the Baltic Sea conditions. The modelled reflectance spectra are shown in Fig. 1.

The main reason of the differences between modelled and measured data is because the modelled spectra are ideal cases, while real measurements include waves, different illumination conditions and other disturbances that occur during real field measurements.

The modelled spectra were simulated using SIOPs of waters sampled from research vessel. Nearshore waters are sometimes optically quite different due to river inflows or resuspension of bottom sediments. In order to expand the open Baltic Sea spectral library (modelled spectra) we used also *in situ* data collected from 77 coastal stations. The data was collected between May and September in Estonia, Latvia and Sweden in 2010—2015 (Figs. 2 and 3, Table 3).

For determination of the concentration of chlorophyll-*a* (in $mg\ m^{-3}$), water samples were filtered through Whatman GF/F-filters (0.7 $\mu$m pore size) and then extracts of the filters

**Table 3** Ranges of measured values.

| Variable | Min | Max | Mean |
|---|---|---|---|
| Chl [$\mu g\ l^{-1}$] | 0.79 | 22.38 | 4.80 |
| TSM [$mg\ l^{-1}$] | 1.20 | 18.00 | 6.26 |
| $a_{CDOM}(412)$ [$m^{-1}$] | 0.28 | 13.46 | 2.28 |

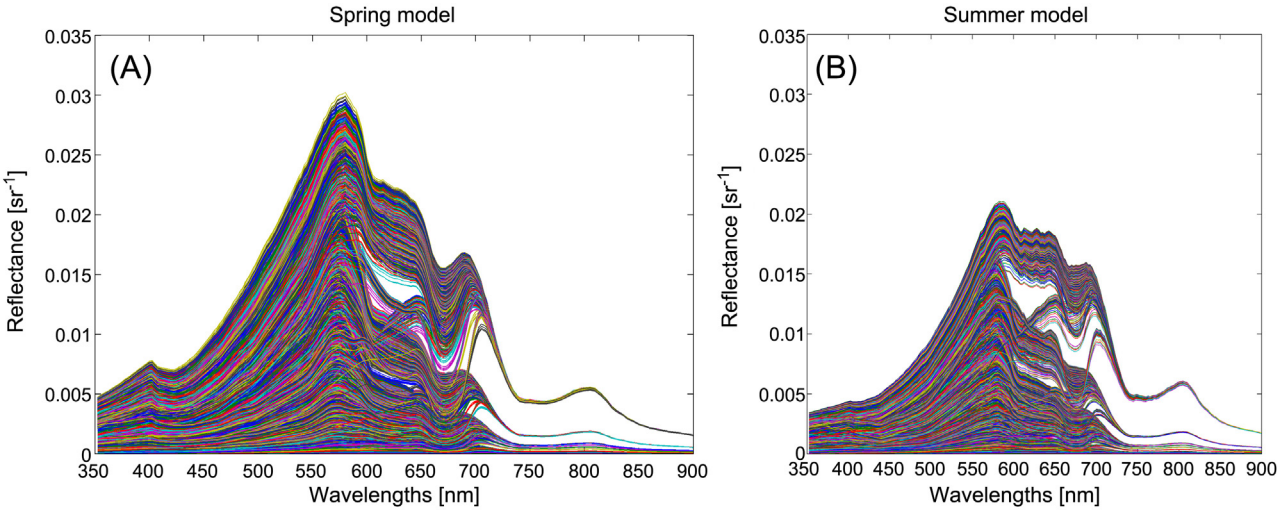


**Figure 1** Reflectance ($R_{rs}$) spectra used in this study: (A) modelled reflectance with spring SIOPs; (B) modelled reflectance with summer SIOPs.

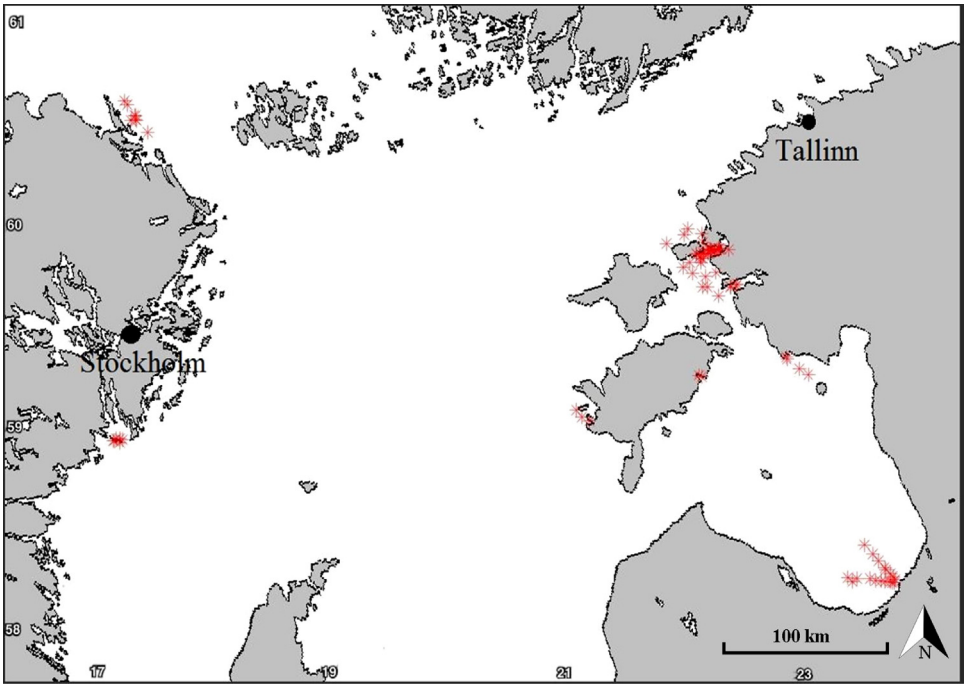


**Figure 2** Locations of the sampling points in the coastal waters of the Baltic Sea.

were investigated spectrophotometrically in 96% ethanol according to the ISO standard method (ISO, 1992). Finally, CHL was calculated using the Lorenzen (Lorenzen, 1967) method.

The concentration of total suspended matter (TSM), was measured gravimetrically after filtration of the same amount of water through pre-weighed and pre-combusted (103–105°C for 1 h) GF/F filters. The inorganic fraction of suspended matter, SPIM, was measured after combustion at 550°C for 30 min. The organic fraction of suspended matter, SPOM, was determined by subtraction of SPIM from TSM (ESS, 1993).

Absorption by coloured dissolved organic matter ($a_{CDOM}$) was measured with a spectrometer (Hitachi U-3010 UV/VIS, at the range of 350–750 nm) in water filtered through a Millipore 0.2 μm filter. Measurements were carried out in a 5-cm cuvette against distilled water and corrected for residual scattering according to Davies-Colley and Vant (1987). $a_{CDOM}$(412) was used for measuring CDOM concentration in the algorithm analyses. Different algorithms use different wavelengths for CDOM, but as Kowalczuk et al. (2005a) has shown, the slope of the CDOM in the Baltic Sea is relatively stable throughout the year so using a different wavelength as reference should not change the performance of the algorithm.

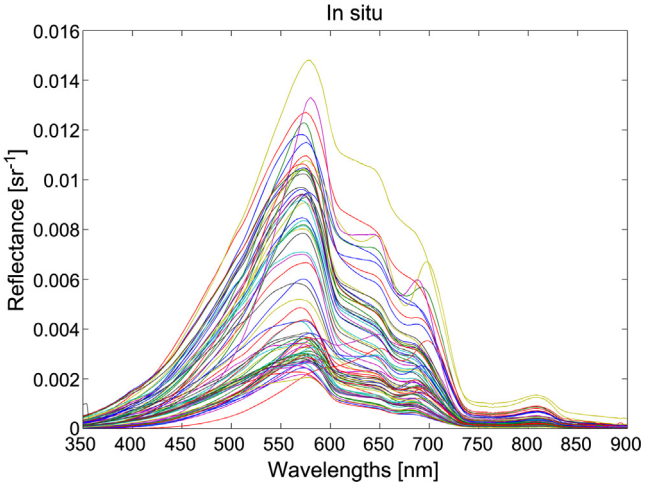


**Figure 3** *In situ* measured reflectance ($R_{rs}$) spectra used in this study.

Above water remote sensing reflectance measurements were carried out with two TriOS RAMSES sensors, where RAMSES-ACC-VIS measures sky irradiance and RAMSES-ARC upwelling radiance. The downwelling irradiance sensor was looking straight up and the upwelling radiance sensor was looking straight down. The methodology was described in more detail in Kutser et al. (2013). RAMSES measures with a 3.3 nm spectral interval at the wavelength range of 350–900 nm. In order to avoid errors in reflectance spectra that occur due to the slight wavelength differences between the two sensors both radiance and irradiance values were interpolated to a 2-nm step before calculating the reflectance as a ratio of upwelling radiance to downwelling irradiance.

To evaluate the performance of the algorithms we used correlation between known concentrations (*in situ* results and model inputs) and algorithm outputs. From the outputs, concentrations were calculated and the mean normalized bias, MNB (systematic error), as well as the normalized rms error (random error), RMS, was calculated, as suggested by Darecki et al. (2005). These errors were defined as follows:

$$\mathrm{MNB} = \mathrm{mean}\left(\frac{x_{calculated} - x_{input}}{x_{input}}\right) \times 100\%,$$

$$\mathrm{RMS} = \mathrm{stdev}\left(\frac{x_{calculated} - x_{input}}{x_{input}}\right) \times 100\%,$$

where $x_{calculated}$ is the chlorophyll concentration estimated from the algorithm and $x_{input}$ is the measured (*in situ*) or model input concentration.

## 3. Results and discussion

There are no empirical algorithms or other image processing methods that have demonstrated good performance in retrieving chlorophyll-*a*, CDOM or TSM with high accuracy in all parts of the Baltic Sea and during the whole ice-free season. For example the Copernicus Marine Environment Monitoring Service uses chlorophyll-*a* algorithm that has nearly negligible correlation with measured chlorophyll ($r^2 = 0.21$) (Garnesson and Krasemann, 2016). The latest results by Pitarch et al. (2015) got slightly better results ($r^2 = 0.42$) with OC4v6. One of the main reasons is optical properties of the Baltic Sea. For example, standard satellite chlorophyll products rely on the ratio of blue and green spectral bands (Darecki and Stramski, 2004). Baltic Sea waters are rich in CDOM that absorbs most of the light in the blue part of the spectrum (Darecki et al., 2003; Kowalczuk et al., 2005b). Therefore, the water leaving radiance in blue is very small. Sun and sky glint also affect the measured signal mostly in the blue part of the spectrum. Consequently, using the blue band in empirical algorithms is not favoured in optically complex waters like the Baltic Sea. Nevertheless, we tested the suitability of a widely used OC4v6 algorithm by means of model simulations. Coefficient of determination between the chlorophyll-*a* concentrations used in the model and estimated based on the simulated reflectance spectra by means of the OC4v6 was poor – $R^2 = 0.0054$. The results match with the previous findings (Beltran-Abaunza et al., 2014; Darecki and Stramski, 2004; Kratzer et al., 2008; Pitarch et al., 2015; Reinart and Kutser, 2006) that the blue-green ratio is not suitable for retrieval of chlorophyll-*a* in waters where the remote sensing signal in blue part of spectrum is determined by absorption of CDOM not chlorophyll-*a*. On the other hand results by Pitarch et al. (2015) are better than our modelling results. This is surprising as we calculated the OC4v6 from perfect modelled reflectance whereas Pitarch et al. (2015) used satellite data that contains different sources of noise, atmospheric correction errors, *etc*. To certain extent the results by Pitarch et al. (2015) were improved by including about one third of stations from Skagerrak and Kattegat where the physical water properties (salinity) and optical water properties are quite different from the actual Baltic Sea. However, this does not explain all the difference. The results for all other band ratios tested by us are provided in Table 4.

Phytoplankton succession in the Baltic Sea has a strong seasonal component. A spring bloom, dominated by diatoms, starts after ice melts. It is followed by a phytoplankton minimum in June and dominance of cyanobacteria typically in July–August. The optical properties of cyanobacteria differ significantly from other phytoplankton (Groetsch et al., 2014; Kutser et al., 2006; Simis et al., submitted for publication). Therefore, we produced two different spectral libraries – one with SIOPs of spring algal assemblage and one with SIOPs of cyanobacterial season. It was surprising that several band ratio algorithms performed well in estimating CHL, TSM and CDOM from the reflectance spectra of both spring and summer spectral libraries as well as when combined with *in situ* results. It is seen in Figs. 4–7 that the results for spring and summer seasons are slightly different, but some band ratio algorithms provided still acceptable results when spring and summer data was combined. The differences between spring and summer are not large (Fig. 4), but grouping exists and when only results from one season is used, then the statistics are slightly improved. It is also seen in Fig. 4 that the data from most of the *in situ* sampling stations (green circles) fit with the results obtained from modelled spectral libraries. The grouping of points, seen in Fig. 4 (and following figures), occurs because for every chlorophyll concentration used in the model simulation there were several sets with different TSM and CDOM concentrations. This produces the horizontal scattering of points for the same concentration of chlorophyll-*a*. Note that the *in situ* points were not taken into account in calculating the

**Table 4** List of algorithms used in this study.

| Reference | General form | Code | $R^2$ IS | MNB% IS | RMS% IS | $R^2$ model | MNB% model | RMS% model |
|---|---|---|---|---|---|---|---|---|
| Chlorophyll | | | | | | | | |
| Zimba and Gitelson (2006) | (1/R650 − 1/R710) × R740 | CHL1 | 0.259 | 43 | 99 | 0.838 | 305 | 4581 |
| Moses et al. (2009a) | (1/R665 − 1/R708) × R753 | CHL2 | 0.403 | 36 | 93 | 0.948 | −9 | 1970 |
| Gitelson et al. (2009) | (1/R670 − 1/R710) × R750 | CHL3 | 0.414 | 35 | 93 | 0.964 | −144 | 1750 |
| Mayo et al. (1995) | (R485 − R660)/R570 | CHL4 | 0.194 | 47 | 99 | 0.001 | 2497 | 6908 |
| Hunter et al. (2008) | log10(R710/R670) | CHL5 | 0.499 | 31 | 91 | 0.812 | −1021 | 5477 |
| Han and Jordan (2005) | log10(R482.5)/log10(R660) | CHL6 | 0.224 | 45 | 96 | 0.003 | 2475 | 6880 |
| Schalles et al. (1998) | max(R670 − R850) − (R670 − R850) line value at the location of maximum | CHL7 | 0.469 | 41 | 103 | 0.041 | 2270 | 6456 |
| Brezonik et al. (2005) | R482.5/R660 | | | | | | | |
| | Linear | CHL8 | 0.172 | 47 | 101 | 0.014 | 2231 | 7146 |
| | Exponential | | 0.219 | 22 | 82 | 0.005 | 560 | 1869 |
| | Power | | 0.191 | 21 | 82 | 0.020 | 579 | 1910 |
| Östlund et al. (2001) | R565/(R482.5 + R565 + R660) | CHL9 | 0.074 | 55 | 119 | 0.020 | 2333 | 6887 |
| Wang et al. (2006) | R660/R565 | CHL10 | 0.167 | 49 | 104 | 0.002 | 2540 | 7061 |
| Dierberg and Carriker (1994) | R693.5/R679 | | | | | | | |
| | Linear | CHL11 | 0.556 | 29 | 86 | 0.856 | −1125 | 4198 |
| | Power | | 0.429 | 16 | 75 | 0.725 | 119 | 486 |
| Duan et al. (2007), Menken et al. (2006) and Dierberg and Carriker (1994) | R700/R670 | CHL12 | 0.552 | 30 | 88 | 0.934 | −524 | 2804 |
| Kutser et al. (1999) and Kallio et al. (2001) | R702/R674 | CHL13 | 0.551 | 30 | 88 | 0.951 | −522 | 2569 |
| Koponen et al. (2007) and Ammenberg et al. (2002) | R705/R664 | CHL14 | 0.503 | 32 | 94 | 0.924 | −145 | 2732 |
| Kallio et al. (2003) | R705/R673 | CHL15 | 0.549 | 30 | 88 | 0.957 | −399 | 2337 |
| Kallio et al. (2001) | R706.5/R677.5 | CHL16 | 0.526 | 31 | 91 | 0.966 | −447 | 2317 |
| Kallio et al. (2001) and Moses et al. (2009a) | R707.5/R664 | CHL17 | 0.501 | 33 | 93 | 0.928 | −97 | 2679 |
| Kallio et al. (2001) | R709.5/R673.5 | CHL18 | 0.545 | 31 | 88 | 0.962 | −319 | 2237 |
| Jiao et al. (2006) | R719/R665 | | | | | | | |
| | Linear | CHL19 | 0.465 | 35 | 99 | 0.938 | −48 | 2736 |
| | Power | | 0.337 | 18 | 82 | 0.581 | 226 | 954 |
| Härmä et al. (2001) | R730/R710 | CHL20 | 0.005 | 59 | 121 | 0.243 | 1600 | 6867 |
| Härmä et al. (2001) | R735/R720 | CHL21 | 0.004 | 58 | 116 | 0.127 | 1956 | 6507 |
| Moses et al. (2009b) | R748/R667 | CHL22 | 0.163 | 50 | 116 | 0.938 | −79 | 2843 |
| Yacobi et al. (1995) | Rmax(670 − 850)/R670 | CHL23 | 0.397 | 46 | 149 | 0.960 | 90 | 869 |
| Schalles et al. (1998) | Sum (R670 − R850) − (sum R670 − R850) Linear | CHL24 | 0.006 | 59 | 119 | 0.211 | 1197 | 7752 |
| Kutser et al. (2016) | R710 − (R676 − R770 linear at R710) | CHL25 | 0.480 | 40 | 97 | 0.089 | 1962 | 5580 |
| Kutser et al. (2016) | R810 − (R770 − R840 linear at R810) | CHL26 | 0.202 | 49 | 111 | 0.000 | 2538 | 7002 |

**Table 4** (*Continued*)

| Reference | General form | Code | $R^2$ IS | MNB% IS | RMS% IS | $R^2$ model | MNB% model | RMS% model |
|---|---|---|---|---|---|---|---|---|
| Anon (2015) | 10^($a + b \times X + c \times X$^2 + $d \times X$^3 + $e \times X$^4), $X$ = log 10(R489/R555) | CHL27 | 0.064 | 55 | 112 | 0.005 | 2504 | 7004 |
| Darecki et al. (2003) | R550/R590 | CHL28 | 0.160 | 48 | 98 | 0.057 | 1857 | 7146 |
| Darecki et al. (2005) | 10^(log($R$(550)/$R$(590))) | CHL29 | 0.160 | 48 | 98 | 0.057 | 1857 | 7146 |
| Woźniak (2014) | R555/R645 | CHL30 | 0.182 | 47 | 104 | 0.049 | 1998 | 7141 |
| Total suspended matter | | | | | | | | |
| Dekker et al. (2002) | (R545 + R645)/2 | | | | | | | |
| | Linear | TSM1 | 0.294 | 32 | 80 | 0.793 | −235 | 690 |
| | Exponential | | | | | 0.427 | 142 | 424 |
| Dekker et al. (2002) | (R565 + R660)/2 | | | | | | | |
| | Linear | TSM2 | 0.291 | 32 | 80 | 0.794 | 252 | 719 |
| | Exponential | | | | | 0.425 | 139 | 418 |
| Kutser et al. (1999) | (Rmax − R750)/(R476 − R750) | TSM3 | 0.005 | 45 | 101 | 0.000 | 1899 | 4437 |
| Kutser et al. (2016) | R810 − (R770 − R840)base | TSM4 | 0.207 | 36 | 86 | 0.997 | 86 | 214 |
| Wang and Ma (2001) | ln((R660 + R825)/(R482.5 + R565)) | TSM5 | 0.014 | 44 | 99 | 0.179 | 782 | 3713 |
| Neukermans et al. (2009) | R635/(0.162 − R635) | TSM6 | 0.260 | 33 | 79 | 0.900 | −63 | 187 |
| Miller and McKee (2004) | R645 | TSM7 | 0.263 | 33 | 79 | 0.913 | −139 | 370 |
| Doxaran et al. (2006) and Wang et al. (2006) | R660/R565 | | | | | | | |
| | Linear | TSM8 | 0.007 | 45 | 100 | 0.088 | 1548 | 3909 |
| | Exponential | | 0.015 | 21 | 83 | 0.178 | 433 | 1330 |
| Kallio et al. (2001) | R702 | TSM9 | 0.230 | 35 | 83 | 0.987 | −69 | 172 |
| Kallio et al. (2001) | R702 − R751 | TSM10 | 0.235 | 34 | 81 | 0.970 | −106 | 266 |
| Koponen et al. (2007) and Ammenberg et al. (2002) | R705 | TSM11 | 0.228 | 35 | 83 | 0.991 | −62 | 152 |
| Thiemann and Kaufmann (2000) | R705/R678 | TSM12 | 0.040 | 43 | 98 | 0.005 | 1844 | 4314 |
| Härmä et al. (2001) | R705 − R754 | TSM13 | 0.233 | 34 | 81 | 0.976 | −100 | 249 |
| Kallio et al. (2001) | R709.5 | TSM14 | 0.225 | 35 | 84 | 0.994 | −38 | 91 |
| Doxaran et al. (2003) and Doxaran et al. (2006) | R825/R565 | | | | | | | |
| | Linear | TSM15 | 0.000 | 46 | 102 | 0.118 | 1360 | 3192 |
| | Exponential | | 0.008 | 22 | 86 | 0.196 | 367 | 992 |
| Doxaran et al. (2003) and Onderka and Pekarova (2008) | R840/R545 | | | | | | | |
| | Linear | TSM16 | 0.000 | 46 | 102 | 0.097 | 1413 | 3253 |
| | Exponential | | 0.003 | 22 | 85 | 0.181 | 367 | 972 |
| Doxaran et al. (2002) and Doxaran et al. (2005) | R850/R550 | | | | | | | |
| | Linear | TSM17 | 0.001 | 46 | 101 | 0.098 | 1407 | 3238 |
| | Exponential | | 0.001 | 22 | 85 | 0.181 | 367 | 971 |
| | Polynomial | | 0.001 | 42 | 97 | 0.181 | 522 | 4231 |
| Doxaran et al. (2003) | R855/R55 | | | | | | | |
| | Linear | TSM18 | 0.001 | 45 | 101 | 0.101 | 1398 | 3225 |
| | Exponential | | | | | 0.183 | 367 | 973 |
| Kutser et al. (2016) | R710 − (R676 − R770 linear at R710) | TSM19 | 0.000 | 46 | 102 | 0.594 | 932 | 2207 |
| Woźniak (2014) | R555/R645 | TSM20 | 0.023 | 44 | 98 | 0.163 | 678 | 4659 |

**Table 4** (*Continued*)

| Reference | General form | Code | $R^2$ IS | MNB% IS | RMS% IS | $R^2$ model | MNB% model | RMS% model |
|---|---|---|---|---|---|---|---|---|
| Coloured dissolved organic matter | | | | | | | | |
| Brezonik et al. (2005) | R482.5 − 0.657 (R482.5/R825) | CDOM1 | 0.334 | 20 | 99 | 0.040 | 720 | 2019 |
| Koponen et al. (2007) | R663/R490 | CDOM2 | 0.807 | 21 | 68 | 0.827 | 91 | 975 |
| Doxaran et al. (2005) | R400/R600 | | | | | | | |
| | Linear | CDOM3 | 0.337 | 19 | 58 | 0.061 | 514 | 2145 |
| | Exponential | | 0.654 | 10 | 50 | 0.417 | 127 | 362 |
| | Power | | 0.606 | 10 | 57 | 0.631 | 67 | 264 |
| Kallio et al. (2008) | R560/R660 | | | | | | | |
| | Linear | CDOM4 | 0.357 | 27 | 67 | 0.325 | 144 | 2615 |
| | Exponential | | 0.571 | 14 | 64 | 0.636 | 136 | 521 |
| | Power | | 0.464 | 13 | 64 | 0.557 | 118 | 535 |
| Kutser et al. (2005a) | R565/R660 | | | | | | | |
| | Linear | CDOM5 | 0.345 | 28 | 70 | 0.343 | 133 | 2603 |
| | Exponential | | 0.558 | 15 | 65 | 0.636 | 168 | 542 |
| | Power | | 0.448 | 13 | 65 | 0.549 | 122 | 560 |
| Ammenberg et al. (2002) | R664/R550 | CDOM6 | 0.791 | 19 | 60 | 0.831 | 94 | 1239 |
| Menken et al. (2006) | R670/R571 | CDOM7 | 0.735 | 22 | 66 | 0.796 | 139 | 1342 |
| Kowalczuk et al. (2005) | 10^(−0.29 − 0.708 × $x$ + 1.12 × $x$^2), $X$ = log 10(R490/R550) | CDOM8 | 0.242 | 24 | 73 | 0.000 | 917 | 1621 |

statistics shown in the figure. It is also worth mentioning, that several algorithms were showing very similar results when *in situ* statistics and correlation with modelled data was taken into account, but RMS and MNB values for model data differed significantly. For example the MNB of CHL2 was several times lower than the rest of the algorithms. Also when power function is used, then CHL11 algorithm's MNB and RMS values are relatively low, but correlation is not that good, compared to others.

The results for suspended matter are similar to that of chlorophyll-*a*. The band ratios calculated from *in situ* reflectance spectra are not correlating well with the TSM concentrations. However, if the *in situ* results are plotted together with the results obtained from modelled reflectance spectra

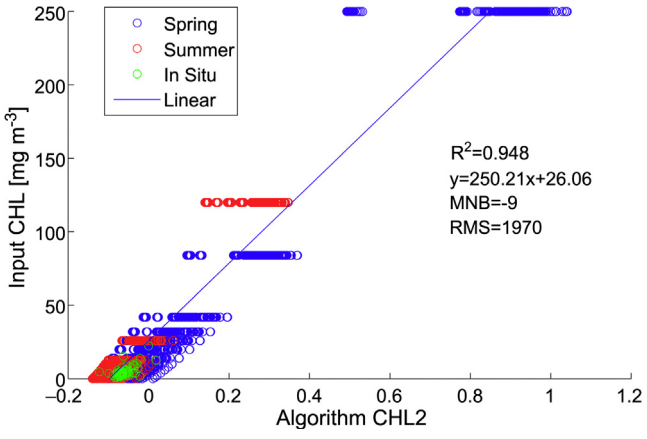


**Figure 4** Correlation between the chlorophyll algorithm No. 2 − (1/R665 − 1/R708) × R753 (Moses et al., 2009a) and chlorophyll concentrations [μg $l^{-1}$] measured *in situ* (for green circles) or used in the model simulations (red — summer and blue — spring circles). Determination coefficients for summer and spring data separately are $r^2$ = 0.96 and 0.94 respectively. Correlation for the field data separately was lower ($r^2$ = 0.40).

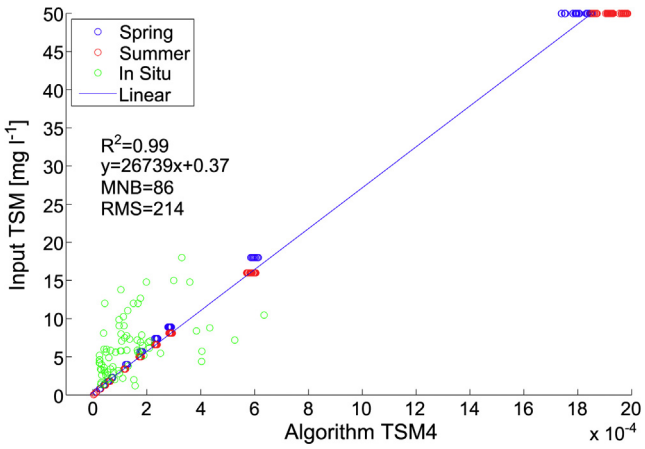


**Figure 5** Correlation between TSM algorithm No. 4 — R812 — (R770 — R840)base (Kutser et al., 2016) and the TSM values [mg $l^{-1}$] used in model simulations (red — summer and blue — spring circles) or measured *in situ* (green circles). Note that the determination coefficient in the figure is for modelling results and does not include *in situ* data. For *in situ* data $r^2$ = 0.210.

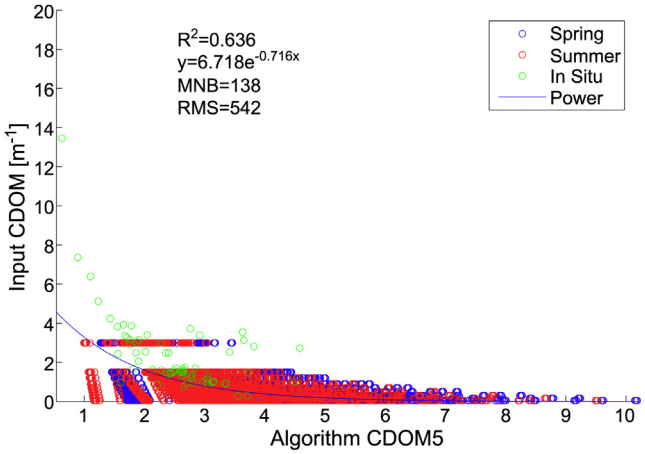


**Figure 6** Correlation between CDOM algorithm No. 5 — R565/R660 (Kutser et al., 2005) and the CDOM values [$m^{-1}$] used in model simulations (red — summer and blue — spring circles) or measured *in situ* (green circles). Note that the determination coefficient in the figure is for modelling results and does not include *in situ* data.

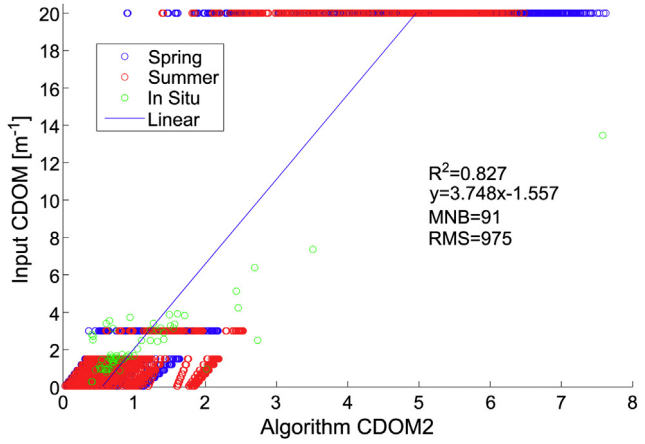


**Figure 7** Correlation between CDOM algorithm No. 2 — R663/R490 (Koponen et al., 2007) and the CDOM values [$m^{-1}$] used in model simulations (red — summer and blue — spring circles) or measured *in situ* (green circles). Note that the determination coefficient in the figure is for modelling results and does not include *in situ* data.

then they fit with the general trend. For example, the correlation between the 810 nm peak height (Kutser et al., 2016) and the TSM concentration was very high ($r^2$ close to 1) if we used only modelled spectra, but very low for *in situ* data ($r^2$ = 0.29). On the other hand, *in situ* values follow the trend from the model data (Fig. 5). The higher variation in *in situ* data may be caused by the fact that mineral to organic ratio in suspended matter is highly variable in near coastal waters. The amount of mineral particles may be high due to resuspension in shallow water areas or river inflow but the amount of mineral particles should be minimal in open parts of the Baltic Sea due to sedimentation. On the other hand the modelled spectral library was created using SIOPs of open Baltic Sea waters where the TSM was predominantly phytoplankton. Interesting phenomenon is with algorithms TSM6 and TSM16. Both show good results, but tend to overestimate the tsm concentrations for *in situ* data, compared to underestimation for the model data.

For CDOM we found results that are just the opposite compared to the CHL and TSM example — some algorithms gave better results with *in situ* data than against simulated data. For example, the green circles (*in situ* data) in Fig. 6 follow the power law function between green/red band ratio and CDOM better than the band-ratio calculated from modelled spectra (red and blue circles). One explanation that comes out from Fig. 6 is that CDOM retrieval with this algorithm is problematic if CDOM values are low, but chlorophyll and TSM values vary in great extent. Lower CDOM values usually occur in the middle of the Baltic Sea where TSM is also low and chlorophyll values are high only during bloom situations. This means that this band-ratio algorithm may actually work better than predicted by Fig. 6 modelling part as situations where CDOM is low, but TSM and chlorophyll are high, are not very probable in the Baltic Sea. Such situation may occur either in bloom conditions or in river estuaries bringing low CDOM turbid waters to the Baltic Sea. If all the statistics are taken into account, then the CDOM2 (Koponen et al., 2007, Fig. 7) tends to show the best results.

Most of the successful CHL algorithms used the peak near 700—710 nm. Many algorithms use the ratio of this peak to minima in reflectance caused by chlorophyll-*a* absorption (using bands near 675 nm). Such band combinations are available on both Sentinel 3 OLCI and Sentinel 2 MSI sensors. OLCI data has 300 m spatial resolution that is too coarse in many geomorphologically sophisticated coastal areas of the Baltic Sea. Sentinel 2 will provide similar band configuration (665 nm and 705 nm) with 20 m spatial resolution. We have demonstrated (Toming et al., 2016) that the height of the 705 nm peak in MSI data is very useful for mapping lake chlorophyll, but Sentinel 2 should perform as well in coastal regions with sophisticated geomorphology. It has been demonstrated (Kutser, 2004) that 30 m spatial resolution is not sufficient in the case of cyanobacterial blooms and the chlorophyll concentration may vary by more than two orders of magnitude within one 300 m pixel. Optical water properties may vary as dramatically in river estuaries. Therefore, the launch of Sentinel 2 opened a great new potential in coastal and inland water studies. Sentinel 2 imagery will be available nearly every second day when both S2a and S2b are on orbit, meaning that the high resolution monitoring of coastal waters becomes feasible from technical point of view and there are suitable algorithms for retrieving water quality parameters.

The most successful TSM algorithm used the height of 810 nm peak as a descriptor of suspended matter concentration whereas other good algorithms used the height of the peak at 700—710 nm. Both Sentinel 2 and Sentinel 3 have spectral bands in the 700—710 nm peak region as was mentioned above. We have demonstrated (Kutser et al., 2016) that the Sentinel 2 MSI band 7 (783 nm) can be used to detect the peak at 810 nm although the spectral band is not located optimally to capture this feature. Sentinel 3 OLCI has band 16 at 778.75 nm. It should potentially be used in the same way like the MSI 783 nm band, but this has to be tested with real data.

One of the useful CDOM retrieval algorithms is based on the blue to red band ratio whereas others are based on the red to green band ratio. In general, use of the blue band in retrieving CDOM is hampered by low water leaving radiance in CDOM-rich waters. Another issue is atmospheric correction that has the largest errors in the blue part of spectrum. It has been demonstrated in the case of lakes (Kutser et al., 2005b) that green to red band ratios perform the best in retrieving CDOM content of the water. We have also demonstrated with Sentinel 2 imagery that the band ratio works well in retrieving CDOM concentrations in lakes (Toming et al., 2016). Therefore, one may assume that the band ratio works well also in the CDOM-rich coastal waters of the Baltic Sea.

Most of the spectral bands used in the successful band-ratio algorithms match with the Sentinel 3 OLCI band configuration or are very close to it. This suggests that the empirical algorithms can be used in retrieving concentrations of CHL, TSM and CDOM in the Baltic Sea provided atmospheric correction of the imagery produces reliable reflectance spectra. According to our results, the best OLCI channel ratios to use for chlorophyll retrieval are band11/band9 (CHL14 — chla = 89.97 × R705/R664 − 66.10) and band11/band10 (CHL16 — chla = 82.10 × R706.5/R677.5 − 63.38); as the OLCI sensor bands are wider, these bands also include wavelengths used in this study. As the OLCI sensor does not have a band near 810 nm, band11-band12 (TSM13 tsm = 5670.34 × (R705 − R754) − 0.53 and TSM14 tsm = 4141.74 × R709.5 − 0.23) might be something that is worth testing. OLCI bands match very well with our best CDOM results (CDOM6 — band8/band6 — cdom412 = 10.80 × R664/R550 − 2.82) and CDOM2 (band8/band4 — cdom412 = 3.75 × R663/R490 − 1.56).

## 4. Conclusions

The results confirm the assumption that seasonal remote sensing algorithms provide the best results in the Baltic Sea. However, the results of the study also show that there are band ratio algorithms that can be used all year round to get reliable estimates of chlorophyll-*a*, CDOM and TSM.

Several of the best performing algorithms use spectral bands available on both Sentinel 2 and Sentinel 3 meaning that these satellites can be used in retrieving concentrations of optically active substances in the Baltic Sea by means of band ratio algorithms. We would recommend using CHL14 (Ammenberg et al., 2002; Koponen et al., 2007) and CHL16 (Kallio et al., 2001) for chlorophyll-*a* retrieval, TSM13 (Härmä et al., 2001) and TSM14 (Kallio et al., 2001) for total suspended matter, and CDOM2 (Koponen et al., 2007) and CDOM6 (Ammenberg et al., 2002) for cdom absorption.

## Acknowledgements

Field data used in this study was collected in the framework of the Interreg IVA project Hispares and the PECS project "Simulating Performance of ESA Future Satellites for Water Quality Monitoring of the Baltic Sea". Model simulation and analysis were supported by the Finnish national project EOMORE, the BONUS program project FerryScope, the European Comission programs GLaSS and WaterS; and the Republic of Estonia Ministry of Education and Research grants SF0180009As11 and SF0180009Bs11.

## References

Alikas, K., Kango, K., Randoja, R., Philipson, P., Asuküll, E., Pisek, J., Reinart, A., 2015. Satellite-based products for monitoring optically complex inland waters in support of EU Water Framework Directive. Int. J. Remote Sens. 36 (17), 4446—4468, http://dx.doi.org/10.1080/01431161.2015.1083630.

Ammenberg, P., Flink, P., Lindell, T., Pierson, D., Strombeck, N., 2002. Bio-optical modelling combined with remote sensing to assess water quality. Int. J. Remote Sens. 23 (8), 1621—1638, http://dx.doi.org/10.1080/01431160110071860.

Anon, 2015. OCV6 (Ocean Color Chlorophyll (OC) v6), http://oceancolor.gsfc.nasa.gov/cms/reprocessing/r2009/ocv6.

Arst, H., Kutser, T., 1994. Data processing and interpretation of sea radiance factor measurements. Polar Res. 13 (1), 3—12.

Attila, J., Kallio, K., Kutser, T., Koponen, S., Simis, S., Böttcher, M., Brockmann, C., 2015. FerryScope D2.1 Hydrolight Baltic, Version 1.2. 30.06.2015.

Attila, J., Koponen, S., Kallio, K., Lindfors, A., Kaitala, S., Ylöstalo, P., 2013. MERIS Case II water processor comparison on coastal sites of the northern Baltic Sea. Remote Sens. Environ. 128, 138—149, http://dx.doi.org/10.1016/j.rse.2012.07.009.

Beltran-Abaunza, J.M., Kratzer, S., Brockmann, C., 2014. Evaluation of MERIS products from Baltic Sea coastal waters rich in CDOM. Ocean Sci. 10, 377—396, http://dx.doi.org/10.5194/os-10-377-2014.

Brezonik, P., Menken, K.D., Bauer, M., 2005. Landsat-based remote sensing of lake water quality characteristics, including chlorophyll and colored dissolved organic matter (CDOM). Lake Reserv. Manage. 21 (4), 373—382, http://dx.doi.org/10.1080/07438140509354442.

Darecki, M., Ficek, D., Krezel, A., Ostrowska, M., Majchrowski, R., Wozniak, S.B., Bradtke, K., Dera, J., Wozniak, B., 2008. Algorithms for the remote sensing of the Baltic ecosystem (DESAMBEM). Part 2: Empirical validation. Oceanologia 50 (4), 509—538.

Darecki, M., Kaczmarek, S., Olszewski, J., 2005. SeaWiFS ocean colour chlorophyll algorithms for the southern Baltic Sea. Int. J. Remote Sens. 26 (2), 247—260, http://dx.doi.org/10.1080/01431160410001720298.

Darecki, M., Stramski, D., 2004. An evaluation of MODIS and SeaWIFS bio-optical algorithms in the Baltic Sea. Remote Sens. Environ. 89 (3), 326—350, http://dx.doi.org/10.1016/j.rse.2003.10.012.

Darecki, M., Weeks, A., Sagan, S., Kowalczuk, P., Kaczmarek, S., 2003. Optical characteristics of two contrasting Case 2 waters and their influence on remote sensing algorithms. Cont. Shelf Res. 23 (3—4), 237—250, http://dx.doi.org/10.1016/S0278-4343(02)00222-4.

Davies-Colley, R.J., Vant, W.N., 1987. Absorption of light by yellow substance in freshwater lakes. Limnol. Oceanogr. 32 (2), 416—425, http://dx.doi.org/10.4319/lo.1987.32.2.0416.

Dekker, A.G., Phinn, S.R., Anstee, J., Bissett, P., Brando, V.E., Casey, B., Fearns, P., Hedley, J., Klonowski, W., Lee, Z.P., Lynch, M., Lyons, M., Mobley, C., Roelfsema, C., 2011. Intercomparison of shallow water bathymetry, hydro-optics, and benthos mapping techniques in Australian and Caribbean coastal environments. Limnol. Oceanogr. Meth. 9 (9), 396—425, http://dx.doi.org/10.4319/lom.2011.9.396.

Dekker, A.G., Vos, R.J., Peters, S.W., 2002. Analytical algorithms for lake water TSM estimation for retrospective analyses of TM and SPOT sensor data. Int. J. Remote Sens. 23 (1), 15—35, http://dx.doi.org/10.1080/01431160010006917.

Dierberg, F.E., Carriker, N.E., 1994. Field testing two instruments for remotely sensing water quality in the Tennessee Valley. Environ. Sci. Technol. 28 (1), 16—25, http://dx.doi.org/10.1021/es00050a004.

Doerffer, R., Schiller, H., 1997. Algorithm Theoretical Basis Document (ATBD 2.12). Pigment Index, Sediment and Gelbstoff Retrieval from Directional Water Leaving Radiance Reflectances using Inverse Modelling Technique. GKSS Research Centre.

Doerffer, R., Schiller, H., 2007. The MERIS Case 2 algorithm. Int. J. Remote Sens. 28 (3—4), 517—535, http://dx.doi.org/10.1080/01431160600821127.

Doxaran, D., Castaing, P., Lavender, S., 2006. Monitoring the maximum turbidity zone and detecting finescale turbidity features in the Gironde estuary using high spatial resolution satellite sensor (SPOT HRV, Landsat ETM) data. Int. J. Remote Sens. 27 (11), 2303—2321, http://dx.doi.org/10.1080/01431160500396865.

Doxaran, D., Cherukuru, R., Lavender, S., 2005. Use of reflectance band ratios to estimate suspended and dissolved matter concentrations in estuarine waters. Int. J. Remote Sens. 26 (8), 1763—1770, http://dx.doi.org/10.1080/01431160512331314092.

Doxaran, D., Froidefond, J.M., Castaing, P., 2002. A reflectance band ratio used to estimate suspended matter concentrations in sediment-dominated coastal waters. Int. J. Remote Sens. 23 (23), 5079—5085, http://dx.doi.org/10.1080/0143116021000009912.

Doxaran, D., Froidefond, J.M., Castaing, P., 2003. Remote-sensing reflectance of turbid sediment-dominated waters. Reduction of sediment type variations and changing illumination conditions effects by use of reflectance ratios. Appl. Opt. 42 (15), 2623—2634, http://dx.doi.org/10.1364/AO.42.002623.

Duan, H.T., Zhang, Y., Zhang, B., Song, K., Wang, Z., 2007. Assessment of chlorophyll-*a* concentration and trophic state for Lake Chagan using Landsat TM and field spectral data. Environ. Monit. Assess. 129 (1), 295—308, http://dx.doi.org/10.1007/s10661-006-9362-y.

Erm, A., Väli, G., Lips, I., Lips, U., 2008. Optical properties of northeastern Baltic Sea (Conf. paper). In: IEEE/OES US/EU-Baltic Int. Symp. 27—29 May 2008, Tallinn, EEE, http://dx.doi.org/10.1109/BALTIC.2008.4625547 7 pp.

ESS, 1993. EES Method 340.2: Total suspended solids, mass balance (dried at 103—105°C), volatile suspended solids (ignited at 550°C). Environ. Sci. Section, Madison 189—192.

Feistel, R., Günther, N., Wasmund, N., 2008. State and Evolution of the Baltic Sea, 1952—2005: A Detailed 50-year Survey. John Wiley & Sons, Hoboken, 441—481.

Garnesson, P., Krasemann, H., 2016. Quality Information Document. Ocean Colour. Baltic Chlorophyll Observation Products, CMEMS, http://marine.copernicus.eu/documents/QUID/CMEMS-OC-QUID-009-080-097.pdf.

Giardino, C., Candiani, G., Bresciani, M., Lee, Z., Gagliano, S., Pepe, M., 2012. BOMBER: a tool for estimating water quality and bottom properties from remote sensing images. Comput. Geosci. 45, 313—318, http://dx.doi.org/10.1016/j.cageo.2011.11.022.

Gitelson, A.A., Gurlin, D., Moses, W.J., Barrow, T., 2009. A bio-optical algorithm for the remote estimation of the chlorophyll-*a* concentration in case 2 waters. Environ. Res. Lett. 4 (4), 5 pp. 045003.http://iopscience.iop.org/article/10.1088/1748-9326/4/4/045003/meta.

Groetsch, P.M., Simis, S.G., Eleveld, M.A., Peters, S.W., 2014. Cyanobacterial bloom detection based on coherence between ferrybox observations. J. Marine Syst. 140 (A), 50—58, http://dx.doi.org/10.1016/j.jmarsys.2014.05.015.

Han, L., Jordan, K., 2005. Estimating and mapping chlorophyll *a* concentration in Pensacola Bay, Florida using Landsat ETM data. Int. J. Remote Sens. 26 (23), 5245—5254, http://dx.doi.org/10.1080/01431160500219182.

Hunter, P., Tyler, A.N., Willby, N.J., Gilvear, D.J., 2008. The spatial dynamics of vertical migration by *Microcystis aeruginosa* in a eutrophic shallow lake: a case study using high spatial resolution time-series airborne remote sensing. Limnol. Oceanogr. 53 (6), 2391—2406, http://dx.doi.org/10.4319/lo.2008.53.6.2391.

Härmä, P., Vepsäläinen, J., Hannonen, T., Pyhälahti, T., Kämäri, J., Kallio, K., Eloheimo, K., Koponen, S., 2001. Detection of water quality using simulated satellite data and semi-empirical algorithms in Finland. Sci. Total Environ. 268 (1—3), 107—121, http://dx.doi.org/10.1016/S0048-9697(00)00688-4.

ISO 1.1., 1992. Water Quality — Measurement of Biochemical Parameters — Spectrophotometric Determination of Chlorophyll *a* Concentration.

Jiao, H.B., Zha, Y., Gao, J., Li, Y.M., Wei, Y.C., Huang, J.Z., 2006. Estimation of chlorophyll *a* concentration in Lake Tai, China using in situ hyperspectral data. Int. J. Remote Sens. 27 (19), 4267—4276, http://dx.doi.org/10.1080/01431160600702434.

Kallio, K., Attila, J., Härmä, P., Koponen, S., Pulliainen, J., Hyytiäinen, U.-M., Pyhälahti, T., 2008. Landsat ETM+ images in the estimation of seasonal lake water quality in boreal river basins. Environ. Manage. 42 (3), 511—522, http://dx.doi.org/10.1007/s00267-008-9146-y.

Kallio, K., Koponen, S., Pulliainen, J., 2003. Feasibility of airborne imaging spectrometry for lake monitoring — a case study of spatial chlorophyll *a* distribution in two meso-eutrophic lakes. Int. J. Remote Sens. 24 (19), 3771—3790, http://dx.doi.org/10.1080/0143116021000023899.

Kallio, K., Kutser, T., Hannonen, T., Koponen, S., Pulliainen, J., Vepsäläinen, J., Pyhälahti, T., 2001. Retrieval of water quality from airborne imaging spectrometry of various lake types in different seasons. Sci. Total Environ. 268 (1—3), 59—77, http://dx.doi.org/10.1016/S0048-9697(00)00685-9.

Koponen, S., Attila, J., Pulliainen, J., Kallio, K., Pyhälahti, T., Lindfors, A., Rasmus, K., Hallikainen, M., 2007. A case study of airborne and satellite remote sensing of a spring bloom event in the Gulf of Finland. Cont. Shelf Res. 27 (2), 228—244, http://dx.doi.org/10.1016/j.csr.2006.10.006.

Kowalczuk, P., Darecki, M., Zabloka, M., 2010. Validation of empirical and semi-analytical remote sensing algorithms for estimating absorption by colored dissolved organic matter in the Baltic Sea from SeaWiFS and MODIS imagery. Oceanologia 52 (2), 171—196, http://dx.doi.org/10.5697/oc.52-2.171.

Kowalczuk, P., Olszewski, J., Darecki, M., Kaczmarek, S., 2005a. Empirical relationships between coloured dissolved organic matter (CDOM) absorption and apparent optical properties in Baltic Sea waters. Int. J. Remote Sens. 26 (2), 345—370, http://dx.doi.org/10.1080/01431160410001720270.

Kowalczuk, P., Ston-Egiert, J., Cooper, W.J., Whitehead, R.F., Durako, M.J., 2005b. Characterization of chromophoric dissolved organic matter (CDOM) in the Baltic Sea by excitation emission matrix fluorescence spectroscopy. Mar. Chem. 96 (3—4), 273—292, http://dx.doi.org/10.1016/j.marchem.2005.03.002.

Kratzer, S., Brockmann, C., Moore, G., 2008. Using MERIS full resolution data to monitor coastal waters — a case study from Himmerfjärden, a fjord-like bay in the northwestern Baltic Sea. Remote Sens. Environ. 112 (5), 2284—2300, http://dx.doi.org/10.1016/j.rse.2007.10.006.

Kutser, T., 2004. Quantitative detection of chlorophyll in cyanobacterial blooms by satellite remote sensing. Limnol. Oceanogr. 49 (6), 2179—2189, http://dx.doi.org/10.4319/lo.2004.49.6.2179.

Kutser, T., Herlevi, A., Kallio, K., Arst, H., 2001. A hyperspectral model for interpretation of passive optical remote sensing data from turbid lakes. Sci. Total Environ. 268 (1—3), 47—58, http://dx.doi.org/10.1016/S0048-9697(00)00682-3.

Kutser, T., Kallio, K., Eloheimo, K., Hannonen, T., Pyhälahti, T., Koponen, S., Pulliainen, J., 1999. Quantitative monitoring of water properties with the airborne imaging spectrometer AISA. Proc. Estonian Acad. Sci. Biol. Ecol. 48 (1), 25—36.

Kutser, T., Metsamaa, L., Strömbeck, N., Vahtmäe, E., 2006. Monitoring cyanobacterial blooms by satellite remote sensing. Estuar. Coastal Shelf Sci. 67 (1—2), 303—312, http://dx.doi.org/10.1016/j.ecss.2005.11.024.

Kutser, T., Paavel, B., Verpoorter, C., Ligi, M., Soomets, T., Toming, K., Casal, G., 2016. Remote sensing of black lakes and using 810 nm reflectance peak for retrieving water quality parameters of optically complex waters. Remote Sens. 8 (6), 497, http://dx.doi.org/10.3390/rs8060497.

Kutser, T., Pierson, D.C., Kallio, K.Y., Reinart, A., Sobek, S., 2005a. Mapping lake CDOM by satellite remote sensing. Remote Sens. Environ. 94 (4), 535—540, http://dx.doi.org/10.1016/j.rse.2004.11.009.

Kutser, T., Pierson, D.C., Tranvik, L., Reinart, A., Sobek, S., Kallio, K., 2005b. Using satellite remote sensing to estimate the colored dissolved organic matter absorption coefficient in lakes. Ecosystems 8 (6), 709—720, http://dx.doi.org/10.1007/s10021-003-0148-6.

Kutser, T., Vahtmäe, E., Paavel, B., Kauer, T., 2013. Removing glint effects from field radiometry data measured in optically complex coastal and inland waters. Remote Sens. Environ. 133, 85—89, http://dx.doi.org/10.1016/j.rse.2013.02.011.

Lorenzen, C.J., 1967. Determination of chlorophyll and phaeopigments; spectrophotometric equations. Limnol. Oceanogr. 12 (2), 343—346.

Mayo, M., Gitelson, A., Yacobi, Y.Z., Ben-Avraham, Z., 1995. Chlorophyll distribution in Lake Kinneret determined from Landsat Thematic Mapper data. Int. J. Remote Sens. 16 (1), 175—182, http://dx.doi.org/10.1080/01431169508954386.

Menken, K.D., Brezonik, P.L., Bauer, M.E., 2006. Influence of chlorophyll and colored dissolved organic matter (CDOM) on lake reflectance spectra: implications for measuring lake properties by remote sensing. Lake Reserv. Manage. 22 (3), 179—190, http://dx.doi.org/10.1080/07438140609353895.

Metsamaa, L., Kutser, T., Strömbeck, N., 2006. Recognising cyanobacterial blooms based on their optical signature: a modelling study. Boreal Environ. Res. 11 (6), 493—506.

Miller, R.L., McKee, B.A., 2004. Using MODIS Terra 250 m imagery to map concentrations of total suspended matter in coastal waters. Remote Sens. Environ. 93 (1—2), 259—266, http://dx.doi.org/10.1016/j.rse.2004.07.012.

Mobley, C.D., 1994. Light and Water: Radiative Transfer in Natural Waters. Academic Press, San Diego, 608 pp.

Mobley, C.D., Sundman, L.K., 2013a. HydroLight 5.2 — EcoLight 5.2 Technical Documentation. Sequoia Scientific. Inc., 115 pp.

Mobley, C.D., Sundman, L.K., 2013b. HydroLight 5.2 — EcoLight 5.2 Users' Guide. Sequoia Scientific. Inc., 109 pp.

Moses, W.J., Gitelson, A.A., Berdnikov, S., Povaznyy, V., 2009a. Satellite estimation of chlorophyll-*a* concentration using the red and NIR bands of MERIS — the Azov Sea case study. IEEE Geosci. Remote Sci. 6 (4), 845—849, http://dx.doi.org/10.1109/LGRS.2009.2026657.

Moses, W.J., Gitelson, A.A., Berdnikov, S., Povaznyy, V., 2009b. Estimation of chlorophyll-*a* concentration in case II waters using MODIS and MERIS data — successes and challenges. Environ. Res. Lett. 4 (4), 045005, http://dx.doi.org/10.1088/1748-9326/4/4/045005.

Neukermans, G., Ruddick, K., Bernard, E., Ramon, D., Nechad, B., Deschamps, P.-Y., 2009. Mapping total suspended matter from geostationary satellites: a feasibility study with SEVIRI in the Southern North Sea. Opt. Express 17 (16), 14029—14052, http://dx.doi.org/10.1364/OE.17.014029.

Onderka, M., Pekarova, P., 2008. Retrieval of suspended particulate matter concentrations in the Danube River from Landsat ETM data. Sci. Total Environ. 397 (1—3), 238—243, http://dx.doi.org/10.1016/j.scitotenv.2008.02.044.

Östlund, C., Flink, P., Strömbeck, N., Pierson, D., Lindell, T., 2001. Mapping of the water quality of Lake Erken, Sweden, from imaging spectrometry and Landsat Thematic Mapper. Sci. Total Environ. 268 (1—3), 139—154, http://dx.doi.org/10.1016/S0048-9697(00)00683-5.

Pitarch, J., Volpe, G., Colella, S., Krasemann, H., Santoleri, R., 2015. Remote sensing of chlorophyll in the Baltic Sea at basin scale from 1997 to 2012 using merged multisensor data. Ocean Sci. 12 (2), 2283—2313, http://dx.doi.org/10.5194/os-12-379-2016.

Reinart, A., Kutser, T., 2006. Comparison of different satellite sensors in detecting cyanobacterial bloom events in the Baltic Sea. Remote Sens. Environ. 102 (1—2), 74—85, http://dx.doi.org/10.1016/j.rse.2006.02.013.

Schalles, J.F., Gitelson, A.A., Yacobi, Y.Z., Kroenke, A.E., 1998. Estimation of chlorophyll *a* from time series measurements of high spectral resolution reflectance in an eutrophic lake. J. Phycol. 34 (2), 383—390.

Simis, S.G., Olsson, J., 2013. Unattended processing of shipborne hyperspectral reflectance measurements. Remote Sens. Environ. 135, 202—212, http://dx.doi.org/10.1016/j.rse.2013.04.001.

Simis, S.G.H., Ylöstalo, P., Kallio, K., Spilling, K., Kutser, T., Optical biogeochemical models of the Baltic Sea in spring and summer. PLOS ONE, submitted for publication.

Thiemann, S., Kaufmann, H., 2000. Determination of chlorophyll content and trophic state of lakes using field spectrometer and IRS-1C satellite data in the Mecklenburg lake district, Germany. Remote Sens. Environ. 73 (2), 227—235, http://dx.doi.org/10.1016/S0034-4257(00)00097-3.

Toming, K., Kutser, T., Laas, A., Sepp, M., Paavel, B., Nõges, T., 2016. First experiences in mapping lake water quality parameters with Sentinel-2 MSI imagery. Remote Sens. 8, 640, 14 pp.

Wang, F., Han, L., Kung, H.T., Van Arsdale, R.B., 2006. Applications of Landsat-5 TM imagery in assessing and mapping water quality in Reelfoot Lake, Tennessee. Int. J. Remote Sens. 27 (23), 5269—5283, http://dx.doi.org/10.1080/01431160500191704.

Wang, X.J., Ma, T., 2001. Application of remote sensing techniques in monitoring and assessing the water quality of Taihu Lake. Bull. Environ. Contam. Toxicol. 67 (6), 863—870, http://dx.doi.org/10.1007/s001280202.

Wasmund, N., Uhlig, S., 2003. Phytoplankton trends in the Baltic Sea. ICES J. Mar. Sci. 60 (2), 177—186, http://dx.doi.org/10.1016/S1054-3139(02)00280-1.

Woźniak, A.B., 2014. Simple statistical formulas for estimating biogeochemical properties of suspended particulate matter in the southern Baltic Sea potentially useful for optical remote sensing applications. Oceanologia 56 (1), 7—39, http://dx.doi.org/10.5697/oc.56-1.007.

Woźniak, B., Krężel, A., Darecki, M., Woźniak, S.B., Majchrowski, R., Ostrowska, M., Kozłowski, L., Ficek, D., Olszewski, J., Dera, J., 2008. Algorithm for the remote sensing of the Baltic ecosystem (DESAMBEM). Part 1: Mathematical apparatus. Oceanologia 50 (4), 451—508.

Yacobi, Y.Z., Gitelson, A., Mayo, M., 1995. Remote sensing of chlorophyll in Lake Kinneret using high spectral-resolution radiometer and Landsat TM: spectral features of reflectance and algorithm development. J. Plankton Res. 17 (11), 2155—2173, http://dx.doi.org/10.1093/plankt/17.11.2155.

Zimba, P.V., Gitelson, A., 2006. Remote estimation of chlorophyll concentration in hypereutrophic aquatic systems: model tuning and accuracy optimization. Aquaculture 256 (1—4), 272—286, http://dx.doi.org/10.1016/j.aquaculture.2006.02.038.

Oceanologia (2017) 59, 69—80

Available online at www.sciencedirect.com

ScienceDirect

journal homepage: www.journals.elsevier.com/oceanologia/

ORIGINAL RESEARCH ARTICLE

# Processes and factors influencing the through-flow of new deepwater in the Bornholm Basin

**Anders Stigebrandt** *

*Department of Marine Sciences, University of Gothenburg, Gothenburg, Sweden*

Received 3 June 2016; accepted 11 September 2016
Available online 23 September 2016

**KEYWORDS**
Vertical mixing;
Inflow of new deepwater;
Salinity;
Currents;
Baltic Sea

**Summary** This paper is based on the idea that the hydrographical conditions in the Bornholm Basin, and any other basin, can be understood from knowledge of general hydromechanical principles and basin-specific factors. Published results on the variability of the vertical stratification are shown and discussed. Such analyses demonstrate the residence time of water at different depth levels. Different modes of currents forced by winds and by stratification gradients at open vertical boundaries are presented. Vertical mixing is discussed and published results for the Bornholm Basin are shown. An experiment demonstrates that the diffusive properties of the enclosed basin, i.e. below the sill depth of the Słupsk Furrow, can be computed quite well from the horizontal mean vertical diffusivity obtained from historical hydrographical observations. A published two decades long simulation of the vertical stratification shows that the through flow and modification of new deepwater in the Bornholm Basin can be well described based on existing knowledge regarding crucial hydromechanical processes. It also suggests, indirectly, that there should be a weak anticyclonic circulation above the sill depth, which is supported by current measurements.


* Correspondence to: Department of Marine Sciences, University of Gothenburg, PO Box 460, 40530 Gothenburg, Sweden. Tel.: +46 708772851.
*E-mail address:* anders.stigebrandt@marine.gu.se.
Peer review under the responsibility of Institute of Oceanology of the Polish Academy of Sciences.

Production and hosting by Elsevier

http://dx.doi.org/10.1016/j.oceano.2016.09.001

## 1. Introduction

When the sea level is higher in Kattegat than in the Arkona Basin, salty water flows across the shallow sills in Fehmarn Belt and the Öresund into the Arkona Basin. Because this water has higher salinity and density than the surface water of the Arkona Basin, it descends along the seabed whereby the potential energy of the dense water is transferred to kinetic energy. Due to friction against the seabed and the overlying water, kinetic energy is transformed to turbulent energy that causes entrainment of the overlying water whereby the volume flow of the inflowing water increases and its salinity decreases. The inflowing saline water is the source of new deepwater in the Baltic proper. In the present paper it is called the new deepwater. Finally, the new deepwater is added to the dense bottom pool in the Arkona Basin. The water from this pool is evacuated through the Bornholm Channel. When this occurs it will undergo further dilution with less dense ambient water in the Bornholm Basin. If the new deepwater has sufficiently high density, it will penetrate into the enclosed part of the Bornholm Basin, below the level of the deepest connection with the Gdańsk Basin (the so-called sill depth) through the Stolpe Channel (Słupsk Furrow). Otherwise it will be interleaved in the halocline above the sill depth from where it may escape the Bornholm Basin through the Stolpe Channel.

The oxygen conditions in the basin water, below the sill level, depend on the rates of supply and consumption of oxygen. Oxygen supply is essentially due to inflowing new deepwater while oxygen consumption primarily depends on decomposition of organic matter sinking down from the surface layer where it is produced. Since the salinity of the new deepwater during an inflow event increases as the inflow progresses (Stigebrandt, 1987a; Stigebrandt et al., 2015), only the later-coming part of very large inflows has high enough salinity to replace the residing deepwater. This means that with the actual rate of vertical mixing, it may take a couple of years before an initially very salty deepwater becomes exchanged. If the long-term oxygen consumption is larger than the oxygen supply, the basin may become exhausted in oxygen and hydrogen sulfide may be added to the water column before the next event of deepwater renewal brings in new oxygen as demonstrated by observations and model simulations in Stigebrandt et al. (2015).

The oxygen conditions are very important for the ecology and the water quality in a basin. Higher forms of life may have difficulties in getting enough of oxygen in hypoxic conditions ($O_2 < 2$ mg $L^{-1}$). In the Bornholm Basin the bottoms in the deepest part are episodically anoxic (no $O_2$) and azoic, i.e. they lack animals. This is a large disadvantage for e.g. cod that largely feed on benthic animals. For successful recruitment, cod is depending on the existence of oxic ($O_2 > 2$ mg $L^{-1}$) water with salinity >11 PSU (e.g. Stigebrandt et al., 2015; and references therein). When oxygen disappears (anoxic), red-ox reactions are reversed and, for instance, the bottom sediment starts to leak phosphorus (e.g. Stigebrandt and Kalén, 2013). This is eventually mixed into the surface layers which increase the biological production which leads to increased oxygen consumption in the deepwater implying expanding bottom areas with anoxic conditions which further increase the phosphorus leakage.

This paper describes and discusses the mixing and through-flow of new deepwater in the Bornholm Basin. The applied approach is to first describe the topography and the hydrographical properties. Thereafter the oceanographic processes influencing the mixing and the through-flow are described. The idea is that the conditions in the Bornholm Basin can be understood from knowledge of general principles and basin-specific factors. Finally some results from a vertical advection-diffusion circulation model are described.

## 2. Topography, sediment conditions and other external facts

In the central parts, the Bornholm Basin reaches about 100 m depth (Fig. 1). The deepest connection between the Bornholm Basin and the basins east and north of it is 59 m and it goes through the Stolpe Channel. East of the isle of Öland there is an about 46 m deep connection to the West Gotland Basin. Consequently the Bornholm Basin is closed beneath 59 m depth. The horizontal area at this depth equals about 14 150 $km^2$ and the volume of the closed part beneath this depth equals about 200 $km^3$ (e.g. Stigebrandt and Kalén, 2013). The vertical circulation of the Bornholm Basin can be thought of as taking place in a so-called diffusive filling-box where new deepwater enters essentially through the Bornholm Strait in the northwest and leaves through the Stolpe Channel in the southeast. During strong inflow events with highly elevated halocline in the Arkona Basin some deepwater may likely enter the Bornholm Basin also across the ~29 m deep sill southwest of Bornholm Island (Lass et al., 2001; Stigebrandt, 1987a).

A map of surficial sediment types shows that bottoms in the deeper parts of the Bornholm Basin usually are muddy and covered by soft material. However, in an area stretching southeastwards from the Bornholm Channel, east of Bornholm Island, bottoms are made up of sand and hard clay (Fig. 2). As further discussed in Section 4.3, it is obvious that the hard bottoms are swept clear of soft matter during occasional events with high-speed dense bottom currents, carrying new deepwater to the Bornholm Basin. Svikov and Sviridov (1994) constructed a map of occasional high bottom speeds based on the properties of the surface sediment.

The Bornholm Basin is the area with the lowest frequency of ice cover in the whole Baltic Sea. The hundred-year wind wave height has been estimated to be 15 m, see Ödalen and Stigebrandt (2013b) for additional information.

The studies referred to in the present paper have largely used hydrographical data from stations BY4 and BY5 in the Bornholm Basin (Fig. 1) but also from stations in neighboring basins. All data can be obtained from official databases. Additional data are available from HELCOM. Furthermore, Nord Stream collected data on salinity, temperature and currents with high vertical resolution in two locations using moored instruments. These and other data are available from Nord Stream (see https://www.nord-stream.com/environment/data-and-information-fund/dif/).

## 3. Hydrography

Salinity and oxygen concentrations of the water column in the Bornholm Basin are shown in Fig. 3 for the period

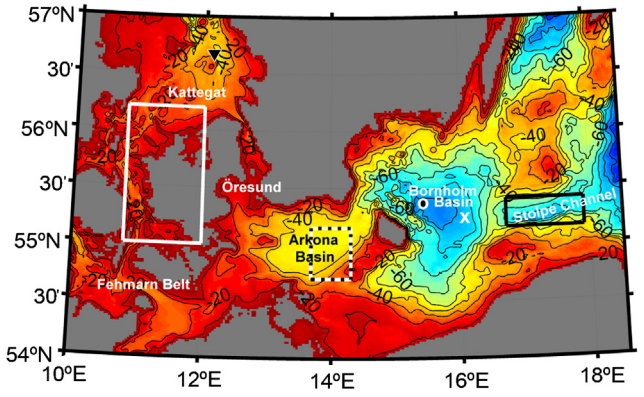


**Figure 1** Map of the southern Baltic Sea area (hypsographic data from Seifert et al. (2001)). Reference data for the Arkona Basin originates from the area within the white and black dashed rectangle and reference data station BY4 and BY5 in the Bornholm Basin is marked by a white ○ and × respectively. Data from the Stolpe Channel used for forcing of the model originate from the area within the black rectangle. The forcing data for the freshwater pool model were obtained from within the white rectangle and from the Anholt E station marked by ▼ (from Stigebrandt et al., 2015).

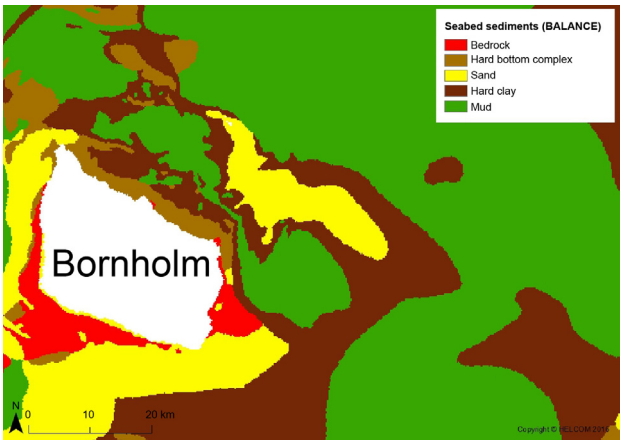


**Figure 2** Sediment types in the Bornholm Basin and surrounding waters. Fine grained, muddy sediments (green) and sand (yellow) are dominant in the deep basin, with some areas of more course hard clay (brown). Courser sediments are also found in and around the sand bank (yellow) extending from Christiansø toward the deep basin (Map from HELCOM Map and Data Service). (For interpretation of the references to color in this figure legend, the reader is referred to the web version of this article.)

1958–2016. As can be seen there are large variations in time, in particular in the deepwater. Variability and long-term averages of salinity, temperature, density and oxygen concentration for the period 1970–2010 were investigated by Ödalen and Stigebrandt (2013a). The long term means and their standard deviations are given in Table 1.

It is interesting to note that the largest variability of temperature (variability equals StD squared) occurs in the surface layer due to the annual heating–cooling cycle while the largest variability of salinity and oxygen occurs around and below the sill depth (Table 1). The large variability below the sill depth is due to long periods of stagnation during which

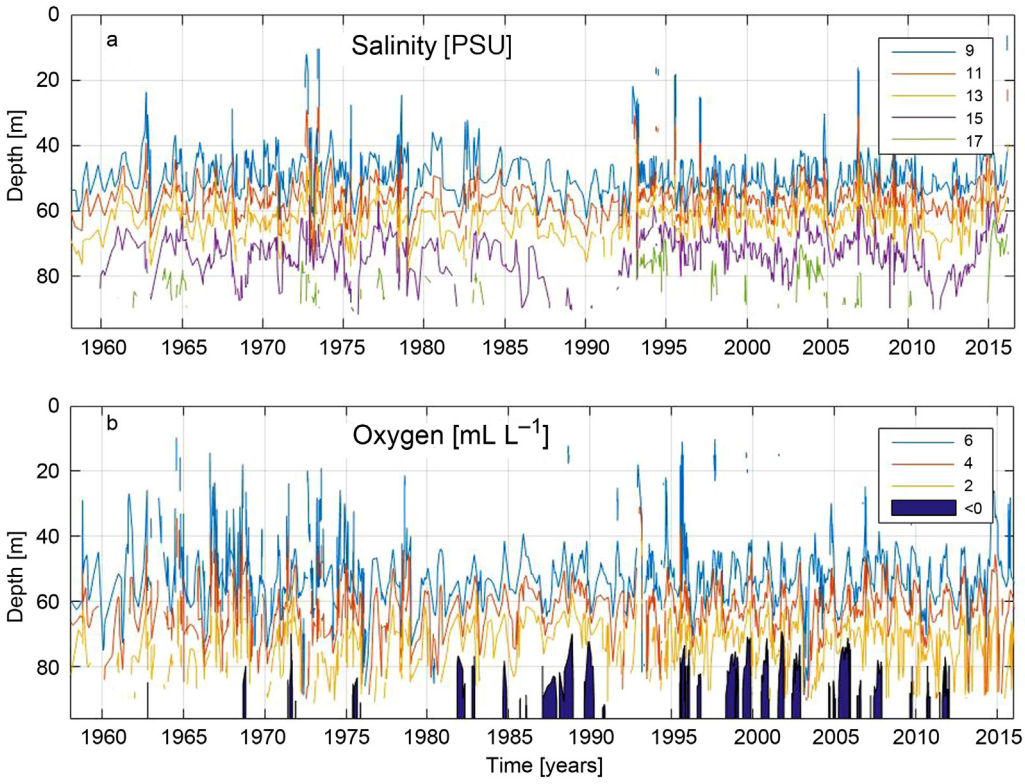


**Figure 3** Isopleth diagram of (a) salinity [PSU] and (b) oxygen [mL $O_2$ $L^{-1}$] at BY5 from February 12, 1958 to July 22, 2016. Negative oxygen values in (b) denote the presence of anoxia with hydrogen sulfide in the water (data from SMHI).

**Table 1** Long-term averages and standard deviations (StD) of temperature, salinity and oxygen ($O_2$) at selected standard observational depths from 1970 to 2010 inclusive (after Ödalen and Stigebrandt, 2013a).

| Depth [m] | Temperature [°C] | ±StD T [°C] | Salinity [PSU] | ±StD S [PSU] | $O_2$ [g m$^{-3}$] | ±StD $O_2$ [g m$^{-3}$] |
|---|---|---|---|---|---|---|
| 0 | 9.6 | 5.6 | 7.5 | 0.3 | 11.4 | 1.5 |
| 10 | 9.2 | 5.4 | 7.5 | 0.3 | 11.4 | 1.5 |
| 20 | 8.2 | 4.6 | 7.5 | 0.3 | 11.3 | 1.5 |
| 30 | 6.4 | 3.4 | 7.6 | 0.3 | 11.4 | 1.4 |
| 40 | 5.0 | 2.2 | 7.8 | 0.4 | 11.3 | 1.3 |
| 50 | 5.0 | 2.0 | 8.9 | 1.3 | 9.8 | 2.1 |
| 60 | 6.4 | 2.4 | 12.1 | 1.7 | 6.7 | 2.3 |
| 70 | 6.8 | 1.8 | 14.7 | 1.1 | 3.6 | 2.2 |
| 80 | 6.9 | 1.7 | 16.0 | 0.9 | 1.9 | 2.4 |

salinity decreases steadily owing to vertical diffusion and oxygen decreases due to biological consumption. Seldom occurring water renewals furnish the basin below the sill depth with salt and oxygen. The variabilities of salinity, temperature and oxygen concentration due to the seasonal cycle and periods shorter and longer than this, respectively, are discussed below.

Following Stigebrandt (2012), the variability was partitioned in three period bands viz. periods longer than 1 year, the period 1 year exactly and periods shorter than 1 year (Ödalen and Stigebrandt, 2013a). The result is shown in Fig. 4 where the variability for the three different timescales is shown. It can be seen that the period 1 year, i.e. the annual cycle, which often is called the seasonal cycle,

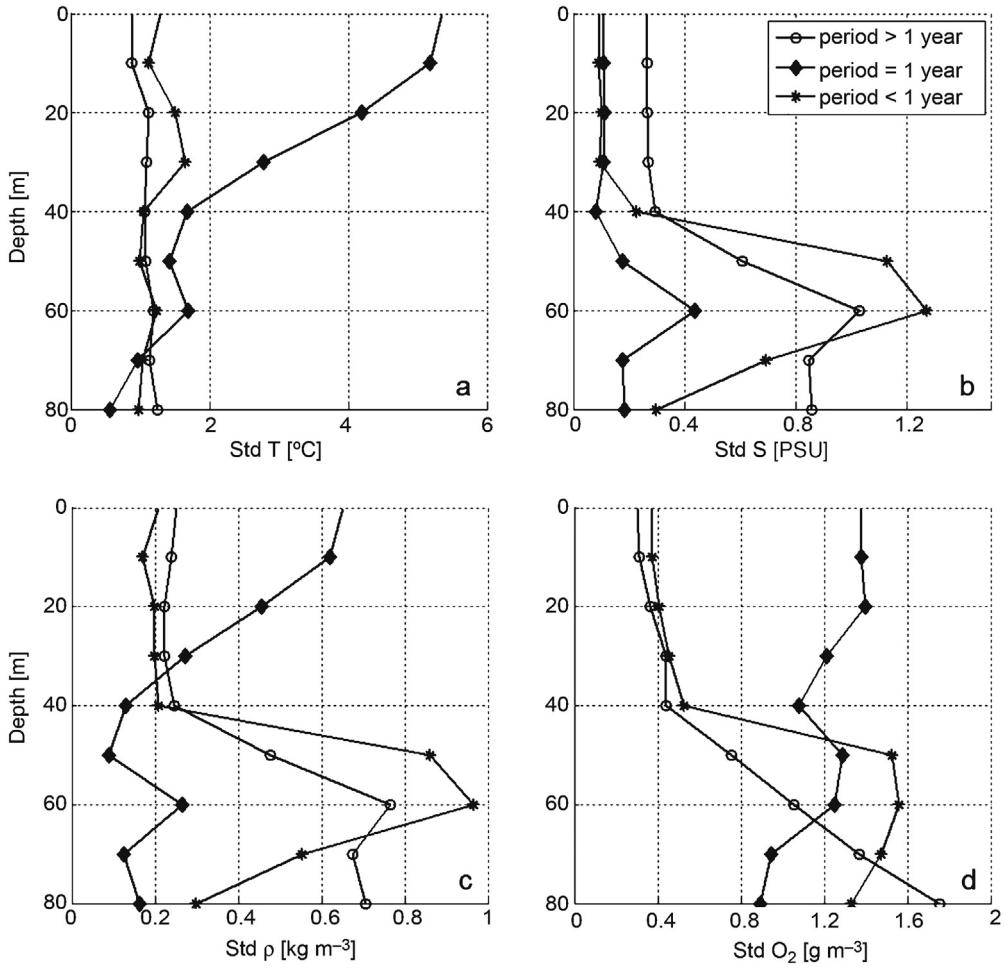


**Figure 4** Standard deviation of (a) temperature [°C], (b) salinity [PSU], (c) density [kg m$^{-3}$] and (d) oxygen [g $O_2$ m$^{-3}$] partitioned into three period bands, viz. periods longer than 1 year, the period 1 year and periods shorter than 1 year, respectively (from Ödalen and Stigebrandt, 2013a).

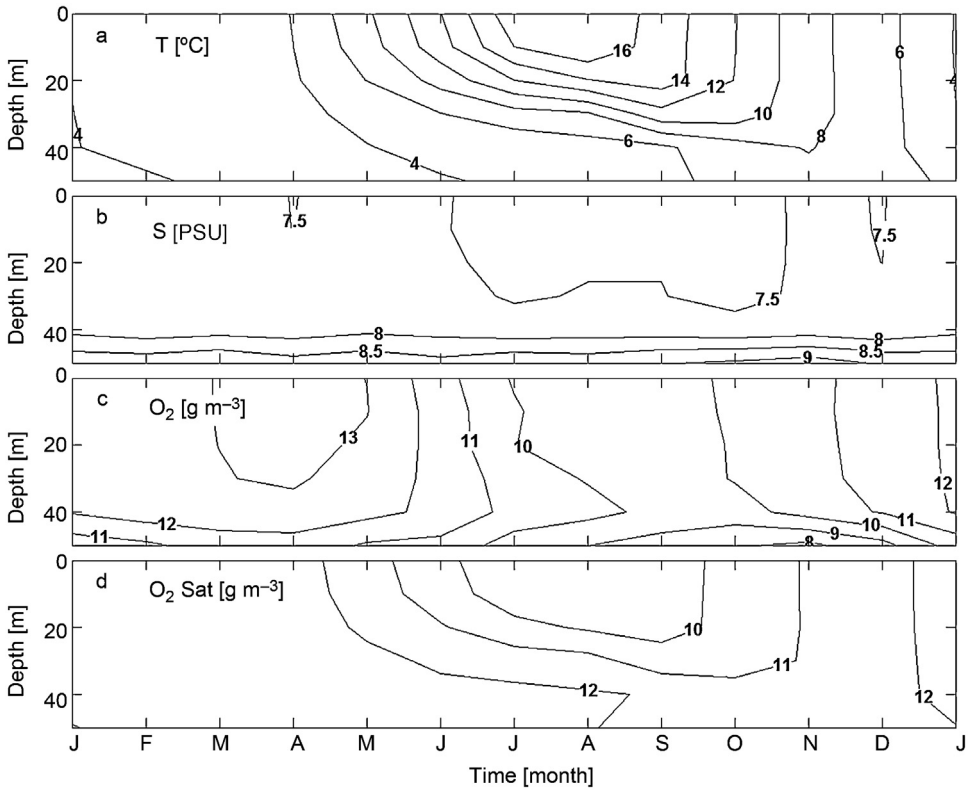


**Figure 5** Annual cycles of (a) temperature [°C], (b) salinity [PSU], (c) oxygen concentration [g $O_2$ $m^{-3}$] and (d) oxygen saturation concentration [g $O_2$ $m^{-3}$] between 0 and 50 m for the period 1970—2010 (from Ödalen and Stigebrandt, 2013a).

dominates the variability of temperature, density and oxygen in the upper layer (about 40 m thick).

The mean seasonal cycles of temperature, salinity, oxygen concentration and oxygen saturation concentration between 0 and 50 m for the period 1970—2010 are shown in Fig. 5. The surface layer shows effects of seasonal local heating/cooling cycles, of precipitation/runoff and of oxygen production and use coupled to production and decomposition of organic matter. A comparison between oxygen concentration (Fig. 5c) and oxygen saturation concentration (Fig. 5d) shows that surface water is super-saturated in spring and under-saturated in autumn. There is also an effect of an annual cycle of new deepwater inflows, which shows up clearly in the salinity increase at 50 m depth in autumn. The oxygen concentration is simultaneously depressed (Fig. 5c), suggesting that the salinity increase at 50 m is due to upward advection of saltier and oxygen-depleted water.

The vertical salt stratification in the Bornholm Basin can be described roughly by two layers on top of each other that are separated by a 5—20 m thick halocline. The top of the halocline is usually at about 50 m depth but it is up-lifted in periods of larger inflows of new deepwater from the Arkona Basin. The halocline top deepens by outflow of halocline water through the Stolpe Channel and also by entrainment of halocline water into the surface layer during events with strong winds. Compared to the situation in the basins east and north of Bornholm Basin, the top of the halocline is elevated in the Bornholm Basin. The rather shallow sill of the Stolpe Channel (59 m) is responsible for the elevated halocline by blocking outflow from the density stratified basin water below the sill depth. However, the salinity of the lower layer, below the halocline, is quite variable on time-scales longer than 1 year due to relatively strong vertical mixing, which reduces the salinity, in combination with large long-time variability of the salinity of the inflowing new deepwater, which occasionally increases the salinity, as can be seen in Fig. 3a.

## 4. Currents

Currents are generated in several ways, which are briefly summarized below. The direct action of the atmosphere on the sea surface, in particular through the wind stress, generates quasi-steady and time dependent wind-drift currents in the surface layer. The response to the wind stress depends on the vertical stratification, in particular on the thickness of the well-mixed surface layer, and on the buoyancy fluxes through the sea surface caused by local heating/cooling and precipitation/evaporation. Convergence and divergence of drift currents in the surface layer at coasts and density fronts may generate horizontal pressure gradients and thereby horizontal circulation in a basin. It may also generate internal waves in the stratified part of the water column, beneath the well-mixed surface layer. Internal waves may also be generated by interaction between barotropic currents varying in time and bottom topography. The internal waves generated this way have the same frequencies as the barotropic currents generating them. In addition, currents may be generated by horizontal pressure gradients at the open vertical

boundaries of a basin. In the Bornholm Basin such pressure gradients may be caused by e.g. inflow of new deepwater through the Bornholm Channel. Since the new deepwater has relatively high density, the currents carrying this water takes, initially, place along the seabed in so-called dense bottom currents. The water in the dense bottom current is mixed with ambient water, that is why the negative buoyancy decreases and eventually the dense bottom current loses its buoyancy and contact with the seabed. The water is then interleaved in the water column at the level where the density equals that of the current. This process sustains stratification above the sill depth in the Stolpe Channel, which drives currents out of, and circulation within, the Bornholm Basin. In this section various types of currents occurring in the Bornholm Basin are discussed together with examples of observations of currents.

### 4.1. Wind-forced drift currents and inertial currents in the surface layer

In deep non-stratified water, a steady wind in the Northern Hemisphere will transport surface water perpendicular to the right of the wind direction. The Coriolis force acting on the vertically integrated transport (the so-called Ekman transport) is balanced by the wind stress on the sea surface. If there are buoyancy fluxes through the sea surface, due to fluxes of heat and water, and if the water column is stably stratified, the dynamics of the wind drift becomes more complicated and the transport will also obtain a component parallel to the wind direction as shown by Nerheim and Stigebrandt (2006) who analyzed current data from moored rigs in the Baltic Proper. When the wind drift converges, either against coasts or at density fronts in the open sea, barotropic and baroclinic pressure fields are created due to sloping sea surface and density surfaces, respectively. These force large-scale barotropic and baroclinic currents. On large scales in the open ocean, wind drift due to steady wind systems, like the trade winds and the west wind belt, create permanent large-scale current systems. In the Baltic Sea, the winds are often shifting direction and speed and it seems that no permanent large-scale circulation is sustained by the wind drift.

The response to the unsteady component of the wind stress takes the form of inertial currents that manifest themselves as damped clockwise (Northern Hemisphere) circulation as shown theoretically by Ekman (1905). Observations of damped inertial currents from the Baltic Sea were presented by Gustafsson and Kullenberg (1935). The period of inertial currents equals $T_f = 12/\sin(\varphi)$ h where $\varphi$ is the latitude; for e.g. $\varphi = 55^\circ$N the formula gives $T_f \approx 14.6$ h. The inertial period is the upper limit for periods of free internal waves. Inertial currents in the surface layer may transfer energy to free internal waves (of slightly shorter period than $T_f$) in the stratified deepwater, see Section 4.2, and to internal waves of periods longer than $T_f$ that are bound to move along topography like e.g. internal Kelvin waves. In the surface layer, the typical amplitude of inertial currents is 0.1 m s$^{-1}$ and the damping time scale is 1 day. It was assumed that the damping of inertial currents in the surface layer of the Baltic Proper is due to vertical transfer of power to internal waves in the stratified water column beneath the well-mixed surface layer (Liljebladh and Stigebrandt, 2000). From observations obtained during the DIAMIX experiment, these authors estimated that the average vertical transfer of power from inertial currents in the surface layer to internal waves in the deepwater is about 0.3 mW m$^{-2}$. This power is believed to eventually be transferred to deepwater turbulence as further discussed in Section 5.

### 4.2. Internal waves

Free internal waves have frequencies in the interval between the inertial frequency ($\approx$0.00012 s$^{-1}$) and the buoyancy frequency $N$ defined by $N^2 = g/\rho \cdot (d\rho/dz)$ (symbols are defined in connection to Eq. (1)) that typically is about 0.03 s$^{-1}$ in the strongly stratified Bornholm Basin. In this frequency interval, the orbital motion of water particles caused by the internal waves goes from vertical at the buoyancy frequency to horizontal at the inertial frequency. The vertical structure of internal waves varies with the shape of the vertical stratification of the water column. If the vertical stratification is constant with depth, the oscillation may have evident vertical modes (similar to oscillations of e.g. a violin string). In other cases the stratification can be described by two-layers on top of each other and the orbital motions in the two layers are horizontal and in opposite directions. A common property of all types of internal waves is that the vertically integrated horizontal transport vanishes, i.e. there is no horizontal net transport by internal waves.

The speed $c_i$ of internal waves in two-layer stratification, with density difference $\Delta\rho$ and layer thicknesses $h$ and $H$, respectively, and with $h$ much less than $H$, equals

$$c_i = (g'h)^{1/2}. \quad (1)$$

Here $g' = g\Delta\rho/\rho_0$, where $g$ is the acceleration of gravity and $\rho_0$ a reference density. Example: with $\Delta\rho/\rho_0 = 0.01$, $h = 20$ m, and $g = 10$ m s$^{-2}$ one obtains $c_i = 1.4$ m s$^{-1}$.

Oscillating barotropic currents flowing across sloping bottoms in stratified waters will generate baroclinic (internal) currents that get their energy from the barotropic currents. The most well-known example is the generation of internal tides by the flow of surface tides over ridges and sills in the bottom. Internal waves are not very stable why they lose energy to turbulence by different mechanisms (e.g. Stigebrandt, 1976, 2012). Most of the power driving the turbulence responsible for the mixing of the deepwater of the oceans (and fjords) comes from tides via internal tides generated at sloping bottoms.

In the Baltic, tides are quite small and therefore the energy transfer from tides to deepwater turbulence should be negligible. However, time-dependent wind-forced barotropic currents occur frequently and these may lose power to internal waves and deep water turbulence. This was investigated by Nohr and Gustafsson (2009) who estimated the mean energy transfer from time-dependent barotropic currents for the Baltic proper but they did not discuss the Bornholm Basin specifically.

### 4.3. Dense bottom currents

The density of new deepwater, emanating from Kattegat and the Belt Sea, is higher than the density of water above the halocline. For small bottom slopes, the speed $c$ of dense

bottom current increases with the bottom slope up to the so-called critical slope when the speed equals the speed of $c_i$ of the internal wave in the actual vertical stratification, see e.g. Stigebrandt (1987b). However, if the bottom slope is supercritical, $c$ will still be close to $c_i$ because in this case hydrodynamic instabilities grow rapidly at the interface and cause energy losses and strong apparent flow resistance by entrainment of overlying water. The two-layer stratification applied in the example of internal wave speed, just below Eq. (1), should also be typical of dense bottom currents during major inflows. Dense bottom currents during major inflows should thus in extreme cases be expected to reach velocities up to about 2 m s$^{-1}$, depending on the layer thickness and the density difference. Piechura and Beszczyńska-Möller (2003) observed current speeds up to 0.75 m s$^{-1}$ during an inflow they characterized as medium-sized.

The new deepwater that moves as a dense bottom current along the seabed entrains lighter water from above. It has been estimated that entrainment of ambient water into the dense bottom current in the Bornholm Basin increases the volume flow of the bottom current by about 1% for every meter it descends but in the Arkona Basin the corresponding figure is rather 2% (Stigebrandt et al., 2015). These authors suggest that the difference might be due to differences between the two basins with respect to the large-scale bottom topography where the dense bottoms currents run. Slightly simplified, the bottom currents run on a sloping plane in the Arkona Basin while they run in a valley, or canyon, in the Bornholm Basin, see also Stigebrandt et al. (2006).

An ambitious observational program to estimate the supply of new deepwater to the Bornholm Basin/Baltic Proper was performed in the Bornholm Channel during the period 1973–1977 (Walin, 1981) The flow through a fixed vertical cross-section was observed on 32 different days using gelatin pendulum current meters and CTD. Walin reported that the salinity of the new deepwater is typically 10–20 PSU and the speed 10–50 cm s$^{-1}$. A short time after the major inflow to the Baltic Sea in January 1993, the flow in several vertical cross-sections in both the Bornholm Channel and the Arkona Basin was observed using ship ADCP and CTD (Liljebladh and Stigebrandt, 1996). These authors reported transports of new deepwater in the interval 60 000–120 000 m$^3$ s$^{-1}$ but did not explicitly report currents speeds.

### 4.4. Circulation due to inflow/outflow from the basin

In the Bornholm Basin, new deepwater entering from the Arkona Basin contributes to an upward motion above its level of interleaving. Much of the new deepwater is not dense enough to penetrate into the closed basin, below the sill depth of the Stolpe Channel, that is why the through-flow of this water occurs entirely above the sill depth. The outflow of halocline water takes place through the Stolpe Channel, and probably occasionally also through the shallower channel east of the island of Öland. In model computations by Stigebrandt et al. (2015), further discussed in Section 6, it was assumed that a geostrophic baroclinic current, driven by the horizontal pressure difference between the Bornholm Basin and Stolpe Channel, exits through the Stolpe Channel. However, comparison with hydrographical observations showed that the modeled pool of halocline water in the Bornholm Basin was drained too fast.

One reason for too fast draining of the modeled halocline water could be that just a fraction of the computed baroclinic transport exits through the Stolpe Channel while the residual is re-circulated within the Bornholm Basin. One would then expect that the outflow sustains a dome-structure of the halocline water in the Bornholm Basin, with the isopycnal surfaces sloping downwards from the central parts of the basin toward the periphery, implying a radial horizontal baroclinic pressure gradient in the basin sustaining an anticyclonic, clockwise, circulation of halocline water. ADCP observations performed by the Polish research vessel Oceania, reported by Bulczak et al. (2016), support the expectation of a clockwise circulation of halocline water in the Bornholm Basin. Rak (2016) documented effects on hydrography and currents of the major inflow in the period December 2014–January 2015.

## 5. Vertical mixing

Different mechanisms of vertical mixing are very important for the modification and through-flow of new deepwater in the Bornholm Basin. The horizontal mean rate of vertical mixing in the deepwater can be estimated using the budget method described by e.g. Stigebrandt and Kalén (2013) that is applicable under so-called stagnation periods, i.e. periods lacking water exchange by advection. During such periods, storage changes of conservative entities below a horizontal surface at a specified depth $z$ are due to transport by vertical diffusion through that surface. The horizontally averaged value of the vertical diffusivity $\kappa$ at the specified depth can be estimated using the following equation:

$$\kappa_{z=u} = \left(A\frac{\partial S}{\partial z}\right)^{-1}_{z=u}\int_d^u \frac{\partial S}{\partial t} A\, dz. \tag{2}$$

Here $A = A(z)$ equals the horizontal area of the basin at the depth $z$ and $S(z,t)$ the horizontally averaged value of $S$ at depth $z$ and time $t$ obtained from observations. The value of the first factor on the right hand side of Eq. (2) is the value at the upper level of integration $z = u$, which must be below the sill level. The greatest depth in the basin equals $z = d$. This equation may be used to compute $\kappa$ at $n - 1$ levels if there are $n$ levels of measurements of a conservative property like sea salt $S = S(z,t)$. Concentrations of non-conservative dissolved substances like oxygen and nutrients depend in addition on internal sources and sinks due to e.g. decomposition of organic compounds in the water column or the seabed. Table 2 shows results reported by Stigebrandt and Kalén (2013) who used virtually all available salinity observations from the hydrographical stations BY4 and BY5 for the period 1957–2011 for their computations.

For modeling purposes, Stigebrandt (1987b) parameterized $\kappa$ using the stratification parameter $N$, defined in Section 4.2, in the following way

$$\kappa = a_0 N^{-1}. \tag{3}$$

Here $a_0$ is an empirical intensity factor (velocity squared) accounting for the horizontal mean mixing activity of turbulence. Using a vertical advection-diffusion filling-box model with an entraining dense bottom current carrying new

**Table 2** Average and standard deviation of vertical diffusivity $\kappa$ [$m^2\ s^{-1}$] at depth $z$ [m], and work $W$ [$W\ m^{-2}$] against the buoyancy forces and $a_0$ [$m^2\ s^{-2}$] below the depth $z$ in the Bornholm Basin based on hydrographical data from BY4 and BY5. 'No $\kappa$' is the number of estimates of vertical diffusivity.

| $z$ [m] | $\kappa$ [$\times 10^{-6}\ m^2\ s^{-1}$] | No $\kappa$ [–] | $W$ [$\times 10^{-4}\ W\ m^{-2}$] | $a_0$ [$\times 10^{-7}\ m^2\ s^{-2}$] |
|---|---|---|---|---|
| 65 | $2.5 \pm 1.7$ | 12 | $1.0 \pm 0.5$ | $1.1 \pm 0.8$ |
| 75 | $4.5 \pm 3.6$ | 35 | $0.7 \pm 0.5$ | $1.3 \pm 0.9$ |
| 85 | $8.0 \pm 7.2$ | 88 | $0.4 \pm 0.4$ | $1.4 \pm 1.3$ |

deepwater into the basin, Stigebrandt (1987b) estimated $a_0 = 2.0(\pm 0.7) \times 10^{-7}\ m^2\ s^{-2}$ for the Baltic Proper. Later circulation models for the Baltic Proper (Gustafsson, 2003; Meier, 2001; Omstedt, 2011) use this parameterization with $a_0 = 1.5 \times 10^{-7}$, which incidentally is quite close to the values presented in Table 2 for the Bornholm Basin.

The total rate of work against the buoyancy forces $P$ by mixing processes below the level $z = u$ in a basin is obtained by integrating the buoyancy flux, $b = \kappa N^2$, from the greatest depth $z = d$ to the depth $z = u$:

$$P = \int_d^u \rho_0 \kappa(z) N^2(z) A(z)\, dz. \tag{4}$$

To compare the power used by buoyancy fluxes in various basins, one may divide $P$ by the area of the basin at the upper integration limit $u$. This gives the normalized power $W(u) = PA^{-1}(u)$ spent to buoyancy fluxes in the water column of the basin water beneath the depth $u$. The results for the Bornholm Basin obtained by Stigebrandt and Kalén (2013) are shown in Table 2. The estimated rate of work beneath 65 m is thus 100 $\mu W\ m^{-2}$. It should be underlined that if $\kappa$ is estimated using the budget method, the value of $P$ is only dependent on the hydrographical observations; no empirical coefficient is involved in the estimate. The error in $P$ should thus only depend on the quality and the number of hydrographical observations used.

Only a minor fraction $Rf$ of the supplied energy $E$ is used for work against the buoyancy forces $W$. Thus $W = Rf \cdot E$. Most of the supplied turbulent energy is dissipated to heat $D = (1 - Rf)E$. With $Rf = 0.07$, as discussed below, the result from Stigebrandt and Kalén (2013) gives $E \approx 1.5\ mW\ m^{-2}$. The horizontal and time mean dissipation $D$ in the deepwater of the Bornholm Basin should then be about $1.4\ mW\ m^{-2}$. Since tides are very small in the Baltic, it should be obvious that the power $E$ ultimately is derived essentially from the wind. Axell (1998) found that the annual variation in mixing is well correlated with the variation in wind stress. This result is supported by Stigebrandt and Kalén (2013) who found that the ratio between the powers $W$ used against buoyancy forces in summer and winter, respectively, equals 0.65.

It is however not clarified by which mechanisms the wind energy is transferred to the deepwater. Liljebladh and Stigebrandt (2000) estimated that decaying inertial currents in the surface layer east of Gotland might deliver about $0.3\ mW\ m^{-2}$ to deepwater turbulence, see Section 4.1. Nohr and Gustafsson (2009) found that oscillating barotropic currents may supply substantial power to deepwater turbulence via internal waves generated at sills and sloping bottoms, see Section 4.2.

The budget method accounts for the integrated action of all vertical mixing taking place in a stagnant basin but it does not tell when and where in the basin that mixing was carried out. Probably the first model of boundary mixing in a closed basin was presented by Stigebrandt (1976) who applied it to the inner part of the Oslo Fjord. A few years later, a tracer cloud experiment in the deepwater of the Oslo Fjord (Bjerkeng et al., 1978) showed that vertical mixing estimated from the evolution of the tracer cloud that had no contact with the side boundaries, was only about 10% of the vertical mixing estimated from the budget method applied on sea salt ($S$), which proves the dominance of boundary mixing (Stigebrandt, 1979). Boundary mixing versus interior mixing in the eastern Gotland Basin was one of the major research questions of the DIAMIX project, another was the overall energy budget of deepwater turbulence (Stigebrandt et al., 2002). Holtermann and Umlauf (2012) report results from a large-scale tracer experiment in the East Gotland Basin that verified the dominance of boundary mixing. Van der Lee and Umlauf (2011) estimated dissipation in the basin water of Bornholm Basin from microstructure profiles. It was an order of magnitude smaller than that estimated above from the estimate of $W$. This strongly suggests that the observed mixing was interior mixing, which should be of less importance for basin mixing, cf. also Section 6.

It follows from the dense bottom current model in Stigebrandt (1987b) that the efficiency $Rf$ of turbulence generated by combined bottom and interfacial drag in dense bottom currents equals approximately 0.04 (Stigebrandt et al., 2006). This is rather low compared to e.g. the mixing efficiency in fjord basins where numerous estimates typically give an (overall) *system Rf* in the range of 0.06–0.07, see Stigebrandt (2012). This is less than half of the value 0.2 which is often used in oceanography. However, this value seems to be obtained from laboratory process studies. Arneborg (2002) explained that the *process Rf* includes both the work done against the buoyancy forces on the system level and short lived potential energy in turbulent patches. The latter dissipates when patches collapse. He concluded that the *system Rf* should equal about half the *process Rf*.

Possible hydrographical effects upon inflowing deepwater of a pipeline crossing the route of the dense bottom current carrying new deepwater was investigated by Borenäs and Stigebrandt (2009). Referring to Stigebrandt et al. (2006), they assumed that the total dissipation of the dense bottom current, i.e. the dissipation integrated from the entrance sills in Fehmarn Belt and Öresund to Słupsk Furrow, is essentially determined by the potential energy of the dense water when passing the entrance sills. They estimated that a pipeline that rises 1.5 m above the seabed is capable of dissipating up to 0.5% of the total potential energy of the dense bottom current, depending on the speed of the dense bottom current in the crossing section. The mixing of the new

deepwater might increase if the mixing efficiency $Rf_{pipe}$ of pipeline-generated turbulence is greater than 0.04, which is the efficiency of turbulence generated by combined bottom and interfacial friction as mentioned above. It is not an easy task to estimate the system efficiency of mixing induced by pipes using in situ observations. Ingenious methods must probably be invented.

## 6. Modeling of mixing and through-flow in the Bornholm Basin

A vertical advection-diffusion circulation model was applied to the closed, lower parts of the Bornholm Basin (Stigebrandt and Kalén, 2013). Empirical values of the vertical diffusion were applied using the diffusivity described by Eq. (3), with $a_0$ changing with depth according to Table 2. The model was run for a year-long stagnation period in the basin water that started with high salinity. Fig. 6 shows the development of the salinity as observed (upper) and according to the model run (lower). There is a large oscillation in observed salinity in November 2003 but there are no signs of water exchange, implying that the oscillation might be real and caused by large horizontal water displacements within the basin or false and due to erroneous observational data. The salinity computed by the model declines at about the same rate as observed showing that the vertical diffusivity, derived from historic salinity data, describes the vertical diffusion quite well during the modeled period.

To be able to compute the water exchange of the Bornholm Basin during even longer periods, the model had to be supplemented with a model that computes the inflow of new deepwater from the Arkona Basin and the outflow of water through the Stolpe Channel. A simple mechanistic model computing inflow from and outflow to the entrance area, i.e. the Belt Sea and Kattegat, was constructed by Stigebrandt et al. (2015). Flow rates were estimated from volume changes of the Baltic Sea inside the entrance area corrected for volume changes due to the freshwater supply. In practice they used 5 days moving averages of the sea level in Stockholm and the monthly supply of freshwater inside the entrance area. The surface water flowing from the Arkona Basin to the entrance area has low salinity and sustains a usually several meters thick fictive freshwater layer in the entrance area. In reality the freshwater is mixed into the surface layer. Changes of the freshwater layer thickness were computed in response to inflows and outflows, for details see Stigebrandt et al. (2015). The presence of a fresher surface layer together with relatively shallow sills, restricts (partially blocks) the inflow of saltier sea water from the entrance area to the Arkona Basin. As long as there is much freshwater in the entrance area surface layer, the salinity of inflowing new deepwater will be low. However, during events with inflow to the Baltic Sea, the salinity of inflowing water increases with the duration of the inflow (Stigebrandt, 1987a) because the thickness of the freshwater layer in the entrance area diminishes during such episodes due to export to both the Arkona Basin and Skagerrak.

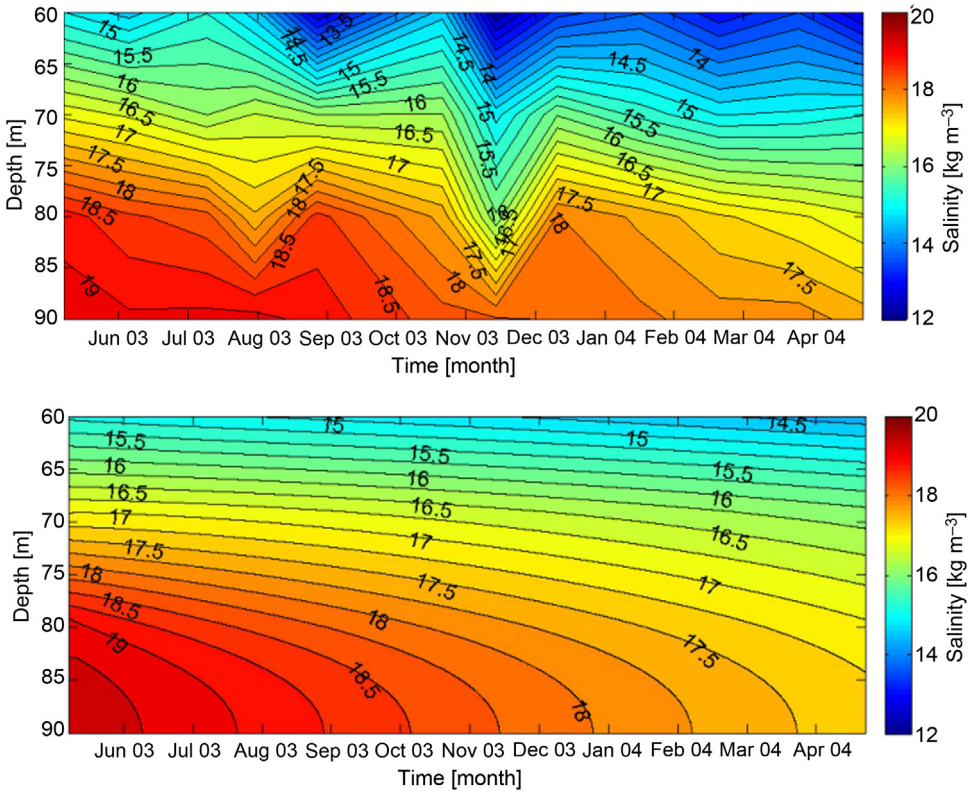


**Figure 6** Observed salinity [PSU] at BY5 (upper panel) and modeled salinity [PSU] (lower panel) in the basin water of the Bornholm Basin during the period 7 May 2003 to 21 April 2004 (from Stigebrandt and Kalén, 2013).

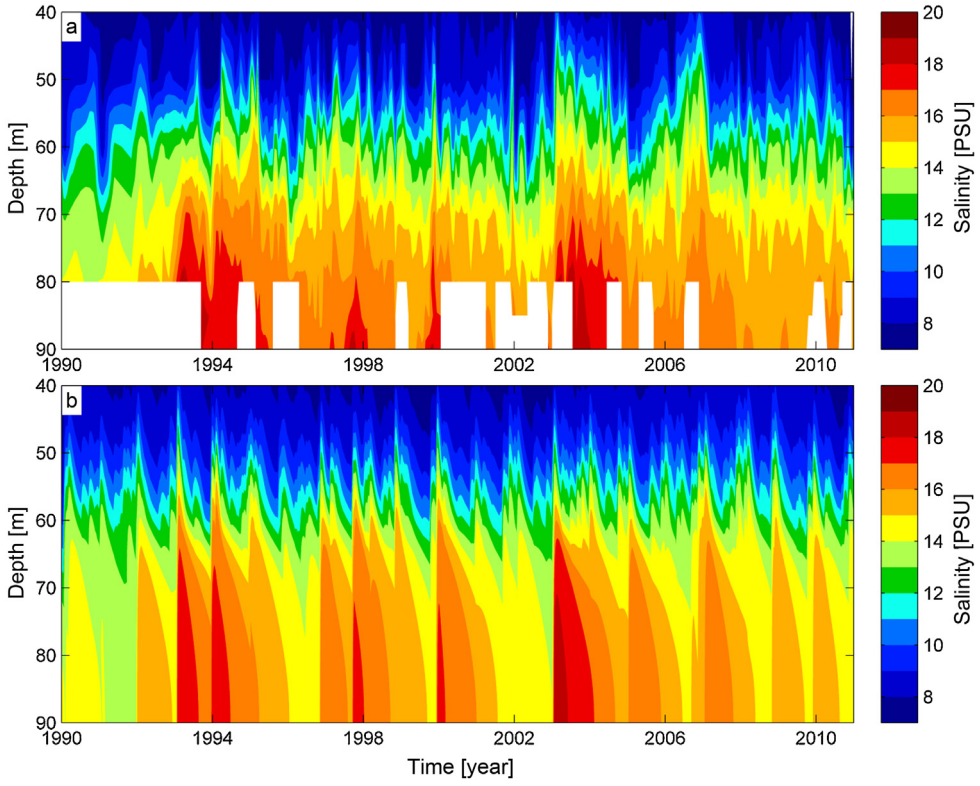


**Figure 7** The observed salinity [PSU] from BY4 (a) and the modeled salinity [PSU] (b). White areas in (a) indicate lack of data (from Stigebrandt et al., 2015).

The vertical advection-diffusion model supplemented with the through-flow model was run for the lower part of the Bornholm Basin for the period 1990–2011 (21 years) (Stigebrandt et al., 2015). Fig. 7 shows the observed salinity (a) and the modeled salinity (b). As can be seen, the model quite well describes the evolution of salinity in the lower part of the basin. The modeled salinity shows seemingly abrupt increases of salinity due to inflows of new deepwater. The observed salinity increases are more diffuse because the observational data grid is coarse and because horizontal displacements within the basin (cf. Fig. 7a) as well as internal waves create a large variability that influences the observations. A closer inspection shows that the heightened salinity above 60 m depth due to halocline uplift after larger inflows, such as the one in early 2003, can persist for up to 1 year. In the model, the effect of such uplifts seems to decay more quickly, suggesting that the baroclinic outflow through the Stolpe Channel might be too fast in the model as discussed in Section 4.4. In the model by Stigebrandt et al. (2015) the upper part of the water column changes as a result of data

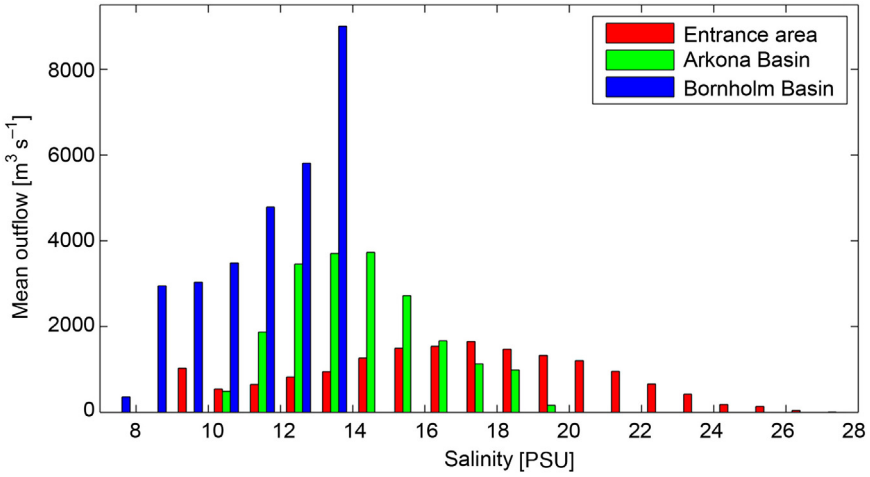


**Figure 8** Distribution of average volume flow among different salinities for the modeled deepwater flows from the entrance area, the Arkona Basin and the Bornholm Basin (from Stigebrandt et al., 2015).

assimilation. Thus, there is no model that computes e.g. the dynamics of the mixed surface layer because this was considered of less importance for the evolution of the stratification in the lower part of Bornholm Basin. In the simulations, the temperature field shows that the model misses some instances of strong mixing in the surface layer (see Stigebrandt et al., 2015).

The salinity of the deepwater in the Baltic Proper east of the Słupsk Furrow is only about 1/3rd of the salinity of Kattegat deepwater. The very large decrease of the salinity of new deepwater is taking place in the Arkona and Bornholm Basins. Due to efficient mixing between inflowing water and residing Baltic Sea surface water, the salinity range of inflowing new deepwater decreases the further into the Baltic Sea the deepwater intrudes. Accordingly, the high salinity end of new deepwater from the entrance area has salinities in the range of 20—28 PSU; the high salinity end of new deepwater from the Arkona Basin is in the range of 15—20 while the highest salinity is less than 15 from the Bornholm Basin (Fig. 8). By looking at e.g. the upper panel of Fig. 6 it can be understood that the mixing of residing water in the Bornholm Basin is paramount to reduce the high salinity end of new deepwater imported from the Arkona Basin. The salinity range of new deepwater is a very important factor for the vertical stratification and the length of stagnation periods in the Baltic Proper as discussed in Stigebrandt (1987b). Increased mixing in the Bornholm Basin by pipelines and other man-made devices should thus contribute to shorter stagnation periods, and thereby decrease the occurrence of anoxia in the Baltic Proper, see also Stigebrandt et al. (2015).

## 7. Concluding remarks

Scientific knowledge about the hydrography of the Bornholm Basin has increased drastically during the last decade. One reason for this is the increased interest in using the Bornholm Basin for various purposes that has required analyses to quantify and understand the dynamics of this sea. Thus, investigations of environmental effects of various possible man-made operations and building of physical constructions have forced interest into this particular sea which has led to increased scientific knowledge. After thorough investigations of possible environmental effects, the company Nord Stream has now laid down two gas pipelines on the seabed crossing the Bornholm Basin in the SSW—NNE direction. There have been also theoretical investigations of possible man-made oxygenation of the nowadays often anoxic deepwater and its effects, in order to reduce the leakage of phosphorus from anoxic bottoms. Oxygenation would improve the water quality at greater depths so that the now azoic bottoms may be colonized which would imply more food for the cod, for instance. Improved pelagic water quality would also lead to better conditions for cod recruitment.

## Acknowledgement

Josefina Almén adapted the figures borrowed from other publications to *Oceanologia* standards and drew Fig. 3.

## References

Arneborg, L., 2002. Mixing efficiencies in patchy turbulence. J. Phys. Oceanogr. 32 (5), 1496—1506.

Axell, L.B., 1998. On the variability of Baltic Sea deepwater mixing. J. Geophys. Res. 103 (C10), 21667—21682.

Bjerkeng, B., Göransson, C.G., Magnusson, J., 1978. Investigations of different alternatives for waste water disposal from Sentralanlegg Vest. Part 1, NIVA Rep. No. O-132/76, 74 pp., (in Norwegian).

Borenäs, K., Stigebrandt, A., 2009. Possible hydrographical effects upon inflowing deep water of a pipeline crossing the flow route in the Baltic Proper. Swedish Meteorological and Hydrological Institute (SMHI), Report No. 2007-61, ver. 3.0, 49 pp., (accessed online: http://www.ft.dk/samling/20091/almdel/mpu/spm/78/svar/663190/760021.pdf).

Bulczak, A., Rak, D., Beldowski, K., 2016. Observations of near-bottom currents in Bornholm Basin, Słupsk Furrow and Gdańsk Deep. Deep Sea Res. Part II 128, 96—113.

Ekman, V.W., 1905. On the influence of the earth's rotation on ocean currents. Ark. Mat. Astron Fys. 2 (11), 1—52.

Gustafsson, B.G., 2003. A time-dependent coupled-basin model of the Baltic Sea. Rep. No. C47, Earth Sci. Centre, Göteborg Univ. 61 pp.

Gustafsson, T., Kullenberg, B., 1935. Untersuchungn von Trägheitsströmungen in der Ostsee. Svenska Hydrogr.-Biol. Komm. Skr. Ny. Ser. Hydrogr. 13, 1—28.

Holtermann, P.L., Umlauf, L., 2012. The Baltic Sea Tracer Release Experiment 2: mixing processes. J. Geophys. Res. 117, C01021.

Lass, H.U., Mohrholz, V., Seifert, T., 2001. On the dynamics of the Pomeranian Bight. Cont. Shelf Res. 21 (11—12), 1237—1261.

Liljebladh, B., Stigebrandt, A., 1996. Observations of the deepwater flow into the Baltic Sea. J. Geophys. Res. 101, 8895—8912. http://www.academia.edu/25127985/Observations_of_the_deepwater_flow_into_the_Baltic_Sea.

Liljebladh, B., Stigebrandt, A., 2000. The contribution from the surface layer via internal waves to the energetics of deepwater mixing in the Baltic. In: Liljebladh, B. (Ed.), Experimental Studies of Some Physical Oceanographic Processes. Earth Sci. Centre, Publ. A56, Univ. Gothenburg (Ph.D. Thesis).

Meier, H.E.M., 2001. On the parameterization of mixing in three-dimensional Baltic Sea models. J. Geophys. Res. 106 (C12), 30997—31016.

Nerheim, S., Stigebrandt, A., 2006. On the influence of buoyancy fluxes on wind drift currents. J. Phys. Oceanogr. 36 (8), 1591—1604.

Nohr, C., Gustafsson, B.G., 2009. Computations of energy for diapycnal mixing in the Baltic Sea due to internal wave drag acting on wind-driven barotropic currents. Oceanologia 51 (4), 461—494, http://dx.doi.org/10.5697/oc.51-4.461.

Ödalen, M., Stigebrandt, A., 2013a. Hydrographical conditions in the Bornholm Basin of importance for oxygenation of the deepwater by pumping down oxygen saturated water from above the halocline. Box-Win Tech. Rep. No. 1, Rep. C96, Univ. Gothenburg, 19 pp.

Ödalen, M., Stigebrandt, A., 2013b. Factors of potential importance for the location of wind-driven water pumps in the Bornholm Basin. Box-Win Tech. Rep. No. 2, Rep. C97, Univ. Gothenburg, 36 pp.

Omstedt, A., 2011. Guide to Process-based Modeling of Lakes and Coastal Seas. Springer, Berlin, 258 pp., http://dx.doi.org/10.1007/978-3-642-17728-6.

Piechura, J., Beszczyńska-Möller, A., 2003. Inflow water in the deep regions of the southern Baltic Sea — transport and transformations. Oceanologia 45 (4), 593—621.

Rak, D., 2016. The inflow in the Baltic Proper as recorded in January—February 2015. Oceanologia 58 (3), 241—247, http://dx.doi.org/10.1016/j.oceano.2016.04.001.

Seifert, T., Tauber, F., Kayser, B., 2001. A high resolution spherical grid topography of the Baltic Sea — 2nd edition. In: Baltic Sea Sci. Congr. Stockholm, 25—29 November 2001 Poster #147.

Stigebrandt, A., 1976. Vertical diffusion driven by internal waves in a sill fjord. J. Phys. Oceanogr. 6 (4), 486—495.

Stigebrandt, A., 1979. Observational evidence for vertical diffusion driven by internal waves of tidal origin in the Oslo fjord. J. Phys. Oceanogr. 9 (2), 435—441.

Stigebrandt, A., 1987a. Computations of the flow of dense water into the Baltic from hydrographical measurements in the Arkona Basin. Tellus A 39 (2), 170—177.

Stigebrandt, A., 1987b. A model for the vertical circulation of the Baltic deep water. J. Phys. Oceanogr. 17 (10), 1772—1785.

Stigebrandt, A., 2012. Hydrodynamics and circulation of fjords. In: Bengtsson, L., Herschy, R.W., Fairbridge, R.W. (Eds.), Encyclopedia of Lakes and Reservoirs. Springer Science+Business Media B.V., Dordrecht, Heidelberg, New York, London, 327—344.

Stigebrandt, A., Johnson, M., Wüest, J., 2006. Mixing efficiency of turbulence in dense gravity-forced bottom currents. In: Johnson, M. (Ed.), Studies in Coastal Seas of Small Scale Mixing Processes Related to Topography. Publ. A 106, (Licentiate thesis), Göteborg Univ..

Stigebrandt, A., Kalén, O., 2013. Improving oxygen conditions in the deeper parts of Bornholm Sea by pumped injection of winter water. Ambio 42 (5), 587—595.

Stigebrandt, Lass, A., Liljebladh, H.U., Alenius, B., Piechura, P., Hietala, J., Beszczyńska, R., 2002. DIAMIX — an experimental study of diapycnal deepwater mixing in the virtually tide-less Baltic Sea. Boreas Environ. Res. 7 (4), 363—369.

Stigebrandt, A., Rosenberg, R., Råman, L., Ödalen, M., 2015. Consequences of artificial deepwater ventilation in the Bornholm Basin for oxygen conditions, cod reproduction and benthic biomass — a model study. Ocean Sci. 11 (1), 93—110.

Svikov, V.V., Sviridov, N.I., 1994. The relation between erosional-accumulative forms of bottom relief and near bottom currents in the Bornholm deep. Oceanology 34 (2), 266—270, (English translation).

Van der Lee, E.M., Umlauf, L., 2011. Internal wave mixing in the Baltic Sea: near-inertial waves in the absence of tides. J. Geophys. Res. 116, C10016.

Walin, G., 1981. On the deep water flow into the Baltic. Geophysica 17, 75—93.

Oceanologia (2017) 59, 81—84

Available online at www.sciencedirect.com

ScienceDirect

journal homepage: www.journals.elsevier.com/oceanologia/

SHORT COMMUNICATION

# New data on benthic Naididae (Annelida, Clitellata) in Polish brackish waters

Lena Marszewska [a,*], Elżbieta Dumnicka [b], Monika Normant-Saremba [a]

[a] Institute of Oceanography, University of Gdańsk, Gdynia, Poland
[b] Institute of Nature Conservation, Polish Academy of Sciences, Kraków, Poland

Received 26 February 2016; accepted 23 June 2016
Available online 22 July 2016

**KEYWORDS**
Oligochaeta;
Tubificidae;
Soft bottom infauna;
Port of Gdynia;
Gulf of Gdańsk;
Baltic Sea

**Summary** This paper presents new findings on oligochaete species inhabiting Polish brackish waters. Identification of 455 specimens collected in September 2013 and July 2014 during the macrozoobenthos survey in the Port of Gdynia (the Gulf of Gdańsk, the southern Baltic Sea, Poland) showed the presence of six species belonging to two subfamilies Naidinae and Tubificinae.


## 1. Introduction

Oligochaetous clitellates (subclass Oligochaeta) are a diverse, widely distributed group in both marine and freshwater ecosystems all over the world in which they play various roles. Despite their importance, and the fact that oligochaetes are an abundant group within soft-bottom communities in the Baltic Sea, they are often identified only to the subclass level (Boström and Bonsdorff, 1997; Gic-Grusza et al., 2009; Masłowski, 2010), what can give a different result when considering, for example, species richness or number or non-indigenous species (NIS), considered these days a major threat to coastal ecosystems' biodiversity (Bax et al., 2003; Ojaveer et al., 2014). Because of intense international vessel traffic and favorable environmental conditions, the Baltic Sea is particularly susceptible to NIS introductions (Leppäkoski et al., 2002). Moreover, ballast water and ballast tank sediment are the most probable vectors of introduction of annelids (Gollasch et al., 2002), hence it is likely that a new species from this phylum will be recorded in port areas in the future (Kotta et al., 2015; Leppäkoski et al., 2002; Paavola et al., 2005).

In this paper, we present new data on oligochaete worms, native and introduced, from shallow waters of southern part of the Baltic Sea (Poland), based on the example of the Port of Gdynia. In 2013 and 2014, during testing the protocol for comprehensive sampling of alien species in ports recommended by HELCOM (2013), we analyzed the taxonomic composition of benthic macrofauna, including the identification of oligochaetes to the species level.

* Corresponding author at: Institute of Oceanography, University of Gdańsk, al. Marszałka J. Piłsudskiego 46, 81-378 Gdynia, Poland. Tel.: +48 585236866.
*E-mail address:* lena.marszewska@ug.edu.pl (L. Marszewska).
Peer review under the responsibility of Institute of Oceanology of the Polish Academy of Sciences.

Production and hosting by Elsevier

http://dx.doi.org/10.1016/j.oceano.2016.06.003

## 2. Material and methods

Samples of benthic infauna were taken in September 2013 and July 2014 in the Port of Gdynia (Gulf of Gdańsk, Poland) from three sampling sites at the depth of 8.7—13.6 m. Bottom temperature during sampling varied from 18.5 to 18.9°C in 2013 and from 16.1 to 19.5°C in 2014, salinity was between 6.7 and 6.8 PSU in 2013 and 7.0 PSU in 2014, water oxygenation at the bottom ranged from 65.7 to 76.7% in 2013 and from 62.1 to 89.9% in 2014. Samples were collected with a Van Veen grab of 0.1 $m^2$ sampling area. Sediment was sieved through a 0.5 mm sieve; the residue was placed in 1000 $dm^3$ bottles and preserved with 4% formaldehyde. In a laboratory, Oligochaeta specimens were selected from samples, placed in Amman's lactophenol to display chitinous structure of chaetae and penial sheaths and then they were identified to the species level based on features given by Kasprzak (1981) and Timm (2009).

## 3. Results

Altogether, 455 individuals belonging to the family Naididae were collected. Among them one species from the subfamily Naidinae and five from the subfamily Tubificinae were identified, moreover, 136 immature specimens were classified as Tubificinae gen. spp. juv.

Each year of the study, five species were recorded. In September 2013, *Tubificoides heterochaetus* (Michaelsen, 1926) was the most abundant taxon ($n = 135$) followed by mature specimens of *Limnodrilus hoffmeisteri* Claparède, 1862 ($n = 61$). *Tubifex blanchardi* Vejdovský, 1891 was distinctly less numerous ($n = 4$), whereas both *Baltidrilus costatus* (Claparède, 1863) and *Paranais litoralis* (Müller, 1780) were represented by only one specimen (Fig. 1A). Juvenile Tubificinae, not determined to the species level, were not numerous ($n = 7$) in 2013, while they were the most abundant group ($n = 129$) in July 2014. In 2014, the number of mature specimens of *L. hoffmeisteri* ($n = 63$) was similar to the number determined in 2013, while the number of mature *T. blanchardi* was higher ($n = 22$). *T. heterochaetus* was represented by 22 individuals, whereas *B. costatus* — by 8 individuals. Moreover, the presence of *Limnodrilus profundicola* (Verrill, 1873) ($n = 2$) was determined (Fig. 1B). The density of the subclass Oligochaeta reached 697.67 $\pm$ 872 ind. $m^{-2}$ in 2013 and 820 $\pm$ 771 ind. $m^{-2}$ in 2014.

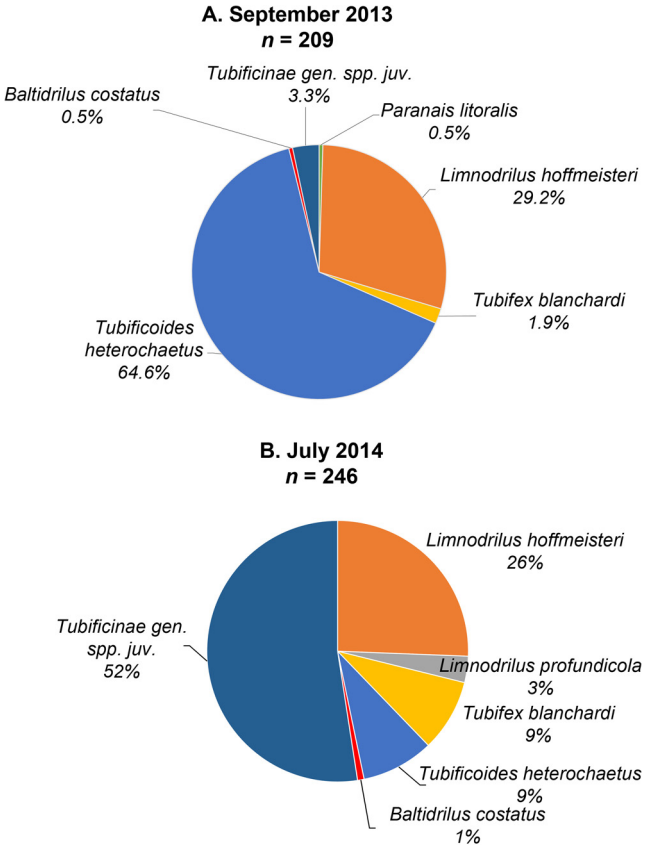


**Figure 1** Abundance of Oligochaeta species in three sample replicates collected form the Port of Gdynia in 2013 (A) and 2014 (B).

## 4. Discussion

Only a few authors analyzed the subclass Oligochaeta (e.g. Gogina et al., 2010; Jabłońska-Barna et al., 2013; Legeżyński, 1979) in the Southern Baltic. As evidenced by the research conducted by Włodarska-Kowalczuk et al. (2015) in the Vistula River prodelta, oligochaete individuals can represent from less than 1% up to 82% of the total number of benthic macrofauna and, based on the literature (Zettler and Daunys, 2007), it might be assumed that they could be one of the most diverse groups within the macrobenthic community. Of the six species identified in the Port of Gdynia, four are typical marine or brackish water inhabitants (*T. heterochaetus*, *P. litoralis*, *B. costatus*, and *T. blanchardi*), previously found in Polish coastal waters. *T. heterochaetus*, *P. litoralis*, and *B. costatus* were noted by Legeżyński (1979) in the Gulf of Gdańsk, whilst Żmudziński (1990) mentioned only *T. heterochaetus* and *P. litoralis* and described them generally as Baltic Sea inhabitants. So far, euryhaline species *T. blanchardi* and *L. hoffmeisteri* were found in the Vistula Lagoon only by Dumnicka et al. (2014). Our study reports for the first time the occurrence of *L. profundicola* in Polish coastal waters but this species was previously recorded in brackish water. Pfannkuche (1981) found it in the Elbe estuary, Verdonschot et al. (1982) — in brackish inland waters of the southwestern part of The Netherlands, and Seys et al. (1999) — in the Scheldt estuary. Generally, *L. profundicola* was present, except for freshwater ecosystems, in localities where the salinity was usually low (about 2 PSU) and did not exceed 7 PSU (Verdonschot et al., 1982). According to Weigel et al. (2015) and Warzocha (pers. comm.), the most abundant species in the western Baltic Sea and the Polish Exclusive Economic Zone were *B. costatus* and *Tubificoides benedii* (Udekem, 1855). Surprisingly, only few specimens of the former were found during our work. Our study revealed that both the species composition and the abundance may vary seasonally and annually, but in this case this kind of variation could be explained by patchy distribution of oligochaetes and perhaps collection of more samples would have given a better, overall picture of their abundance and taxonomic composition.

Almost all specimens collected in the Port of Gdynia in 2013 and 2014 belong to the subfamily Tubificinae, typical inhabitants of muddy sediments at depths ranging from a few centimeters to several dozen meters. The depth on sampling sites and type of sediment could be the reason for almost complete absence of Naidinae species, despite that some species from this subfamily (*Nais elinguis* Müller, 1774, *Amphichaeta sannio* Kallstenius, 1892) tolerate salinity up to 15 PSU (Pfannkuche, 1980).

As an effect of marine traffic, new species can be introduced into the Port of Gdynia and possibly further expand their range. Therefore, the origin of some Clitellata species is not certain, for instance *T. heterochaetus* with unknown status (Timm and Erséus, 2015) was listed by Gherardi et al. (2009) as an alien species in Europe. The origin of cosmopolitan *P. litoralis* (Timm, 2009) is also unknown — probably speciation of this genus took place in the Ponto-Caspian region and *P. litoralis* colonized other continents before oligochaetological studies; two other species from this genus were listed by Gherardi et al. (2009) as non-indigenous to Europe. Moreover, *T. blanchardi* described from North Africa (Vejdovský, 1891) and found in some countries of Southern Europe (Giani, 2013) could also be an introduced species in Poland.

Our study shows that even in a relatively small area with quite severe conditions for living organisms, fairly high species diversity can be noted, even when analyzing only one taxonomic group. Without a doubt these are valuable information, especially in the context of the EU Marine Strategy Framework Directive, where non-indigenous species, listed as one of the descriptors of "Good Environmental Status" of an aquatic ecosystem, constantly challenge marine biodiversity.

## Acknowledgements

This research was conducted in cooperation with the Port of Gdynia, the Environmental Protection Department within "The Baltic Sea Pilot Project: Testing new concepts for integrated environmental monitoring of the Baltic Sea" (BALSAM) financed by the European Commission DG Environment in years 2013—2015.

We would like to thank Mrs. Paulina Kunkel for her help in the sample collection process and laboratory work.

## References

Bax, N., Williamson, A., Aguero, M., Gonzalez, E., Geeves, W., 2003. Marine invasive alien species: a threat to global biodiversity. Mar. Policy 27 (4), 313—323, http://dx.doi.org/10.1016/s0308-597x(03)00041-1.

Boström, C., Bonsdorff, E., 1997. Community structure and spatial variation of benthic invertebrates associated with *Zostera marina* (L.) beds in the northern Baltic Sea. J. Sea Res. 37 (1—2), 153—166, http://dx.doi.org/10.1016/s1385-1101(96)00007-x.

Dumnicka, E., Jabłońska-Barna, I., Rychter, A., 2014. The first record of a new alien species *Limnodrilus cervix* Brinkhurst, 1963 (Annelida, Clitellata) in the Vistula Lagoon (southern Baltic Sea). Oceanologia 56 (1), 151—158, http://dx.doi.org/10.5697/oc.56-1.151.

Gherardi, F., Gollasch, S., Minchin, D., Olenin, S., Panov, V.E., 2009. Alien invertebrates and fish in European inland waters. In: Handbook of Alien Species in Europe. Berlin, Springer, 81—92.

Giani, N., 2013. Fauna Europaea: Tubificinae. In: de Jong, Y. (Ed.), Fauna Europaea: Tubificida. Fauna Europaea ver. 2.6.2, http://www.faunaeur.org.

Gic-Grusza, G., Kryla-Staszewska, L., Urbański, J., Warzocha, J., Węsławski, J.M. (Eds.), 2009. Atlas of Marine Benthic Habitats in Polish Marine Areas. Broker-Innowacji, Gdynia, 180 pp.

Gogina, M., Glockzin, M., Zettler, M.L., 2010. Distribution of benthic macrofaunal communities in the western Baltic Sea with regard to near-bottom environmental parameters. 1. Causal analysis. J. Mar. Syst. 79 (1—2), 112—123, http://dx.doi.org/10.1016/j.jmarsys.2009.07.006.

Gollasch, S., Macdonald, E., Belson, S., Botnen, H., Christensen, J.T., Hamer, J.P., Houvenaghel, G., Jelmert, A., Masson, I.L.D., McCollin, T., Olenin, S., Persson, A., Wallentinus, I., Wetsteyn, L.P.M.J., Wittling, T., 2002. Life in Ballast Tank. In: Leppäkoski, E., Gollasch, S., Olenin, S. (Eds.), Invasive Aquatic Species of Europe. Distribution, Impacts and Management. Springer Sci., Business Media, Dordrecht, 217—231.

HELCOM, 2013. HELCOM ALIENS 2 — Non-native Species Port Survey Protocols, Target Species Selection and Risk Assessment Tools for the Baltic Sea. 34 pp.

Jabłońska-Barna, I., Rychter, A., Kruk, M., 2013. Biocontamination of the western Vistula Lagoon (south-eastern Baltic Sea Poland). Oceanologia 55 (3), 751—763, http://dx.doi.org/10.5697/oc.55-3.751.

Kasprzak, K., 1981. Skąposzczety wodne, I. Rodziny: Aeolosomatidae, Potamodrilidae, Naididae, Tubificidae, Dorydrilidae, Lumbriculidae, Haplotaxidae, Glossoscolecidae, Branchiobdellidae. PWN, Warszawa, 226 pp.

Kotta, J., Kotta, I., Bick, A., Bastrop, R., Väinölä, R., 2015. Modelling habitat range and seasonality of a new, non-indigenous polychaete *Laonome* sp. (Sabellida, Sabellidae) in Pärnu Bay, the north-eastern Baltic Sea. Aquat. Icol. 10 (3), 275—285, http://dx.doi.org/10.3391/ai.2015.10.3.03.

Legeżyński, P., 1979. Skąposzczety (Oligochaeta, Annelida) Zatoki Gdańskiej. (Ph.D. thesis). UG, Gdynia, 99 pp.

Leppäkoski, E., Gollasch, S., Gruszka, P., Ojaveer, H., Olenin, S., Panov, V., 2002. The Baltic — a sea of invaders. Can. J. Fish. Aquat. Sci. 59 (7), 1175—1188, http://dx.doi.org/10.1139/f02-089.

Masłowski, J., 2010. Macrobenthos of the Pomeranian Bay in 1976—2005. Wyd. A. Marszałek, Toruń, 123 pp., (in Polish).

Ojaveer, H., Galil, B.S., Minchin, D., Olenin, S., Amorim, A., Canning-Clode, J., Chainho, P., Copp, G.H., Gollasch, S., Jelmert, A., Lehtiniemi, M., McKenzie, C., Mikuš, J., Miossec, L., Occhipinti-Ambrogi, A., Pećarević, M., Pederson, J., Quilez-Badia, G., Wijsman, J.W.M., Zenetos, A., 2014. Ten recommendations for advancing the assessment and management of non-indigenous species in marine ecosystems. Mar. Policy 44, 160—165, http://dx.doi.org/10.1016/j.marpol.2013.08.019.

Paavola, M., Olenin, S., Leppäkoski, E., 2005. Are invasive species most successful in habitats of low native species richness across European brackish water seas? Estuar. Coast. Shelf Sci. 64 (4), 738—750, http://dx.doi.org/10.1016/j.ecss.2005.03.021.

Pfannkuche, O., 1980. Distribution and abundance of Tubificidae and Naididae (Oligochaeta) in a brackish-water fjord, with special reference to the α-mesohaline zone. Neth. J. Sea Res. 14 (1), 78—93.

Pfannkuche, O., 1981. Distribution, abundance and life cycles of aquatic Oligochaeta (Annelida) in a freshwater tidal flat of the Elbe estuary. Arch. Hydrobiol. Suppl. 43 (4), 506—524.

Seys, J., Vincx, M., Meire, P., 1999. Spatial distribution of oligochaetes (Clitellata) in the tidal freshwater and brackish parts of the Schelde estuary (Belgium). Hydrobiologia 406 (0), 119—132, http://dx.doi.org/10.1023/A:1003751512971.

Timm, T., 2009. A guide to the freshwater Oligochaeta and Polychaeta of the Northern and Central Europe. Lauterbornia 66, 235 pp.

Timm, T., Erséus, C., 2015. Tubificoides heterochaetus (Michaelsen, 1926), World Register of Marine Species at: http://www.marinespecies.org/aphia.php?.p=taxdetails&id=137577 (accessed on 23.07.15).

Vejdovský, F., 1891. Note sur un Tubifex d'Algérie. Mém. Soc. Zool. De France 4, 596—603.

Verdonschot, P.F.M., Smies, M., Sepers, A.B.J., 1982. The distribution of aquatic oligochaetes in brackish inland water in the SW Netherlands. Hydrobiologia 89 (1), 29—38.

Weigel, B., Andersson, H., Meier, H., Blenckner, T., Snickars, M., Bonsdorff, E., 2015. Long-term progression and drivers of coastal zoobenthos in a changing system. Mar. Ecol. Prog. Ser. 528, 141—159, http://dx.doi.org/10.3354/meps11279.

Włodarska-Kowalczuk, M., Mazurkiewicz, M., Jankowska, E., Kotwicki, L., Damrat, M., Zajączkowski, M., 2015. Effects of fluvial discharges on meiobenthic and macrobenthic variability in the Vistula river prodelta (Baltic Sea). J. Mar. Syst. 157, 135—146, http://dx.doi.org/10.1016/j.jmarsys.2015.12.009.

Zettler, M.L., Daunys, D., 2007. Long-term macrozoobenthos changes in a shallow boreal lagoon: comparison of a recent biodiversity inventory with historical data. Limnologica 37 (2), 170—185, http://dx.doi.org/10.1016/j.limno.2006.12.004.

Żmudziński, L., 1990. Świat zwierzęcy Bałtyku, WSiP, Warszawa, 106—109.

Oceanologia (2017) 59, 85—91

Available online at www.sciencedirect.com

ScienceDirect

journal homepage: www.journals.elsevier.com/oceanologia/

SHORT COMMUNICATION

# The killer shrimp *Dikerogammarus villosus* (Crustacea, Amphipoda) invades Lithuanian waters, South-Eastern Baltic Sea

**Eglė Šidagytė [a,*], Sabina Solovjova [b], Viktė Šniaukštaitė [a], Andrius Šiaulys [b], Sergej Olenin [b], Kęstutis Arbačiauskas [a]**

[a] *Nature Research Centre, Vilnius, Lithuania*
[b] *Marine Science and Technology Centre, Klaipėda, Lithuania*

Received 5 August 2016; accepted 29 August 2016
Available online 9 September 2016

**KEYWORDS**
Alien species;
Ponto-Caspian invaders;
First records;
Invasive crustaceans in Lithuania

**Summary** The killer shrimp *Dikerogammarus villosus* was recorded for the first time in Lithuanian waters in 2015. The species was detected in three sites in the Curonian Lagoon (on two buoys in the lagoon strait and the harbour, and one littoral sampling site) and in the mouth of the Šventoji River. The species presence in the buoy fouling suggests the involvement of shipping in species introduction. Most likely *D. villosus* has arrived to the Curonian Lagoon with commercial ships, while the invasion into the mouth of the Šventoji River may be associated with leisure shipping as the port situated therein is not currently functioning. Further northward expansion of the killer shrimp in the Baltic Sea basin seems very probable. As the species is highly aggressive, alterations of local macroinvertebrate assemblages can also be predicted.


* Corresponding author at: Nature Research Centre, Akademijos Str. 2, LT-08412 Vilnius, Lithuania. Tel.: +370 687 25477.
*E-mail addresses:* e.sidagyte@gmail.com (E. Šidagytė), sabina.lt@gmail.com (S. Solovjova), vikte.sn@gmail.com (V. Šniaukštaitė), andrius.siaulys@jmtc.ku.lt (A. Šiaulys), sergej.olenin@jmtc.ku.lt (S. Olenin), arbas@ekoi.lt (K. Arbačiauskas).
Peer review under the responsibility of Institute of Oceanology of the Polish Academy of Sciences.


http://dx.doi.org/10.1016/j.oceano.2016.08.004

## 1. Introduction

The killer shrimp *Dikerogammarus villosus* (Sowinsky, 1894) is an amphipod originating from the Ponto-Caspian region which began its range expansion across European waters in the 20th century after the re-opening of the Rhine-Main-Danube canal (Bij de Vaate et al., 2002). The crustacean is considered a highly invasive and aggressive aquatic species due to its large body, high fecundity, wide environmental tolerance and is often denoted as a voracious predator; it is capable of severe alteration of local communities and reduction or even extermination of native and other resident amphipods as well as of other macroinvertebrates (Dick and Platvoet, 2000; Grabowski et al., 2007a; Haas et al., 2002). The killer shrimp is the only amphipod included in the list of 100 most invasive non-indigenous species of Europe (Devin and Beisel, 2009).

The killer shrimp is unique for utilising all three main European invasion corridors from the Ponto-Caspian region (Bij de Vaate et al., 2002; Rewicz et al., 2014). The southern invasion corridor, connecting the basins of the Black and Northern seas along the Danube, Main and Rhine rivers, was the main pathway of expansion of *D. villosus*. The species was recorded in the lower Rhine for the first time in 1994 (Bij de Vaate and Klink, 1995). Recently it is widely distributed in all major rivers of Western Europe (reviewed in Bij de Vaate et al., 2002; Bollache et al., 2004; Jażdżewski and Konopacka, 2002; Nesemann et al., 1995). The invader originating from the southern route was also detected in the United Kingdom in 2010 (MacNeil et al., 2010; Rewicz et al., 2015). In 2003, the species was detected in the Bug River (Konopacka, 2004), indicating its expansion through the central invasion corridor along the Dnieper, Pripyat, Bug and Vistula rivers as well (see also Mastitsky and Makarevich, 2007). Molecular studies have shown that the southern and central invasion routes correspond with two distinct source populations residing in the Danube and Dnieper deltas (Rewicz et al., 2015) which may soon meet in Poland (Grabowski et al., 2007b). By the middle of the 20th century, *D. villosus* has also spread via the northern corridor (the Volga River system), within which its most northern record was made in the Kuybyshev Reservoir in 2000 (Rewicz et al., 2014; Yakovleva and Yakovlev, 2010).

A rapid further expansion of the killer shrimp across European waters is still ongoing. So far, *D. villosus* has approached the waters of the Baltic States and Lithuania in particular. In the vicinity of the Baltic Sea (Fig. 1), *D. villosus* was recorded in 2002 in the brackish-water Szczecin Lagoon, and this suggested that the lagoon was colonised by the descendants of invaders in the Oder River coming through the southern invasion corridor (Gruszka and Woźniczka, 2008). It also established populations in the Vistula Lagoon and the Gulf of Gdansk during 2010–2012 (Dobrzycka-Krahel et al., 2013, 2015).

It was already anticipated several years ago that *D. villosus* will inevitably reach Lithuania (Arbačiauskas et al., 2011), namely the middle reaches of the Nemunas River (southern Lithuania), through the Augustów canal which connects the Nemunas and the invaded Vistula basin. In this work we report the first records of *D. villosus* in Lithuanian waters, which, however, appear to be a result of a marine invasion along the Baltic Sea coast.

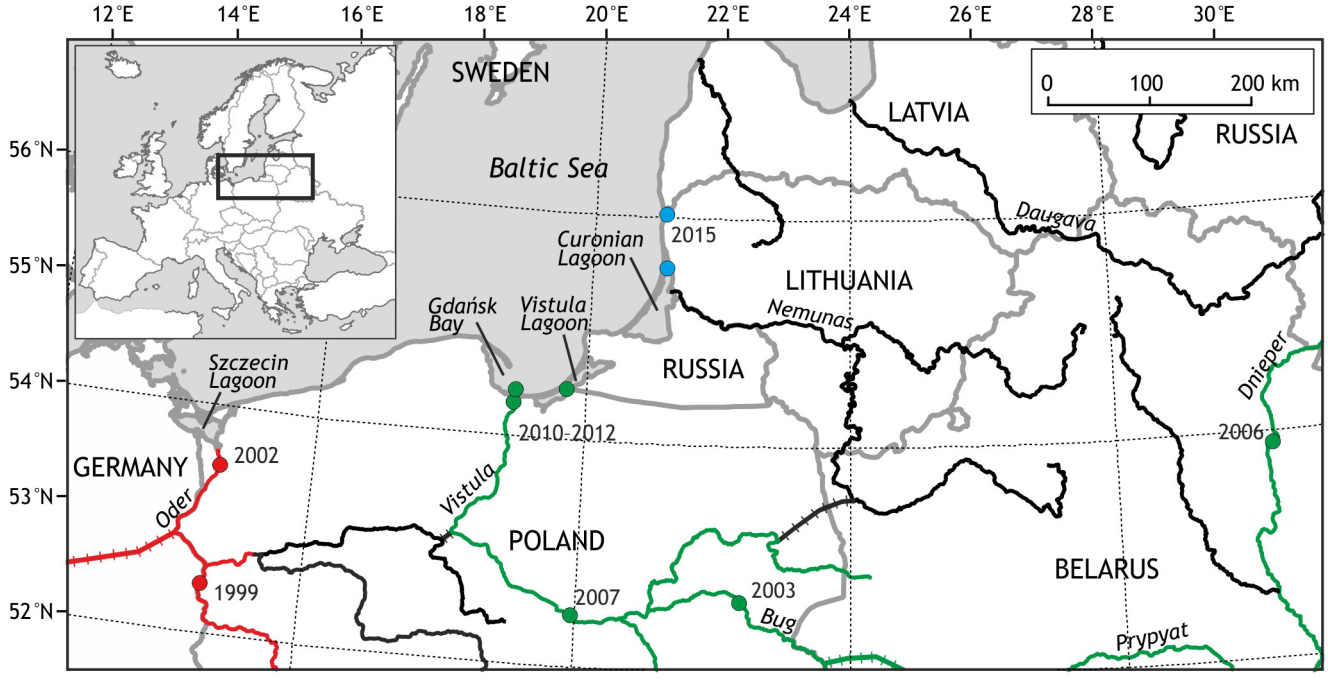


**Figure 1** European invasion routes of *Dikerogammarus villosus* in the vicinity of the Baltic Sea: southern corridor denoted in red and central corridor denoted in green. Recently invaded Lithuanian water bodies are denoted by blue dots. Dates are first records of the species. Based on Rewicz et al. (2015) and Dobrzycka-Krahel et al. (2015). (For interpretation of the references to colour in this figure legend, the reader is referred to the web version of this article.)

## 2. Material and methods

Investigations of amphipod assemblages were performed in the Šventoji River, which empties into the Baltic Sea, and the Curonian Lagoon during 2015. In the Šventoji River, the mouth and two other upstream sites were investigated in early September. In the Curonian Lagoon, a survey of fouling of five navigation buoys and a water level ruler located in the Klaipėda port and its vicinity was undertaken in June, and benthic sampling of three stations distributed within the lagoon was performed in September.

Samples from buoys were each taken by scraping off a 0.04-$m^2$ area of fouling, using a 20 cm × 20 cm sampling frame; 17 such samples in total were collected from surfaces located on buoys at different depths below the water level (Fig. 2). For composition of amphipod assemblages in the Šventoji River and the Curonian Lagoon, material was taken using a standard dip net with a 25 cm × 25 cm opening and a 0.5-mm mesh size. Semi-quantitative samples were collected in wadeable depths covering all substrate types and putting a sampling effort of 10 min per site.

In the field, all collected samples were fixed in 4% formaldehyde solution. In the laboratory, they were examined for the presence of amphipods that were sorted and preserved in 70% ethanol. The amphipod *D. villosus* was identified based on the shape of conical protuberances on urosomes I–II and dense tufts of long setae on the flagellum of antennae II and on the propodus of gnathopods in males (Dobson, 2013).

**Figure 2** A buoy in the Malkų Bay, the Klaipėda port. Photograph by M. Orlov.

## 3. Results

Locations of study sites where *D. villosus* was recorded are given in Table 1 and Fig. 3. In the Šventoji River, *D. villosus* (Fig. 4A) was present in the mouth and absent from the other two upstream study sites. There were only two specimens per sample that comprised around 1% of amphipods in the sample. Alien amphipods *Gammarus tigrinus* Sexton, 1939 of North American origin, and *Pontogammarus robustoides* (Sars, 1894) and *Chaetogammarus warpachowskyi* (Sars, 1894) originating from the Ponto-Caspian region dominated in the mouth of the river.

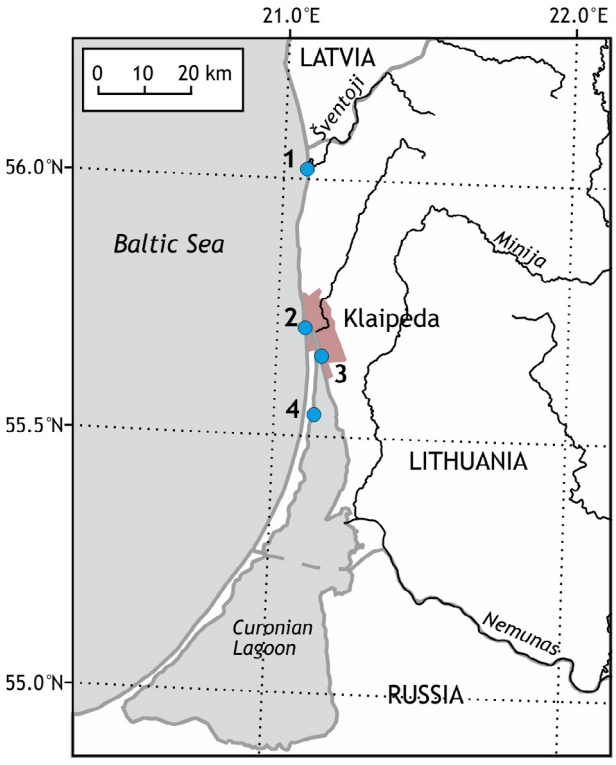


**Figure 3** Geographic location of sampling sites in Lithuanian waters where *Dikerogammarus villosus* was recorded. Site numbers correspond to those in Table 1.

**Table 1** Description of sampling sites in the Šventoji River and the Curonian Lagoon where *Dikerogammarus villosus* was recorded. Sampled substrates: buoy fouling (BF), sand (SA), silt (SI), stones (ST), macrophytes (MA); number of specimens per sample (*N*), proportion among amphipods (*P*).

| No | Site | Coordinates | Date | Substrate | *N* | *P* |
|---|---|---|---|---|---|---|
| | *Šventoji River* | | | | | |
| 1 | River mouth | 56°01′45″N, 21°04′22″E | 2015-09-04 | SA, SI, MA | 2 | 0.01 |
| | *Curonian Lagoon* | | | | | |
| 2 | Lagoon strait | 55°43′12″N, 21°06′05″E | 2015-06-22 | BF | 16 | 0.18 |
| 3 | Malkų Bay, Klaipėda port | 55°39′15″N, 21°09′10″E | 2015-06-18 | BF | 48 | 0.10 |
| 4 | Near Juodkrantė town | 55°33′14″N, 21°07′44″E | 2015-09-25 | ST, SI, MA | 44 | 0.19 |

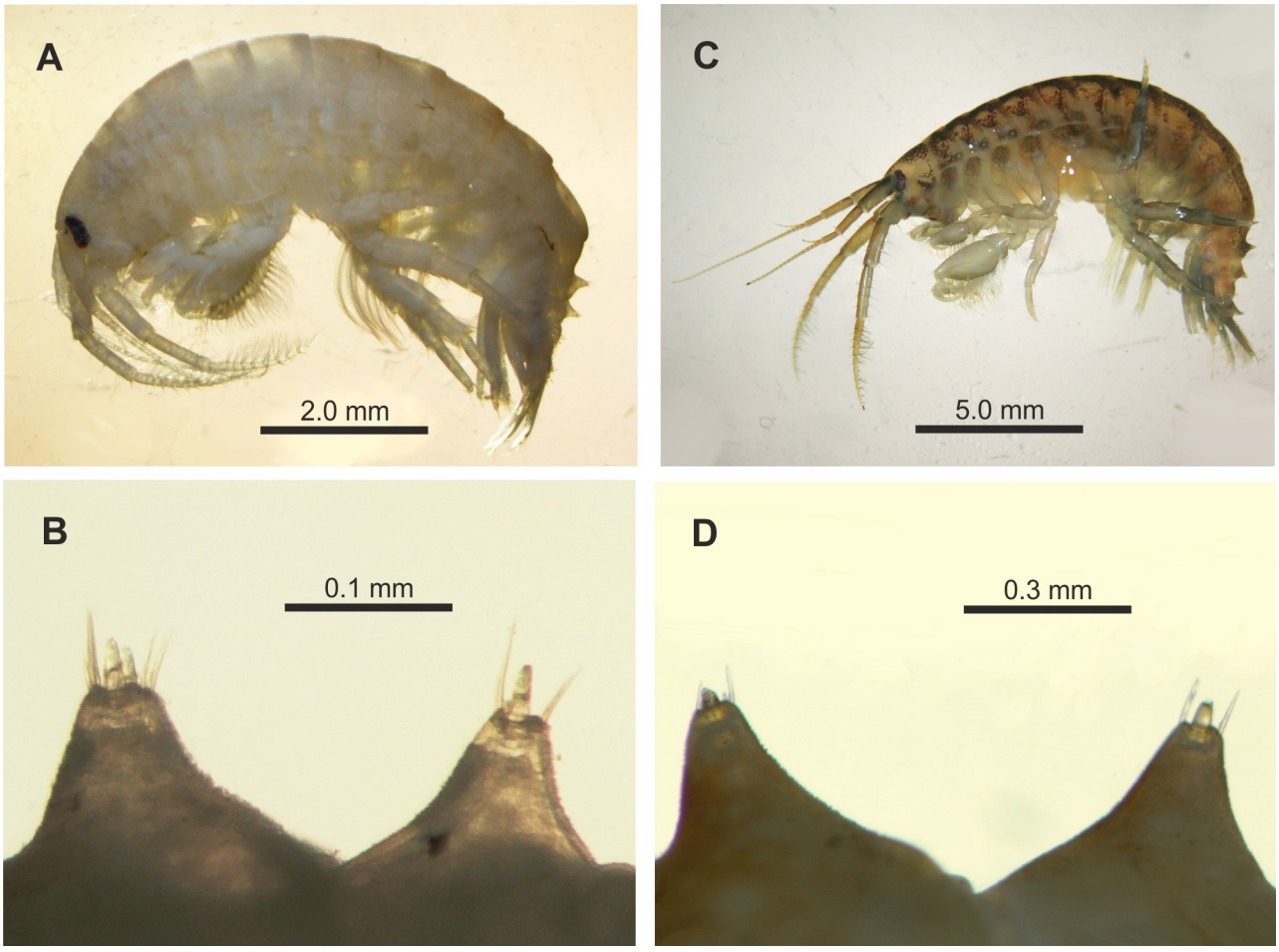


**Figure 4** *Dikerogammarus villosus* from Lithuanian waters: ethanol preserved 11-mm male from the mouth of the Šventoji River (A) and its urosomal protuberances (B); defrosted 21-mm male from the Curonian Lagoon (C) and its urosomal protuberances (D). Note that both specimens have only two spines on each of the protuberances, the characteristic typical of most male *D. villosus* currently observed in Lithuanian waters. Photographs by E. Šidagytė.

In the Curonian Lagoon, the species (Fig. 4C) was detected on two (out of five studied) navigation buoys located in the strait and the port in the Malkų Bay. The abundance of the killer shrimp per fouling sample was larger on the buoy from the port in the Malkų Bay, however, due to large abundance of other amphipods the proportion of the new invader here was about twofold lower than that observed on the buoy from the strait (Table 1). The dominant amphipods on the buoys were other alien amphipods, *Obesogammarus crassus* (Sars, 1894) and *Chelicorophium curvispinum* (Sars, 1894) of Ponto-Caspian origin, and *G. tigrinus*.

From the three littoral sites sampled in the Curonian Lagoon, *D. villosus* was detected only in one site located close to Juodkrantė Town. Here, 44 specimens of the killer shrimp were found. They comprised 19% of all sampled amphipods which were represented almost exclusively by alien species *G. tigrinus*, *O. crassus*, *C. curvispinum* and *C. warpachowskyi*.

## 4. Discussion

Our results clearly indicate that Lithuanian waters in the close vicinity of the Baltic Sea have been invaded by the killer shrimp *D. villosus*. A survey of macroinvertebrate assemblages in 17 sites along the Nemunas River in Lithuania, the northern branch of the central invasion corridor, failed to detect *D. villosus* in 2015 (unpublished results), thus we conclude that the newcomer had arrived through the sea. The most probable source of this amphipod invader into Lithuanian waters is the Polish coastal waters. Because of possible intermixture of invaders from the two invasion routes in the region, fine-scale molecular studies are warranted to determine the origin of Lithuanian populations. However, their origination from the central invasion corridor seems more presumable. So far, the Šventoji River mouth is the most northern recorded site of *D. villosus* presence in the Baltic Sea basin.

The presence of the species in the fouling of navigation buoys located in the Klaipėda port and its vicinity suggests that *D. villosus* probably was transferred by commercial ships, whether within the hull fouling or in ballast waters. Introduction of the species into the mouth of the Šventoji River may be associated with leisure shipping as the port at this site is not currently functioning. On the other hand, a possibility of natural dispersal over the coastal waters of the Baltic Sea should not be excluded. This is possible as the species proved

to be an osmotic hyper-regulator capable of resisting a wide range of external salinities (Bruijs et al., 2001; Dobrzycka-Krahel et al., 2015).

While quite abundant (when present) in the samples from the Curonian Lagoon, this amphipod only occasionally occurred in the mouth of the Šventoji River. In June 2016, abundant individuals of various size, precopula pairs and ovigerous females of *D. villosus* were observed in the stony littoral habitats of the Curonian Lagoon near Juodkrantė, while in the sandy mouth of the Šventoji River its abundance did not seem to be high. Only 16 specimens of the killer shrimp (just 3% of all sampled amphipods) were identified after rigorous sampling carried out by three people. This pattern suggests that the invasion of *D. villosus* into the lagoon may have occurred at least a year before its first detection, while colonisation of the Šventoji River has started only recently. However, the differences in abundance may also be related to the scarcity of hard substrates preferred by *D. villosus* (Devin et al., 2003; Kley and Maier, 2005) in the predominantly sandy habitat of the mouth of the Šventoji River.

The characteristic temperature and salinity ranges of the Curonian Lagoon (respectively 0—24°C and 0—8 PSU; Olenin and Daunys, 2004), as well as these conditions in most Lithuanian inland waters, should be easily tolerated by such a plastic species as *D. villosus* (Bruijs et al., 2001; Devin and Beisel, 2009; Dobrzycka-Krahel et al., 2015). It has been reported that the species largely prefers hard substrates (from gravel to boulders, artificial embankments, roots, dreissenid colonies) and avoids sand and silt (Boets et al., 2010; Devin et al., 2003; Kley and Maier, 2005; MacNeil et al., 2010). Most of invasive pontogammarids are oxyphilic species, however, the lethal oxygen concentration for the killer shrimp (0.38 mg $L^{-1}$) is the highest among them (Dedyu, 1980). As a result, the species has also been noticed to be more restrained by pollution than other pontogammarid invaders (Boets et al., 2010; Dobrzycka-Krahel et al., 2015). It has been suggested that *D. villosus* prefers slow-flowing waters and therefore should not invade small rivers, even if the water quality is good (Boets et al., 2010). Thus it can be preliminarily concluded that ecosystems from large rivers, reservoirs and lakes to lagoons and bays of the eastern Baltic Sea, especially habitats with any kind of hard substrate and no substantial pollution, are vulnerable to the new invader.

It is of interest to note that Ponto-Caspian amphipod *O. crassus* usually dominated amphipod assemblages in the northern part of the Curonian Lagoon, at least in the areas affected by the brackish sea water. However, in over 50 years the species did not manage to colonise the mouth of the Šventoji River located just 35 km north (Arbačiauskas et al., 2011; current study), although it was once observed in the Baltic coastal waters at Palanga town, around 20 km north from the Curonian Lagoon (Solovjova, unpublished results). *Dikerogammarus villosus*, on the other hand, was recorded in both ecosystems simultaneously, indicating a huge potential of the species to spread across marine waters. Therefore, it is not surprising that the killer shrimp is considered the most probable future amphipod invader in the North American waters (Ricciardi and Rasmussen, 1998). Future northward expansion of *D. villosus* in the basin of the Baltic Sea and invasion of the Latvian waters seems inevitable. It is also likely that the species is already there (as well as in the Russian Kaliningrad region) but is not yet recorded.

There are three species of the genus *Dikerogammarus* invading the European waters, the other two being *Dikerogammarus haemobaphes* (Eichwald, 1841) and *Dikerogammarus bispinosus* Martynov 1925; the latter only recently being promoted to a species from a subspecies of *D. villosus* (Müller et al., 2002). It is often noted that adult males of *D. villosus* are easily distinguishable from the congeneric invaders using a combination of three identification features: (1) short setation of the peduncle but dense and long setation on the flagellum of antennae II, (2) long setation of the propodus of gnapthopods, and (3) 3—5 spines on each of the two pointed dorsal protuberances of the urosomes I—II (Dobson, 2013; Müller et al., 2002). In Lithuanian populations, however, male individuals confined to the first two identification features very clearly, but most of them had two main spines on both protuberances (Fig. 4B and D). MacNeil et al. (2010) have mentioned personal observations of D. Platvoet that only adult males of *D. villosus* over 16-mm body length (may reach up to 30 mm; Dobson, 2013) usually have 3—5 spines. The largest individuals in our study reached slightly over 20 mm. They all, however, had two spines on at least one of the protuberances, and very often two spines on both protuberances. Smaller males of 10—11-mm length consistently had only two spines on both protuberances, while variation from 2 + 2 to 3 + 5 spines was observed in medium 14—15 mm long males. Thus, it seems that the number of spines on dorsal urosomal protuberances should be used with caution for species identification. So far, only A. Konopacka (2004) has clearly pointed out that urosomal protuberances of *D. villosus* may contain from 2 to 5 spines.

The killer shrimp has been repeatedly reported as a voracious predator (Dick and Platvoet, 2000; Grabowski et al., 2007a; Haas et al., 2002), thus it is ecologically aggressive towards resident macroinvertebrate species and is capable of impacts on their communities. The other Ponto-Caspian amphipod, *P. robustoides*, is the dominant alien amphipod species in the inland freshwaters of Lithuania (Arbačiauskas et al., 2011) and the central part of the Curonian Lagoon (Solovjova, unpublished results). This amphipod species is also characterised as an ecologically aggressive species which is capable of extermination of native amphipods and alteration of composition of macroinvertebrate assemblages (Arbačiauskas and Gumuliauskaitė, 2007; Gumuliauskaitė and Arbačiauskas, 2008). In Polish dams, *P. robustoides* has been reported to out-compete the preceding invader, the daemon shrimp *D. haemobaphes* (Jażdżewska and Jażdżewski, 2008). Some experimental studies confirm that *P. robustoides* stands close to *D. villosus* according to interference competitiveness (Kobak et al., 2016).

Although *P. robustoides* prefers more lentic habitats than *D. villosus* (Jazdzewski et al., 2002), localities recently invaded by *D. villosus* and *P. robustoides* coincide in some reservoirs of Poland and Russia. In these reservoirs, they are currently able to coexist by occupying different habitats: *P. robustoides* dwells in the sandy shallows while *D. villosus* prevails in higher depths (Kobak et al., 2014; Yakovleva and Yakovlev, 2010). It may be that *D. villosus* is a stronger competitor but is more restricted to hard substrates (Boets et al., 2010) and less resistant to desiccation

(Poznańska et al., 2013) and pollution (Boets et al., 2010; Dobrzycka-Krahel et al., 2015) than *P. robustoides*.

These two aggressive invaders will definitely clash in Lithuanian waters as well, and it would be of interest to reveal the outcomes of their interaction. Alterations, even severe ones, of local macroinvertebrate assemblages in waters suitable for the killer shrimp can definitely be expected in the near future.

## Acknowledgement

The study was supported by the Research Council of Lithuania, Project No. SIT-10/2015.

## References

Arbačiauskas, K., Gumuliauskaitė, S., 2007. Invasion of the Baltic Sea basin by the Ponto-Caspian amphipod *Pontogammarus robustoides* and its ecological impact. In: Gherardi, F. (Ed.), Biological Invaders in Inland Waters: Profiles, Distribution, and Threats. Springer, Dordrecht, Netherlands, 463—477, http://dx.doi.org/10.1007/978-1-4020-6029-8_25.

Arbačiauskas, K., Višinskienė, G., Smilgevičienė, S., Rakauskas, V., 2011. Non-indigenous macroinvertebrate species in Lithuanian fresh waters. Part 1: Distributions, dispersal and future. Knowl. Manag. Aquat. Ecosyst. 402, art. ID 12, 18 pp., http://dx.doi.org/10.1051/kmae/2011075.

Bij de Vaate, A., Jazdzewski, K., Ketelaars, H.A.M., Gollasch, S., Van der Velde, G., 2002. Geographical patterns in range extension of Ponto-Caspian macroinvertebrate species in Europe. Can. J. Fish. Aquat. Sci. 59 (7), 1159—1174, http://dx.doi.org/10.1139/f02-098.

Bij de Vaate, A., Klink, A.G., 1995. *Dikerogammarus villosus* Sowinsky (Crustacea: Gammaridae) a new immigrant in the Dutch part of the Lower Rhine. Lauterbornia 20, 2—5.

Boets, P., Lock, K., Messiaen, M., Goethals, P.L.M., 2010. Combining data-driven methods and lab studies to analyse the ecology of *Dikerogammarus villosus*. Ecol. Inform. 5 (2), 133—139, http://dx.doi.org/10.1016/j.ecoinf.2009.12.005.

Bollache, L., Devin, S., Wattier, R., Chovet, M., Beisel, J.-N., Moreteau, J.-C., Rigaud, T., 2004. Rapid range extension of the Ponto-Caspian amphipod *Dikerogammarus villosus* in France: potential consequences. Arch. Hydrobiol. 160 (1), 57—66, http://dx.doi.org/10.1127/0003-9136/2004/0160-0057.

Bruijs, M.C.M., Kelleher, B., Van der Velde, G., Bij de Vaate, A., 2001. Oxygen consumption, temperature and salinity tolerance of the invasive amphipod *Dikerogammarus villosus*: indicators of further dispersal via ballast water transport. Arch. Hydrobiol. 152 (4), 633—646, http://dx.doi.org/10.1127/archiv-hydrobiol/152/2001/633.

Dedyu, I.I., 1980. Amphipods of Fresh and Salt Waters of the South-West Part of the USSR. Shtiintsa Publishers, Kishinev, 223 pp., (in Russian).

Devin, S., Beisel, J.-N., 2009. *Dikerogammarus villosus* (Sowinsky), killer shrimp (Gammaridae, Crustacea). In: Drake, J.A. (Ed.), Handbook of Alien Species in Europe. Springer, Dordrecht, Netherlands, 309 pp.

Devin, S., Piscart, C., Beisel, J.N., Moreteau, J.C., 2003. Ecological traits of the amphipod invader *Dikerogammarus villosus* on a mesohabitat scale. Arch. Hydrobiol. 158 (1), 43—56, http://dx.doi.org/10.1127/0003-9136/2003/0158-0043.

Dick, J.T., Platvoet, D., 2000. Invading predatory crustacean *Dikerogammarus villosus* eliminates both native and exotic species. Proc. R. Soc. London B 267 (1447), 977—983, http://dx.doi.org/10.1098/rspb.2000.1099.

Dobrzycka-Krahel, A., Kendzierska, H., Szaniawska, A., 2013. Ponto-Caspian gammarids — a new species in the Gulf of Gdańsk (Southern Baltic Sea). J. Ecol. Health 17 (3), 110—114.

Dobrzycka-Krahel, A., Melzer, M., Majkowski, W., 2015. Range extension of *Dikerogammarus villosus* (Sowinsky, 1894) in Poland (the Baltic Sea basin) and its ability to osmoregulate in different environmental salinities. Oceanol. Hydrobiol. Stud. 44 (3), 294—304, http://dx.doi.org/10.1515/ohs-2015-0028.

Dobson, M., 2013. Identifying Invasive Freshwater Shrimps and Isopods. Freshwater Biological Association, Ambleside, 30 pp.

Grabowski, M., Bacela, K., Konopacka, A., 2007a. How to be an invasive gammarid (Amphipoda: Gammaroidea) — comparison of life history traits. Hydrobiologia 590 (1), 75—84, http://dx.doi.org/10.1007/s10750-007-0759-6.

Grabowski, M., Jażdżewski, K., Konopacka, A., 2007b. Alien crustacea in Polish waters — Amphipoda. Aquat. Invasions 2 (1), 25—38, http://dx.doi.org/10.3391/ai.2007.2.1.3.

Gruszka, P., Woźniczka, A., 2008. *Dikerogammarus villosus* (Sowinsky, 1894) in the River Odra estuary — another invader threatening Baltic Sea coastal lagoons. Aquat. Invasions 3 (4), 395—403, http://dx.doi.org/10.3391/ai.2008.3.4.4.

Gumuliauskaitė, S., Arbačiauskas, K., 2008. The impact of the invasive Ponto-Caspian amphipod *Pontogammarus robustoides* on littoral communities in Lithuanian lakes. Hydrobiologia 599 (1), 127—134, http://dx.doi.org/10.1007/s10750-007-9209-8.

Haas, G., Brunke, M., Streit, B., 2002. Fast turnover in dominance of exotic species in the Rhine River determines biodiversity and ecosystem function: an affair between amphipods and mussels. In: Leppäkoski, E., Gollasch, S., Olenin, S. (Eds.), Invasive Aquatic Species of Europe: Distribution, Impacts and Management. Springer, Dordrecht, Netherlands, 426—432, http://dx.doi.org/10.1007/978-94-015-9956-6_42.

Jażdżewska, A., Jażdżewski, K., 2008. *Pontogammarus robustoides* (G. O. Sars, 1894) (Crustacea, Amphipoda), a new Ponto-Caspian invader in Great Masurian Lakes (NE Poland). Fragm. Faun. 51 (1), 1—7, http://dx.doi.org/10.3161/00159301FF2008.51.1.001.

Jażdżewski, K., Konopacka, A., 2002. Invasive Ponto-Caspian species in waters of the Vistula and Oder basins and of the southern Baltic Sea. In: Leppäkoski, E., Gollasch, S., Olenin, S. (Eds.), Invasive Aquatic Species of Europe: Distribution, Impacts and Management. Springer, Dordrecht, Netherlands, 384—398, http://dx.doi.org/10.1007/978-94-015-9956-6_39.

Jazdzewski, K., Konopacka, A., Grabowski, M., 2002. Four Ponto-Caspian and one American gammarid species (Crustacea Amphipoda) recently invading Polish waters. Contrib. Zool. 71 (4), 115—122.

Kley, A., Maier, G., 2005. An example of niche partitioning between *Dikerogammarus villosus* and other invasive and native gammarids: a field study. J. Limnol. 64 (1), 85—88, http://dx.doi.org/10.4081/jlimnol.2005.85.

Kobak, J., Jermacz, Ł., Płąchocki, D., 2014. Effectiveness of zebra mussels to act as shelters from fish predators differs between native and invasive amphipod prey. Aquat. Ecol. 48 (4), 397—408, http://dx.doi.org/10.1007/s10452-014-9492-1.

Kobak, J., Rachalewski, M., Bącela-Spychalska, K., 2016. Conquerors or exiles? Impact of interference competition among invasive Ponto-Caspian gammarideans on their dispersal rates. Biol. Invasions 18 (7), 1953—1965, http://dx.doi.org/10.1007/s10530-016-1140-3.

Konopacka, A., 2004. Inwazyjne skorupiaki obunogie (Crustacea, Amphipoda) w wodach Polski. Przegląd Zool. 48 (3—4), 141—162.

MacNeil, C., Platvoet, D., Dick, J.T.A., Fielding, N., Constable, A., Hall, N., Aldridge, D., Renals, T., Diamond, M., 2010. The Ponto-Caspian "killer shrimp", *Dikerogammarus villosus* (Sowinsky, 1894), invades the British Isles. Aquat. Invasions 5 (4), 441—445, http://dx.doi.org/10.3391/ai.2010.5.4.15.

Mastitsky, S.E., Makarevich, O.A., 2007. Distribution and abundance of Ponto-Caspian amphipods in the Belarusian section of the

Dnieper River. Aquat. Invasions 2 (1), 39—44, http://dx.doi.org/10.3391/ai.2007.2.1.4.

Müller, J., Schramm, S., Seitz, A., 2002. Genetic and morphological differentiation of *Dikerogammarus* invaders and their invasion history in Central Europe. Freshw. Biol. 47 (11), 2039—2048, http://dx.doi.org/10.1046/j.1365-2427.2002.00944.x.

Nesemann, H., Pöckl, M., Wittmann, K.J., 1995. Distribution of epigean Malacostraca in the middle and upper Danube (Hungary, Austria, Germany). Misc. Zool. Hung. 10, 49—68.

Olenin, S., Daunys, D., 2004. Coastal typology based on benthic biotope and community data: The Lithuanian case study. In: Schernewski, G., Wielgat, M. (Eds.), Baltic Sea Typology, Coastline Reports 4. The Coastal Union, Leiden, 65—83.

Poznańska, M., Kakareko, T., Krzyżyński, M., Kobak, J., 2013. Effect of substratum drying on the survival and migrations of Ponto-Caspian and native gammarids (Crustacea: Amphipoda). Hydrobiologia 700 (1), 47—59, http://dx.doi.org/10.1007/s10750-012-1218-6.

Rewicz, T., Grabowski, M., MacNeil, C., Bącela-Spychalska, K., 2014. The profile of a "perfect" invader — the case of killer shrimp, *Dikerogammarus villosus*. Aquat. Invasions 9 (3), 267—288, http://dx.doi.org/10.3391/ai.2014.9.3.04.

Rewicz, T., Wattier, R., Grabowski, M., Rigaud, T., Bącela-Spychalska, K., 2015. Out of the Black Sea: phylogeography of the invasive killer shrimp *Dikerogammarus villosus* across Europe. PLoS One 10 (2), e0118121, http://dx.doi.org/10.1371/journal.pone.0118121.

Ricciardi, A., Rasmussen, J.B., 1998. Predicting the identity and impact of future biological invaders: a priority for aquatic resource management. Can. J. Fish. Aquat. Sci. 55 (7), 1759—1765, http://dx.doi.org/10.1139/cjfas-55-7-1759.

Yakovleva, A.V., Yakovlev, V.A., 2010. Modern fauna and quantitative parameters of invasive invertebrates in zoobenthos of upper reaches of the Kuybyshev Reservoir, Russia. Russ. J. Biol. Invasions 1 (3), 232—241, http://dx.doi.org/10.1134/S2075111710030161.